

**CHARACTERISATION OF THE FUNDAMENTAL
INTERACTIONS BETWEEN WATER AND
CELLULOSE ETHER POLYMERS**

by

Conor B. McCrystal BSc., MRPharmS, MPSNI

Thesis submitted to Liverpool John Moores University for the
degree of Doctor of Philosophy



School of Pharmacy and Chemistry
Liverpool John Moores University

May 1998

Defeat is not an option

anon.

Acknowledgements

I would like to thank the following people for helping me achieve this goal:

My supervisors; Dr. Ali R. Rajabi-Siahboomi for his tuition, patience and industry and Professor James L. Ford for his wisdom and sense of humour. I offer you both my sincerest thanks and heartfelt appreciation for your help and guidance.

The staff of Liverpool John Moores University for the help which I received during my period of research including all technical staff especially Mr Roland Collins, the library staff and the staff at computing services who were always available for consultation.

Dr. D.Q.M. Craig and Dr. R. He (School of Pharmacy, University of London) for their guidance with Dielectric Spectroscopy analysis.

Dr. K. Vyas (Bristol-Myers Squibb, Moreton, Merseyside) and the staff at Surface Measurement Systems Ltd.(London) for their advice with Dynamic Vapour Sorption studies.

I acknowledge the funding provided by Liverpool John Moores University to support this research and allow conference attendance.

Special thanks to the following: Dr. A. Nokhodchi, Dr. G.P. Moss, Dr. M.M. Tunney and all post-graduate (please see previous page) and undergraduate students I had the privilege of meeting in Liverpool. A word of thanks also to the staff in the School of Pharmacy, The Queen's University of Belfast, where this thesis was largely written.

Finally, I would like to thank my family, my brother Barry and in particular Clare, for being with me through both bad times and good in Liverpool.

Contents

	Page number
Abstract	i
Glossary of abbreviations	ii
<u>CHAPTER 1 INTRODUCTION</u>	
1.1 Cellulose ethers	1
1.1.1 Structure	1
1.1.2 Source	1
1.1.3 Preparation	3
1.1.4 Degree of substitution	6
1.1.5 Viscosity grades	7
1.1.6 Glass Transition temperature	9
1.1.7 Properties of MC and HPMC solutions	10
1.1.7.1 Hydration and thermal gelation	10
1.1.7.2 Mechanism of thermal gelation	11
1.1.7.3 Viscosity-Temperature behaviour of methylcellulose	14
1.1.7.4 Factors influencing thermal gelation	14
1.1.7.5 Surface activity	19
1.1.8 Applications	19
1.1.8.1 Non-pharmaceutical applications	20
1.1.8.2 Pharmaceutical applications	21
1.2 Cellulose Ethers and sustained release formulations	23
1.2.1 Sustained release formulation	23
1.2.2 Hydrophilic matrix (HM) controlled release systems	24
1.2.3 Mechanism of drug release from HM systems	26
1.2.4 Factors affecting drug release from HPMC matrix systems	28
1.2.4.1 Active ingredient	28
1.2.4.2 Polymer factors	29

1.2.4.2.1	Polymer viscosity grade	29
1.2.4.2.2	Polymer substitution type	30
1.2.4.2.3	Particle size and concentration effects	31
1.3	Interactions between water and cellulose ethers	32
1.3.1	Mechanism of the water-polymer interaction	32
1.3.2	Techniques employed in the differentiation and measurement of different types of water in hydrophilic polymers	39
1.3.2.1	Nuclear Magnetic Resonance (NMR)	39
1.3.2.2	Differential Scanning Calorimetry (DSC)	40
1.3.2.3	Thermogravimetric analysis (TGA)	40
1.3.2.4	Thermomechanical Analysis (TMA) or Dilatometry	41
1.3.2.5	Dielectric spectroscopy	41
1.3.2.6	Vapour Sorption	41
1.4	Thesis Aims and Objectives	42

CHAPTER 2 MATERIALS, METHODS AND CHARACTERISATION

2.1	Materials	43
2.1.1	Cellulose ethers	43
2.1.2	Propranolol Hydrochloride	43
2.1.3	Diclofenac Sodium	45
2.2	Experimental Methods	45
2.2.1	Preparation of cellulose ether gels	45
2.2.2	Thermal methods	47
2.2.2.1	Differential Scanning Calorimetry	47
2.2.2.2	Thermogravimetric Analysis (TG)	49
2.2.3	Powder Characterisation	52
2.2.3.1	X-ray Powder Diffraction	52

2.2.3.2 Surface Area Determination	52
2.2.3.3 Glass Transition Determination	56
2.2.4 Other Methods	63

CHAPTER 3 CHARACTERISATION OF WATER DISTRIBUTION WITHIN HPMC K15M GELS USING DIFFERENTIAL SCANNING CALORIMETRY

3.1	Introduction	64
	3.1.1 Objectives	67
3.2	Materials	67
3.3	Methods	67
	3.3.1 Gel Preparation	67
	3.3.2 Thermal Analysis	68
3.4	Results and Discussion	68
	3.4.1 Differential Scanning Calorimetry studies	68
	3.4.1.1 The influence of HPMC K15M on DSC spectra of water	68
	3.4.1.2 Effect of gel storage time on water distribution	72
	3.4.1.3 Further moisture characterization of HPMC K15M gels	74
	3.4.1.3.1 Quantitative analysis of water distribution within HPMC K15M gels	77
	3.4.1.4 Effect of cooling and heating rates during DSC analysis on the nature of the thermal events	79
	3.4.1.5 Study of batch to batch variation on the water distribution within HPMC K15M gels	86
	3.4.1.6 Influence of water temperature during gel preparation on water distribution within HPMC K15M gels	92
3.5	Conclusions	97

CHAPTER 4 CHARACTERISATION OF WATER DISTRIBUTION WITHIN HPMC K15M GELS USING THERMOGRAVIMETRIC ANALYSIS

4.1	Introduction	99
	4.1.1 Objectives	99
4.2	Materials	103
4.3	Methods	103
	4.3.1 Gel Preparation	103
	4.3.2 Thermal Analysis	103
4.4	Results and Discussion	104
	4.4.1 Thermogravimetric analysis studies	104
	4.4.1.1 Thermogravimetric analysis of HPMC K15M gels of different concentrations	104
	4.4.1.2 Effect of heating rate on moisture loss from HPMC K15M gels	108
	4.4.1.3 Kinetic analysis of water loss from HPMC K15M gels	113
4.5	Conclusions	116

CHAPTER 5 EFFECT OF MOLECULAR WEIGHT AND SUBSTITUTION TYPE ON WATER DISTRIBUTION WITHIN CELLULOSE ETHER POLYMERS

5.1	Introduction	117
	5.1.1 Objectives	118
5.2	Materials	118

5.3	Methods	118
	5.3.1 Gel preparation	118
	5.3.2 Thermal Analysis	119
5.4	Results and Discussion	119
	5.4.1 Effect of polymer molecular weight on the water distribution within cellulose ether polymers	119
	5.4.2 Effect of polymer substituent type on the nature of water distribution within cellulose ether polymers	131
	5.4.3 Quantitative analysis of the effect of molecular weight and substitution type on water distribution within cellulose ether polymers	140
	5.4.3.1 Water distribution within cellulose ether polymers as calculated by the method proposed by Ford and Mitchell	140
	5.4.3.2 Comparison of two methods used to estimate bound water content of hydrophilic polymers using DSC	143
5.5	Conclusions	147

**CHAPTER 6 DYNAMIC WATER VAPOUR SORPTION/DESORPTION
STUDIES ON CELLULOSE ETHER POLYMERS**

6.1	Introduction	149
	6.1.1 Objectives	153
6.2	Materials	153
6.3	Methods	153
	6.3.1 Sample preparation	153
	6.3.2 Dynamic Vapour Sorption	153

6.4	Results and Discussion	
6.4.1	Water sorption characteristics of HPMC's with different molecular weights	154
6.4.1.1	The influence of polymer molecular weight on hysteresis area	157
6.4.2	Water sorption characteristics of HPMC's with different substitution levels	162
6.4.2.1	The influence of polymer substitution level on hysteresis area	162
6.4.3	Application of the Young-Nelson Theory to moisture sorption/desorption of cellulose ether polymers	166
6.4.3.1	Influence of polymer molecular weight and substitution levels on the water distribution within cellulose ether polymers	169
6.4.4	BET analysis of dynamic vapour sorption data for cellulose ether polymers	183
6.5	Conclusions	186

CHAPTER 7 DIELECTRIC PROPERTIES OF CELLULOSE ETHER GELS

7.1	Introduction	188
	7.1.1 Objectives	192
7.2	Materials	192
7.3	Methods	192
	7.3.1 Gel preparation	192
	7.3.2 Dielectric Spectroscopy Analysis	193
7.4	Results and Discussion	193

7.4.1 Dielectric response of HPMC K15M gels	193
7.4.1.1 Effect of temperature on the nature of the dielectric response	193
7.4.1.2 Effect of HPMC K15M concentration on the dielectric response	198
7.4.1.3 Effect of polymer molecular weight on the dielectric response in cellulose ether gels	201
7.4.1.4 The influence of polymer substitution level on the dielectric response of cellulose ether gels	211
7.4.1.5 Effect of drug addition on the nature of the dielectric response in HPMC K15M gels	216
7.5 Conclusions	225

**CHAPTER 8 INFLUENCE OF DRUGS ON WATER DISTRIBUTION
WITHIN CELLULOSE ETHER POLYMER GELS**

8.1 Introduction	227
8.1.1 Objectives	228
8.2 Materials	228
8.3 Methods	229
8.3.1 Gel and solution preparation	229
8.3.2 Thermal Analysis	230
8.4 Results and Discussion	230
8.4.1 Determination of the eutectic point for the propranolol hydrochloride : water system	230
8.4.2 The influence of propranolol hydrochloride on the water distribution in HPMC K15M gels	235

8.4.3	Quantitative analysis on the effect of propranolol hydrochloride concentration on water distribution within HPMC K15M gels	239
8.4.4	Effect of propranolol hydrochloride (50mM) and diclofenac sodium (50mM) on water distribution in cellulose ether polymer gels	243
8.4.4.1	Influence of propranolol hydrochloride and diclofenac sodium on the thermal events occurring within a series of cellulose ether polymers of varying molecular weight	244
8.4.4.2	Influence of propranolol hydrochloride and diclofenac sodium on the thermal events occurring within a series of cellulose ether polymers of different substitution types	246
8.4.5	Effect of drug addition on the melting point of free water in HPMC K15M gels	252
8.4.6	Quantitative analysis of the effect of propranolol hydrochloride (50mM) and diclofenac sodium (50mM) on the bound water content of cellulose ether gels	252
8.4.7	Thermogravimetric analysis studies	
8.4.7.1	Effect of propranolol hydrochloride and diclofenac sodium on thermal events in HPMC K15M gels	255
8.4.7.2	Kinetic studies on the effect of drug addition on water loss from HPMC K15M gels	261
8.5	Conclusions	264

CHAPTER 9 GENERAL DISCUSSION

9.1	Introduction	266
9.2	Characterisation of the interaction between water and HPMC K15M polymer gels	266

9.3	Characterisation of the interaction between water and a range of polymers of varying molecular weight and substitution type	271
------------	--	------------

9.4	Influence of drugs on the water distribution within cellulose ether polymer gels	275
------------	---	------------

CHAPTER 10 CONCLUSIONS AND RECOMMENDATIONS FOR FUTURE WORK

10.1	Conclusions	278
-------------	--------------------	------------

10.2	Recommendations for future work	280
-------------	--	------------

REFERENCES	282
-------------------	------------

PUBLICATIONS	316
---------------------	------------

Abstract

The thesis characterises the behaviour of water in gels of cellulose ether polymers that are commonly used in hydrophilic matrix systems. Detailed studies on the hydrated polymer which forms a gel and more specifically on the types of water which exist within this gel are fundamental in the optimisation of cellulose ethers for their applications in sustained release formulations.

Characteristic thermal events were apparent in the DSC scans of HPMC K15M gels, which were dependent on gel hydration time, polymer concentration and the cooling and heating rates utilised during scanning. These events were related to the presence of different types of water in HPMC K15M gels; free water, the main endothermic peak at around 0°C, bound water and loosely bound water, giving rise to smaller peaks prior to the main peak at temperatures from -15 to 0°C. These pre-endothermic events were unaffected when gel samples were cooled to -50°C, heated to -9°C and subsequently re-cooled and reheated to +35°C. Upon cooling to -50°C, heating to -9°C and holding for 10mins, and then re-cooling and reheating again, their occurrence and the temperature at which they appeared remained unaffected. Therefore it was concluded that these pre-endothermic events were real and they were reproducible. TGA and dielectric spectroscopy studies also provided evidence for the existence of more than one type of water within HPMC K15M gels. Water evaporating in more than one event was visible from the first derivative of the TGA weight loss curve, which was dependent on polymer concentration and scanning rates. The behaviour of water in HPMC K15M gels was characterised using low frequency dielectric spectroscopy from -30 to +22°C. The shape of the dielectric response curves showed that in addition to the melting of free water, a number of other processes were occurring indicating that the melting of different types of water prior to the melting of free water. These processes were dependent on polymer concentration and the results were in agreement with the DSC findings, confirming the presence of different types of water in these gel systems.

The amount of water bound per PRU in HPMC K15M gels were calculated using DSC results based on methods previously reported. The characteristic events visible in both DSC and LFDS studies were dependent on polymer molecular weight, substitution type and hydration time. The BW per PRU for cellulose ethers after 96h hydration were; HPMCs K100LV (4.4), K4M (4.5), K15M (6.5), K100M (6.6), E4M (5.6), F4M (5.4), MC A4M (3.8) and HPC (6.1). The distinctive events visible in both DSC and LFDS studies and the separation of evaporation events in TGA were influenced by the addition of a drug. Propranolol hydrochloride (water-soluble) reduced the amount of water bound to the majority of polymers, the so called 'salting-in' effect. However, more water was required to fully hydrate the majority of polymers in the presence of diclofenac sodium (poorly water-soluble) in comparison with the effects seen in the presence of propranolol hydrochloride, the so called 'salting-out' effect.

Polymer molecular weight had little effect on their moisture sorption/ desorption characteristics in comparison to polymer substitution type which appeared to have an effect on these properties. HPMC K4M sorbed more moisture at all RH values and had a larger hysteresis area compared to that for HPMCs E4M, F4M and MC A4M.

Glossary of abbreviations

BDC	Broadband dielectric converter
BET	Brunauer-Emmett-Teller
BW	Bound water
CMC	Carboxymethylcellulose
CPT	Cloud point temperature
DIC Na	Diclofenac sodium
DMA	Dynamic mechanical analysis
DMAA	Dimethylacetamide
DMSG	Dynamic moisture sorption gravimetry
DS	Degree of substitution
DSC	Differential scanning calorimetry
DTA	Differential temperature analysis
dTGA	Derivative of the TGA weight loss curve
DVS	Dynamic vapour sorption
Ea	Energy of activation
GAB	Guggenheim, Anderson, and DeBoer
GLM	General linear model
HM	Hydrophilic matrix
HPC	Hydroxypropylcellulose
HPMC	Hydroxypropylmethylcellulose
IPT	Incipient precipitation temperature
LFDS	Low frequency dielectric spectroscopy
MC	Methylcellulose

MCC	Microcrystalline cellulose
MS	Molar substitution
NaCl	Sodium chloride
NaCMC	Sodium carboxymethylcellulose
NMR	Nuclear magnetic resonance
p(HEMA)	poly(hydroxyethylmethacrylate)
P.H.	Propranolol hydrochloride
PEG	Polyethylene glycol
PRU	Polymer repeating unit
RH	Relative humidity
SD	Standard deviation
SDC	Self-diffusion coefficient
SEM	Scanning electron microscopy
SSA	Specific surface area
T _g	Glass transition temperature
TGA	Thermogravimetric analysis
TGP	Thermal gelation point
TMA	Thermomechanical analysis
TSDC	Thermally stimulated depolarisation current

CHAPTER 1

INTRODUCTION

Chapter 1 Introduction

1.1 Cellulose Ethers

1.1.1 Structure

A general structure of cellulose ethers is shown in figure 1.1, where the R-group can be a single entity or a combination of substituents. Properties such as solubility, surface activity, thermoplasticity, film characteristics, thermal gelation and biodegradation are dependent on the chemical nature, quantity and distribution of the substituent groups. These properties make cellulose ethers suitable for use in a wide spectrum of industries such as the adhesive, pharmaceutical, agriculture, ceramic, construction, cosmetic, food, paper, paint, leather, printing ink and resin (DOW Chemical Company, 1983).

In methylcellulose (MC) the hydrogen atoms of some of the hydroxyl groups of the cellulose backbone are substituted by methyl groups (Figure 1.1). In the case of hydroxypropylmethylcellulose (HPMC) the cellulose backbone is substituted by methoxyl and hydroxypropoxyl groups ($-\text{CH}_2\text{CH}(\text{OH})\text{CH}_3$).

1.1.2 Source

Cellulose is a predominantly crystalline material, consisting either of ordered crystalline regions or crystalline regions connected by disordered or amorphous regions. Chemically, cellulose consists of an anhydroglucose backbone with 1-4 glycosidic linkages (section 1.1.1). Cellulose molecules may consist of several thousand linked units running through crystalline and amorphous regions (Savage, 1965). Cellulose is abundant in nature and is available from a host of sources such as cotton seed fiber, wood fibers (hardwoods and softwoods), bast fibers (flax, hemp, jute and ramie), grasses, algae and bacteria. Cotton seed fiber and wood fiber are the principal sources used to manufacture cellulose ethers (Just and Majewicz, 1985), with economics favouring the use of wood pulp (Greminger, 1979).

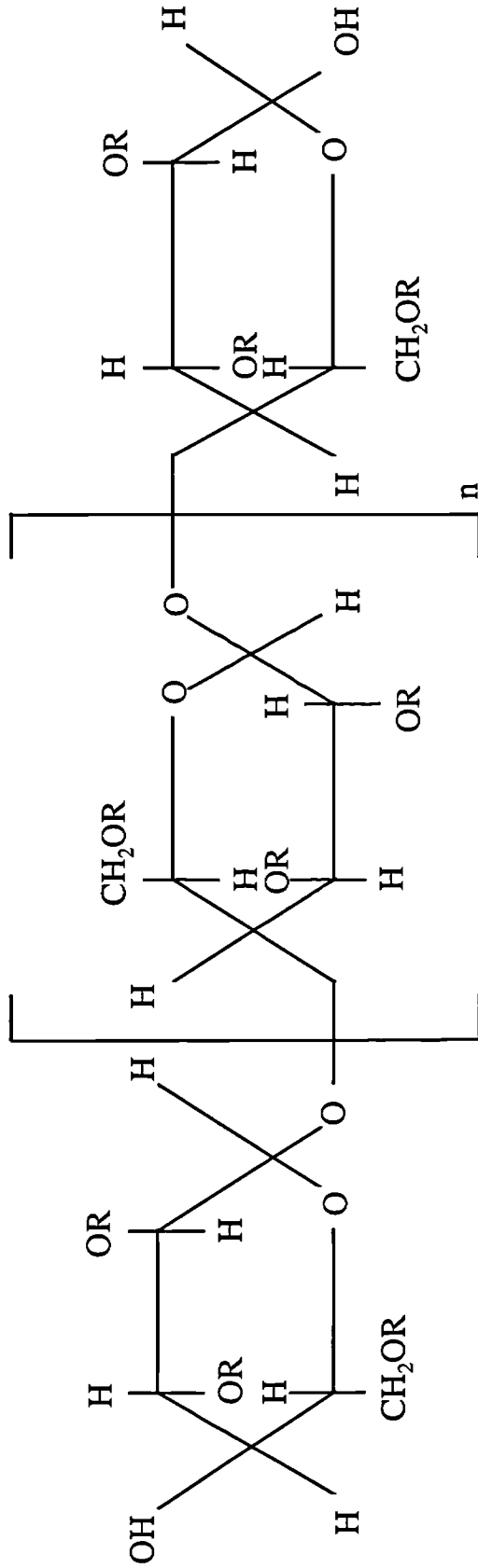


Figure 1.1 : Chemical structure of a typical cellulose ether showing substitution on the cellulose backbone (DOW Chemical Company, 1983)

Substituents R	Product
-H, -CH ₃	Methylcellulose (MC)
-H, -CH ₃ , -CH ₂ CH(OH)CH ₃	Hydroxypropylmethylcellulose (HPMC)
-H, -CH ₂ CH(OH)CH ₃	Hydroxypropylcellulose (HPC)
-H, -CH ₂ COONa	Sodium Carboxymethylcellulose (NaCMC)

At source, wood and cotton cellulose have similar high molecular weights with an estimated degree of polymerisation of 10,000 (Goring and Timell, 1962). The native cellulose is not easily converted to cellulose ethers due to impurities. Therefore, isolation and purification processes are required prior to etherification. These processes are severe and result in a lower molecular weight substrate, especially in the case of wood cellulose, compared to that derived from cotton cellulose. This drop in molecular weight is due to chain cleavage and, as a result, the degree of polymerisation ranges from 1,000 to 7,000 for purified cotton cellulose and from 500 to 2,000 for purified wood pulp cellulose (Just and Majewicz, 1985). The molecular weight differences between the two purified forms of cellulose provide a method to control solution viscosity, with low viscosity grades being made from wood cellulose and high viscosity grades coming from cotton cellulose. Intermediate grades may be made from either substrate or from a mixture of both. The isolation and purification processes are also responsible for differing crystallinity and molecular weight distributions which in turn can influence reactivity and the product properties (Just and Majewicz, 1985).

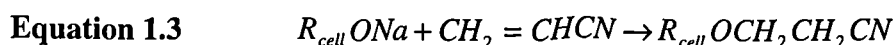
The alpha (α)-cellulose content of cotton and wood cellulose reflect the differences in their purity. Alpha-cellulose is the part of high molecular-weight cellulose that is insoluble in sodium hydroxide (NaOH) solution. The remainder consists of alkali-soluble hemicelluloses i.e. low molecular weight polysaccharides and lignin, which is a polymeric phenolic substance having structural adhesive properties. A low α -cellulose content indicates the presence of hemicellulose and lignin impurities, which may affect the yield of high purity cellulose. Wood cellulose has a low α -cellulose content (87-97%) compared to cotton cellulose (99%) and this is indicative of the lower purity of wood cellulose (Just and Majewicz, 1985).

1.1.3 Preparation

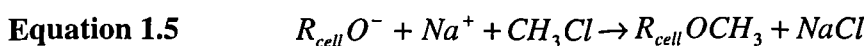
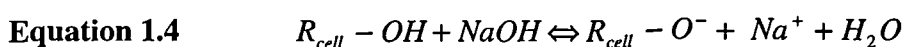
Cellulose ether preparation has evolved from the first reports in 1912 (Lilienfeld, 1913), and these developments have been described by a number of authors (Savage et al, 1954; Savage, 1954; Savage, 1965; Greminger, 1979; Just and Majewicz, 1985). The building blocks of cellulose are anhydroglucose units bound through

acetal (1-4 glycosidic) linkages. There are three hydroxyl groups on the anhydroglucose ring, a primary at C-6 and two secondary at the C-2 and C-3 positions. The crystalline nature of the cellulose structure has left it largely impenetrable to chemical reagents. Therefore, the hydroxyl groups in the crystalline regions can be gradually made accessible by swelling in sodium hydroxide solution (35-60%) (Ranby, 1963) in a process called mercerisation (Dahlgren, 1987). The initial stages in substitution reactions thus involve disrupting the crystalline regions, spreading apart the cellulose, and leaving the molecules accessible to chemical attacks by substitution reagents. Non-uniformity of NaOH distribution within the cellulose can dramatically affect product quality (Greminger, 1979).

There are two types of etherification reactions that are used, the Michael reaction and nucleophilic substitution (Touzinsky, 1965). The Michael reaction involves the reversible addition of an alkali-catalysed activated vinyl group to cellulose. An example of this reaction type is cyanoethylation (Nicholson and Merritt, 1985) e.g. cyanoethylcellulose (where $R_{cell}OH$ is the cellulose molecule) as given in equations 1.1 - 1.3:



However, the more common etherification reaction used is irreversible nucleophilic substitution (Ingold, 1969). For example, methylation of alkali cellulose with methyl halide produces methylcellulose as shown in equations 1.4 and 1.5:



where $R_{cell} - OH$ is the cellulose molecule, $R_{cell} - O^- + Na^+$ is the alkali cellulose, and $R_{cell} OCH_3$ is methylcellulose.

Hydroxypropylmethylcellulose (HPMC), a mixed cellulose ether, is prepared by the reaction of mixtures of methyl chloride and propylene oxide with alkali cellulose as shown, in equation 1.6:

Equation 1.6



where $R_{cell} - O^-$ is methylcellulose, CH_2CHOCH_3 is propylene oxide and $R_{cell} OCH_2CH(OH)CH_3$ is HPMC.

The relative amounts of methoxyl and hydroxypropoxyl substitutions are controlled by the weight ratio and concentration of NaOH and the weight ratios of methyl chloride and propylene oxide per unit weight of cellulose (Greminger and Krumel, 1980). These etherification or alkylation processes are either homogeneous or heterogeneous (Just and Majewicz, 1985). Heterogeneous processes are used industrially where the cellulose and the cellulose ether remain in a fibrous or particulate state throughout the reaction. They may be further divided into organic diluent-mediated or diluent-free processes. In homogeneous processes, solvent systems are used, and the cellulose and the cellulose ether remain in solution throughout the procedure. They are less economical and are seldom used. Recent advances in production methods of methylcellulose derivatives are reviewed by Grover (Grover, 1993).

These reactions have important commercial value to the manufacturers who produce thousands of tons of cellulose ethers annually. Commercially available cellulose ethers include: methylcellulose (MC), ethylcellulose (EC), hydroxyethylcellulose (HEC), hydroxypropylcellulose (HPC), carboxymethylcellulose (CMC), hydroxypropylmethylcellulose (HPMC) and hydroxyethylmethylcellulose (HEMC). These cellulose ethers are supplied by various manufacturers which have different trade names for the various viscosity grades and substitution levels. For example,

DOW Chemical Co., USA supply cellulose ethers as Methocel®, while Shin Etsu Chemical Products Ltd., Japan supply cellulose ethers as Metolose®.

1.1.4 Degree of substitution

Substitution involves the splitting of the cellulose chains by breaking the bonds between neighbouring hydroxyl groups (Lorand, 1938). Thus the bigger the hydrophobic group available to open up the cellulose chains and allow water in, the fewer of these groups are required (Morss and Ogg, 1966). The solubility may not simply be assumed to arise due to the hydrophilic nature of the groups introduced as the overall hydrophilic nature of the polymer does not change significantly on substitution. Introducing small degrees of substitution into a cellulose molecule which has its crystalline structure largely non-disrupted, results in surface modification only (Savage, 1965).

Each anhydroglucose ring of the cellulose contains three hydroxyl groups available for substitution. The relative availabilities of each of the hydroxyl groups are not identical (Spurlin, 1939; Sönnerskog, 1948; Rowland et al, 1971; Rowland and Wade, 1980). Rowland et al (1969) found that in cotton cellulose, for every hydroxyl group at C-2 that was accessible for reaction in 1M and 2M NaOH, only 0.75 hydroxyl group at C-6 and 0.30 hydroxyl group at C-3 were accessible. This decreased accessibility is related to a higher state of order of the hydroxyl groups due to strong H-bonding between reactive groups of the three available hydroxyl ring sites. Not all will take part in the etherification reactions and therefore, the degree of substitution (DS) is defined as the number of hydroxyl groups per monosaccharide unit that have been etherified (Klug, 1971; Greminger, 1979; Greminger and Krumel, 1980; Grover, 1993). The maximum value of DS is 3. In some cases, side-chain formation is possible due to the introduction of further reactive groups and hence the term molar substitution (MS) is used, which is the average number of moles of substituent added per sugar unit. The value of MS may exceed three and the average side-chain length may be obtained by dividing MS by DS. Methylcellulose products have DS ranges from 1.5 to 2.0 while for HPMC products the degree of substitution of methyl group ranges from 0.9 to 1.8 (Greminger and Krumel, 1980). The quantity

and type of substituent groups on the ring determine the properties of cellulose ether products.

Methocel A products contain approximately 30% methoxyl (D.S. 1.64 - 1.92) which gives maximum water solubility. A lower DS gives products with lower water solubility and a higher DS gives products which are soluble only in organic solvents.

Methocel products are available with varying substituents and degrees of substitution. Methylcellulose is the Methocel A brand products and hydroxypropylmethylcellulose is the Methocel E, F and K brand products (Table 1.1). The United States Pharmacopoeia (USP) describes Methocel products differently and Methocel A4M, E4M, F4M and K4M are known as methylcellulose, hydroxypropylmethylcellulose (HPMC) 2910, HPMC 2906 and HPMC 2208 respectively.

Properties such as surface activity, water solubility, cross-linking and stability in the presence of salts and other ionic entities depend mainly on the amount and chemical nature of the substituents, which will also influence the type and range of uses of a particular cellulose ether.

1.1.5 Viscosity grades

The intrinsic or limiting viscosity of a particular polymer is a measure of its chain length or molecular weight. This relationship between the molecular weight of a polymer and its intrinsic viscosity has been shown by the Mark-Houwink equation as equation 1.7:

Equation 1.7
$$[\eta] = KM^a$$

where $[\eta]$ is intrinsic viscosity, K and a are empirically derived constants for a given polymer, and M is the molecular weight of the polymer (Just and Majewicz, 1985). The molecular weight distributions of cellulose ethers are regulated by controlling the cleavage of the glycosidic linkages during the treatment of cellulosic substrate

itself or during etherification (Just and Majewicz, 1985). When etherified, water soluble cellulose ethers are graded based on the viscosity (centipoise, cP) of their 2% w/v aqueous solution at 20°C (Greminger and Savage, 1959). Different viscosity grades of cellulose ethers are available commercially, for example, the DOW Chemical Company produces Methocel products of different viscosity grades include: Methocel K100LV (80 - 120cP), K4M (3, 500 - 5, 600cP), K15M (12, 000 - 18, 000cP), and K100M (80, 000 - 120, 000cP) (DOW Chemical Company, 1983).

Dilute solutions of low viscosity cellulose ethers exhibit Newtonian flow. However, increasing the concentration to over 5% w/v will produce some thixotropy due to weak interactions between polymer chains. In addition, it has been reported that in dilute solutions, methylcellulose (MC) molecules are relatively compact coils and that an increase in polymer molecular weight was accompanied by an increase not only in molecular size but also in the intermolecular interaction in solution (Tomioka and Matsumura, 1987). As the molecular weight increases, pseudoplastic flow is exhibited and this is the classical behaviour of MC and HPMC solutions at 20°C. In summary, the solutions are generally nonthixotropic, exhibiting no hysteresis loop, but showing characteristic shear-thinning behaviour (Greminger and Savage, 1959; Savage, 1965; Morss and Ogg, 1966; Greminger, 1979; Greminger and Krumel, 1980; Just and Majewicz, 1985; Grover, 1993).

The relationship between viscosity and concentration is exponential and may be summarised by Philippoff's equation (Philippoff, 1936), equation 1.8:

Equation 1.8
$$\frac{\eta}{\eta_0} = \left(1 + \frac{[\eta]c}{8}\right)^8$$

where η is apparent viscosity

η_0 is solvent viscosity

$[\eta]$ is intrinsic viscosity, dL/g

c is concentration, g/dL

If measurements are made at 20°C in water where $\eta_0 = 1.0$ and $K = \frac{[\eta]}{8}$ the equation

simplifies into equation 1.9:

Equation 1.9 $\eta^{1/8} = 1 + Kc$

The viscosities of MC and HPMC aqueous solutions decrease with increasing temperature until the thermal gelation point (DOW Chemical Company, 1983) (section 1.1.7). The apparent viscosities of some cellulose ethers are further affected by temperature and the presence of additives (section 1.1.7).

1.1.6 Glass Transition temperature

Amorphous solids are supercooled liquids in which the molecules are arranged in a somewhat random manner as in the liquid state (Martin et al, 1983). They do not have definite melting points and tend to flow when subjected to sufficient pressure over a period of time. Many pharmaceutical solids possess a certain degree of amorphous character which is the case for polymers. This may be due to their large molecular size or to the processing conditions they undergo. When a liquid carbohydrate is cooled below its melting temperature, in the absence of crystallization, the viscosity of the liquid increases until at the glass transition, the amorphous material show characteristics typical of a solid (Parker and Ring, 1995). The temperature at which a glassy polymer becomes rubbery on heating and a rubbery polymer reverts to a glassy one on cooling is called the glass transition temperature (T_g) (Martin et al, 1983). The T_g of an amorphous solid determines its chemical and physical stability and its viscoelastic properties. The T_g becomes critical when it is approached or exceeded by the temperature encountered during experimental or product processing conditions (Hancock and Zografi, 1994).

A number of methods have been employed to measure the T_g in amorphous materials. These have included differential scanning calorimetry (DSC) (Entwistle and Rowe, 1979; Porter and Ridgeway, 1983; Okhamafe and York, 1985; Sakellariou et al, 1985; Hatakeyama et al, 1989; Oksanen and Zografi, 1990; Roos and Karel, 1991; Omelczuk and McGinity, 1993; Hancock and Zografi, 1994; Parker and Ring, 1995); the torsional braid pendulum (Rowe et al, 1984); thermomechanical

analysis (TMA) (Huang et al, 1996); dielectric spectroscopy (Huang et al, 1996; Noel et al, 1996); and dynamic mechanical analysis (DMA) (Kararli et al, 1990; Appelqvist et al, 1993; Davè et al, 1995).

Components that lower the T_g of a substance are said to have a plasticizing effect. On the other hand, when T_g is raised, there is an anti-plasticizing effect. Water is well known for its plasticizing properties and thus when an amorphous material such as HPMC absorbs water, it is possible that an increase in free volume followed by a lowering of the T_g may occur (Levine and Slade, 1988). Material properties are markedly different either side of the T_g and as a result a knowledge and understanding of the T_g has very important implications for storage stability and processing both in the pharmaceutical and food industries (Slade and Levine, 1993; Schenz, 1995). Hancock and Zografi (1994) have attempted to address the issue by establishing a predictive relationship between T_g and water content which would provide information on how much a given water content would reduce the T_g of a material. It would then be possible to predict any resultant physicochemical problems.

Glass transition temperature has special implications for cellulose ether polymers in terms of their hydration and their applications.

1.1.7 Properties of MC and HPMC solutions

1.1.7.1 Hydration and thermal gelation

Soluble cellulose ethers dissolve in water by a swelling mechanism followed by successive hydration of the structural layers. The concentration required of a particular cellulose ether is very much dependent on the desired viscosity and type of product ultimately being used. Some cellulose ethers are insoluble at higher temperatures while being soluble at lower temperatures. Solutions of these polymers undergo sol-gel transformation when heated (Figure 1.2) which is reversible within a narrow temperature range indicating that the cross-linked structure may be attributed to the action of secondary valence forces as opposed to any disruption of covalent bonds.

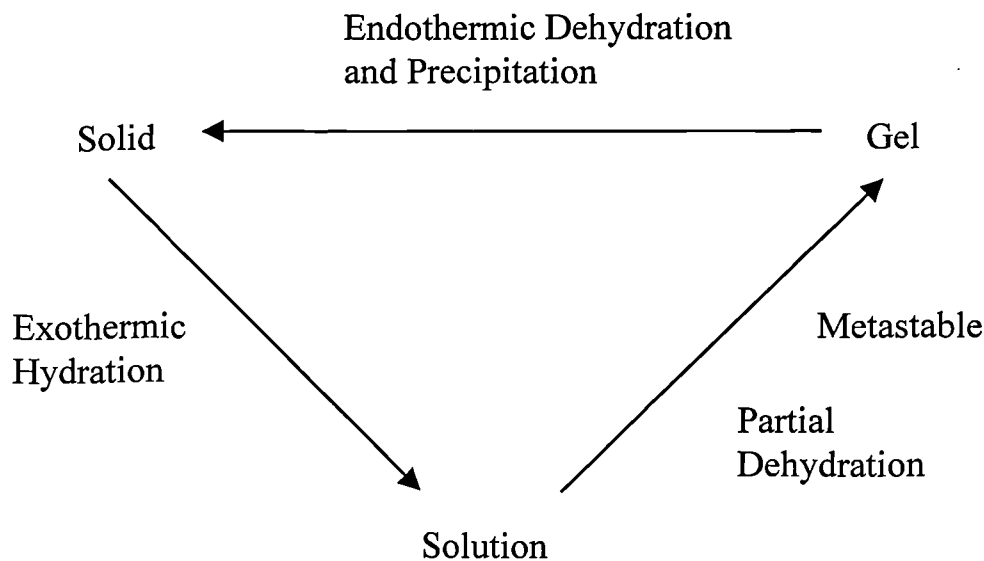


Figure 1.2 : Typical ‘sol-gel’ transformation of MC and HPMC aqueous solutions (taken from Sarkar and Walker, 1995)

The temperature at which sol-gel transformation occurs is commonly known as the thermal gelation point. The type and quantity of substituent groups on a cellulose ether polymer will govern the thermal gelation temperature. Prior to gel formation, polymer molecules undergo precipitation which may be observed via light transmission measurements (Klug, 1971; Sarkar, 1979). The temperatures at which light transmission reaches 97.5% and 50% have been defined as the incipient precipitation temperature (IPT) and cloud point temperature (CPT) respectively (Sarkar, 1979).

1.1.7.2 Mechanism of thermal gelation

The thermally reversible sol-gel transformation of MC was initially reported by Heymann (1935) and the theory that gel formation was primarily due to dehydration when the temperature was raised, was discussed.

A degree of controversy exists regarding the actual mechanism of thermal gelation of cellulose ethers. Kuhn et al (1961) suggested that the aggregation of MC molecules,

held together by dipole forces, leads to gelation. It has also been proposed that gel formation involves association of chain fragments resulting in a three-dimensional framework containing solvent in the interstices (Rees, 1969). These associated regions have been termed junction zones and have been described in terms of a micelle model (Rees, 1972). Methylcellulose gels have a structuring effect on surrounding water molecules which are disrupted upon heating. Phase separation occurs and the aggregates resemble detergent micelles which are liquid-like in the interior. As a result, cellulose ether gels show their characteristic property of setting upon heating and liquefying upon cooling. Replacement by substitution of some methoxyl groups with more hydrophilic groupings such as hydroxyl or hydroxypropyl, will not interfere greatly with the primary micellar structure, however the thermal gelation temperature and gel texture may be affected. Savage (1957) previously indicated that the tendency to gel is increased with an increase in proportion of di- and tri-O-methyl-D-glucose residues, suggesting that highly substituted regions of MC chains form the junction zones. The sparsely substituted regions thus confer solubility in water. Sarkar (1979) and Vigouret (1996) have attributed this theory of gel formation to interaction between hydrophobic methoxyl groups causing gel formation. From x-ray diffraction studies, Kato et al (1978) concluded that these junction zones in MC gels are in fact crystallites of trimethyl glucose sequences and are between 4 and 8 units long. It was further argued that the micellar model, which is assumed to be a liquid-liquid phase transition, cannot be conclusively accepted as there is insufficient evidence to assume that the onset of gelation is in fact a liquid-liquid transition as opposed to a crystal-liquid transition (Kato et al, 1978).

The marked change in the structure of methylcellulose\water systems, when they pass through the thermal gelation point, would lead us to believe that the mobility of water in the polymer may be affected. However, a nuclear magnetic resonance (NMR) study covering the sol-gel transition point of an aqueous methylcellulose solution employing the pulsed field gradient spin-echo technique on a standard Fourier transform NMR spectrometer, produced a series of self-diffusion measurements indicating that the diffusion rate of the water molecules is unaffected by passing through the sol-gel transition point (Roots et al, 1980).

Haque and Morris (1993) and Haque et al (1993) described the thermal gelation of MC as a two stage process. Their work involved oscillatory measurements of steady-shear viscosity as a method for determining liquid-like (viscous) and solid-like (elastic) response to imposed deformation. They characterised solid and liquid responses in terms of storage (G') and loss (G'') moduli respectively. When the temperature is increased two distinct waves of increase in storage modulus (G') occur. The first is due to the sheath of water molecules being removed from highly aggregated cellulosic bundles, causing the ends of the cellulosic bundles to come apart, resulting in a large increase in hydrodynamic volume. Heymann (1936) attributed this change in volume to a decrease in hydration of the colloid particles, since the water bound by secondary forces to the bundles has a smaller specific volume than the free water. The second wave increase in storage modulus occurs at higher temperatures when the methyl substituents shed structured water to form a cross-linked network via hydrophobic interaction. Similarly, Sarkar (1995), has reported gelation to be a two stage process using an oscillating rheometry technique. Sarkar and Walker (1995) have identified dehydration of cellulose ethers in aqueous solution using high sensitivity differential scanning microcalorimetry. They found that dehydration of MC was a single precipitation process, whereas dehydration of HPMC samples occurred with characteristic broad endotherms suggesting phase separation according to molecular weight distribution, with overlapping peaks. Further characterisation of the thermal gelation process in MC systems has been carried out using rheological studies (Boчек and Petropavlovsky, 1995), and by means of a polarised light scattering technique (Boчек et al, 1996). In both these cases, differences between the behaviour of MC solutions in water and dimethylacetamide (DMAA), approaching the thermal gelation point were highlighted. They found that in water, MC behaved like a semi-rigid chain polymer and showed a larger increase in viscosity approaching the thermal gelation point than MC in DMAA which showed the characteristics of a flexible chain polymer.

The non-ionic nature of MC and HPMC results in stability over a wide pH range of 2 - 12. However, gradual decrease in viscosity is apparent over a period of time at extremes of pH (Dow Chemical Company, 1983).

1.1.7.3 Viscosity-Temperature behaviour of methylcellulose

Heymann (1935) described that an aqueous solution of MC at 44.1°C showed a reversible decrease in viscosity with ageing. The decrease in viscosity was accompanied by an increase in intensity of the Tyndall light indicating that dehydration rather than depolymerisation (which would not be reversible) of the MC was occurring. Similar phenomena had been reported to occur with HPMC solutions (Lapidus and Lordi, 1968 and Sarkar, 1979).

The viscosity-temperature relationship for a MC solution is depicted in figure 1.3. As the temperature of the solution is increased, there is an initial viscosity decrease indicating the first and second stages of dehydration. Just before the thermal gelation point, there is a sharp increase in viscosity. Neely (1963) described this sharp increase in viscosity as being due to the increased molecular weight of the polymer as it associates via hydrophobic interaction. On cooling, the viscosity increases, reaches a maximum, then decreases until it merges with the original heating curve returning to the original viscosity (Sarkar, 1979). A hysteresis loop is apparent due to the breaking of the gel structure upon shear and also because the rehydration of the precipitants does not occur completely in a short time (Heymann, 1935; Haque and Morris, 1993; Haque et al, 1994).

1.1.7.4 Factors influencing thermal gelation

(i) Substituents and degree of substitution (DS)

Substituent type is critical to the ability of cellulose ethers to thermally gel as exemplified by HPC which does not undergo thermal gelation but instead, when heated, precipitates out of solution (Klug, 1971). The degree of substitution is equally as important in the thermal gelation properties of MC and HPMC (Table 1.1). Vacher (1940) attributed gelation to the presence of trisubstituted units in the molecule and observed that the gelation temperature was lower for polymers which

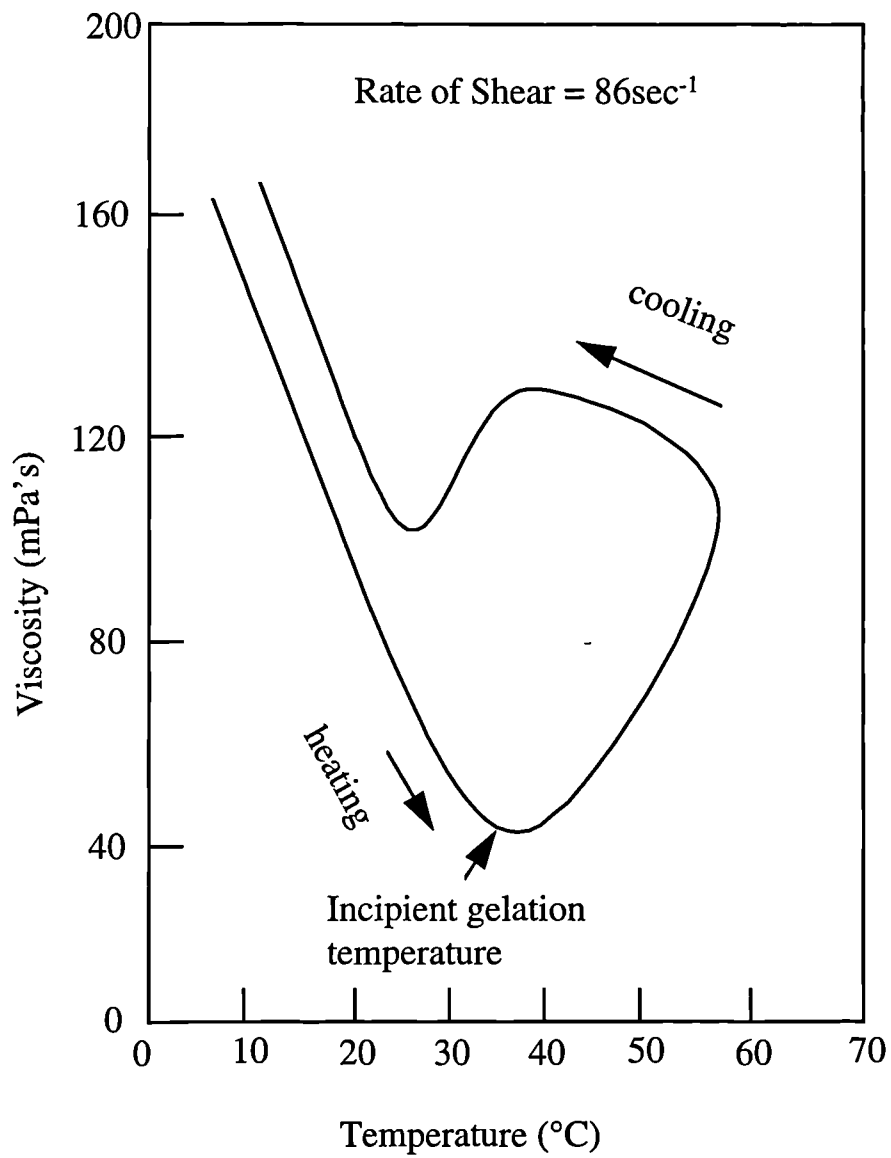


Figure 1.3 : Viscosity versus temperature for an aqueous solution of MC (2% w/v) heated at $0.25^{\circ}\text{Cmin}^{-1}$ (adapted from Grover, 1993)

Table 1.1 : Thermal gelation point (TGP) and gel texture of Methocel cellulose ethers with different substitution levels (DOW Chemical Company, 1983)

Product	Methoxyl (DS)	Methoxyl (%)	Hydroxypropoxyl (DS)	Hydroxypropoxyl (%)	Thermal gelation point (°C)	Gel texture
Methocel A	1.8	30	-	-	50 - 55	firm
Methocel E	1.9	29	0.23	8.5	58 - 64	semi-firm
Methocel F	1.8	28	0.13	5.0	62 - 68	semi-firm
Methocel K	1.4	22	0.21	8.1	70 - 90	mushy

were more highly substituted. This is due to increased hydrophobic interaction between methoxyl substituents (Sarkar, 1979). Gel texture is also influenced by degree of substitution (Table 1.1).

Thermal gelation temperatures of HPMC solutions are higher than those for MC solutions. Klug (1971) and Morss & Ogg (1966) attributed this to an increase in hydrophilicity of HPMC due to the addition of hydroxypropoxyl substituent groups. However, Sarkar (1979) indicated that because both methoxyl and hydroxypropoxyl substitutions render the cellulose hydrophobic, the higher gelation temperature of HPMC may be attributed to steric influence of the larger hydroxypropoxyl substituent. Haque et al, (1993) combined both lines of thinking and detailed that inhibition of thermal gelation until higher temperatures in HPMC gels, was partly due to the increase in hydrophilic character caused by the introduction of the hydroxypropoxyl group and partly due to steric reasons.

(ii) Additives

Heymann (1935) and Levy & Schwarz (1958) have reported that some additives depress the gelation point of MC. Heymann (Heymann, 1935; Heymann et al, 1938) suggested that most electrolytes depress the thermal gelation point (TGP) by dehydration of the polymer. Generally, as the concentration of ions in a polymer solution increases, there is a resultant decrease in polymer solubility. This is because water is required to maintain the ions in solution and less water is available to hydrate the polymer (Johnson et al, 1993). The ability of an electrolyte to 'salt out' a polymer from its solution generally follows its position in the lyotropic series. Some salts can carry water and adsorb to the polymer causing an increase in hydration and solubility and therefore increasing the TGP. For example, I^- and CNS^- (10^{-1} M) in a MC -water (MC was Tylose MH; methylcellulose which has undergone a minor ethoxylation process) system increased the TGP from 74°C to 77°C (Touitou and Donbrow, 1982). An adsorption theory was proposed by Katz and Muschter (1933) in which weakly hydrated ions e.g. CNS^- and I^- , increase the hydration because they are strongly adsorbed onto the polymer molecules. Ions such as SO_4^{2-} ,

although strongly hydrated, do not cause an increase in polymer hydration because their adsorption is weak.

A number of studies have described ionic effects on the hydration of cellulose ether polymers. Fagan et al (1989) and Johnson et al (1993) examined the effect of ionic strength on the hydration of hydroxyalkylcelluloses including hydroxypropylcellulose (HPC). Mitchell et al (1990a; 1993c) examined the influence of electrolytes on HPMC gels and the influence of drugs on the properties and swelling characteristics of MC and HPMC gels. They found that both propranolol hydrochloride and tetracycline hydrochloride caused an increase in cloud-point in HPMC K15M gels. This was thought to be due to 'salting in' of the polymer by the drugs. Rajabi-Siahboomi et al (1994) have shown that diclofenac sodium depresses the cloud-point of HPMC E4M, K4M and F4M, a so called 'salting out' effect. Further investigations using component parts of the drug molecule have identified the effect as being attributable to the 2,6-dichloroaniline structure within diclofenac.

(iii) Molecular weight

It has been reported that the molecular weight of cellulose ether polymers has very little effect on their thermal gelation point and cloud point (Sarkar, 1979). This was related to samples possessing a very wide molecular weight distribution (Kato et al, 1982; Rowe, 1980; 1982a; 1982b), which is just as important as the average molecular weight. All samples contain some high molecular weight fractions, which separate out first in the gelation process, thus different samples exhibit similar TGP's. Some properties of cellulose ethers, including tensile strength, are dependent on the smaller molecules, while other properties such as solution viscosity are dependent on intermediate to large size molecules. Yet other properties, such as melt elasticity are dependent on the amounts of large chain molecules that are present (Van Krevelen, 1972).

Sarkar (1979) has shown that at low concentrations (0.25% w/v), low molecular weight MC exhibited a lower cloud point temperature (CPT) than higher molecular weight MC samples. This was attributed to the presence of polymer aggregates in solution. Low molecular weight MC can aggregate more via parallel alignment than

the high molecular weight samples (Kuhn et al, 1961). Sarkar (1979) reported that gel strength increases with molecular weight up until an average molecular weight of 140,000 (Methocel A4C), at which point the effect levels off. HPMC solutions undergo gelation at higher temperatures than MC (Table 1.1).

(iv) Polymer concentration

Increase in concentration of Methocel cellulose ethers results in a lowering of the thermal gelation temperature for Methocel F50 up until a critical concentration of between 2 - 3% (w/v) is reached. Thereafter, the effect of concentration becomes negligible (Sarkar, 1979).

CPT decreases initially as the concentration of the polymer is increased up to a certain point, thereafter, the effect of concentration is negligible. In low concentrations of HPMC (< 6.5% w/v), the solutions become turbid upon heating before gelation occurs. However above this concentration, a gel is produced before turbidity is apparent (Sarkar, 1979).

1.1.7.5 Surface activity

In solution, HPMC and MC exhibit surfactant or surface active properties. They exhibit moderate surface tension and interfacial tension values which results in their effectiveness as stabilizers and protective colloids. The surface activity increases with an increase in solution temperature up until polymer dehydration begins to occur resulting in a decrease in surface activity (Dow Chemical Company, 1983; Grover, 1993).

1.1.8 Applications

Methylcellulose derivatives are used in a wide spectrum of applications in industries such as the paper, cosmetic, construction, ceramic, agricultural, adhesive, paint, leather, foods and the pharmaceutical industry (Dow Chemical Company, 1983). A number of these applications will be described in more detail outlining the specific properties of the cellulose ether derivatives.

1.1.8.1 Non-pharmaceutical applications

Methylcellulose derivatives are used as protective films, spray adherents, fungicide stickers and dispersing agents. Methylcellulose (15cP) may be used as a protective coating preventing dehydration of bulbs and roots during transplantation (Greminger and Savage, 1959).

They are used in hypoallergenic preparations to provide viscosity control and stabilisation as well as feel, clarity, and surfactant compatibility in face/hand creams, shampoos and deodorants (Greminger and Krumel, 1980).

Methylcellulose derivatives including HPMC but not other hydroxyalkyl-methylcellulose derivatives are used in food products such as in bakery products, fried foods, milkshake drinks and fruit pie fillings (Grover, 1993) in order to obtain greater customer palatability. Properties utilised include binding, thickening, stabilising, emulsifying, suspending and thermal gelation (in fried products). The greater awareness of healthy eating has led to the use of MC and HPMC in low calorie foods, diabetic foods, nonallergenic foods and foods suitable for use in a salt free diet (Glicksman, 1969). The non-ionic, non-toxic, nonallergenic properties allied to the fact that cellulose ethers have no calorific value, make them excellent for use in this regard. They are also used in frozen foods where the properties of stability at low temperatures and lack of syneresis at sub-zero temperatures are utilised.

The combination of the water and organic solubility of HPMCs is exploited in their use as a thickener in paint removers (Greminger and Krumel, 1980). Methylcellulose is employed in water based paints of both the emulsion and dry types as a protective colloid, viscosity stabilizer and pigment dispersant (Dow Chemical Company, 1983).

Cellulose ether products are used in 'dryset' ceramic adhesive and grouting systems, cement based paints, stuccos and formulations for sound insulating systems. They are employed for their workability and water-retention aids (Greminger and Krumel, 1980).

The inherent adhesive properties of cellulose ethers are utilised in plywood

adhesives, latex adhesives and pastes. The thermal gelation point provides setting instead of thinning upon heating.

1.1.8.2 Pharmaceutical applications

Methylcellulose and its derivatives are used extensively in the pharmaceutical industry for a variety of purposes.

(i) Tablet film coatings

Methylcellulose derivatives exhibit excellent film-forming characteristics and are widely used for coating solid dosage forms (Banker et al, 1981; Porter, 1989, Haluska et al, 1992). The fact that methylcelluloses are water soluble and have some degree of organic solubility results in their use as aqueous-based film coatings, as solvent based film coatings and for coating from solvent-water mixtures. Lower molecular weight grades with low viscosities tend to be employed for coating tablets and granules. Film properties have been shown to be affected by the molecular weight of the polymer with higher molecular weight polymers producing harder, less elastic films (Rowe, 1976; Entwistle and Rowe, 1979).

(ii) Ophthalmological applications

Methylcellulose and carboxymethylcellulose (CMC) are used as stabilizers and thickeners for ophthalmic solutions and ointments. These include over-the-counter eye drops and contact lens solutions (Udupa et al, 1976). The methylcelluloses reduce surface tension and improve wetting and spreading of the solution over the surface of the eye.

(iii) Tablet binding

The strong binding properties exhibited by cellulose ethers enable their utilization in granule preparation in moist and dry granulation formulations, to produce an increase in tablet hardness upon compression (Doelker, 1987).

(iv) Suspending agents

Cellulose ether derivatives may be used as suspending agents due to their viscosity enhancing properties (Davies and Rowson, 1957; 1958). Choice of the optimum concentration and viscosity grade is vital, as too high a polymer concentration can cause gelling and failure of the sedimented particles to redisperse.

(v) Emulsifying agents

Cellulose ethers act to stabilize an emulsion by forming a multimolecular film round the dispersed globules at the oil/water interface. They can also increase the viscosity of the continuous phase of an o/w emulsion. Davies and Rowson (1960) found that low viscosity cellulose ether grades were better emulsifying agents than high viscosity grades.

(vi) Miscellaneous pharmaceutical uses

Other pharmaceutical applications of cellulose ethers include use as a bulk laxative and as an alternative to gelatin in the manufacture of hard-shell medicinal capsules (Sarkar, 1979). Methylcellulose may also have contraceptive uses (Loewit, 1977) due to its ability to permanently immobilize human sperm *in-vitro*. HPMC is used in hydrophilic matrix (HM) controlled release systems which will be outlined next.

1.2 Cellulose ethers and sustained release formulations

1.2.1 Sustained release formulation

In the treatment of disease, it is necessary for the drug to quickly reach its therapeutic concentration at the site of action in the body and maintain this concentration for the specified treatment time. Most traditional oral dosage forms require frequent and repeated doses to achieve these criteria. This, however, is far from ideal for reasons such as:

- (a) fluctuation of plasma drug concentration over successive dosing time intervals may lead to overdosing or underdosing of the patient.
- (b) drugs with short biological half-lives require frequent doses to maintain therapeutic concentrations.
- (c) lack of compliance due to a forgotten dose or the overnight no dose period (Proudfoot, 1988).

Due to these problems, 'sustained release' approaches have become popular and applications for incorporating drugs into solid polymers have been developed. By employing polymers as carriers, drugs may be continuously released over long periods of time improving patient compliance and decreasing patient to patient variations in drug administration patterns. Other potential advantages include:

- (a) reduction in possible side-effects related to high peak plasma drug levels.
- (b) reduction in the total amount of drug administered, reducing the side-effects.
- (c) improved patient compliance due to fewer doses.
- (d) decrease in localised gastrointestinal side-effects due to dumping of high concentrations of irritant drugs from traditional oral dosage forms.

Controlled release polymeric systems may be suitably classified based on the mechanism by which drug is released. Zero order release is when drug release is independent of time and it is the ideal drug release profile. Types of controlled release polymeric systems include diffusion controlled devices, chemically

controlled devices, solvent-activated systems and magnetically controlled devices (Peppas, 1984). In this section, solvent activated systems incorporating cellulose ether polymers are considered.

1.2.2 Hydrophilic matrix (HM) controlled release systems

A hydrophilic matrix (HM) consists of a mixture of ingredients including a hydrophilic, water-soluble, viscous polymer and the active ingredient, compressed into the tablet form (or as a hard-shell capsule). When the device comes into contact with an aqueous medium, the polymer hydrates and a gel-layer forms at the tablet surface which provides a method of controlling drug release (Figure 1.4). Within the gel layer the tablet core remains intact, with a store of drug and polymer (Alderman, 1984; Melia, 1991). Many hydrophilic polymers have been used as the rate-controlling polymer in HM devices (Buri and Doelker, 1980). The first report on the use of HPMC in HMs was in 1962 (Christensen and Dale, 1962). Since then its role has been extensively characterised and a number of reviews have been published (Alderman, 1984; Doelker, 1987; Hogan, 1989). It is important to distinguish between hydrogels and hydrophilic matrices. Swellable polymers that are water-insoluble are known as hydrogels, whereas, swellable polymers which are water soluble are called hydrophilic matrices (Ranga Rao and Padmalatha Devi, 1988).

It is possible to include more than one hydrophilic polymer within a HM system to obtain the required drug release profile. Zero-order release profiles have been reported using combinations of pectin and HPMC (Kim and Fassihi, 1997), and NaCMC and HPMC (Vázquez et al, 1995) in HM systems. Some authors have used innovative HM systems to achieve the required drug release profile with the Geomatrix[®] multi-layer matrix system (Conte et al, 1993; Conte and Maggi, 1996) and the development of a polymeric matrix system providing bimodal drug release (Munday, 1996). Both of these systems have incorporated HPMC as the rate controlling polymer.

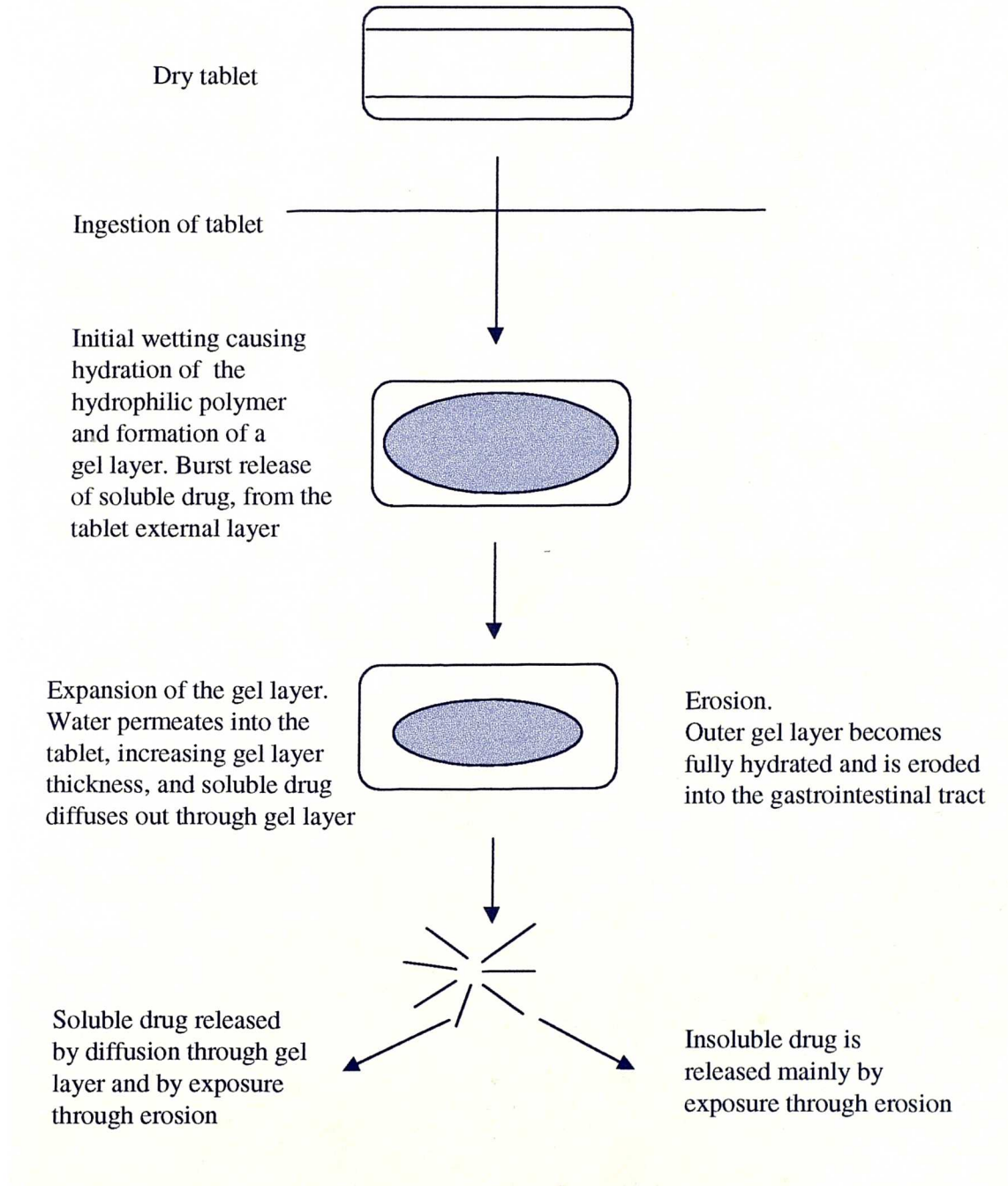


Figure 1.4 : Drug release from a matrix tablet containing a hydrophilic polymer

1.2.3 Mechanism of drug release from HM systems

The mechanism of drug release from HM systems has been the subject of many articles and reviews. Huber et al (1966) proposed the existence of a diffusion mechanism in combination with attrition of a dynamic gel barrier around the external areas of the tablet. Based on the Higuchi model (Higuchi, 1963) for the diffusion of drugs from non-porous solid matrices, the fundamental mathematical principles describing drug release from HM matrices were proposed by Lapidus and Lordi (1966, 1968) (equation 1.10):

Equation 1.10 $Q = [Dt(2A - C_s)C_s]^{0.5}$

where Q is the amount of drug released per unit area after time t, D is the diffusivity of the drug in the matrix, A is the amount of drug in the matrix per unit volume and C_s is the solubility of the drug in the hydrated polymer.

The mechanisms of drug release from both swellable and erodible hydrophilic matrices have been widely examined (Bamba et al, 1979; Lee, 1985; Peppas, 1985; Ritger and Peppas, 1987a, 1987b; Ranga-Rao and Padmalatha Devi, 1988; Peppas and Sahlin, 1989; Ranga-Rao et al, 1990; Skoug et al, 1993; Pham and Lee, 1994; Tahara et al, 1995; Tahara et al, 1996; Talukdar and Kinget, 1997). When a matrix contacts a liquid medium, the polymer relaxes and on hydration, the penetration and the dissolution fronts form around the matrix. Essentially, the polymer is in its glassy (or dry) form initially and when water enters the matrix dosage form, the glass transition temperature of the polymer is lowered to that of the experimental temperature. Polymer relaxation occurs with water interacting with the polymer forming a barrier gel layer (Ranga Rao and Padmalatha Devi, 1988). The penetration (or diffusing front) is the interface between solid drug, dry polymer and the gel. The dissolution (or eroding) front is the interface between the gel and the liquid medium. In swellable soluble matrices, a glassy - rubbery transition boundary has also been considered (Colombo et al, 1987). Hydration and swelling of polymer particles occur at the penetration front whereas matrix dissolution occurs at the dissolution front. Gel

layer thickness is equivalent to the distance between penetration and dissolution fronts (Lee and Peppas, 1987; Skoug et al, 1993; Pham and Lee, 1994; Gao et al, 1995a, 1995b). Thus, drug release from swellable and erodible HM matrices is due to either polymer dissolution (erosion) or drug diffusion through the gel layer (diffusion) or a combination of both. Alderman (1984) suggested that soluble drugs are released mainly by diffusion whereas drugs of poorer solubility are released mainly by erosion. The release mechanisms for many drugs have been determined by fitting data to the Higuchi model (equation 1.10).

This approach, however, is not suitable for eroding HM systems in that the effect of matrix erosion on drug release is not accounted for. Other models have been subsequently developed describing diffusional drug release from non-swellable polymeric devices to include that proposed by Peppas (1985) (equation 1.11):

Equation 1.11
$$M_t/M_\infty = K t^n$$

where K is a constant incorporating characteristics of the drug, and n is the diffusional exponent indicating the transport mechanism which is affected by the geometry of the system employed (Ritger and Peppas, 1987a). When n = 0.5, Fickian diffusion predominates, while non-Fickian diffusion is defined by n greater or less than 0.5. Zero-order release is indicated when n = 1.

Peppas and Sahlin (1989) have addressed the issue of drug release from swellable matrices incorporating a term for relaxational or erosion release which is known as Case II transport (equation 1.12):

Equation 1.12
$$M_t/M_\infty = K_1 t^n + K_2 t^{2n}$$

where $K_1 t^n$ is the Fickian diffusion contribution to drug release and $K_2 t^{2n}$ is the Case II relaxation contribution.

Sung et al (1996) assessed the contribution of matrix erosion by measuring the

amount of polymer released into the dissolution medium. They concluded that for the soluble drug studied (adinazolam mesylate), diffusion of the drug was the predominant drug release mechanism using this technique. Tahara et al (1996) have studied the effect of drug solubility, using seven model drugs, on release rate from HPMC matrices. For poorly soluble drugs it was apparent that the limiting factor for dissolution is erosion of the matrix tablet.

1.2.4 Factors affecting drug release from HPMC matrix systems

1.2.4.1 Active ingredient

The active ingredient, i.e. drug, has been shown to influence its release from HPMC matrix systems. Ford et al (1985a, 1985b, 1985c) studied the release of both water-soluble (promethazine hydrochloride, aminophylline and propranolol hydrochloride) and poorly soluble (indomethacin) drugs from HPMC matrix systems. For indomethacin, both the viscosity grade of HPMC and the particle size of the drug were reported to contribute more to controlling the drug release than was the case for water soluble drugs. This was primarily due to the erosion mechanism of drug release which predominates in the case of poorly soluble drugs. High concentrations of insoluble drugs and excipients, may cause non-uniform swelling of the HM system and ultimately failure of the system by decreasing the area available for wetting. However, careful tailoring of the concentrations of insoluble drug and polymer in a system can be used to slow the dissolution rate of the insoluble drug (Ford et al, 1987).

The presence of a drug in a matrix tablet has been found to influence the way water is bound to, or taken up by the cellulose ether (Mitchell et al, 1989). Differential Thermal Analysis (DTA) data on HPMC gels containing propranolol hydrochloride showed that propranolol affects the hydration of HPMC in gels of low water content, typical of conditions occurring during water penetration into HPMC matrices. The effect of various drugs on polymer cloud-point temperature has been reported and the effects of various drugs on modulating such properties lead to the assumption that the properties of drugs play an important role in their release rate from matrix systems.

(Mitchell et al, 1990a). Propranolol hydrochloride (water-soluble drug) has been reported to increase the thermal gelation point of HPMC solutions, thus increasing apparent solubility of the HPMC, the so called 'salting-in' effect (Mitchell, 1992). Propranolol will therefore help maintain gel structure and provide sustained release of drug in a HM system. This effect was attributed to an increase in concentration of propranolol hydrochloride in HPMC matrices causing a slowing in the release rate of the drug (Mitchell et al, 1993b).

The effect of diclofenac sodium (sparingly soluble drug) on polymer hydration within hydrophilic polymer matrices has been studied using cryogenic scanning electron microscopy (SEM) and has revealed that internal gel structure is modified by drug addition (Binns et al, 1990; Melia et al, 1990). The mechanism of diclofenac sodium release from hydrophilic matrix systems has been widely characterised (Vyas et al, 1989; Lee and Kim, 1991; Sheu et al, 1992; Liu et al, 1993; Liu et al, 1995).

1.2.4.2 Polymer factors

1.2.4.2.1 Polymer viscosity grade

Polymer viscosity depends primarily on the molecular weight of the polymer (section 1.1.4.2). Salomon et al (1979) indicated that HPMC viscosity grade only affected the lag time for potassium chloride diffusion to become quasi-stationary but did not affect the rate of release. Nakano et al (1983) have reported that the rate of theophylline release from hydroxypropylcellulose (HPC) matrices decreased with increase in polymer viscosity grade. Daly et al (1984) similarly reported a decrease in drug release rate with increase in polymer viscosity. Ford et al (1985a; 1985b) found that for aminophylline, promethazine (high water solubility) and propranolol (moderate solubility), while drug release was affected by polymer concentration, there was no dependence on HPMC viscosity grade above 4,000cP. In contrast, for poorly soluble drugs such as indomethacin, viscosity grade appeared to play a major role in drug release rates indicating that indomethacin is released predominantly by gel erosion (Ford et al, 1985c). Vasquez et al (1991) have shown that drug release is only initially influenced by HPMC viscosity grade when using HPMCs with

viscosity grades of 4, 000cP and above, especially when the polymer content is low. Liu et al (1995) have reported that the release rate of diclofenac sodium is mainly controlled by HPMC viscosity grade, however the maximum polymer viscosity studied was 4, 000cP. Further studies have shown that drug release rates decreased to a limiting value with increasing HPMC molecular weight (Hogan, 1989, Gao et al, 1996). Ju et al (1995a, 1995b) described a new mathematical model based on the polymer disentanglement concentration and the diffusion layer. The polymer disentanglement concentration is defined as the polymer concentration at the gelled tablet-diffusion layer interface and the diffusion layer is the transitional phase from a gelled matrix to the bulk solution. Predictions from their model of the effect of molecular weight on drug release from HPMC containing matrices agree well with the experimental data in the literature.

The effect of HPMC viscosity grade on water uptake has previously been characterised. Wan et al (1991) reported that with increase in polymer molecular weight, liquid uptake rates decreased. This was explained as being due to an increase in viscous drag which is dependent on molecular weight. Higher molecular weight HPMCs tend to swell faster causing the pores within the gel to be blocked up very quickly, thus preventing further liquid entry (Wan et al, 1991).

1.2.4.2.2 Polymer substitution type

Different polymer properties have been reported to be responsible for the rate of polymer hydration including substitution type. It was initially proposed (Alderman, 1984) that cellulose ethers of different substitution levels hydrate at different rates and this factor may be used to optimise the formulation of sustained release matrices. However, Mitchell et al (1993a), using a combination of differential scanning calorimetry (DSC) and dissolution studies, have shown that the differences in release rates for HPMCs with different substitution levels are not due to differences in hydration rate. Further studies using thermomechanical analysis (Mitchell et al, 1993a) have shown that gel layer thickness (which will affect the diffusional path length) is similar in HPMCs of different substitution type. Using NMR imaging, Rajabi-Siahboomi et al (1994) have shown that gel layer development in HPMC tablets occurred to the same extent in both axial and radial directions and was similar

in all HPMC types. They have shown that the predominantly axial swelling reported for all HPMC types resulted almost equally from growth of the hydrating gel layer and expansion of the ungelled tablet core. They also reported that the smaller axial expansion in HPMC E4M tablets was due to a smaller expansion of the core.

Differences between the three HPMC substitution types (Methocels K, E and F) have been found when low polymer contents of coarse sieve fractions were examined (Mitchell et al, 1993d). Bonferoni et al (1996) reported differences in drug release profiles between E4M and the other two substitution types (Methocel K4M and F4M) at low polymer concentrations which cannot be explained by differences in their hydrophilic character. Rajabi-Siahboomi et al (1996) used NMR imaging to show that water mobility within the gel layer of different HPMCs varies with degree of substitution of the polymer. The lowest value for water mobility was obtained for HPMC K4M. The distribution and mobility of water within the gel layer would be expected to influence polymer hydration and ultimately drug dissolution and release.

1.2.4.2.3 Particle size and concentration effects

Polymer particle size has an important part in polymer hydration through surface area contact with water. Therefore fine particles have been used to ensure more rapid hydration and gel formation for slow hydrating HPMC polymers such as HPMC E4M. However, particle size and its effects are modulated by matrix composition and polymer concentration (Alderman, 1984). Mitchell et al (1993d) found that at high polymer concentrations, coarse and fine sieve fractions show similar drug release behaviour and even at low concentrations, no differences were visible between different sieve fractions of fine particles (< 210 μ m). Particle size is known to influence compressional behaviour and packing of the powder (Malamataris et al, 1994a, 1994b).

Cellulose ether concentration in HM systems is a major factor in controlling drug release rate. In the majority of cases, an increase in HPMC polymer concentration (HPMC : drug ratio) results in a decrease in drug release rate (Lapidus and Lordi, 1966, 1968; Ford et al, 1985a).

1.3 Interactions between water and cellulose ethers

Many polymers exist in thermodynamically stable forms, however they may also contain metastable regions of amorphous material due to processing conditions. Such polymers can retain large quantities of water in their amorphous portions when exposed to water vapour at various relative humidities (Zografi, 1988). This absorbed water can dramatically influence the physicochemical properties of the polymer and ultimately the resultant pharmaceutical product. Thus, it is important to understand the mechanisms involved in the water-polymer interaction. Such an interaction has a key role to play in the use of cellulose ethers in sustained release formulations as well as in the effect of moisture on the stability of solid state pharmaceuticals (Carstensen, 1977; Carstensen and Li Wan Po, 1992). The rate at which water diffuses into HM devices, reacts with the hydrophilic polymer and forms the gel layer (Bamba et al, 1979) is a major factor in determining the drug release rate from such devices. Detailed study on the gel layer and more specifically on the types of water which exist clearly is fundamental in the optimisation of cellulose ether use in sustained release formulations.

Studies in the literature have identified physicochemical properties of water which are different between those in pure water and those in water associated with a solid. These studies have concluded, generally, that a certain portion of water molecules is tightly bound to the solid while the remainder of the water may be considered as having properties approaching that of pure water (Oksanen and Zografi, 1990). It is thought that a better understanding of the types of water existing within cellulose ether polymers will enable more accurate prediction of the behaviour of such materials when employed in pharmaceutical systems.

1.3.1 Mechanism of the water-polymer interaction

Two possible types of hydration have been proposed by Heymann (1935). These are adsorption-hydration and immobilisation, the former being most prominent in the MC - water system. The mechanism of the interaction between water and MC is assumed to be based on hydrogen bonding of the adsorbed water to the oxygen atoms

in the polymer (Klug, 1971). The hydroxyl groups on the polymer would be expected to have a greater affinity for water than the oxygen atoms but in practice a lot of these sites for fixing water are not available due to intramolecular hydrogen-bonding. The latter, and possibly less important mechanism, immobilization, may occur when the polymer is very long or has a complicated structure. In this case although no actual forces may exist between the solvent and the polymer, the molecules of the solvent may still be influenced by the polymer. Water molecules exhibit a high polarizability and a large permanent dipole moment and thus they tend to interact with polar sites at the surface of macromolecules (Ling, 1972). When the polymer surface carries one type of electric charge, the interaction layer is usually only one molecule in depth. When alternating negative and positive charges are present, the depth of this interaction layer increases. The order of the interaction between water and carbohydrates increases with molecular weight, so that neutral polysaccharides tend to bind large quantities of water (Biswas et al, 1975). The presence of ionized groups will undoubtedly affect the hydration of polysaccharides. Kumsah et al (1976) found that large amounts of water are found associated with sodium carboxymethylcellulose (NaCMC) samples indicating a possible multilayer formation of water molecules around the solute.

Water has been proposed to bind to celluloses by a three stage process (Khan and Pilpel, 1987) (Figure 1.5). Initially, water binds tightly to anhydroglucose units and also to linking units, resulting in two hydrogen bonds per water molecule. Some of these initial bonds between water and cellulose break and extra water molecules now bind at vacant anhydroglucose sites resulting in one hydrogen bond per water molecule, but more water molecules are involved. Finally, a more loosely bound region of sorbed water is formed as hydrogen bonds form between water molecules.

Yasuda et al (1972), in a study on poly-glycerol monomethacrylate (poly-GMA) hydrogels, found that the water transport properties through the gel are dependent on the degree of hydration of the polymer. At a low hydration state, movement is by activated diffusion indicating the existence of water in a molecularly dispersed form. In contrast, in highly hydrated states, viscous flow under pressure may be observed indicating the presence of bulk water. Thus movement of water that is strongly associated with the hydrophilic group of a polymer, will be different from that of

pure water. Such a water molecule is attached directly via H-bonding to a polymer hydroxyl group and does not exhibit any phase transition e.g. melting or crystallization and is therefore known as non-freezing water (Hatakeyama et al, 1987). For insoluble hydrophilic polymers, the amount of non-freezing water is generally about one molecule to each hydroxyl group in the monomer unit. This is dependent on the molecular conformation. For water-soluble hydrophilic polymers the amount of non-freezing water increases by ionic hydration. This non-freezing water is also known as bound water. Nakamura et al (1983b) have defined free water as unbound water in polymers whose transition temperature enthalpy and shape of peak in differential scanning calorimetry (DSC) curves are equal to those of pure (bulk) water.

The majority of workers have classified three different types of water in hydrophilic polymer gels with three types of water being reported experimentally in hyaluronic acid and its esters (Joshi and Topp, 1992); poly(vinyl alcohol) (Hatakeyama et al, 1984); agarose gel (Aizawa et al, 1972); poly(2-hydroxyethyl Methacrylate) (Lee et al, 1975; Sung et al, 1981); cellulose (Nakamura et al, 1981) and in various other systems by Hatakeyama et al, (1979; 1988), Sung (1986), Kim et al (1983), Zhang, (1989) and Joshi and Wilson (1992).

As well as the free water and bound water already mentioned, Taniguchi and Horigome (1975) reported the existence of another type of water, known as freezing bound water. It is characterised as having a phase transition temperature lower than that of bulk water due to a weak interaction of the water with the polymer chain.

In a study of the states of water in cellulose acetate membranes, Taniguchi and Horigome (1975), suggested that four types of water actually exist. These were:

- (a) completely free water
- (b) free water very weakly interacting with polymer
- (c) bound water which can contain salts, and
- (d) bound water which rejects salts.

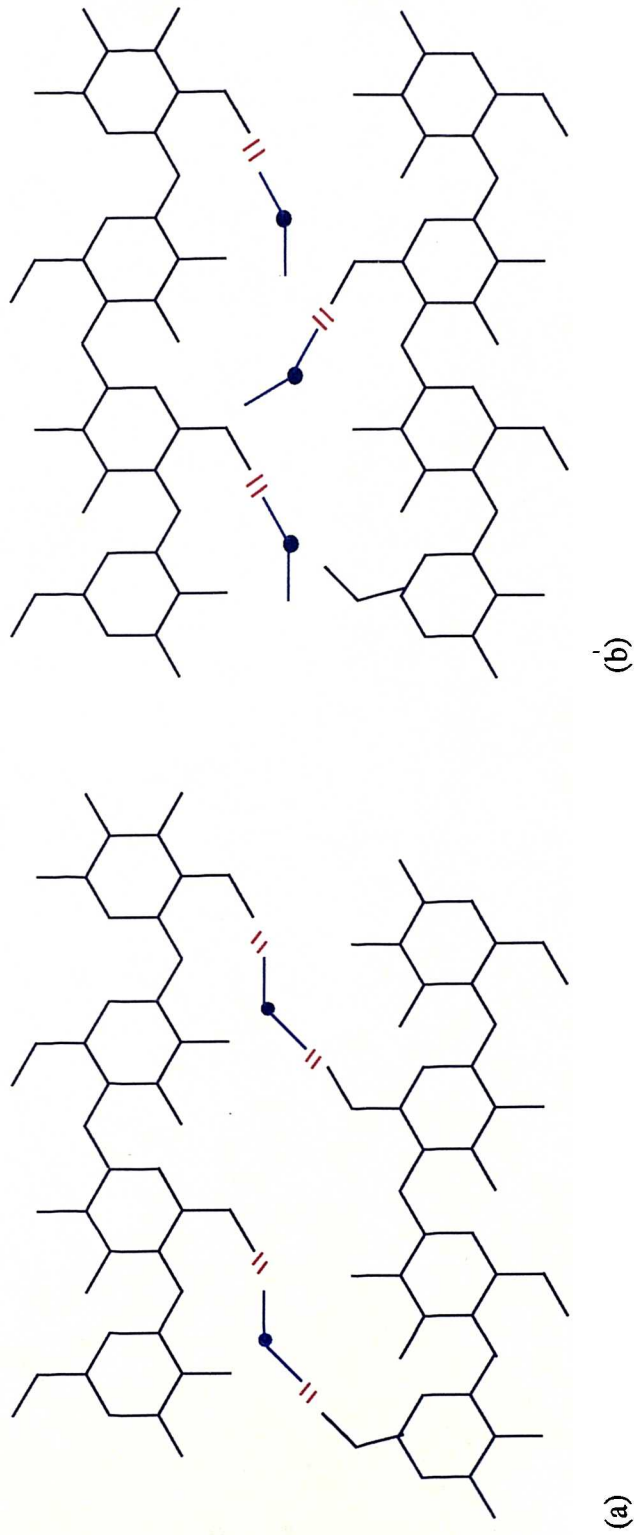
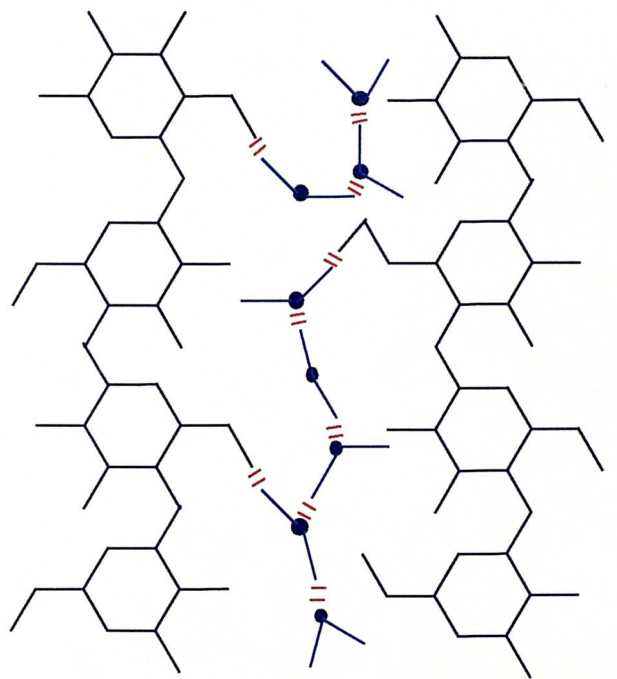


Figure 1.5a and b : Water molecules binding to cellulose depicting the three stages proposed by Khan and Pilpel (1987)

(a) two hydrogen bonds per water molecule

(b) one hydrogen bond per water molecule

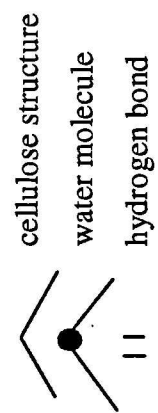
(for key see Figure 1.5c)



(c)

Figure 1.5c : Water molecules binding to cellulose depicting the three stages proposed by Khan and Pilpel (1987)

(c) hydrogen bonding between water – polymer and water - water molecules



They also reported that the semi-permeability of membranes is dependent on the ratio of the four types of water in the membranes with semipermeability increasing with an increasing ratio of completely bound water.

In contrast to the popular models mentioned already, Roorda et al (1988a, 1988b, 1994) have cast doubts on the existence of three (or more) thermodynamically different classes of water. In studies on poly(hydroxyethylmethacrylate) (p(HEMA)) gels they have demonstrated that the abnormal behaviour of water is caused by extremely slow crystallization upon cooling leading to the formation of a metastable non-equilibrium state and not by thermodynamic binding of water to the polymer. The water in pHEMA may be regarded as a single class of water, the average mobility of which is significantly reduced in the presence of a polymer. More recently, Bouwstra et al (1995), extended this work to polymethacrylic acid and copolymers of methacrylic acid and hydroxyethylmethacrylate and concluded that the amount of non-freezable water cannot be explained by different types of water. It was found by glass transition temperature determination that the amount of water required to decrease the T_g to 0°C was approximately equal to the amount of non-freezable (or bound) water in the hydrogels. From this it was concluded that it is not correct to consider the amount of bound water as a thermodynamically distinct class of water. It is due to either a restriction of the diffusion of water in hydrogels or a restriction of a further growth of ice crystals after the polymer has changed from its rubbery to glassy state. A similar hypothesis has been suggested by Levine and Slade (1988) in which water that previously has been known as 'tightly bound' may arise due to the immobility created by the glassy state. Likewise, the free water at higher water contents may be due to the rubbery state of the polymer above the T_g . Slade and Levine (1991) go as far as to refer to 'the mythology of bound water.' They report that if binding does occur, it must be specified in terms of either position, energy, or lifetime and that the binding must be of an equilibrium type. They say that so-called bound water is not energetically bound in any equilibrium thermodynamic sense but it is kinetically retarded due to high local viscosity below the T_g .

Zografi (1988) also considered the absorption of water into amorphous solids and the resultant plasticization which causes a reduction in the T_g . As a result, the measurement of the thermodynamic activity of water in such systems cannot be

interpreted without considering the contribution of the solid to what is being examined. For example, if the water within a polymer system is being analysed by dielectric methods, the property being measured reflects the kinetic effects of the solid on the water in addition to any thermodynamic effects. Thus, techniques used to detect bound water may not reflect bound water, but in fact may reflect that at certain levels of moisture the solid is in its glassy state.

Pre-endothermic events have also been attributed to overlapping ice melting (first order) and glass transition (second order) phase transitions (see section 1.3.1). Roos and Karel (1991) have reported that the temperature difference between the glass transition and onset of ice melting in maltose and maltodextrins decreased with increasing molecular weight. For high molecular weight compounds, the glass transition temperature and the onset of ice melting were found to be equal and as such the glass transition was observed as a step change followed by the main melting endotherm.

Murase (1993) referred to the small endotherm visible in DSC traces for polymer gels below 0°C as different from that due to ice melting of bulk water. In cross-linked dextrans, variation in cooling and heating rates during differential scanning calorimetry (DSC) analysis have suggested that this small endotherm beginning at about -19°C, is not due to a relaxation process e.g. a glass transition. The small endothermic change depends on the preceding cooling treatment and it is thought that as the cooling treatment will affect the size of the crystals produced during freezing, the ice crystallization evident during rewarming may be due to water compartmentalised by the polymer network. Ratto et al (1995) have observed more than one endothermic peak for water in water/chitosan systems which was attributed to cold crystallization. This occurs over a narrow water content range in such systems where only non-freezing and freezing bound water are present. Upon heating, a portion of the non-freezing water becomes mobile and comes into contact with the solidified freezing bound water forming ice, with a subsequent exotherm being visible.

Liu and Lelièvre (1991) have identified two endothermic melting peaks around 0°C for 50% (w/w) starch systems analysed using DSC. They suggested that such peaks

are not due to melting, followed by recrystallization and final melting but are due to changes in machine resolution. In further studies, Liu and Lelièvre (1992) have identified a minor baseline shift at the leading edge of the main endothermic peak for the melting of free water in 30 % starch-water systems analysed by DSC. This shift was entirely reversible and was attributed to a glass transition in agreement with the findings of Slade and Levine (1988). However, in samples containing 45% starch, two major endothermic peaks were visible around 0°C which were reversible. These were attributed to the division of moisture between water in the starch sample and water evaporating from the starch in the DSC pan and condensing on the pan lid.

1.3.2 Techniques employed in the differentiation and measurement of different types of water in hydrophilic polymers

A wide range of studies have been completed on hydrophilic polymer gels to explore the state of water within such systems. Various techniques have been employed in these studies.

1.3.2.1 Nuclear Magnetic Resonance (NMR)

Nuclei, such as hydrogen, with an odd number of protons or neutrons, possess a net spin or angular momentum and an electric charge. This in turn leads to the production of a net magnetic moment pointing along the axis of rotation of the nucleus. If an external magnetic field is applied, the spins align themselves along the applied field adopting parallel or antiparallel orientations. For the majority of nuclei, including that of hydrogen, the spin quantum number is 0.5 and the spins may exist in low (aligned with the field) or high (opposed to the field) energy states. If the spinning nuclei are subject to a radio frequency, the spins release or absorb energy and reach different energy levels. As a result, the mobility of protons may be detected in various energy states. This enables the spin-spin relaxation time (T_2) to be measured and the motional state of water may be estimated with the hydrogen atoms in bound water being at different energy states compared to those in free water. Pulsed-gradient spin-echo NMR has been used to measure the self-diffusion coefficient (SDC) of water. NMR imaging has been used to examine the water mobility within HPMC tablets (Rajabi-Siahboomi et al, 1994; 1996) and by Ashraf et

al (1994) to measure water front penetration in HM capsule plugs. Water states have been further explored using NMR methods in agarose gels (Aizawa et al, 1972); poly (vinyl alcohol) (Hatakeyama et al, 1984); methacrylate polymer networks (Sung et al, 1981); MC and HPMC gels (Ibbett et al, 1992; Gao and Fagerness, 1995a).

1.3.2.2 Differential Scanning Calorimetry (DSC)

Probably the most commonly used technique to examine different types of water is differential scanning calorimetry (DSC). When a hydrophilic polymer sample is cooled below 0°C, free water within the system will freeze while closely associated water will remain non-frozen. Upon heating, in many, but not in all systems, it is possible to identify both free and freezing bound water from DSC traces. However, identification of water tightly bound to the polymer becomes more complex because this water does not freeze and hence is not visible on the DSC trace. The DSC method has been previously used to examine the water distribution within HPMC (Ford and Mitchell, 1995; Nokhodchi et al, 1997) and hydrophilic methacrylate polymer gels (Sung, 1978).

1.3.2.3 Thermogravimetric analysis (TGA)

Different types of water are identifiable from thermogravimetric studies, as they evaporate at different temperatures on the heating cycle (Donescu et al, 1993). These events may be quantifiable from the derivative of the TGA weight loss curve (dTGA) provided that there is no overlap between the temperatures at which the different types of water evaporate. The derivative of the weight loss curve gives an indication of the rate of weight loss with time.

In many cases, TGA studies are used to complement DSC/DTA (differential temperature analysis; an older version of DSC formerly employed in high temperature work) studies as shown in work carried out on theophylline monohydrate (Duddu et al, 1995); polyaniline (Matveeva et al, 1995) and in peat (McBrierty et al, 1996). TGA measurements have been used to calculate total water content (W_t) of certain systems thus enabling the bound water content of the system to be determined by subtraction of the free water content (W_f) which is determined

using DSC. Examples of calculation of total water content by TGA for measurement of bound water in this way include characterization of actin (Kakar and Bettelheim, 1991); various ligno-cellulosic materials (Berthold et al, 1996); and poly (vinyl alcohol) films (Hodge et al, 1996).

1.3.2.4 Thermomechanical Analysis (TMA) or Dilatometry

Thermomechanical analysis (or its predecessor dilatometry) determines the dimensional changes of materials when they are subjected to a controlled temperature programme. In this application, TMA may be used to measure the swelling of HM systems in water and the rate of gel layer formation. Such studies have been carried out on agarose gels and cross-linked dextrans (Aizawa and Suzuki, 1971); p(HEMA) gels (Lee et al, 1975); copolymer hydrogels (Kim et al, 1983) and on HPMC gels (Mitchell et al, 1993a).

1.3.2.5 Dielectric spectroscopy

The behaviour of water in polymeric systems has been previously characterised by analysis of the dielectric response. The relaxation and crystallization of water in a terpolymer hydrogel has been characterised in terms of its dielectric response (Pathmanathan and Johari, 1994). It was found that on cooling, a fraction of the total amount of water crystallized to ice and this is detectable by the appearance of a relaxation peak. Water and ice co-existed at temperatures up to 270°C which may indicate the existence of freezing and non-freezing water in the polymer.

The dielectric response of polymer-water interactions in poly (hydroxyethylacrylate) hydrogels were studied and compared to similar systems studied using DSC and sorption isotherm measurements (Kyritis et al, 1995).

1.3.2.6 Vapour Sorption

The dynamic measurement of water uptake and release by solids has been achieved by employing gravimetric methods in association with electronic microbalances. Water sorption to cellulose and starch based excipients has been studied, with at least three thermodynamic states being identified (Zografis and Kontny, 1986). These

include water which is tightly bound to anhydroglucose units on the cellulose backbone, unrestricted water which has properties similar to bulk water, and water having properties intermediate between the two extremes. Blair et al (1990) studied the water sorption characteristics of starch and microcrystalline celluloses (MCC). They found that starch freely adsorbs water at all relative humidities studied while MCC does so only at raised relative humidities. This was explained as being due to the fact that starch has more free cellulose hydroxyl groups to which water can bind.

1.4 Thesis Aims and Objectives

The aims of this work were to achieve a better understanding of the interactions between water and cellulose ether polymers as summarised below:

- (1) Characterization of water distribution within HPMC K15M gels both qualitatively and quantitatively using the complementary thermal methods of DSC and TGA.
- (2) The influence of polymer molecular weight and substitution levels on water distribution within HPMC gels.
- (3) The influence of drugs on the distribution of water within a range of cellulose ether polymers.
- (4) Characterization of the interaction between water and cellulose ether polymers using dielectric spectroscopy and dynamic vapour sorption.

Chapter 2 Materials, Methods and Characterisation

2.1 Materials

2.1.1 Cellulose ethers

Cellulose ether polymers, 'MethocelTM', of different viscosity grades and substitution levels were obtained from DOW Chemical Co., USA and are listed in Table 2.1 along with certain details from their certificates of analysis including % substitution, apparent viscosity and impurity levels.

Klucel Hydroxypropylcellulose (HPC) MF EP (LOT 12187) with a viscosity of 5950cP and molar substitution 4.2 was obtained from Hercules Limited, Aqualon Division, Salford, U.K.

2.1.2 Propranolol Hydrochloride

Propranolol Hydrochloride, (\pm)-1-Isopropylamino-3-(1-naphthyloxy)propan-2-ol, ($C_{16}H_{21}NO_2$) (BN 12895034) was obtained from Becpharm, Harlow, Essex, England. It has a molecular weight of 259.3 and its structural formula is shown in Figure 2.1. Propranolol hydrochloride is a Beta-adrenoceptor blocking agent with a wide variety of indications including hypertension, angina, arrhythmias and anxiety (British National Formulary, Sept. 1997). It is soluble in water (Martindale: The Extra Pharmacopoeia, 1996).

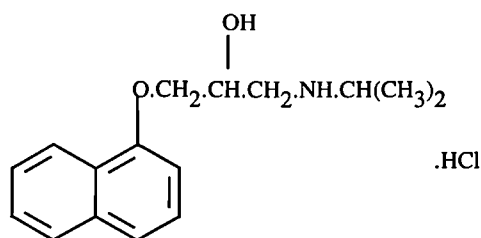


Figure 2.1 : Structural formula of propranolol hydrochloride

Table 2.1 : Methocel cellulose ether polymers obtained from DOW Chemicals, USA.

Key: HPMC (Hydroxypropylmethylcellulose)
MC (Methylcellulose)

Polymer	Batch Number	Viscosity (cP)	Methoxyl (%)	Hydroxypropoxyl (%)	Sodium chloride (%)	Iron (ppm)
HPMC K100LV	MM94051022K	93	22.1	9.2	0.49	20
HPMC K100LV	JE28012N21	100	23.1	8.4	0.28	29
HPMC K4M	MM92031903K	4,196	22.2	8.4	0.36	23
HPMC K15M	MM93042103K	15,256	21.3	9.0	0.52	18
HPMC K15M	MM94112811K	15,825	22.8	8.7	0.16	35
HPMC K100M	JL02012N11	119,768	22.6	10.8	0.28	30
HPMC F4M	QP90121805F	5,218	28.9	6.1	0.30	40
HPMC E4M	MM91061011E	3,970	29.1	8.1	0.14	23
MC A4M	MM94071301A	3,811	29.9	-	0.75	16

2.1.3 Diclofenac Sodium

Diclofenac Sodium, sodium 2-[(2,6-dichlorophenyl)amino]phenylacetate ($C_{14}H_{10}Cl_2NNaO_2$) (BN 0710) was obtained from Profarmaco, Milan, Italy. It has a molecular weight of 318.1 and its structural formula is shown in Figure 2.2. Diclofenac sodium is classified as a non-steroidal anti-inflammatory drug (NSAID) and is indicated for treatment of pain and inflammation in rheumatic disease (including juvenile arthritis), other musculoskeletal disorders and acute gout (British National Formulary, Sept. 1997). It is sparingly soluble in water (Martindale: The Extra Pharmacopoeia, 1996).

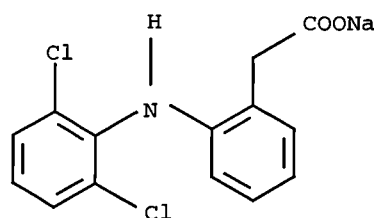


Figure 2.2 : Structural formula of diclofenac sodium

2.2 Experimental Methods

2.2.1 Preparation of cellulose ether gels

Samples of cellulose ether gels (5-25% w/w) (sample size 20g) were prepared by heating the full quantity of distilled water to $\sim 80^{\circ}\text{C}$ and adding in two aliquots to the previously weighed cellulose ether powder in a mortar and pestle. The mixture was triturated vigorously to ensure thorough wetting. Gels were transferred to pyrex storage vessels which were sealed and stored at $4-6^{\circ}\text{C}$ for 2, 24 or 96h before use. Water losses during both preparation and storage were taken into account when determining the final polymer concentrations in the gels.

Gels containing propranolol hydrochloride (0, 1.479 (50mM), 10, 20 and 30% w/v) or diclofenac sodium (50mM) were also prepared. This was accomplished by dissolving the drugs in distilled water by mixing with the aid of gentle heat on a hot plate stirrer (Griffin & George, England), prior to gel preparation. Both drugs were fully soluble in warm water at concentrations of 50mM.

Propranolol hydrochloride solutions (1, 3, 5 & 10% w/v) were prepared in the presence and absence of heat as a control to identify whether propranolol hydrochloride was thermolabile under the gel preparation conditions. A student t-test when applied to the melting enthalpy (J/g; n = 3) data gave a critical value of $t = 2.447$ ($p < 0.05$) from which it was concluded that no significant difference was apparent in solutions prepared either in the absence or presence of heat.

Gel samples (>25% w/w) were prepared by preparing gels initially as detailed above in the 10 - 20% w/w range and storing at 4-6°C for 24h. A series of samples (10-16mg) of the gels were weighed into DSC sample pans (40 μ l, Perkin Elmer) and held at 55°C in an oven. The samples were removed after defined time periods to obtain a measurable % weight loss from which the exact polymer : water ratios could be calculated. The sealed DSC pans were stored for 24 or 96h at ambient temperatures to allow equilibration and uniform water distribution in the gels before analysis. Controls were completed in which a series of sealed DSC pans incorporating HPMC K15M (20% w/w) gel samples were stored at ambient temperatures for 24, 96 or 168h and the moisture loss from the pans was monitored by weight measurement. The average percentage weight loss (\pm SD; n = 8) from the pans were 0.33 ± 0.34 ; 1.39 ± 1.16 and $0.97 \pm 0.83\%$ respectively. Such weight losses during storage were quite small and should not affect the calculated polymer concentration value.

2.2.2 Thermal methods

2.2.2.1 Differential Scanning Calorimetry

Differential Scanning Calorimetry (DSC) is a technique which measures heat flow into, or out of, a sample that is heated as it is held in a controlled environment. Two types of instrumentations are available: the heat-flux DSC, characteristic of TA Instruments, Setaram and Mettler systems, and the power-compensated DSC, typical of Perkin-Elmer systems. Only the theory behind power compensated systems is detailed here.

The Perkin-Elmer DSC7 system works on the principle that energy absorbed or evolved by the sample is compensated by adding or subtracting an equivalent amount of electrical energy to a heater located in the sample holder (Perkin-Elmer DSC7 Operator's Manual, 1986). Platinum resistance heaters and thermometers provide means of measuring the energy and temperature measurements (Figure 2.3). A varying electrical signal related to the changing thermal behaviour of the sample is provided by the adjustment of the heater power (energy per unit time) needed to keep the temperature of both the sample and reference holders identical. The output signal is in milliwatts (mW) providing a direct electrical energy measurement of peak areas. The Perkin-Elmer DSC7 instrument with attached liquid nitrogen cooling accessory is capable of scanning in the temperature range of -170°C to $+730^{\circ}\text{C}$ at heating and cooling rates from $0.1^{\circ}\text{Cmin}^{-1}$ to $200^{\circ}\text{Cmin}^{-1}$ with a calorimetric precision of better than $\pm 0.1\%$ (Perkin-Elmer DSC7 Operator's Manual, 1986).

A Perkin-Elmer DSC7 (Beaconsfield, UK) with an attached liquid nitrogen based cooling accessory controlled by a Perkin-Elmer TAC-7 was employed in the majority of DSC analysis work. Calibrations with indium (m.p. onset 156.60°C) and zinc (m.p. onset 419.47°C) were carried out each time the heating rate was changed. Nitrogen was used as the purge gas with a flow rate of between 0.04 lmin^{-1} to 0.05 lmin^{-1} . Gel samples

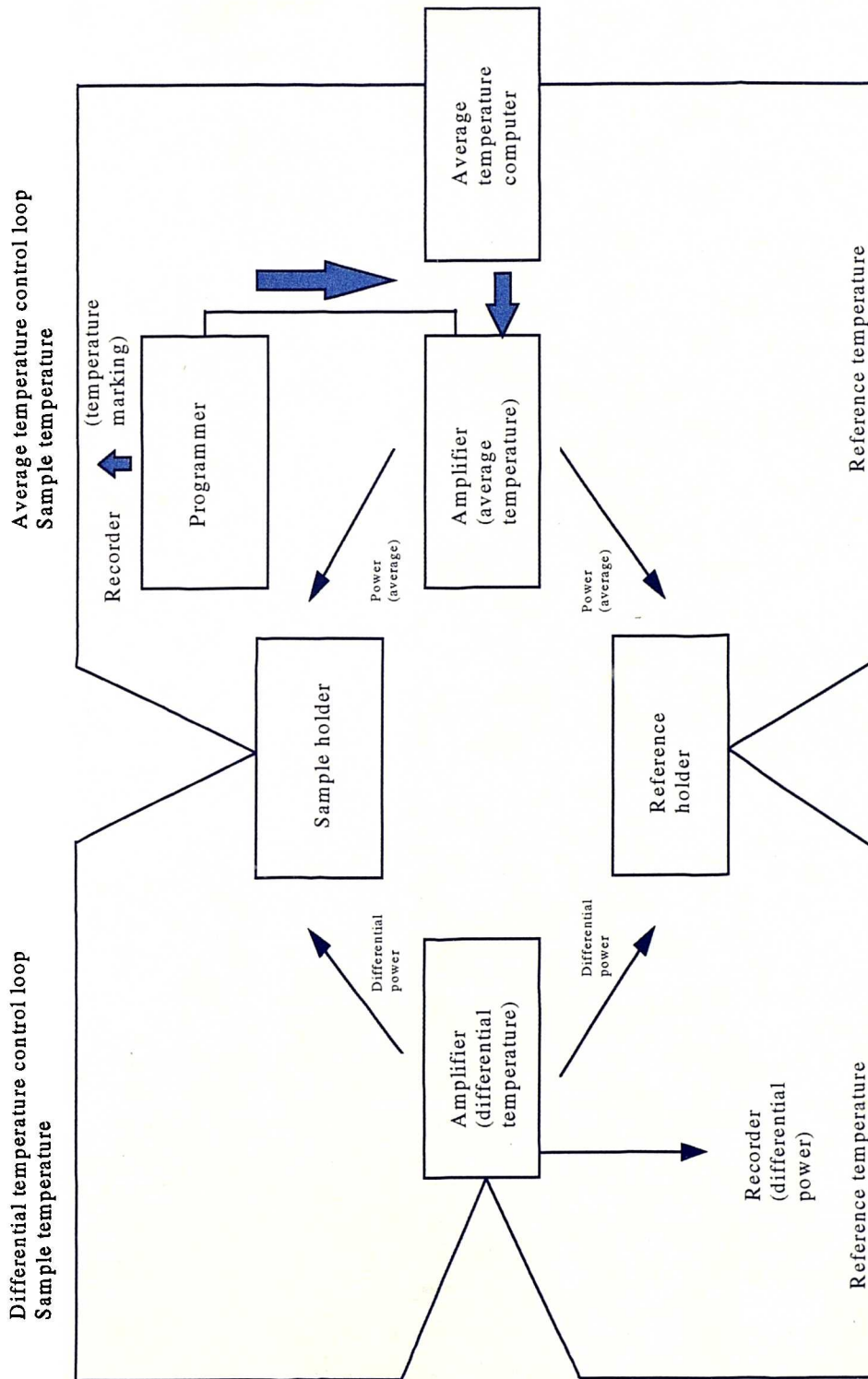


Figure 2.3 : Schematic diagram of a Perkin-Elmer DSC instrument (adapted from Wendlandt, 1986)

(5-15mg) were analysed in aluminium sample pans (40 μ l, Perkin-Elmer, Beaconsfield, UK) while powdered samples were analysed in flat aluminium sample pans (Perkin-Elmer, Beaconsfield, UK). Cooling rates were varied from rapid cooling to $-1^{\circ}\text{Cmin}^{-1}$. In the case of rapid cooling, the DSC head was cooled to -30°C and the sample pan placed on the DSC head providing rapid cooling of the sample. Heating rates varied from $+1^{\circ}\text{Cmin}^{-1}$ to $+100^{\circ}\text{Cmin}^{-1}$. The specific heating and cooling rates employed are further documented in the relevant experimental section. In the literature, some workers have autoclaved aluminium sample pans before use to eliminate any reaction between the aluminium surface and water (Nakamura et al, 1983b). A control experiment was completed in which the effect of autoclaving aluminium sample pans was examined. Subsequent statistical analysis of the melting enthalpy values for a series of HPMC K15M gel samples ($n = 12$) analysed in treated and untreated aluminium sample pans gave a value for student t-test of $t = 0.09$ ($p < 0.05$). It was concluded that there were not significant differences between data obtained from treated and untreated pans and therefore it was not necessary to pretreat aluminium sample pans.

A Perkin-Elmer Pyris 1 DSC system with attached intercooler was employed to characterise the glass transition temperature of a series of cellulose ether polymers. Calibrations with indium and zinc were carried out with changes in heating rate as described for the DSC7 system. Powdered samples (18-30mg) were scanned at $10^{\circ}\text{Cmin}^{-1}$ in the temperature range of 0°C to 230°C in stainless steel pans (50 μ l, Perkin-Elmer, Beaconsfield, UK).

2.2.2.2 Thermogravimetric Analysis

Thermogravimetric analysis (TGA) is a technique in which a change in sample mass is determined as a function of temperature and/or time. This may involve heating at a sustained fixed temperature or alternatively heating or cooling at a linear rate (Wendlandt, 1986). A thermobalance is commonly used to continuously weigh the sample as a function of temperature or time. In the Perkin-Elmer TGA 7 (Figure 2.4), a

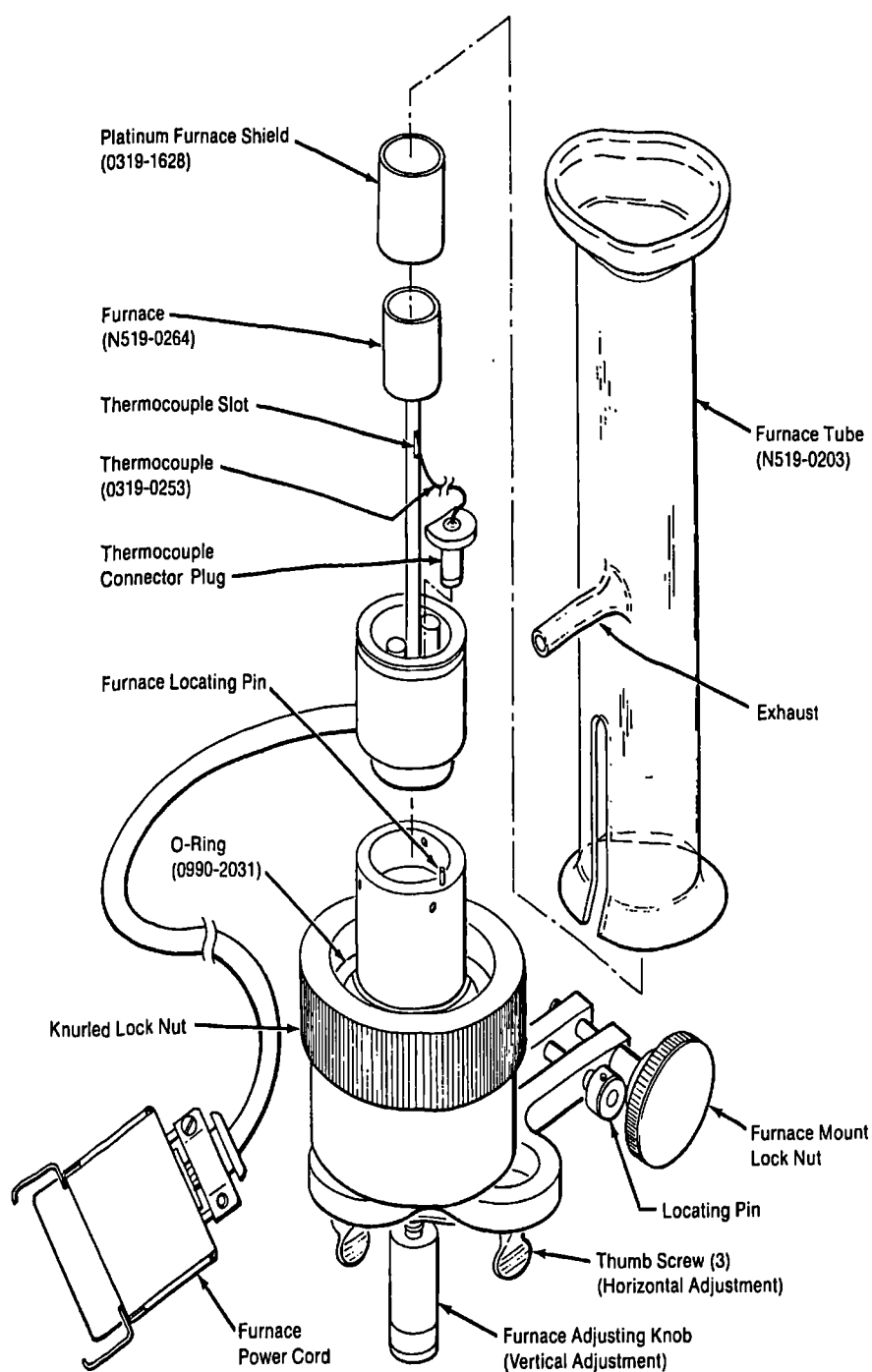


Figure 2.4 : Schematic diagram of the Perkin-Elmer TGA 7 (adapted from Perkin-Elmer TGA 7 Operator's manual 1986)

sensitive ultramicrobalance (detection $\pm 0.1\mu\text{g}$; maximum 130mg) is used along with a furnace element. The microbalance used is a null-type instrument in which the amount of current necessary to maintain the system in the null state is directly proportional to sample weight change (Perkin-Elmer TGA 7 Operator's Manual, 1986). The TGA 7 furnace allows analysis in the temperature range from ambient to 1000°C , at heating rates ranging from $0.1^{\circ}\text{Cmin}^{-1}$ to $200^{\circ}\text{Cmin}^{-1}$ in $0.1^{\circ}\text{Cmin}^{-1}$ increments. The TGA 7 requires the use of two purge gas lines which are separately connected to the balance chamber and the sample/furnace area. Nitrogen gas is commonly used to provide a suitable inert atmosphere with flow rates to the balance of $0.04\text{-}0.06\text{ lmin}^{-1}$ and to the furnace area of $0.02\text{-}0.035\text{ lmin}^{-1}$. The TGA 7 further uses compressed air to operate the furnace removal and cooling features of the analyser.

All analyses were carried out on a Perkin-Elmer TGA 7 system. The machine was calibrated using each of the following three calibration routines:

- (i) *furnace calibration* - temperature calibration which involves heating the TGA between 100°C and 900°C , which linearizes the furnace by matching thermocouple temperature to furnace temperature.
- (ii) *standard calibration* - temperature calibration performed by running Nickel (m.p. 354°C) and iron (m.p. 780°C) standards. Involves entering theoretical and measured values for onset temperatures which are used for calibration.
- (iii) *weight calibration* - calibration using a 100mg calibration standard which allows automatic calibration of the ordinate (weight) axis of the TGA 7.

Powder samples of cellulose ether (about 10mg) were heated from ambient to 200°C at a heating rate of $+10^{\circ}\text{Cmin}^{-1}$. Cellulose ether gels (5-25% w/w) were prepared as in 2.2.1, in the absence and presence of a drug, and samples of about 10mg were scanned at five scanning rates ($+2$, $+5$, $+10$, $+15$ and $+20^{\circ}\text{Cmin}^{-1}$) in an open sample pan. A number of gel samples were analysed in vented aluminium sample pans ($20\mu\text{l}$, Perkin-Elmer) in an attempt to provide a controlled moisture loss from the gel samples. Kinetic analysis of

moisture loss studies was carried out using a TGA 7 PC Series Decomposition kinetics software programme (Perkin-Elmer, Beaconsfield, U.K.) (see section 4.4.1.3).

2.2.3 Powder Characterisation

2.2.3.1 X-ray Powder Diffraction

An x-ray generator model Phillips, PW 1729 fixed $\theta/2\theta$ Goniometer with PW1710 diffractometer (Phillips, Almelo, Netherland) was used to record x-ray diffraction spectra. The sample powders, HPMC K4M, E4M, F4M and MC A4M were transferred to the sample holder and scanned at a rate of $0.04^\circ.2\theta/\text{sec}$ over the range of 5 to $75^\circ.2\theta$.

Typical x-ray diffraction spectra are shown in Figure 2.5. The traces show that all materials examined show non-crystalline or amorphous behaviour. In an amorphous material, beams are scattered by the atoms within the structure in all directions and minimal constructive interference of the beams occurs.

2.2.3.2 Surface Area Determination

A NOVA-2000 Gas Sorption Analyzer (version 1.20; Quantachrome Corporation, Camberley, Surrey, U.K.) was employed to measure the surface area of a range of cellulose ether powder samples. All samples were dried in a hot air oven (Memmert, GmbH, Schwabach, Germany) at 70°C before transfer to a sample cell (12mm, bulb diameter; 1.5-3g, sample weight). The sample cell was transferred to the NOVA outgasser and the sample was prepared by flow outgassing (or degassing) with Helium. The gas pressure was set to give an output of 10 PSI with a flow rate of 1-2 bubbles per second. Outgassing was carried out for either 4 or 12h while heating at 50°C . Samples were analysed using nitrogen gas (output; 10 PSI) with a 7-point BET

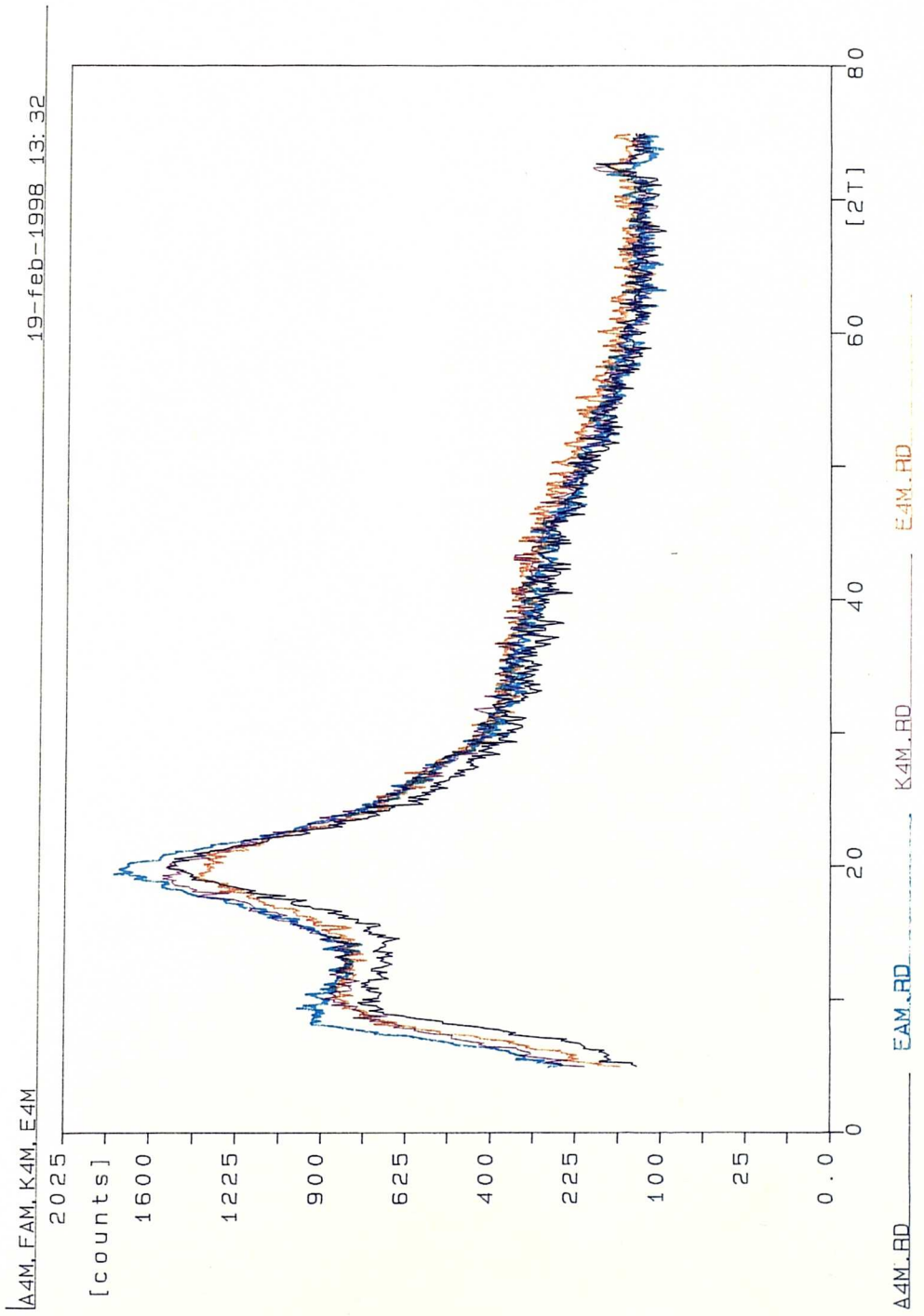


Figure 2.5 : X-ray diffraction spectra of Methocel cellulose ethers HPMC F4M, HPMC K4M, HPMC E4M and MC A4M

(Brunauer-Emmett-Teller) set-up in which the total volume of nitrogen gas (cm^3/g) adsorbed by the sample was measured at each of the seven target relative pressures (0.025, 0.050, 0.100, 0.150, 0.200, 0.250 and 0.300 mmHg) while the sample cell was immersed in liquid nitrogen. Four particle sizes of HPMC K4M were analysed; $<75\mu\text{m}$, $75-90\mu\text{m}$, $90-125\mu\text{m}$ and $125-180\mu\text{m}$. In addition, the surface areas of HPMC E4M, HPMC F4M and MC A4M (all $90-125\mu\text{m}$) were characterised. The following parameters are variable on the NOVA analyser and were adjusted according to the material analysed within certain limits as indicated.

(a) *Pressure tolerance*: chosen range within which the pressure in the cell must remain for the defined equilibration time at each particular target relative pressure:

0.05 or 0.1 (mm Hg) were used.

(b) *Equilibration time*: chosen time during which the pressure in the cell must not change by more than the defined pressure tolerance at each particular target relative pressure:

120 or 60 (sec) were used.

(c) *Dwell time*: time limit which is invoked if the pressure tolerance is not met and if the pressure does not fall below the lower pressure limit:

600 or 240 (sec) were used.

The analysis takes from 33 to 50 min according to the parameters employed. This method of surface area determination is based on the theory of Brunauer-Emmett-Teller (1938), commonly known as the 'BET' theory:

Equation 2.1

$$\frac{1}{W \left(\left(\frac{P_0}{P} \right) - 1 \right)} = \frac{1}{W_m C} + \frac{C - 1}{W_m C} \left(\frac{P}{P_0} \right)$$

where W is the weight of gas adsorbed at a relative pressure P/P_0 , where P is the pressure of water vapour in the environment, and P_0 is the vapour pressure of liquid water at a particular temperature. W_m is the weight of adsorbate constituting a monolayer of surface coverage. The BET constant C , is related to the energy of adsorption in the first adsorbed layer and indicates the magnitude of the adsorbent/adsorbate interactions. The BET equation requires a linear plot of $\frac{1}{W((P_0/P) - 1)}$ against $\{P/P_0\}$ which is found mainly in the P/P_0 range of 0.05 to 0.35. The weight of a monolayer of adsorbate W_m may be obtained from the slope s and intercept i of the BET plot.

$$\text{Equation 2.2} \quad s = \frac{C-1}{W_m C}$$

$$\text{Equation 2.3} \quad i = \frac{1}{W_m C}$$

W_m , the weight of a monolayer, may be obtained by combining equations 2.2 & 2.3, giving equation 2.4:

$$\text{Equation 2.4} \quad W_m = \frac{1}{s+i}$$

The total surface area of the sample S_t may be calculated from equation 2.5:

$$\text{Equation 2.5} \quad S_t = \frac{W_m N A_{cs}}{M}$$

where N is Avogadro's number (6.023×10^{23} molecules/mol) and M is the molecular weight of the adsorbate (nitrogen). The cross-sectional area A_{cs} for nitrogen is 16.2 \AA^2 or $16.2 \times 10^{-10} \text{ m}^2$.

The specific surface area S of the solid can be calculated from equation 2.6:

Equation 2.6
$$S = S_t / w$$

All surface area calculations completed were based on a 5-point BET analysis with the data received at relative pressures 0.025 and 0.050 being omitted so that calculations were completed on the most linear region of the BET plot. The linearity of each BET plot was defined by a regression coefficient (R^2). The five point BET plot for HPMC K4M (125 - 180 μ m) is shown in Figure 2.6.

The results of the surface area analysis are shown in Table 2.2. Characterisation of surface area using this method proved very difficult. The samples could not be heated aggressively in the outgassing procedure and indeed adequate outgassing proved particularly difficult to achieve, particularly in the case of HPMC F4M. Furthermore, the high degree of amorphous content in the powders resulted in low surface areas and adsorption potentials. Large sample sizes and long outgassing times were employed with such factors in mind. Despite this, the technique failed to distinguish between HPMC K4M powders of different particle size fractions. HPMC K4M (125-180 μ m) particles had a larger specific surface area ($0.544 \pm 0.030 \text{ m}^2\text{g}^{-1}$) than HPMC K4M (90-125 μ m) ($0.284 \pm 0.163 \text{ m}^2\text{g}^{-1}$) particles. This is probably an ambiguous result. In light of this, few conclusions can be drawn from the surface area data from the other polymers studied apart from the consistently low specific surface area for all samples.

2.2.3.3 Glass Transition Determination

The glass transition temperatures (section 1.1.6) of a series of cellulose ethers were characterised using powdered samples (18-30mg) scanned in stainless steel pans on a Perkin-Elmer Pyris 1 DSC system as described in section 2.2.2.1. HPMC K15M

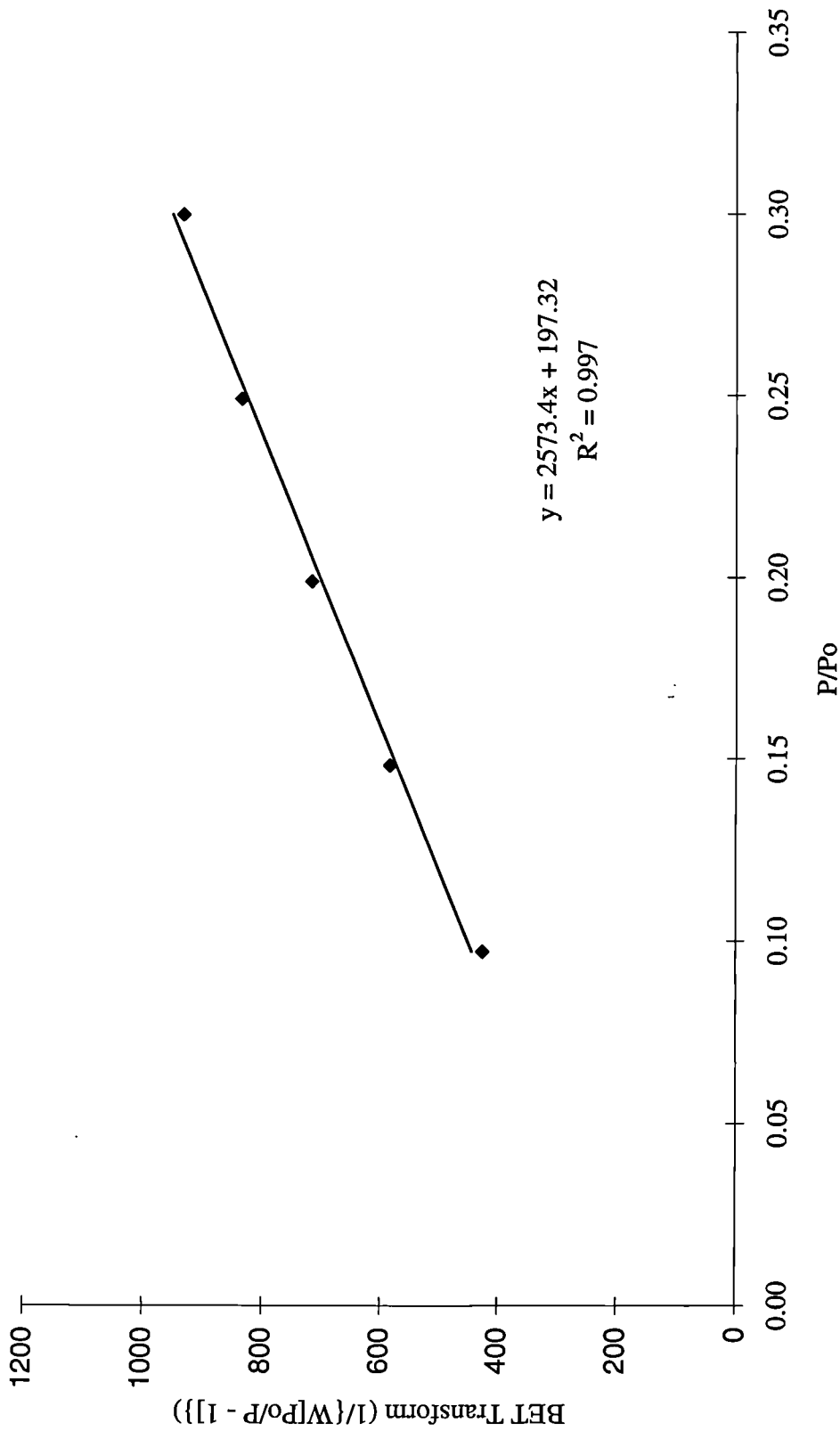


Figure 2.6 : Multi-point BET (Adsorption) plot of BET Transform (1/{W[Po/P - 1]}) against partial pressure for HPMC K4M (125 - 180um)

Table 2.2 : Surface area determination of HPMC and MC A4M powders showing drying and flow outgas conditions in addition to the specific surface area and regression coefficients

Polymer	Powder drying time at 70°C (h)	Flow outgas time (h)	*Specific surface area (m ² g ⁻¹)	Regression coefficient (R ²)
HPMC K4M	12	12	0.697	0.997
(<75µm)			0.596	0.997
HPMC K4M	12	12	0.527	0.995
(75-90µm)			0.579	0.997
HPMC K4M	12	4	0.399	0.983
(90-125µm)			0.168	0.991
HPMC K4M	12	12	0.565	0.997
(125-180µm)			0.522	0.992
MC A4M	12	4	0.344	0.978
(90-125µm)			0.375	0.981
HPMC E4M	12	4	0.244	0.993
(90-125µm)			0.248	0.991
HPMC F4M	24	12	0.526	0.988
(90-125µm)			0.331	0.977
HPMC K4M	12	4	0.399	0.997
(90-125µm)			0.168	0.997

*n = 2 measured at each condition

powders were initially scanned in standard flat aluminium pans. However, poor encapsulation led to baseline drift and the presence of a lot of noise. Using stainless steel pans, a larger sample size was possible along with better encapsulation. Initially, samples were heated from 0°C to +230°C at +10°Cmin⁻¹. The moisture contents in the samples were measured by TGA analysis of powdered samples (10mg approx.), heated from ambient temperatures to 200°C at +10°Cmin⁻¹ and are shown in Table 2.3. Endotherms were visible in the 60-65°C temperature range indicating removal of water from the powders (Figure 2.7). Subsequently, samples were rapidly cooled to 25°C and reheated to 230°C at +10°Cmin⁻¹. No endotherms due to moisture loss were visible in the reheated traces and a decrease in glass transition temperature occurred (Figure 2.8 and Table 2.3). Removal of moisture from the powders during heating should theoretically cause an increase in glass transition temperature because water acts as a plasticizer and causes a reduction in glass transition temperature (Hancock and Zografi, 1994). However, this does not occur and may possibly be due to degradation of the sample during the initial heating run. To investigate this hypothesis, a HPMC K15M powder sample was held at 100°C for three minutes followed by cooling to 25°C and then heating to 230°C. This resulted in an elimination of the water endotherm and an increase in the glass transition temperature to 183.7°C.

Glass transition temperatures of HPMC polymers by DSC have previously been reported in the literature. Entwistle and Rowe (1979) reported a value of 177°C for HPMC Pharmacoat 606 prepared from cast films. Okhamafe and York (1985) reported a value of 155°C while Sakellariou et al (1985) reported a value of 180°C for HPMC powdered samples and a value of 157°C was found from solvent cast films. Kararli et al (1990) reported values of 160 to 175°C using dynamic mechanical analysis (DMA).

Table 4.3 : Glass transition temperatures of cellulose ether polymers¹ moisture content measured using TGA analysis of sample powders (n = 2 ± SD)² sample heated from 0°C to +230°C at a heating rate of +10°Cmin⁻¹³ sample rapidly cooled to +25°C and reheated to +230°C at a heating rate of +10°Cmin⁻¹

Polymer	sample weight (mg)	moisture content (%) ¹	Glass transition 1 (°C) ²	Glass transition 2 (°C) ³
HPMC K100LV	22.80	5.02 ± 0.33	159.7	not visible
HPMC K4M	21.67	4.73 ± 0.03	172.34	
	23.54		172.49	159.20
HPMC K15M	22.57	4.56 ± 0.02	170.35	151.29
	21.92		166.41	145.60
HPMC K100M	22.37	4.00 ± 0.27	167.87	153.96
MC A4M	18.67	4.12 ± 0.27	168.18	161.16
HPMC F4M	19.29	3.98 ± 0.26	159.43	not visible
HPMC E4M	29.48	3.92 ± 0.11	141.42	124.79
HPC	25.65	4.99 ± 0.21	not visible	not visible

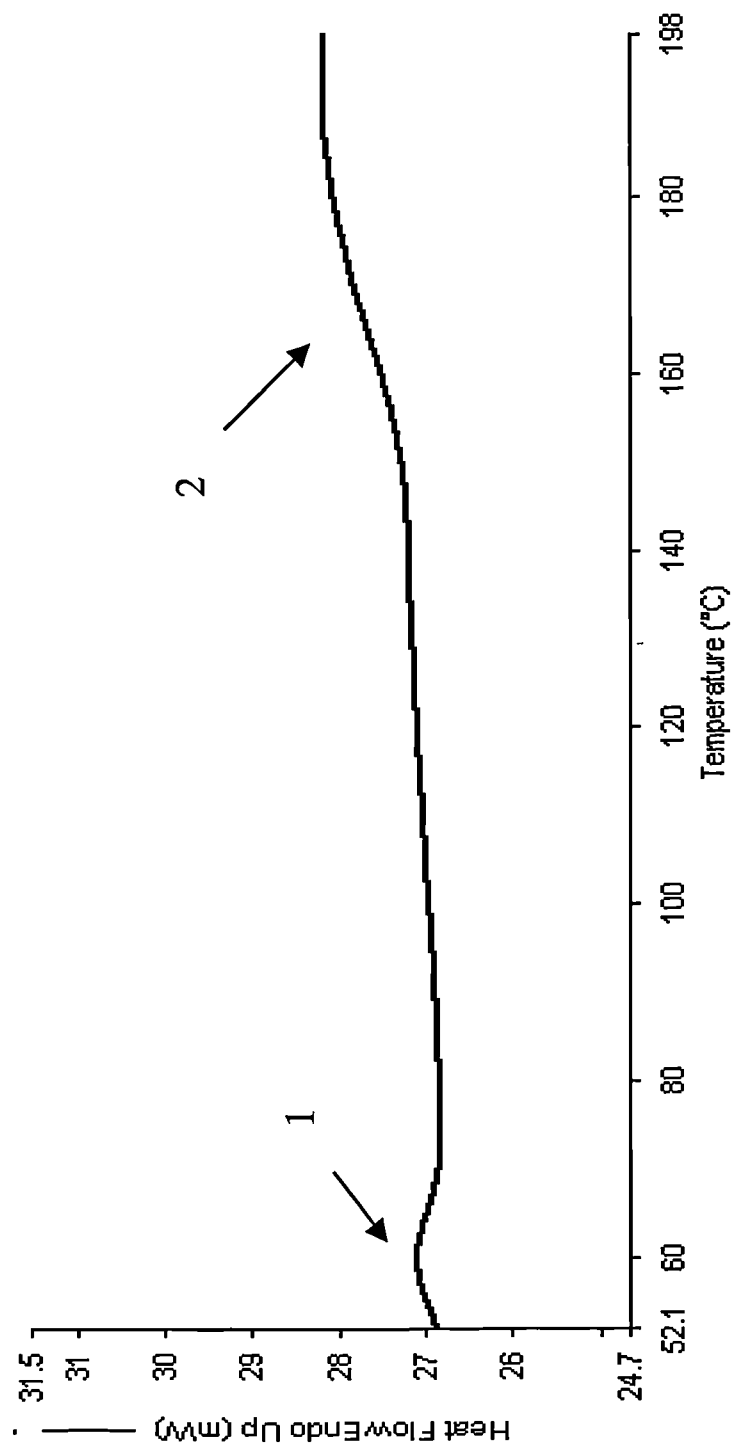


Figure 2.7 : HPMC K15M powder heated from ambient to 200°C at +10°Cmin⁻¹ showing a water endotherm (1) around 60°C and a broad glass transition(2) centring at 170.4°C

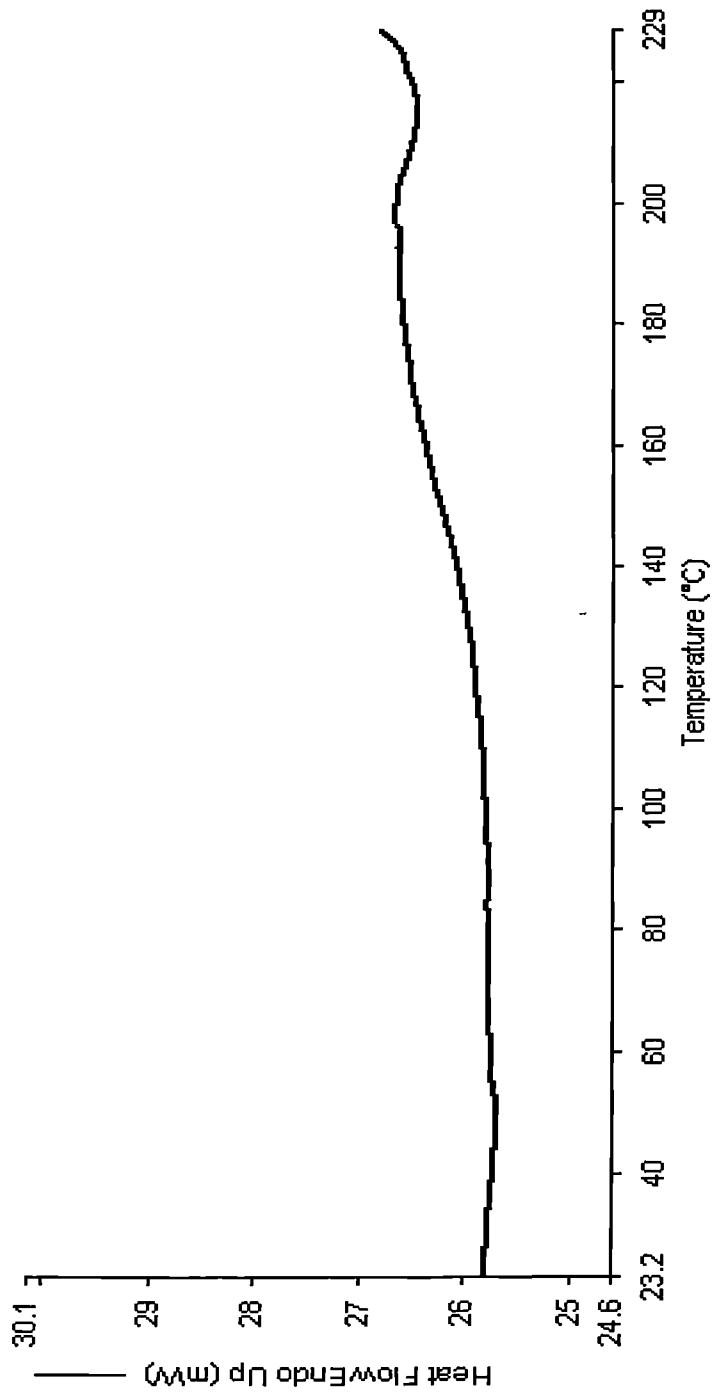


Figure 2.8 : HPMC K15M powder heated from ambient to 200°C at +10°Cmin⁻¹, rapidly cooled to 25°C and then heated to 230°C at +10°Cmin⁻¹

2.2.4 Other Methods

Other methods employed in the characterisation of the interactions between water and cellulose ethers including low frequency dielectric spectroscopy (LFDS) and dynamic vapour sorption (DVS) are outlined in their relevant chapters.

CHAPTER 3

CHARACTERISATION OF WATER DISTRIBUTION WITHIN HPMC K15M GELS USING DIFFERENTIAL SCANING CALORIMETRY

Chapter 3 Characterisation of water distribution within HPMC K15M gels using differential scanning calorimetry

3.1 Introduction

The majority of polymers which are used for their pharmaceutical applications and in particular those used in controlled drug release matrices are employed in aqueous environments. Such polymers form gels in solution and different types of water are known to exist within such gel systems. Detailed studies on the types of water that exist within these gel systems are fundamental to the optimisation and prediction of drug release from their matrices.

The states of water within polymer gel systems have been studied widely using a variety of techniques (section 1.3) including differential scanning calorimetry (DSC) and thermogravimetric analysis (TGA). The majority of workers have identified three classes of water within hydrophilic polymer gels (section 1.3) which may be defined in terms of their thermal analysis as :

- (a) free water i.e. unbound water in polymers whose transition temperature enthalpy and peak shape in DSC curves are equal to those of pure (bulk) water (Nakamura et al, 1983b).
- (b) non-freezing i.e. bound water which is attached directly to polymer hydrophilic groups and does not undergo a phase transition (Hatakeyama et al, 1987).
- (c) freezing bound water which is characterised as having a phase transition temperature lower than that of bulk water due to a weak interaction with the polymer chain (Taniguchi and Horigome, 1975).

DSC has been widely employed as a tool both to identify and quantify the different types of water occurring within polymers and other systems. In many, but not in all systems, it is possible to identify both free and freezing bound water from DSC traces. However,

identification of water tightly bound to the polymer becomes more complex because this water does not freeze and hence is not visible on the DSC trace. Such water must be measured indirectly. In the literature, two lines of thinking have been followed in order to quantify bound water content in various systems.

In the first technique, bound water is found by calculations based on equation 3.1 (Nakamura et al, 1981):

Equation 3.1 $W_{nf} = W_t - W_m$

where W_{nf} = non-freezing (or bound water)

W_t = total water content

W_m = freezing water

By calculating the freezing water content from the DSC endothermic melting peak(s) and subtracting this from the total water content, the difference may be approximated to that water which does not freeze and is tightly bound to the polymer. In some cases, the total amount of freezing water was calculated using the exothermic peaks of crystallization on the DSC cooling curves (Nakamura et al, 1983b; Danjo et al, 1995) due to overlapping melting endotherms for frozen bound water and free water on the DSC heating curves. This hypothesis (equation 3.1) has been applied to quantify the bound water in various cellulose systems (Taniguchi and Horigome, 1975; Deodhar and Luner, 1980; Nakamura et al, 1981, 1983a, 1983b; Hatakeyama et al, 1987; Aoki et al, 1995; Berthold et al, 1996), and in various other diverse systems such as poly (vinyl alcohol) membranes (Zhang et al, 1989); hyaluronic acid and its esters (Joshi and Topp, 1992); actin (Kakar and Bettelheim, 1991); soy proteins (Muffet and Snyder, 1980); bovine corneas (DeMali and Williams, 1994); poly (vinyl alcohol) films (Hodge et al, 1996); and a range of polymer systems (Hatakeyama et al, 1979, 1984, 1985, 1988, 1995).

Alternatively, it is possible to calculate bound water content by plotting enthalpy change (ΔH , Jg^{-1}) (calculated from the DSC endothermic melting peak) against water content and extrapolating through the line of best fit to the intercept on the water content axis which, in theory, should give a value for non-freezing (or bound) water. This method has been employed to examine bound water content in cellulosic materials (Nelson, 1977); co-polymer hydrogels (Kim et al, 1983); various polymers including poly (ethylene oxide) (Ohno et al, 1983); biomedical hydrogels (Sung, 1986); HPMC gels (Ford and Mitchell, 1995); water/chitosan systems (Ratto et al, 1995) and in peat (McBrierty et al, 1996).

Biswas et al (1975) and Kumsah et al (1976) assumed that the amount of non-freezing water may be related to an observed decrease in the enthalpy of fusion values obtained when water within polymer systems melts during DSC analysis, when compared to the enthalpy of fusion values of pure water. The quantity of non-freezing water may be calculated from equation 3.2 (Kumsah et al, 1976):

Equation 3.2

$$\frac{\Delta H_f^1 - \Delta \bar{H}_f}{\Delta H_f^1} \times \text{total weight of water in solution} = \text{non-freezing water}$$

where ΔH_f^1 is the heat of fusion of pure water

$\Delta \bar{H}_f$ is the average molar enthalpy of fusion

Khankari et al (1992) used DSC to determine the water content in a number of pharmaceutical hydrates. The calculations were based on a comparison between the literature value of the enthalpy of fusion of pure water and the enthalpy of fusion values associated with desolvation endotherms. This method of determining water content is

based on the assumption that the enthalpy of binding of n moles of water in the hydrate is the same as that of n moles of water molecules in liquid water.

3.1.1 Objectives

The objectives of the work presented in this chapter are to identify and quantify the water distribution within HPMC K15M gels using DSC. The influences of HPMC K15M concentration, gel storage time, heating and cooling rates during DSC analysis, gel preparation method and the influence of batch to batch variation are studied.

3.2 Materials

Methocel HPMC K15M cellulose ethers were obtained from the DOW Chemical Company (section 2.1.1; Table 2.1). The batches of HPMC K15M characterised were BN MM93042103K and BN MM94112811K respectively.

3.3 Methods

3.3.1 Gel Preparation

HPMC K15M gels (5-25% w/w) were prepared as outlined in section 2.2.1. All gels were stored at 4-6°C from 2 to 96h and water losses during both preparation and storage were taken into account when determining final polymer concentration in the gels. HPMC K15M gels (>25% w/w) were prepared from gels (15-20% w/w) as outlined in section 2.2.1 and were stored for 24 to 96h at ambient temperatures to allow equilibration and uniform water distribution in the gels before analysis. Two batches of HPMC K15M (section 2.1) were examined in this chapter, and the batch numbers are quoted in the text.

3.3.2 Thermal Analysis

A Perkin-Elmer DSC7 (Beaconsfield, UK) with an attached liquid nitrogen based cooling accessory controlled by a Perkin-Elmer TAC-7 was employed as described in section 2.2.2.1. Gel samples were cooled and heated at different scanning rates (section 2.2.2.1) in the temperature range of -30°C to $+35^{\circ}\text{C}$.

3.4 Results and Discussion

3.4.1 Differential Scanning Calorimetry studies

3.4.1.1 The influence of HPMC K15M on DSC spectra of water

In this study, the crystallization and melting of pure water were examined and subsequently the effect of HPMC K15M on the phase transitions of water was characterised. Gels containing 10 and 20% (w/w) HPMC K15M (BN MM93042103K) were used initially to characterise the effects of polymer concentration on the DSC scans of HPMC gels.

Figure 3.1 shows a typical DSC endothermic scan for the melting of double distilled water which was cooled from $+35^{\circ}\text{C}$ to -30°C at $-10^{\circ}\text{Cmin}^{-1}$ and heated to $+35^{\circ}\text{C}$ at $+5^{\circ}\text{Cmin}^{-1}$. A single sharp peak is produced. Typically, the temperature at which water freezes on the cooling run ($-18.90 \pm 3.13^{\circ}\text{C}$; $n = 3$) was lower than the temperature at which ice melts on the heating run ($+0.31 \pm 0.20^{\circ}\text{C}$; $n = 3$). Similarly, the value obtained for the enthalpy of freezing of water ($231.52 \pm 5.12\text{Jg}^{-1}$; $n = 3$) was lower than the enthalpy of melting of ice ($312.28 \pm 9.90\text{Jg}^{-1}$; $n = 3$). This anomaly has been explained by the phenomenon of supercooling which occurs in liquid water. Essentially, supercooling may be defined as the cooling of a liquid below its freezing point without

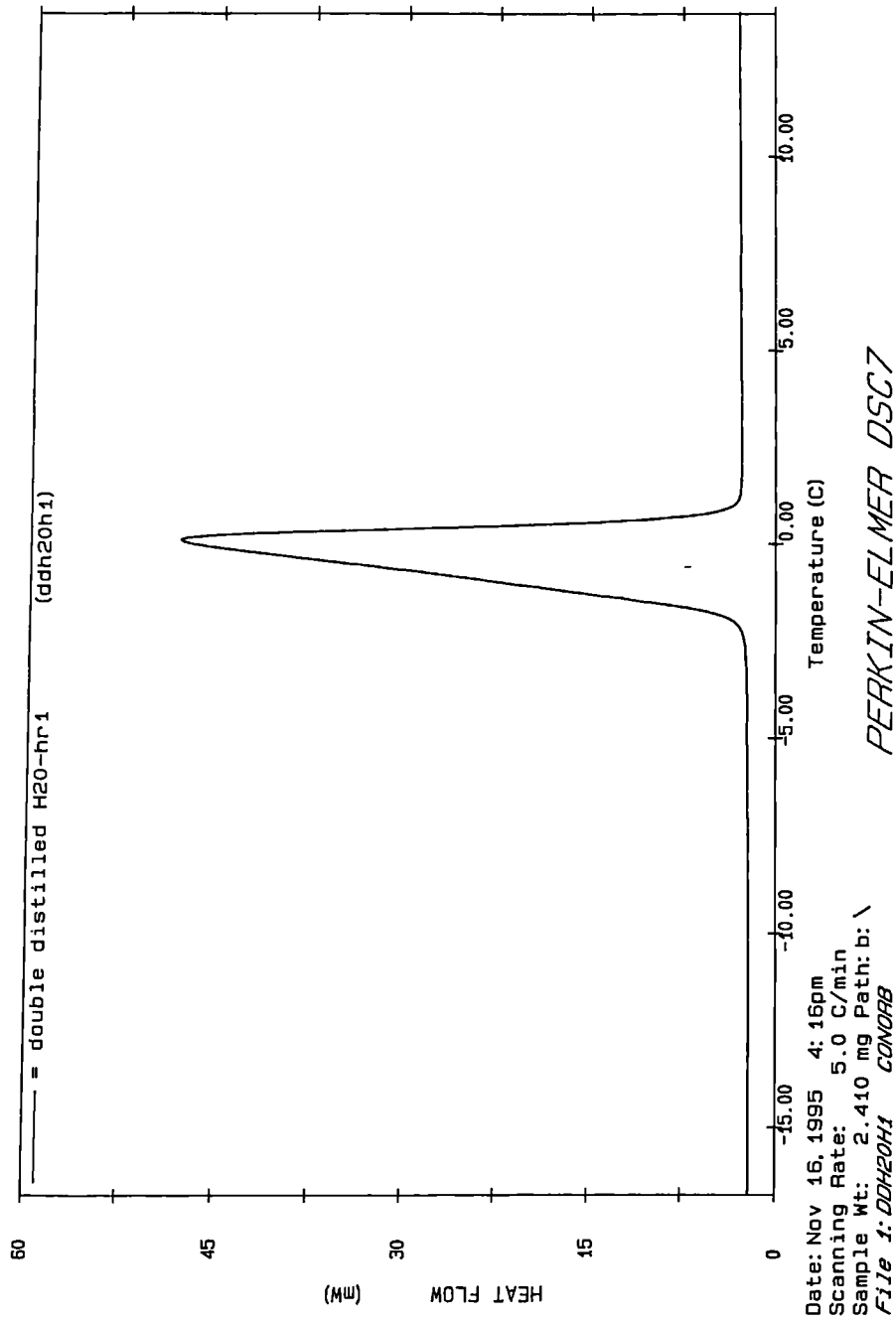


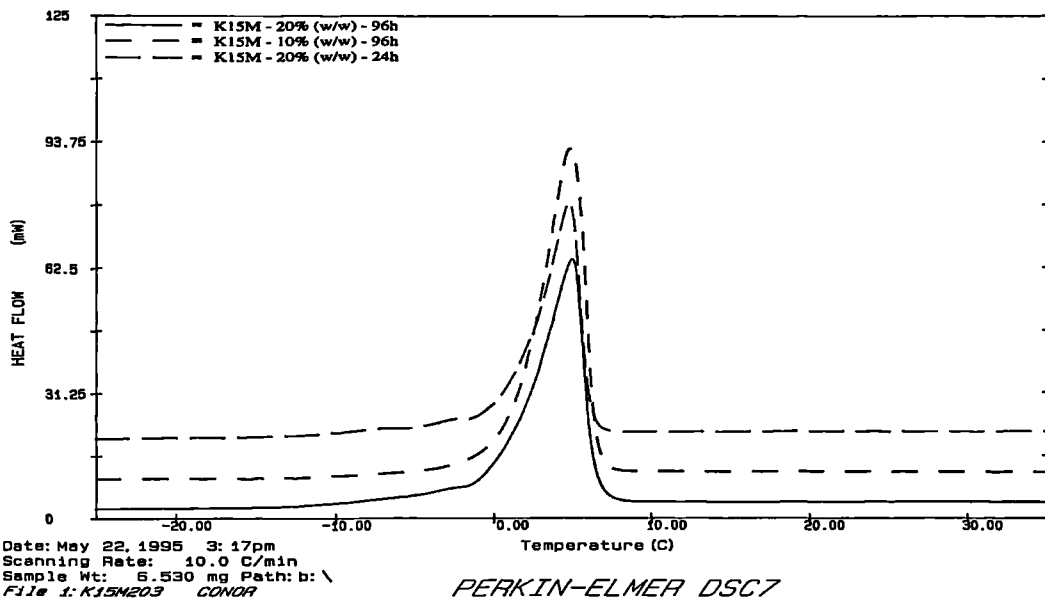
Figure 3.1 : DSC scan of double distilled water cooled at $-10^{\circ}\text{Cmin}^{-1}$ and heated at $+5^{\circ}\text{Cmin}^{-1}$

separation of the solid phase (Harrison, 1976). A characteristic property of supercooled liquids is a high viscosity in the vicinity of the freezing point which has been discussed in the case of water by a number of authors (Bassez et al, 1987; Vedamuthu et al, 1994 and Bartell & Huang, 1994). It is reported (Rasmussen et al, 1973; Angell et al, 1982), that the heat capacity of water increases very rapidly on cooling below -15°C , as expressed by equation 3.3 (Angell et al, 1982):

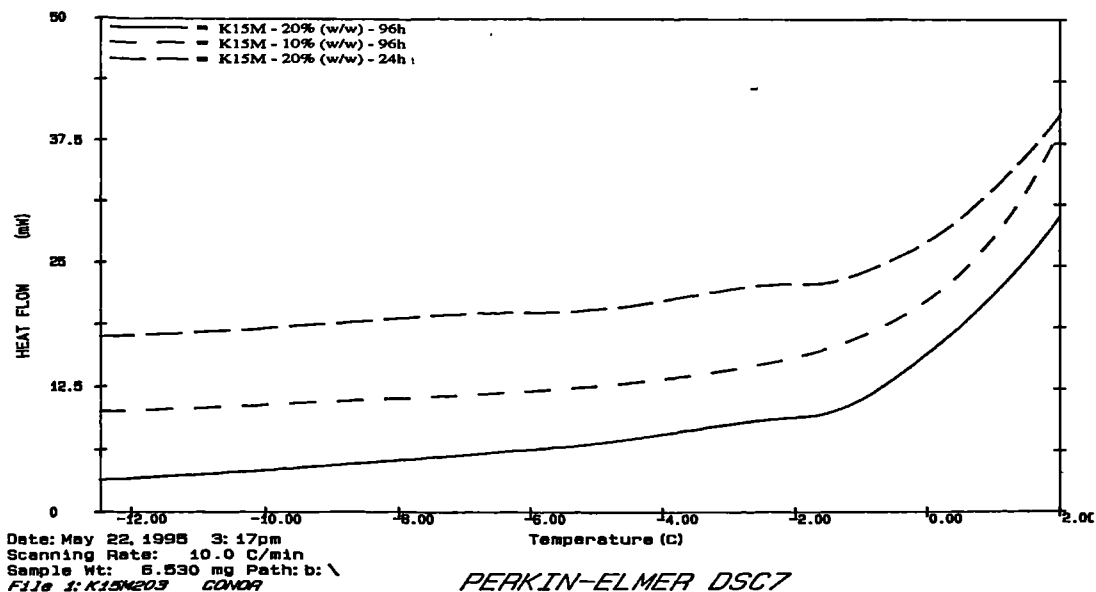
$$\text{Equation 3.3} \quad \Delta H(T) = \Delta H(273) - \int_T^{273} \Delta C_p dT$$

in which the crystallization enthalpy, $\Delta H(T)$, is lower than that of bulk water at 273 K, where ΔC_p is the difference in heat capacities of ice and supercooled water. This equation has been employed to correct the enthalpy of fusion of supercooled water for onset temperatures less than 0°C (Higuchi and Iijima, 1985; Zhang et al, 1989; Joshi and Topp, 1992).

Figure 3.2 shows DSC scans typical of HPMC K15M gels that were stored at $4-6^{\circ}\text{C}$ for 24 or 96h and then cooled from $+35^{\circ}\text{C}$ to -30°C at a variety of cooling rates (rapid cooling to $-5^{\circ}\text{Cmin}^{-1}$) (section 2.2.2.1) and heated to $+35^{\circ}\text{C}$ at a constant $+10^{\circ}\text{Cmin}^{-1}$ heating rate. Figure 3.2b is an expansion of the area to the left of the main endotherm for the melting of free water in Figure 3.2a. Pre-endothermic event(s) were visible at all cooling rates in the case of gels containing 20% w/w HPMC K15M. No such event(s) were apparent for gels containing 10% w/w HPMC K15M. It has been reported that the pre-endothermic events may be related to the presence of different types of water. Pre-endothermic events, typical of those seen in this work have previously been reported in HPMC K4M : carbopol mixtures and identified as different water types being present in the melting process (Perez-Marcos et al, 1994). These pre-endothermic events have also been attributed to overlapping ice melting (first order) and glass transition (second order) phase transitions (see section 1.3.1). Roos and Karel (1991) have reported that the



(a)



(b)

Figure 3.2 : DSC scan of HPMC K15M 20% w/w gel stored for 24h at a heating rate of $+10^{\circ}\text{Cmin}^{-1}$ (top). DSC scans of HPMC K15M 10% w/w and HPMC K15M 20% w/w gels, after 96h storage, scanned at a heating rate of $+10^{\circ}\text{Cmin}^{-1}$, indicating the appearance of a pre-endothermic event at the higher concentration (bottom scans)

(a) from -25 to +35°C

(b) from -12.5 to +2°C

temperature difference between the glass transition and onset of ice melting in maltose and maltodextrins decreased with increasing molecular weight. For high molecular weight compounds, the glass transition temperature and the onset of ice melting were found to be equal. Ratto et al (1995) (section 1.3.1) have attributed pre-endothermic events present in water/chitosan systems as being due to cold crystallization. This occurs in systems where only non-freezing and freezing bound water are present. Upon heating, some of the non-freezing water becomes mobile, comes into contact with solid freezing bound water and forms ice. A crystallization exotherm is subsequently visible.

Further gel concentrations were characterised to establish the concentration at which pre-endothermic events first appeared. HPMC K15M gel samples (10-28% w/w) (BN MM93042103K) were prepared as described in section 2.2.1 and stored at ambient temperature overnight. They were scanned from +35°C to -30°C at -10°Cmin⁻¹ and then heated from -30°C to +35°C at +10°Cmin⁻¹.

Pre-endothermic events occurring on the leading edge of the main endotherm first appeared at 16% (w/w) HPMC K15M. Below this concentration, e.g. 15% (w/w), no such events were visible. As the gel concentration was increased to 28% (w/w), the pre-endothermic events became more exaggerated, possibly indicating increasing amounts of water loosely bound to the polymer.

3.4.1.2 Effect of gel storage time on water distribution

To further characterise the pre-endothermic peaks visible in HPMC K15M gels at 20% (w/w) concentration, the influence of hydration time on the occurrence of these events was studied.

HPMC K15M (20% w/w) (BNMM93042103K) gels were prepared as described in

Table 3.1 : Effect of cooling rate ($^{\circ}\text{Cmin}^{-1}$) and gel storage time (h) on the melting enthalpy of HPMC K15M 20% w/w gels (n = 3)

Cooling rate ($^{\circ}\text{Cmin}^{-1}$)	Melting Enthalpy in Jg^{-1}	
	2 h old samples	24 h old samples
Rapid	251 ± 7	206 ± 9
-100	271 ± 28	232 ± 8
-10	253 ± 13	205 ± 15
-5	261 ± 42	197 ± 1

section 2.2.1 and stored at 4-6 $^{\circ}\text{C}$ for 2 and 24h. Samples were cooled using a variety of cooling rates (rapid cooling to $-5^{\circ}\text{Cmin}^{-1}$) and then heated at a constant heating rate of $+10^{\circ}\text{Cmin}^{-1}$. No pre-endothermic events were visible at any cooling rate for gels stored for 2h. However, a number of pre-endothermic events were visible in the case of 20% w/w HPMC K15M gels stored for 24h (Figure 3.2).

Table 3.1 shows the melting enthalpies of HPMC K15M (20% w/w) gels stored for 2 and 24h at a variety of cooling rates from rapid cooling to $-5^{\circ}\text{Cmin}^{-1}$. It is evident from the standard deviation in Table 3.1, that the enthalpies of melting for gels stored for 2h showed a much wider spread than the data obtained for 24h samples. The 2h gels may have not been homogeneous because such gels take some time to fully hydrate and insufficient time was given for this hydration process to occur. It may be assumed that the DSC peaks in these samples represent the bulk water with little or no influence from the polymer. These results are in contrast to those reported by Ford and Mitchell (1995), where the melting enthalpies increased as the storage time of HPMC K15M gels

increased over a similar time period. Batch to batch variation and, indeed, an exact method of gel preparation may be contributing factors towards this apparent anomaly.

3.4.1.3 Further moisture characterization of HPMC K15M gels

It has been established that the concentration of HPMC K15M (section 3.4.1.1) and hydration time (section 3.4.1.2) are contributing factors to the type and number of endothermic peaks appearing in DSC scans. In this section, the influence of HPMC K15M concentrations from 10 - 55 (%w/w) were explored. The HPMC K15M (10 - 55% w/w) (BN MM93042103K) gel samples were prepared and stored for either 24 or 96h before analysis. Typical DSC scans for 96h-old HPMC K15M gels of different concentrations are shown in Figure 3.3. More than one event is clearly apparent on the endotherms of gels containing more than 10% (w/w) polymer. These events were more exaggerated at the higher polymer concentrations. Similar events were present in the DSC spectra of 24h-old samples. The data from 24 and 96h samples were statistically analysed to determine whether there was a significant difference between the two sets of data. A computer statistical software programme (Minitab V. 10) was employed to carryout analysis of variance using the general linear model (GLM) in the covariate mode. The results (Table 3.2) show that for $c1*c3$, where $c1$ = polymer : water ratio; $c2$ = enthalpy (Jg^{-1}) and $c3$ = number of variables in each subset i.e. 24 or 96h; $p = 0.040$, therefore, $p > 0.01$ which indicates that a significant difference exists between the data for 24 and 96h samples. It would seem that the interaction of water with HPMC K15M polymer is dependent on gel hydration time and this was quantified by calculating the distribution of bound water in HPMC K15M gels after 24 and 96 hours in the following section.

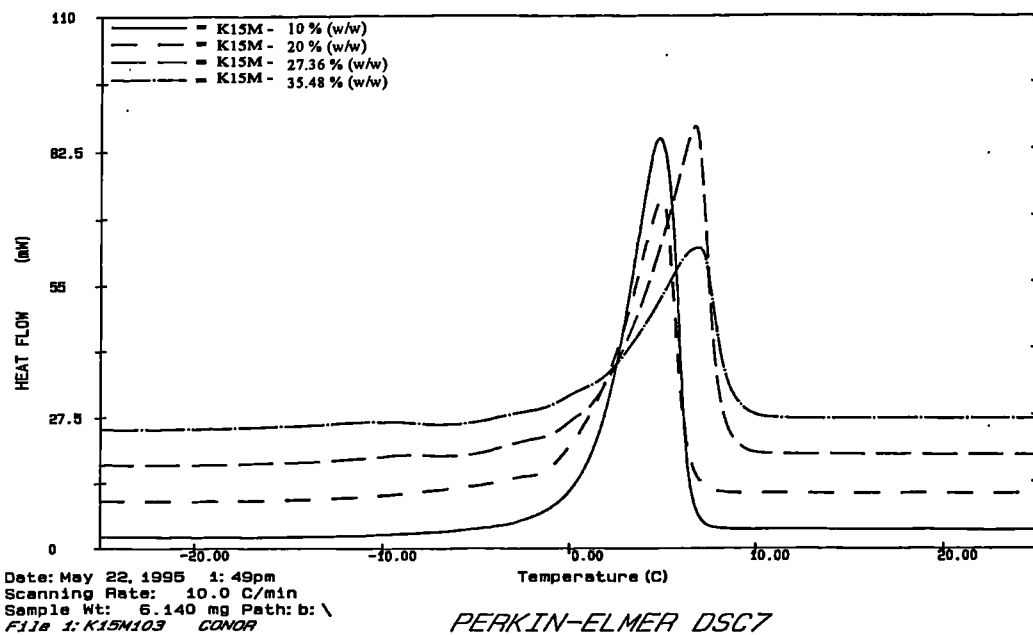
Table 3.2 : Statistical analysis of the water distribution within HPMC K15M (BN MM93042103K) gels after storage for 24 or 96h using GLM (general linear model) in Minitab statistical analysis program

Source	DF	Seq SS	Adj SS	Adj MS	F	p
c1	1	42960	57872	57872	43.71	0.000
c3	1	10365	8038	8038	6.07	0.021
c3*c1	1	6223	6223	6223	4.70	0.040
error	24	31774	31774	1324		
total	27	91322				

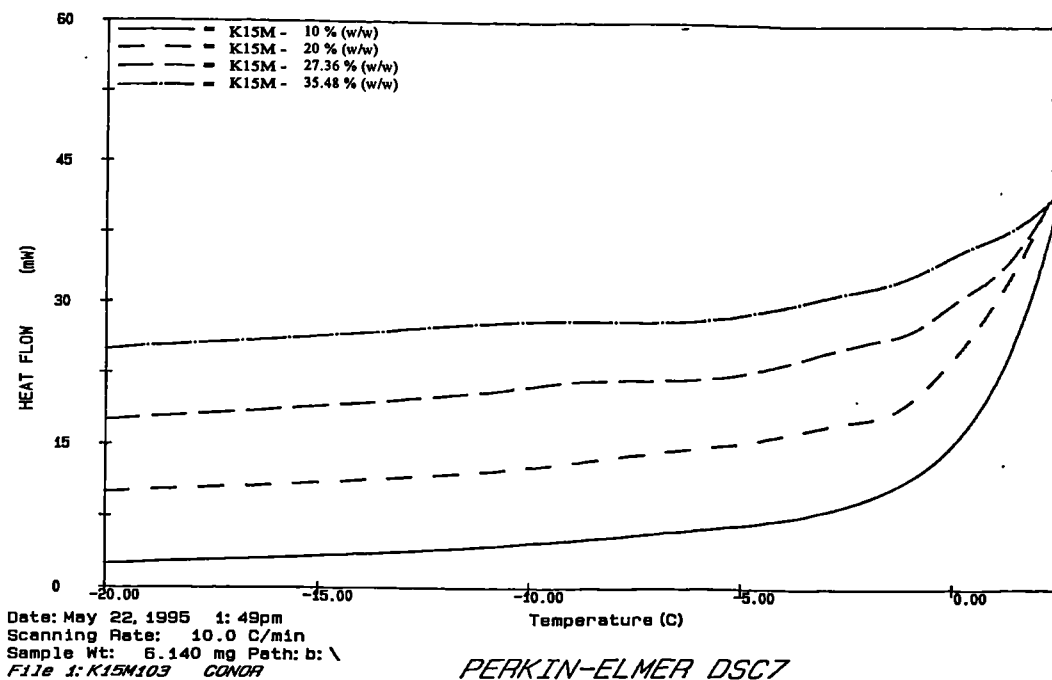
Term	Coefficient	S. D.	t-value	p
constant	-260.27	66.06	-3.94	0.001
c1	6.1208	0.9258	6.61	0.000
c1*c3	2.0071	0.9258	2.17	0.040

Key

Seq SS	sequential sums of squares
Adj SS	adjusted sums of squares
Adj MS	adjusted mean of squares



(a)



(b)

Figure 3.3 : DSC scans of HPMC K15M gels stored for 96h, showing the effect of concentration on endothermic events at a $+10^{\circ}\text{Cmin}^{-1}$ heating rate
 (a) from -25 to $+25^{\circ}\text{C}$ (b) from -20 to $+2^{\circ}\text{C}$

3.4.1.3.1 Quantitative analysis of water distribution within HPMC K15M gels

The number of moles of non-freezing water per polymer repeating unit (PRU) was determined according to the procedure reported by Ford and Mitchell (1995). Enthalpy change (Jg^{-1}) for HPMC K15M gels cooled to -30°C at $-100^{\circ}\text{Cmin}^{-1}$ and heated to $+35^{\circ}\text{C}$ at $+10^{\circ}\text{Cmin}^{-1}$ after 24 and 96h storage was plotted against % water content (Figure 3.4). The plots were extrapolated to zero enthalpy, through the lines of best fit, where the concentration is the minimum water content required for complete hydration of HPMC K15M. All water present at this point was taken as bound water. It is assumed that a linear relationship exists between melting enthalpy and % water content over the full range of polymer concentrations used in this work. However, this assumption may not apply at higher polymer concentrations. The % ratio of HPMC K15M : water at zero enthalpy were found to be 58 : 42 after 24h ($R^2 = 0.588$; $n = 14$; $p < 0.05$ indicating the significance of fit of a straight line) and 74 : 26 after 96h storage ($R^2 = 0.961$; $n = 13$). The number of moles of non-freezing water (bound water) per polymer repeating unit (PRU) were calculated using these data and the previously quoted PRU value of 192 for HPMC K15M (Ford and Mitchell, 1995). These values were ~ 8 and ~ 3.8 mol for 24 and 96h storage times, respectively.

These results show that less bound water (and hence more free water) is present after 96- compared to 24h-old samples. This may suggest that the hydrating water is released from the polymer during storage between 24 and 96h due to gel syneresis (Mattha, 1977). This is in contrast to data obtained for HPMC K15M 20% (w/w) gels stored for 2 and 24h (Table 3.1). The decrease in free water which occurs from 2 to 24h shown in Table 3.1 may be due to the slow hydration of the polymer and thus attributed to initial equilibration within the gel as some free water becomes more tightly bound to the polymer.

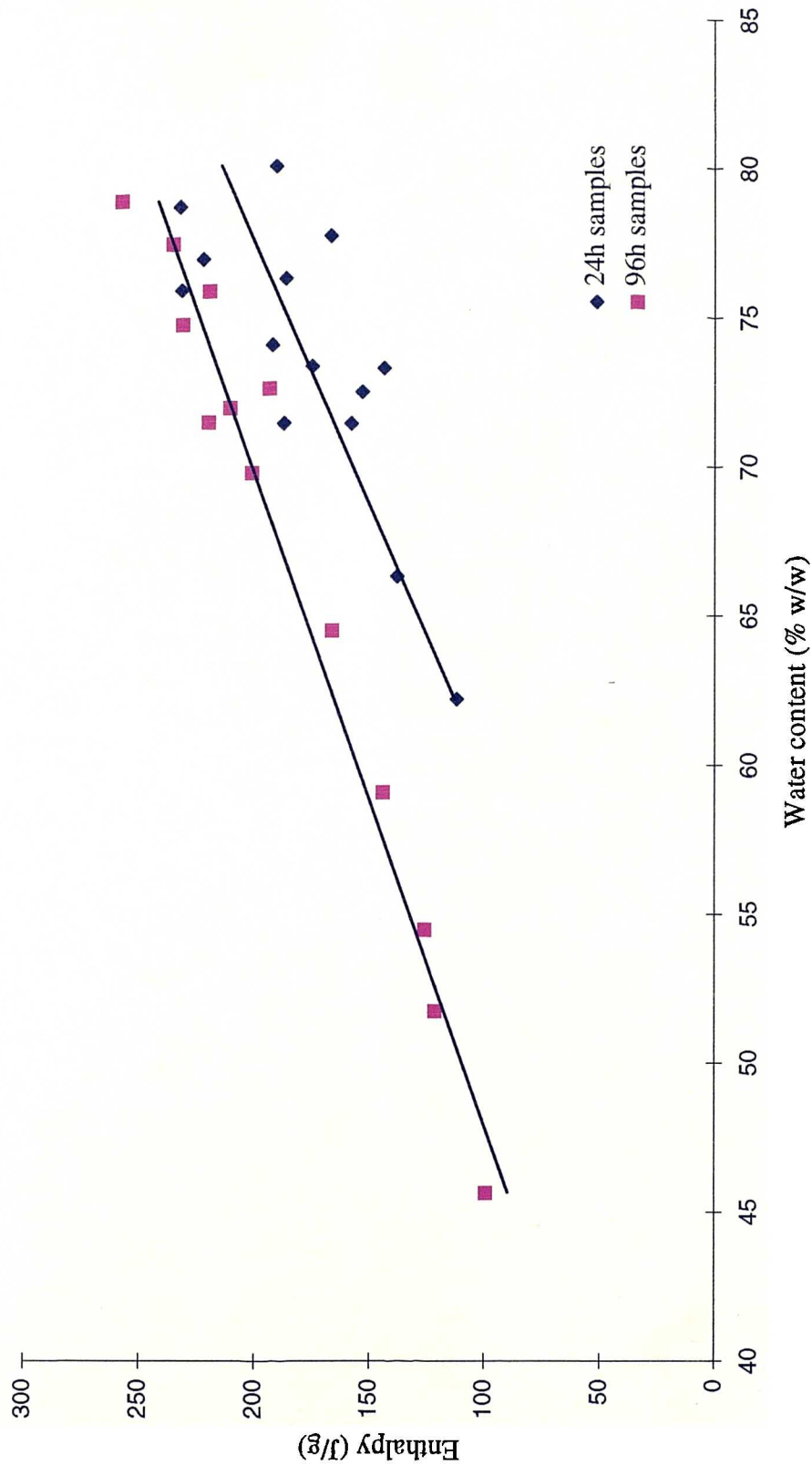


Figure 3.4 : The effect of water content (% w/w) on the melting enthalpy (Jg^{-1}) of HPMC K15M gels after storage for 24 or 96h

3.4.1.4 Effect of cooling and heating rates during DSC analysis on the nature of the thermal events

The occurrence of anomalies around the endotherm produced by the melting of water around 0°C has previously been reported by Nakamura et al (1981) who showed that on DSC heating runs of various cellulose samples, a shoulder existed 'in some cases' on the leading edge of the endotherm. Sung (1986) has also reported the presence of a double endotherm at 0°C in poly(2-hydroxyethylmethacrylate) (pHEMA) hydrogels, whose shape was dependent on the freezing conditions. This was attributed to the presence of different types of water in the pHEMA hydrogels.

After investigation of the effect of polymer concentration and storage time, it would seem logical that if the visible pre-endothermic events were indeed related to different types of water, heating and cooling rates during DSC analysis may influence the occurrence of such events.

The enthalpies of fusion and crystallization temperatures for samples stored for 24 and 96h were unaffected by cooling rate variations (rapid cooling to $-1^{\circ}\text{Cmin}^{-1}$). In the cooling runs, some secondary events were visible (Figure 3.5) (peak from -22.90° to -26.65°C). Although these data were not reproducible, more than one peak on the cooling run may indicate different types of water crystallizing at slightly different temperatures (Nakamura et al, 1983b; Danjo et al, 1995). In the heating runs ($+10^{\circ}\text{Cmin}^{-1}$), it was found that the secondary events were cooling rate dependent. At low cooling rates, e.g. $-5^{\circ}\text{Cmin}^{-1}$, a small endotherm appearing to the left of the main peak was exaggerated (Figure 3.6) (initial peak from -6.84° to $+3.74^{\circ}\text{C}$). Other events were also visible on the leading edge of the main endotherm. As the cooling rate increased (e.g. $-50^{\circ}\text{Cmin}^{-1}$), the initial small endotherms were not as exaggerated. However, the other events on the main endotherm remained visible.

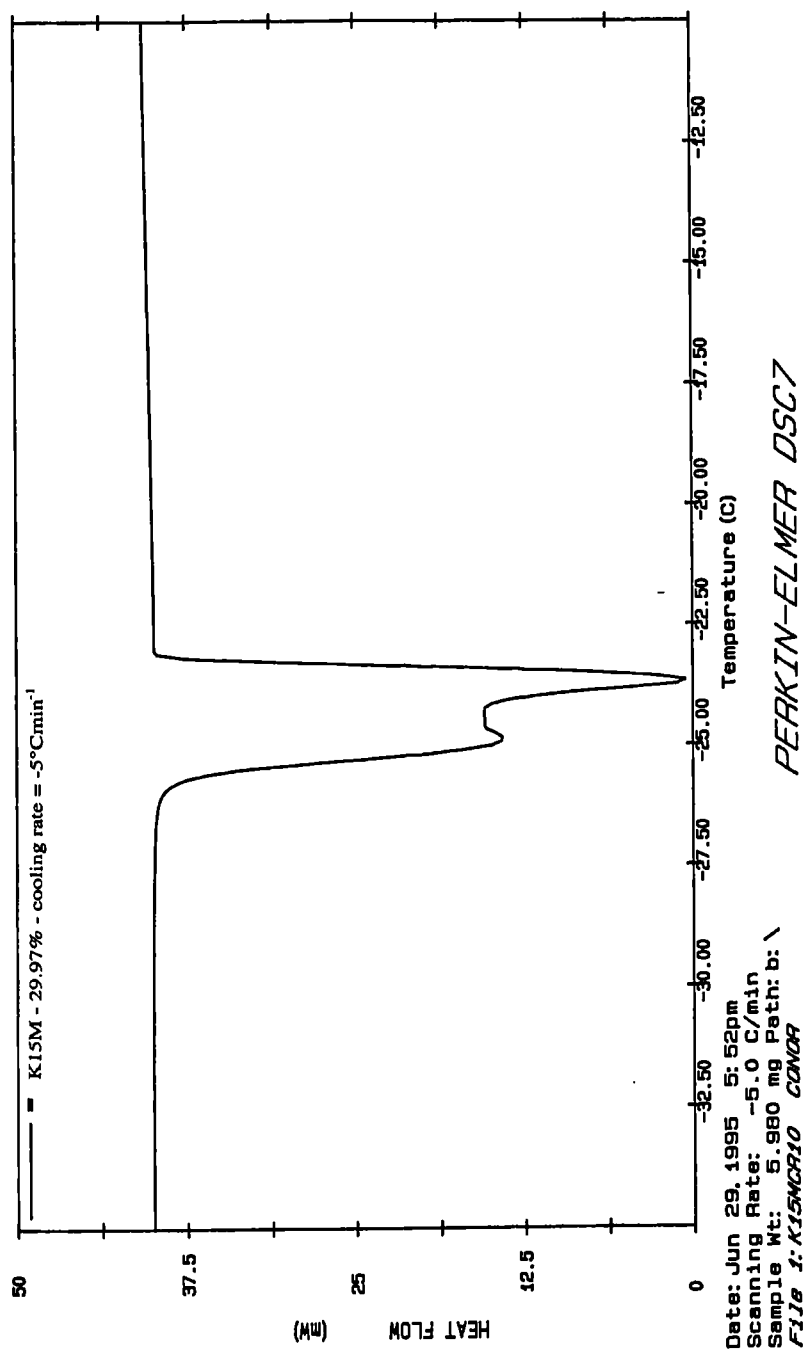
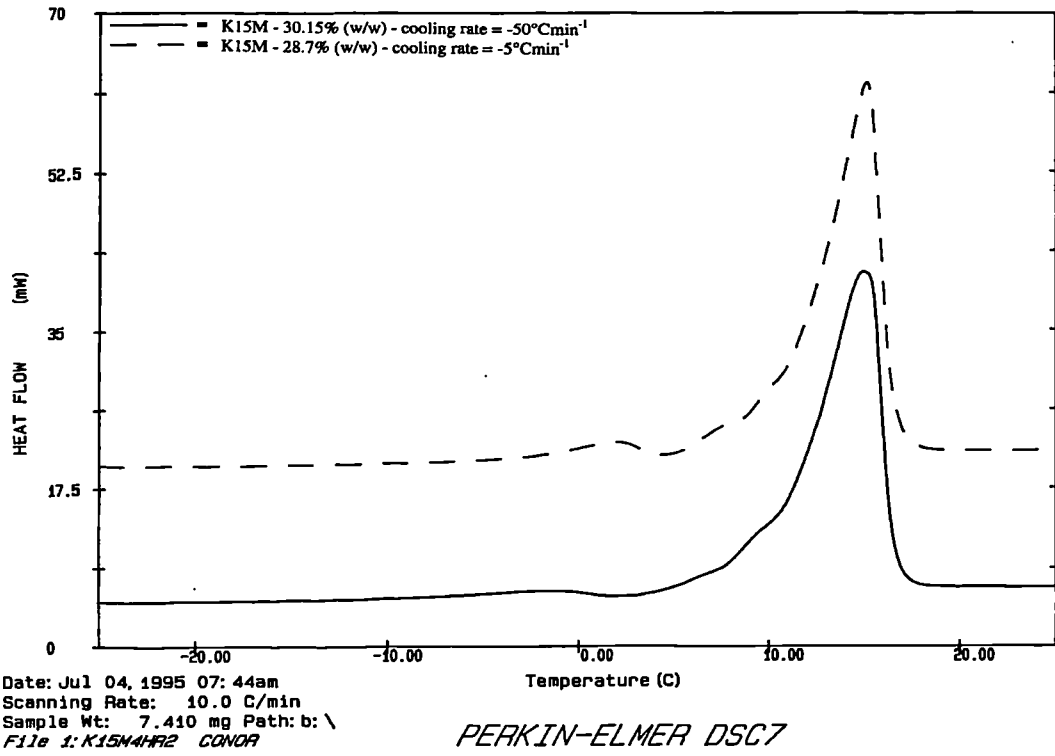
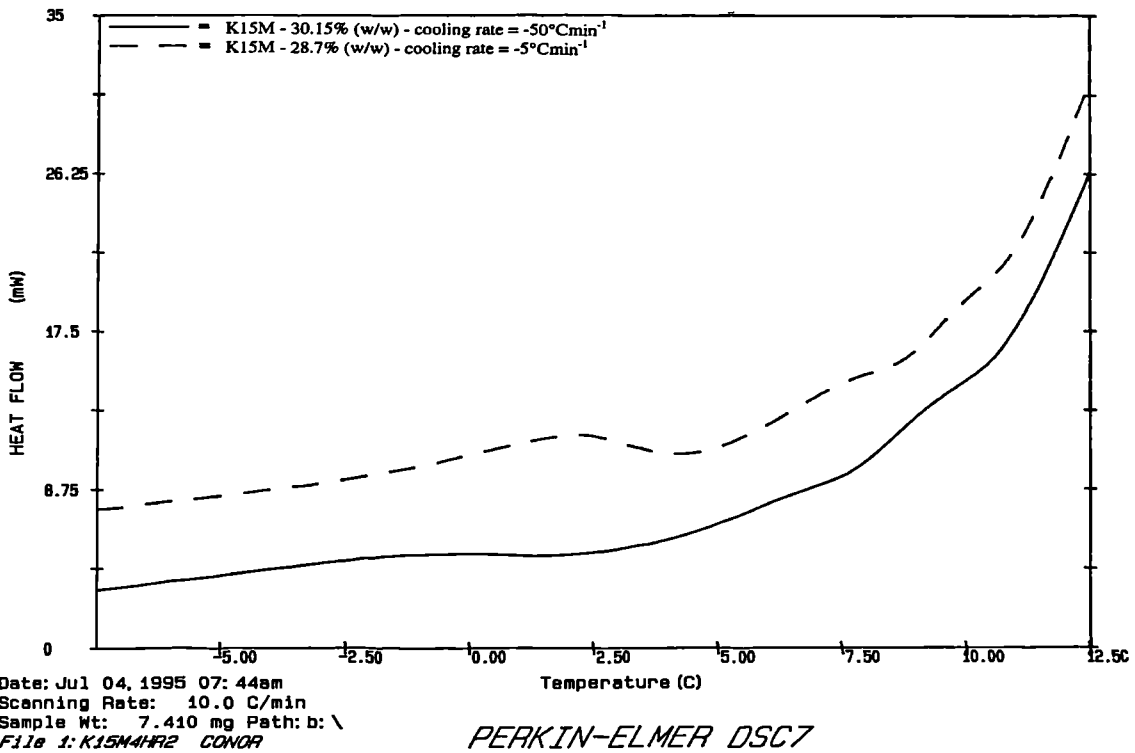


Figure 3.5 : DSC cooling curve of HPMC K15M 29.97% (w/w) gel at a -5°Cmin⁻¹ cooling rate after 24h storage



(a)



(b)

Figure 3.6 : DSC scans of HPMC K15M gels after 96h storage following cooling at $-50^{\circ}\text{Cmin}^{-1}$ or $-5^{\circ}\text{Cmin}^{-1}$

(a) from -25 to $+25^{\circ}\text{C}$

(b) from -7.5 to $+12.5^{\circ}\text{C}$

When a sample of HPMC K15M (20% w/w) (BN MM93042103K) gel was cooled to -50°C , then heated to the point at which secondary events first appeared ($\sim -9^{\circ}\text{C}$) and subsequently re-cooled and reheated to $+35^{\circ}\text{C}$, the secondary events remained visible (heating/cooling rates $\pm 10^{\circ}\text{Cmin}^{-1}$) (Figure 3.7). Upon cooling to -50°C and heating to -9°C and holding for 10mins, and then re-cooling and reheating again indicated that the presence of the secondary events remained unaffected. This would indicate that such events are indeed quite 'real' and may be linked to the presence of different water types that exist in HPMC K15M gels or may indicate the existence of a glass transition around the melting temperature of free water.

The enthalpies of fusion and crystallization for samples stored for both 24 and 96h were unaffected by heating rate variations. In the cooling runs ($-10^{\circ}\text{Cmin}^{-1}$), some secondary events were found to be visible but were not reproducible. This is because recrystallization occurs by nucleation and, as such, is an uncontrolled phenomenon. At a heating rate of $+50^{\circ}\text{Cmin}^{-1}$, an initial small endotherm is clearly seen (Figure 3.8). As the heating rate was decreased to $+1^{\circ}\text{Cmin}^{-1}$, this initial endotherm was not as exaggerated and other inflections became more evident on the main endotherm (Figure 3.9).

At the molecular level, a very low cooling rate would allow the associated water to freeze slowly and combine more tightly with the polymer. In a constantly changing dynamic situation, the amount of bound water will thus tend to increase and will appear as a more pronounced peak to the left of the main endotherm (Figure 3.6). The cooling rate did not affect the other smaller undefined peaks on the edge of the main peak but affected the pre-endothermic peak which may be related to closely associated or 'bound' water. If this pronounced endotherm indicates the presence of a type of 'bound' water, then the other small events visible on the leading edge of the main endotherm may be considered as other, as yet undefined, types of water, or possibly the presence of a glass transition occurring. On the other hand, at high heating rates ($+50^{\circ}\text{Cmin}^{-1}$), this closely associated water, tends to come off as a single small endotherm towards the lower

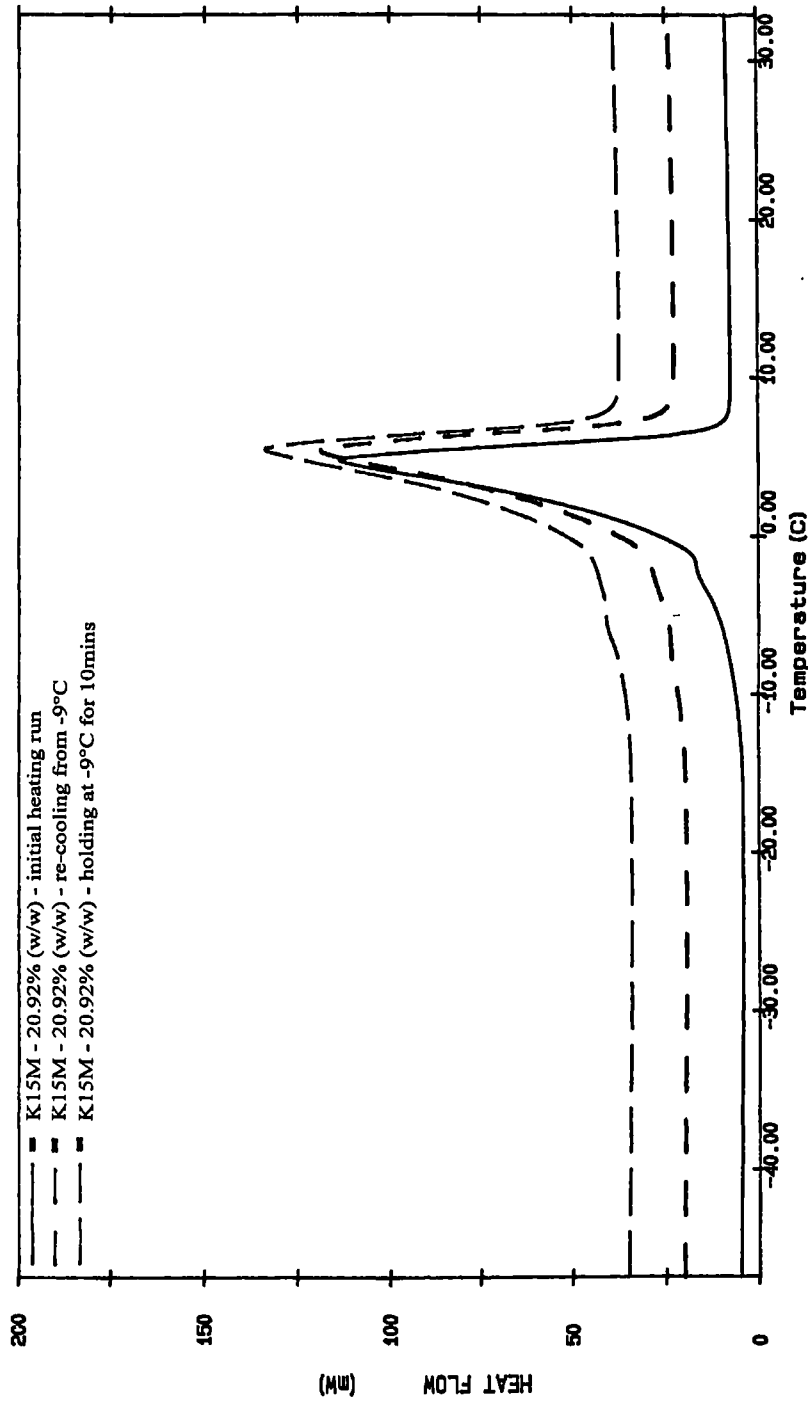


Figure 3.7 : DSC scans of a HPMC K15M 20.92% (w/w) gel sample recooled and reheated around the initial point of inflection of the baseline

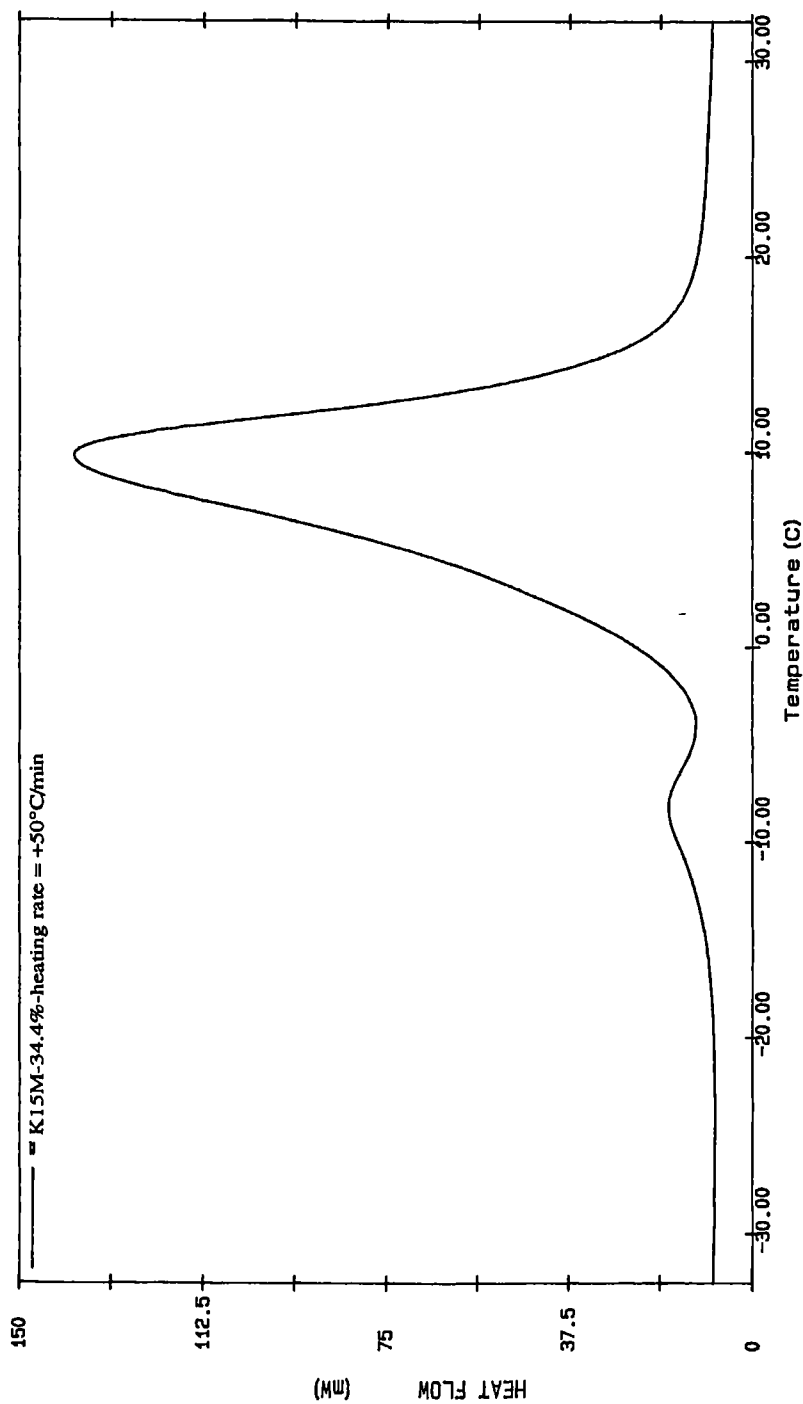


Figure 3.8 : DSC scan of HPMC K15M gel stored for 24h at a heating rate of +50°Cmin⁻¹ following cooling at -10°Cmin⁻¹

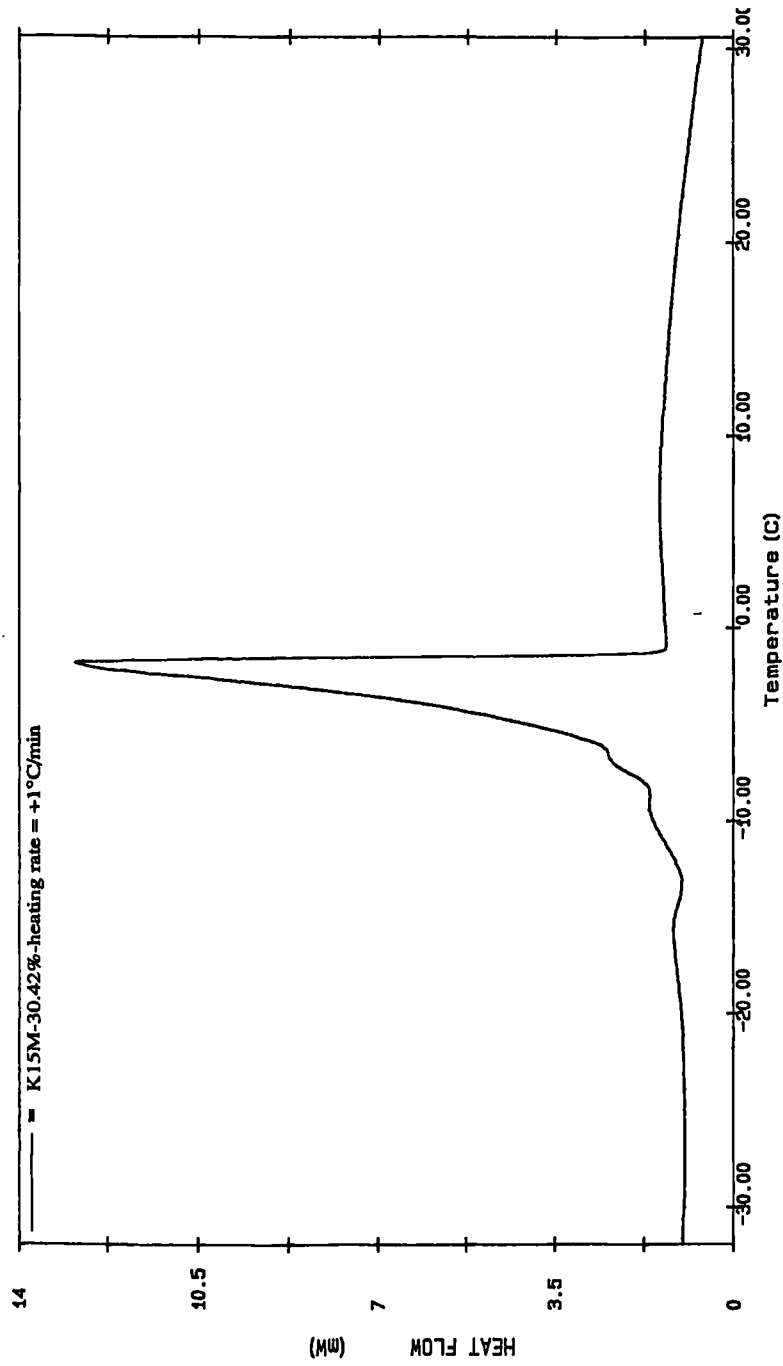


Figure 3.9 : DSC scan of HPMC K15M gel stored for 24h at a heating rate of +1°Cmin⁻¹ following cooling at -10°Cmin⁻¹

temperature side of the main peak (Figure 3.8). When the heating rate is lower ($+1^{\circ}\text{Cmin}^{-1}$), this water comes off as a number of separate events, possibly, indicating the presence of more than one type of closely associated water (Figure 3.9). It appears (from Figure 3.8) that either some recrystallization may be occurring between the two melting events, or alternatively a glass transition is present. This phenomenon of the appearance of a recrystallization exotherm on the DSC heating trace has been previously reported by Murase (1993) in cross-linked dextrans and cross-linked polyacrylamide gels. Similar events have been reported by Ratto et al (1995) using water/chitosan systems. This occurs during the DSC heating run when a portion of the non-freezing water becomes mobile and comes into contact with solid freezing bound water. The mobile water recrystallizes and hence an exotherm is observed during the heating cycle. This exotherm may provide further evidence of the existence of different types of water melting at different temperatures within HPMC K15M gels.

3.4.1.5 Study of batch to batch variation on the water distribution within HPMC K15M gels

The majority of work completed on HPMC K15M gels in this chapter up to this point, was carried out on one particular batch of HPMC K15M (BN MM93042103K). Batch to batch variation may affect the distribution of water within these polymers (see Table 2.1 for comparison of certificates of analysis).

The work completed in section 3.4.1.3 was repeated on a different batch of HPMC K15M (BN MM94112811K) using two gel preparation methods (section 2.2.1). HPMC K15M gels in the 5 - 25% (w/w) concentration range were prepared by mortar and pestle, whereas gels >25% (w/w) were prepared by moisture extraction from gels of lower concentration. Work on gels in the 5 - 25% (w/w) concentration range was repeated twice, and in the second study the storage times examined included both 48, 72 and 120h storage in addition to 24 and 96h storage. The water distribution within the gels after storage was calculated as previously described (section 3.4.1.3.1). Table 3.3

shows that the amount of water bound to the polymer varied both between different batches of HPMC K15M (> 25% w/w concentration range; gels prepared by moisture extraction), and between repeats of the same batch (BN MM94112811K) (5 - 25% w/w concentration range; gels prepared by mortar and pestle) after both 24 and 96h. The release of bound water with time described previously for HPMC K15M (BN MM93042103K) gels prepared by moisture extraction, does not occur in HPMC K15M (BN MM94112811K) gels prepared using either preparation method. Table 3.4 shows that the amount of water bound to HPMC K15M (BN MM94112811K) gels increased with storage time from 24 to 120h. This apparent anomaly may be due either to batch to batch variation or indeed may be due to faults within the gel preparation methods.

Figure 3.10 shows a typical DSC scan for high concentration HPMC K15M (BN MM93042103K) gels stored for either 24 or 96h. Evidence of more than one melting event can be seen to the left of the main melting endotherm for the melting of free water. No events are visible to the right of the main melting endotherm. In high concentration HPMC K15M (BN MM MM94112811K) gels stored for 24h, a double melting peak was present, initially seen in gels of 45.79% (w/w) concentration (Figure 3.11). The second smaller peak to the right of the main melting endotherm, became more accentuated at higher polymer concentrations (Figure 3.12). Similar peaks were visible in HPMC K15M (BN MM MM94112811K) gels stored for 96h, which again were exaggerated with increase in polymer concentration (Figure 3.13).

Clearly, there are differences in water distribution between different batches of HPMC K15M and furthermore, variations exist according to the exact method of gel preparation. Table 3.3 shows that after 24h storage, HPMC K15M (BN MM94112811K) gels (> 25% w/w) prepared by moisture extraction, contain more bound water than HPMC K15M (BN MM94112811K) (5 - 25% w/w) gels prepared by the mortar and pestle method. This may be explained by considering the gel preparation method.

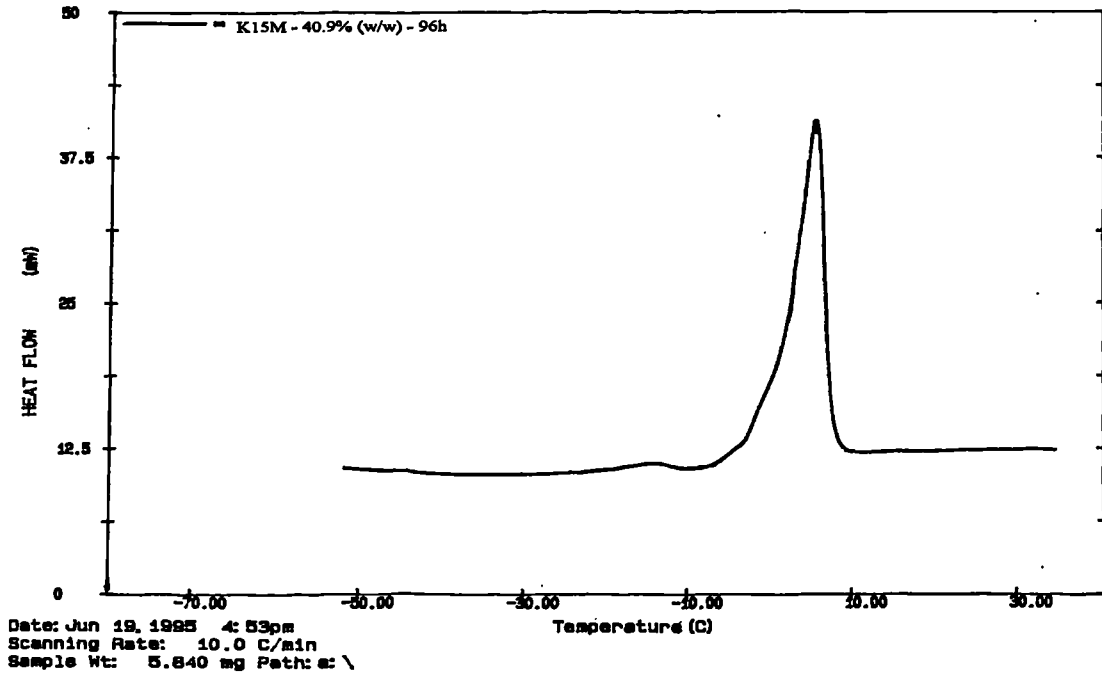


Figure 3.10 : DSC scan of HPMC K15M (BN MM93042103K) 40.9% (w/w) gel cooled at $-100^{\circ}\text{Cmin}^{-1}$ and heated at $+10^{\circ}\text{Cmin}^{-1}$ after 96h storage

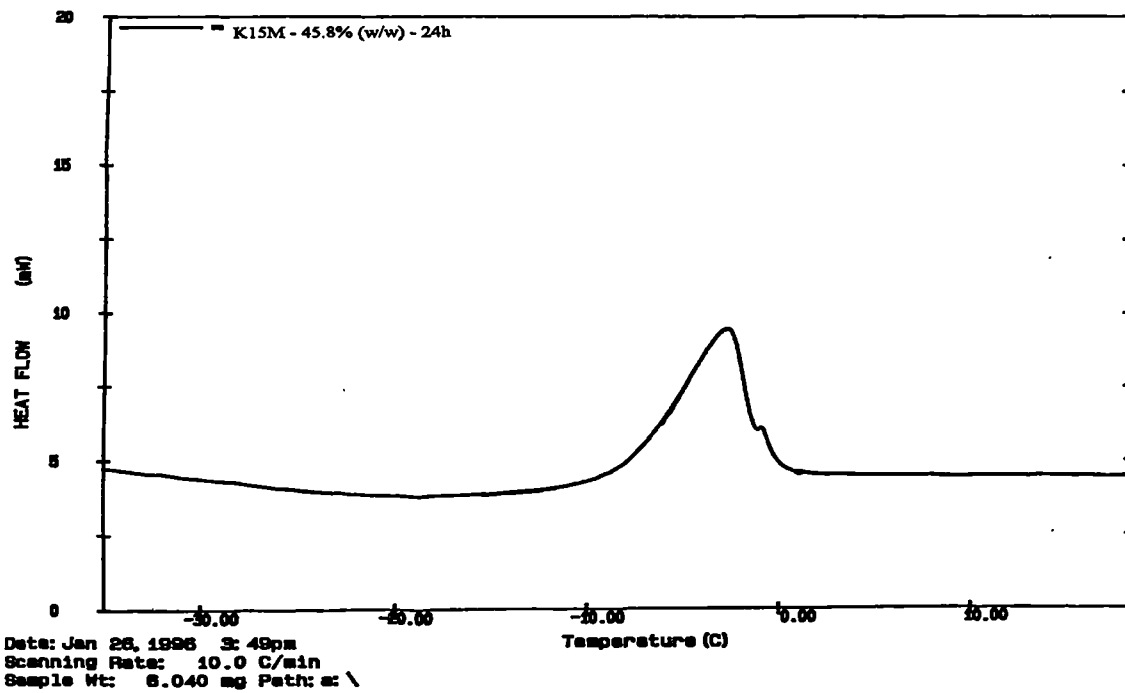


Figure 3.11 : DSC scan of HPMC K15M (BN MM94112811K) 45.8% (w/w) gel cooled at $-100^{\circ}\text{Cmin}^{-1}$ and heated at $+10^{\circ}\text{Cmin}^{-1}$ after 24h storage

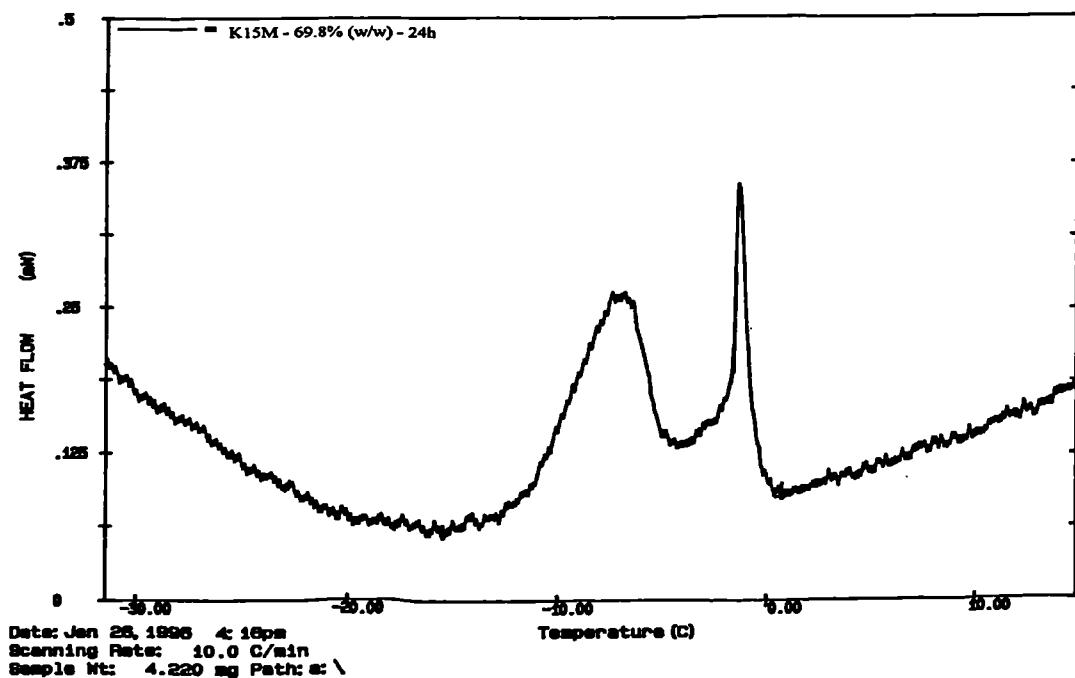


Figure 3.12 : DSC scan of HPMC K15M (BN MM94112811K) 69.8% (w/w) gel cooled at $-100^{\circ}\text{Cmin}^{-1}$ and heated at $+10^{\circ}\text{Cmin}^{-1}$ after 24h storage

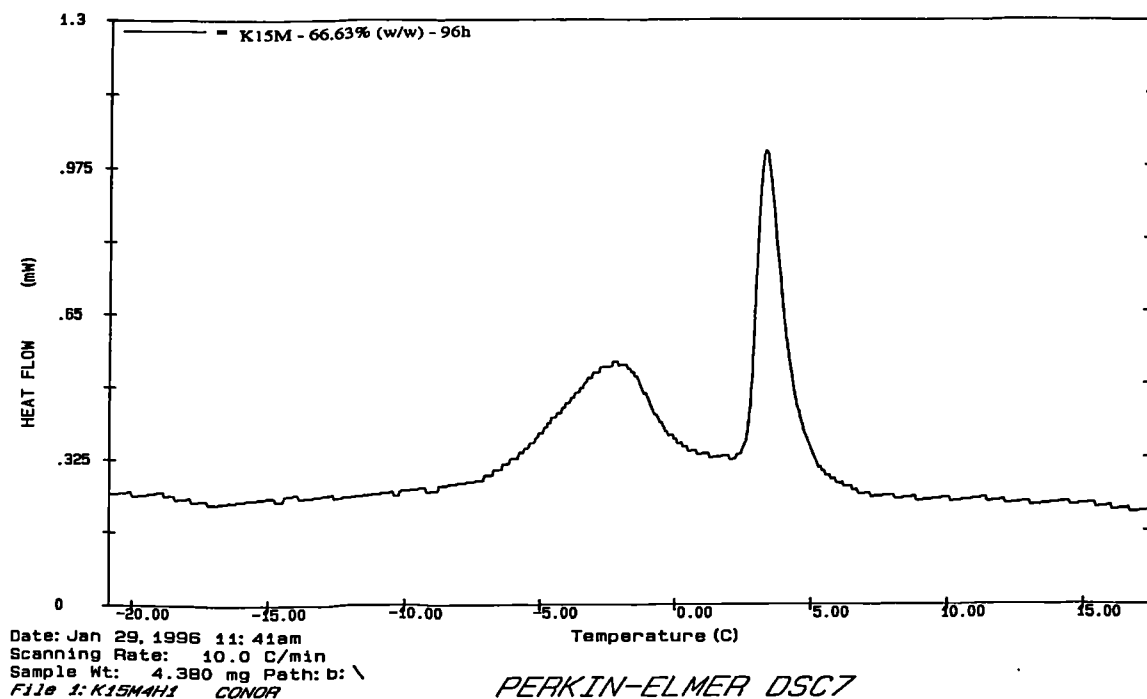


Figure 3.13 : DSC scan of HPMC K15M (BN MM94112811K) 66.6% (w/w) gel cooled at $-100^{\circ}\text{Cmin}^{-1}$ and heated at $+10^{\circ}\text{Cmin}^{-1}$ after 96h storage

Table 3.3 : Effect of batch to batch variation on the water distribution within HPMC K15M gels prepared by mortar and pestle and moisture extraction methods

Preparation method (24h) Batch number	HPMC (% w/w)	H ₂ O (% w/w)	DSC cooling rate (°Cmin ⁻¹)	DSC heating rate (°Cmin ⁻¹)
moisture extraction BN MM93042103K	58	42	-100	+10
moisture extraction BN MM94112811K	60	40	-100	+10
mortar and pestle BN MM94112811K	66	34	-10	+10
mortar and pestle BN MM94112811K	70	30	-10	+10

Preparation method (96h) Batch number	HPMC (% w/w)	H ₂ O (% w/w)	DSC cooling rate (°Cmin ⁻¹)	DSC heating rate (°Cmin ⁻¹)
moisture extraction BN MM93042103K	74	26	-100	+10
moisture extraction BN MM94112811K	59	41	-100	+10
mortar and pestle BN MM94112811K	56	44	-10	+10
mortar and pestle BN MM94112811K	62	38	-10	+10

Table 3.4 : Effect of gel storage time on the water distribution of HPMC K15M (BN MM94112811K) gels prepared using the mortar and pestle method and scanned by DSC at cooling/ heating rates of $\pm 10^{\circ}\text{Cmin}^{-1}$

Gel storage time (h)	HPMC K15M (% w/w)	Mean enthalpy (Jg^{-1}) (\pm SD; n = 3)	HPMC (% w/w)	H ₂ O (% w/w)	Number of moles bound water per PRU
24	4.74	335 \pm 8	70.24	29.76	4.5
	9.32	290 \pm 11			
	14.10	289 \pm 14			
	18.83	264 \pm 16			
	23.82	228 \pm 15			
48	4.75	323 \pm 6	68.20	31.80	5.0
	9.35	292 \pm 9			
	14.12	282 \pm 5			
	18.85	258 \pm 18			
	23.84	219 \pm 11			
72	4.76	332 \pm 8	64.05	35.95	6.0
	9.37	306 \pm 3			
	14.14	272 \pm 11			
	18.86	260 \pm 17			
	23.88	233 \pm 11			
96	4.83	347 \pm 10	61.89	38.11	6.5
	9.38	304 \pm 14			
	14.16	282 \pm 15			
	18.89	246 \pm 11			
	23.92	231 \pm 7			
120	4.89	288 \pm 8	61.62	38.38	6.6
	9.65	265 \pm 0			
	14.03	262 \pm 9			
	19.68	228 \pm 9			
	24.32	185 \pm 7			

In preparing gels using the moisture extraction method, the original gel was, in effect, prepared 24h prior to preparation of higher gel concentrations by removal of moisture. Therefore, DSC analysis after 24h of such samples may be considered as DSC analysis after 48h, thereby allowing more time for polymer hydration. In this chapter and in the remainder of the thesis, determination of bound water contents in cellulose ether gels were completed by examining gels in the 5 - 25% w/w concentration range prepared by the mortar and pestle method. Use of the moisture extraction method of gel preparation was employed only in some specific cases when specific melting events were examined in high concentration gels.

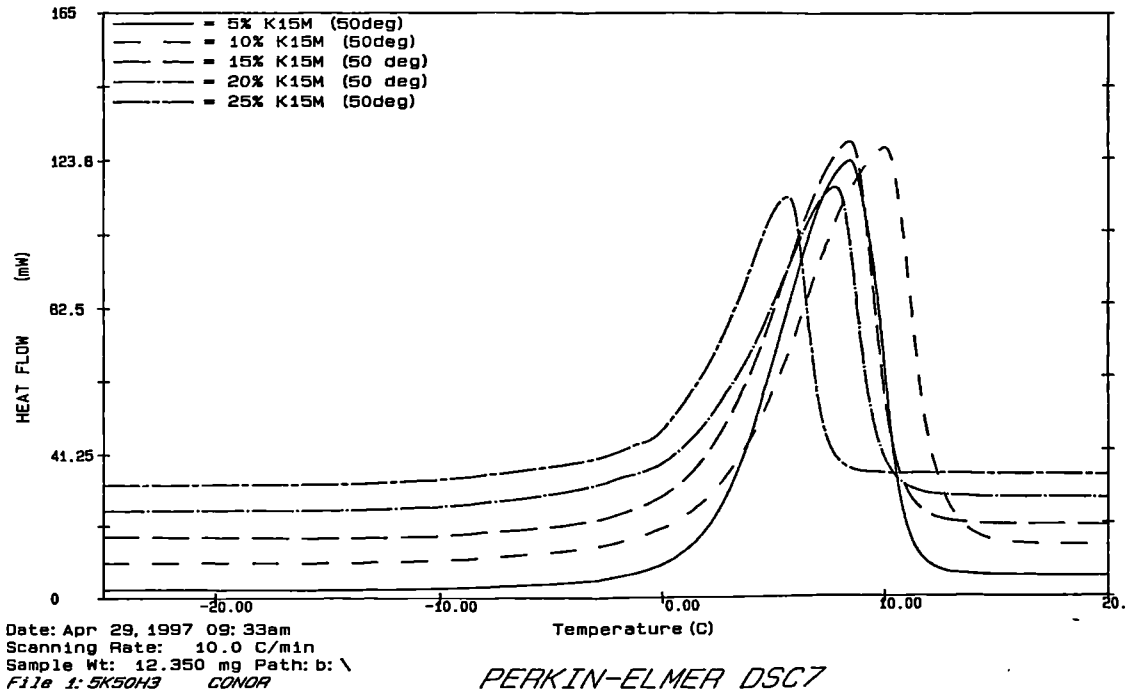
Due to batch availability, all future work on HPMC K15M reported in both this section and in the remainder of the thesis was carried out on HPMC K15M batch BN MM94112811K.

3.4.1.6 Influence of water temperature during gel preparation on water distribution within HPMC K15M gels

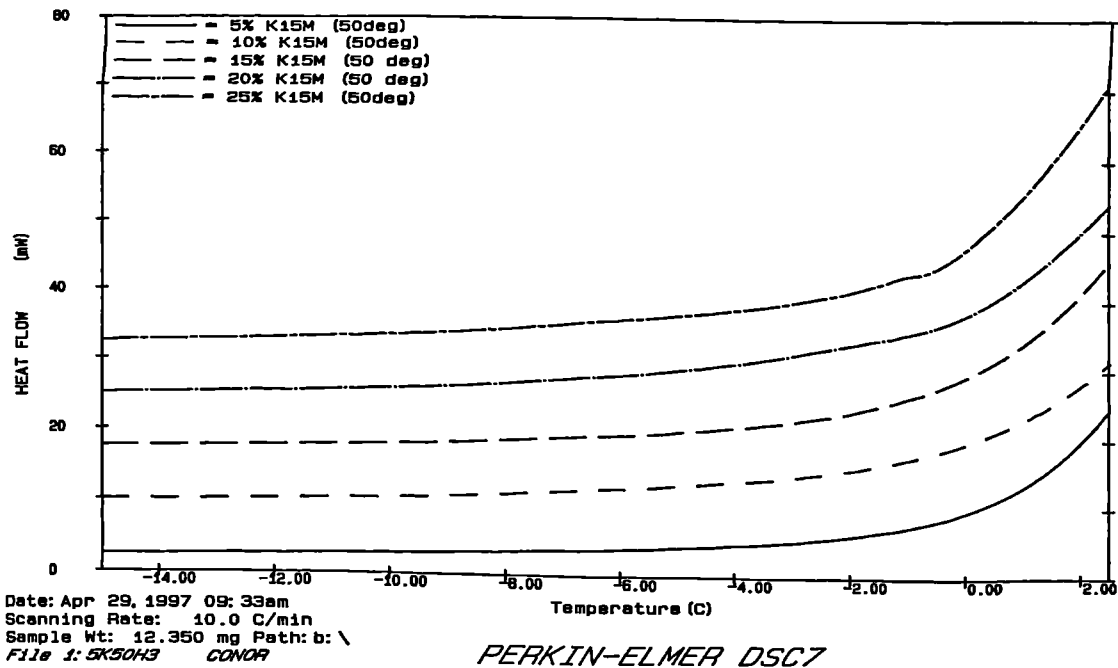
The temperature of water added to the polymer powder to prepare gels may be an important factor in the water distribution in HPMC gels.

The water added to the polymer in gel preparation was preheated to 50, 60, 70 or 80°C (section 2.2.1) in a water bath before addition to HPMC K15M (BN MM94112811K) in two aliquots. All gels were sealed and stored overnight (4-6°C) prior to DSC analysis (section 2.2.2.1). Gel samples were cooled from +20°C to -35°C at -10°Cmin⁻¹ and heated from -35°C to +20°C at +10°Cmin⁻¹.

Gel preparation temperature influenced the appearance of the pre-endothermic events occurring on the leading edge of the main endotherm in HPMC K15M gels. Such events were visible in all 20 & 25% (w/w) gels but were not as exaggerated in gels prepared



(a)

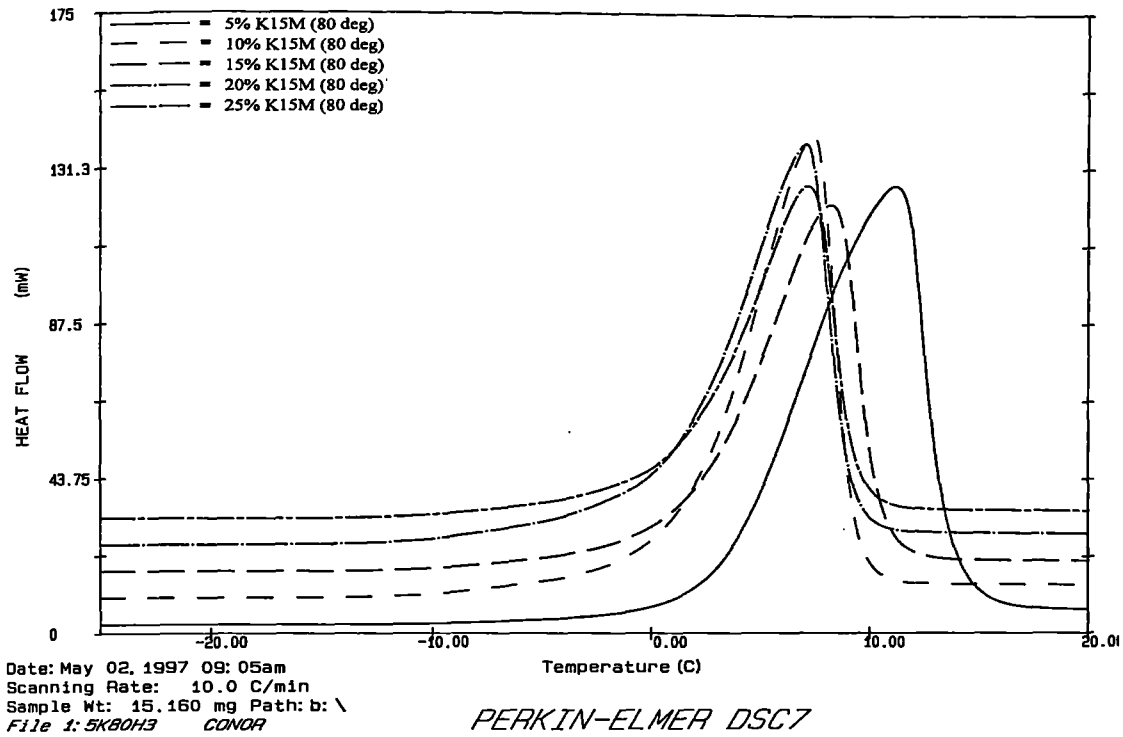


(b)

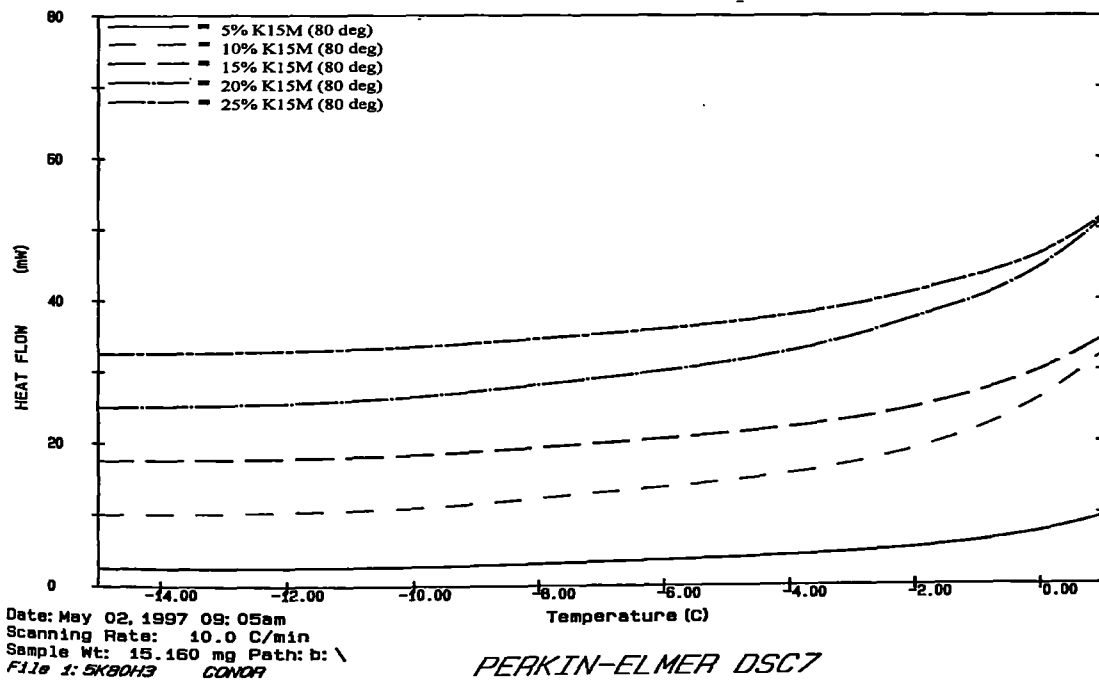
Figure 3.14 : DSC scans of HPMC K15M gels prepared with distilled water heated to +50°C and stored for 24h at a heating rate of +10°Cmin⁻¹ following cooling at -10°Cmin⁻¹

(a) from -22.5 to +20°C

(b) from -15 to +2.5°C



(a)



(b)

Figure 3.15 : DSC scans of HPMC K15M gels prepared with distilled water heated to +80°C and stored for 24h at a heating rate of +10°Cmin⁻¹ following cooling at -10°Cmin⁻¹

(a) from -25 to +20°C

(b) from -15 to +1°C

with water at 80°C (Figure 3.15) compared to such events visible in gels prepared with water at 50 (Figure 3.14), 60 or 70°C (not shown).

The number of moles of BW per PRU of the gel samples prepared at each particular temperature were calculated according to the method described in section 3.4.1.3. (Table 3.5). The regression (R^2) value quoted in table 3.5 gives an indication of the goodness of fit for a straight line through the data points on the plot of enthalpy (J/g) against polymer concentration (% w/w). The p-value indicates the level of significance of the fit of a straight line through the data points. Table 3.5 shows that water distribution within HPMC K15M gels was similar when the temperature of added water was at 50, 60 or 70°C. However, at 80°C, the number of moles of water bound to the polymer backbone was reduced.

This finding has implications for the gel preparation techniques employed in this study (as recommended by the product manufacturers; DOW Chemical Company, 1983). DOW recommend that Methocel cellulose ether powders are dispersed by mixing thoroughly with 1/5 to 1/3 of the required total volume of water as hot water, heated to 80-90°C. The remainder of the water should then be added as cold water to aid complete solubilisation. The rationale for initial dispersion in hot water above 80°C is that better wetting of the particles are ensured. If cold water is mixed directly with the powder, it creates a gelatinous membrane on the particles which causes lumping and acts as a barrier to full hydration of the polymer. It would seem that the temperature of water initially added to the HPMC to aid wetting of the powder is important in the subsequent water distribution within the gels.

Table 3.5 : Influence of temperature of water used to prepare polymer gels on the number of moles of bound water (BW) per polymer repeating (PRU) of HPMC K15M

Water temperature (°C)	HPMC K15M (% w/w)	Mean enthalpy (Jg ⁻¹) (± SD; n = 3)	Number of moles bound water per PRU	Regression coefficient (R ²)	Level of significance
50	4.65	329 ± 14	4.8	0.987	p < 0.1
	9.33	295 ± 4			
	13.90	280 ± 5			
	18.24	247 ± 4			
	23.62	234 ± 12			
60	4.54	339 ± 13	4.2	0.981	p > 0.1
	9.28	298 ± 2			
	13.75	279 ± 4			
	18.71	258 ± 6			
	23.38	239 ± 11			
70	4.66	331 ± 7	4.3	0.875	p > 0.1
	9.26	284 ± 6			
	13.93	286 ± 2			
	18.67	246 ± 7			
	22.83	243 ± 7			
80	4.69	319 ± 7	2.1	0.932	p > 0.1
	9.54	279 ± 6			
	13.81	276 ± 5			
	18.69	258 ± 5			
	23.69	238 ± 2			

3.5 Conclusions

The existence of different types of water within HPMC K15M gels was shown using Differential Scanning Calorimetry (DSC) studies. One or more endothermic events existed on the low temperature side of the endotherm corresponding to the melting of different types of water. These endothermic events were dependent on HPMC K15M concentration in gels, first appearing at 16% (w/w) HPMC K15M. Below this concentration, such events were not visible. As the gel concentration further increased, these events became more exaggerated. Such pre-endothermic events were linked to the presence of different types of water bound to varying degrees to the hydrophilic HPMC polymer. These pre-endothermic events may also be due to the presence of a glass transition temperature occurring close to the temperature of melting of free water.

Polymer hydration time influenced the nature of pre-endothermic events. No pre-endothermic events were visible for gels stored for 2h. It is assumed that the DSC peaks in these samples represent the bulk water with little or no influence from the polymer. Insufficient time had elapsed to allow gel equilibration to occur. Pre-endothermic events were visible for both 24 and 96h storage.

The nature of pre-endothermic events were influenced by variation in both heating and cooling rate during DSC studies. At low cooling rates, pre-endothermic events were exaggerated in nature. Similarly, at low heating rates, water closely associated with the polymer as represented by the pre-endothermic events, was visible as a number of separate melting events. At higher heating rates, fewer melting events were visible to the left of the main endotherm for the melting of bulk water.

Gel preparation method and batch to batch variation influenced the behaviour of HPMC K15M gels, as identified qualitatively by the nature of the melting events visible on DSC traces and quantitatively by analysis of the number of moles of BW per PRU. The nature of such gel systems may lead to problems in accurately characterising water distribution

and thus quantitative work may only provide useful comparative guidelines and may not be regarded as absolute.

DSC analysis inferred that water closely associated with the polymer is visible in DSC traces on the low temperature side of the main melting endotherm i.e. melts at lower temperatures than the bulk or free water. This may be explained by considering the cooling process during DSC analysis. During cooling, water in the polymer system will crystallise (visible as an exothermic event on the DSC cooling curve). Most of the water present in the system will be free water which will form larger crystals than those formed by water which is loosely bound to the polymer. Tightly bound water will not freeze. Upon heating, the smaller crystals will melt first, followed by the larger crystals formed by free water. Thus, the melting of the smaller crystals may be visible as small events to the left of the main melting endotherm.

CHAPTER 4

CHARACTERISATION OF WATER DISTRIBUTION WITHIN HPMC K15M GELS USING THERMOGRAVIMETRIC ANALYSIS

Chapter 4 Characterisation of water distribution within HPMC K15M gels using thermogravimetric analysis

4.1 Introduction

Thermogravimetric analysis (TGA) is a thermal analysis technique often used in conjunction or simultaneously with differential scanning calorimetry (DSC). Different types of water are identifiable from thermogravimetric studies, as they evaporate at different temperatures on the heating cycle. These events may be quantifiable from the derivative of the TGA weight loss curve (dTGA) provided that there is no overlap between the temperatures at which the different types of water evaporate. The derivative of the weight loss curve gives an indication of the rate of weight loss with time. Donescu et al (1993) identified water loss occurring in two stages in poly (vinylacetate) (PVAc) emulsions. Initial water loss in the range of 50-66°C was attributed to the evaporation of free water from the polymer as the majority of the total water content of the sample. This step was followed by a further water loss event in the range of 94-102°C. This event was attributed to the bound water in the polymer which leaves the sample at a higher temperature. Interestingly, the amount of bound water decreased as the polymer content increased. This was linked to an increase in the degree of cross-linking and a decrease in the ratio of PVA/PVAc (PVA = poly (vinyl alcohol)) or hydroxyl/acetate groups. Liron et al (1994) employed TGA in isothermal mode and monitored change of weight and of temperature with time in samples of porcine stratum corneum. From the dTGA curves, three distinct regions of desorption were identified. Initial water desorption was identified as being due to loss of free water. This was followed by loss of bulk water and finally by loss of bound water.

In many cases, TGA studies are used to complement DSC/DTA (differential temperature analysis). Examples include work carried out on poly (hydroxystyrene) and its derivatives (Hatakeyama et al, 1988); theophylline monohydrate (Duddu et al, 1995); polyaniline (Matveeva et al, 1995) and in peat (McBrierty et al, 1996). Zhu et al (1997) undertook TGA studies on nedocromil salt hydrates in open sample pans

and in crimped aluminium pans to simulate the experimental conditions in crimped pan DSC. Various dehydration steps attributed to the presence of loosely bound water in nedocromil salt hydrates were identified from the dTGA curves in open pan TGA. Open pan TGA identified differences in the dehydration behaviour of modifications A and B of the pentahydrate below 100°C, possibly indicating differences in distribution of loosely bound water. These differences, however, disappeared in crimped pans in which the dehydration was shifted to higher temperatures.

TGA has proved a useful analytical technique in the physical characterization of various pharmaceutical and other systems. Sonaglio et al (1995) used TGA as an aid to physical characterization of two types of microcrystalline cellulose. TGA measurements were used to calculate W_t (total water content) of certain systems, thus enabling the bound water content of the system to be determined according to equation 3.1 as outlined in section 3.1. Examples of the calculation of total water content by TGA for measurement of bound water in this way include characterization of actin (Kakar and Bettelheim, 1991); bovine corneas (DeMali and Williams, 1994); various ligno-cellulosic materials (Berthold et al, 1996); and poly (vinyl alcohol) films (Hodge et al, 1996).

The activation energy (Ea) of a thermal event may be directly determined from a number of thermogravimetric runs performed at different scan rates by applying the principles of the Arrhenius equation. The Arrhenius equation predicts the effect of temperature on reaction rate (Martin et al, 1983):

$$\text{Equation 4.1} \quad k = A e^{-Ea/RT}$$

$$\text{Equation 4.2} \quad \log k = \log A - \frac{Ea}{2.303 RT}$$

where k is the specific reaction rate, A is a constant known as the frequency factor, Ea is the energy of activation, R is the gas constant and T is the absolute temperature. By determining k at several temperatures and plotting $\log k$ against $1/T$, the slope of the line obtained (equation 4.2) is $-Ea / 2.303R$, and the intercept on the y-axis is $\log A$, from which Ea and A may be obtained. The activation energy Ea is commonly

described as the energy barrier or threshold that must be overcome to enable the bond distribution steps required to convert products into reactants. The pre-exponential term, or frequency factor A , provides an estimate of the frequency with which the reaction situation occurs (Galwey and Brown, 1995). The Arrhenius equation has been widely applied to rate processes including both homogeneous and heterogeneous reactions. Some discussion has taken place regarding the suitability of such an equation to be applied to solid state reaction processes including thermal dehydration processes (Galwey, 1994a, 1994b; Tanaka et al, 1995).

Flynn and Wall (1966) noted that the E_a of a thermal event can be directly determined from a series of TGA runs performed at different scan rates. If a series of TGA runs are made at different heating rates, each TGA weight loss curve is shifted upward on the temperature scale with an increasing scanning rate. Based on the Arrhenius assumptions, a plot of the log of the heating rate against the inverse of the absolute temperature (at the same conversion or weight loss %) is linear, with a slope directly proportional to the activation energy and known constants. Such theory has been applied in the TGA 7 Decomposition Kinetics software program (section 2.2.2.3). Figure 4.1 shows the Arrhenius plots of scan rate ($^{\circ}\text{Cmin}^{-1}$) against $1/T$ (K) for HPMC K15M gels of 5 - 25% (w/w) concentration scanned at heating rates of +2, +5, +10, +15 and +20 $^{\circ}\text{Cmin}^{-1}$ at weight loss percentages of 2 and 5%. In addition to E_a computations, other factors may be determined from this program where it is assumed that the reaction proceeds according to first order kinetics when the conversion or weight loss % is low (Perkin Elmer TGA 7 Decomposition Kinetics Software Kit, 1989). These include determination of rate constant and half-life profiles. The current study is concerned only with activation energy (E_a) determination.

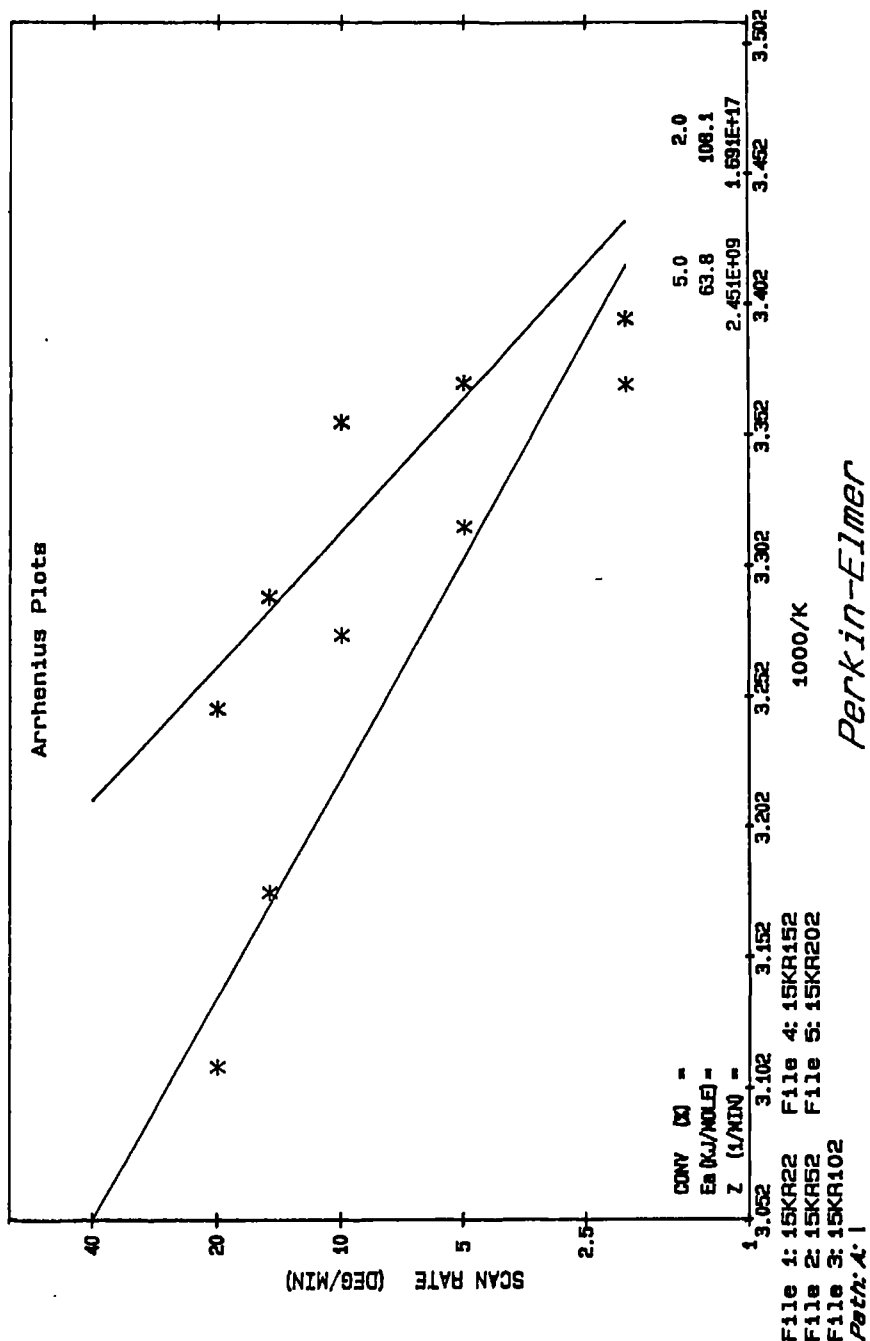


Figure 4.1 : Arrhenius plots of HPMC K15M (5 - 25% w/w) gels scanned at heating rates of +2, +5, +10, +15 and +20°Cmin⁻¹ at weight loss percentages of 2% (right) and 5% (left)

4.1.1 Objectives

The effect of polymer concentration and heating rate during TGA analysis on the nature of water loss from HPMC K15M gels was investigated. The influence of type of sample pan used during TGA analysis on water evaporation from the gel samples was characterised.

4.2 Materials

Methocel HPMC K15M (BN MM94112811K) cellulose ether was obtained from the DOW Chemical Company (section 2.1.1; Table 2.1).

4.3 Methods

4.3.1 Gel Preparation

HPMC K15M gels (5-25% w/w) were prepared as outlined in section 2.2.1. All gels were stored at 4-6°C for 24h and water losses during both preparation and storage were taken into account when determining final polymer concentration in the gels.

4.3.2 Thermal Analysis

Thermogravimetric studies were carried out on HPMC K15M gel samples (5-25% w/w; about 10mg) in both open and vented sample pans on a Perkin Elmer TGA 7 as described in section 2.2.2.2. Vented or pierced aluminium sample pans are sample pans having a hole pierced in their lid providing a controlled release of moisture from the pan.

Kinetic analysis was completed on the data obtained from moisture loss studies using a TGA7 PC Series Decomposition kinetics software programme (Perkin-Elmer, Beaconsfield, U.K.).

4.4 Results and Discussion

4.4.1 Thermogravimetric analysis studies

DSC studies (section 3.4) indicated that there are different types of water present within HPMC polymer gels. These different types of water may be further characterised by thermogravimetric analysis (TGA). It may be hypothesised, that depending on their interaction with HPMC polymer, different types of water evaporate at different temperatures.

4.4.1.1 Thermogravimetric analysis of HPMC K15M gels of different concentrations

Figure 4.2 shows a typical TGA weight loss trace showing weight loss against temperature for the evaporation of distilled water scanned at a heating rate of $+5^{\circ}\text{Cmin}^{-1}$. The first derivative curve is also shown indicating the rate ($\%/min$) at which water was lost from the gel. Water continually evaporates from the sample pan with increasing temperature and is completely removed by approximately 140°C .

HPMC K15M gels of concentration 5-25% w/w were prepared as detailed in section 2.2.1 and stored overnight at low temperatures ($4-6^{\circ}\text{C}$). They were then scanned from ambient to 200°C in open sample pans at a heating rate of $+5^{\circ}\text{Cmin}^{-1}$.

Figure 4.3 shows both the weight loss and the first derivative curves of HPMC K15M (4.73 and 23.68% w/w) gels scanned at $+5^{\circ}\text{Cmin}^{-1}$. The curves show that HPMC K15M concentration affected evaporation of water from their gels. Figure 4.4 shows the first derivative curves of a range of concentrations of HPMC K15M (4.73 - 23.68% w/w). At higher polymer concentrations it is apparent that a second evaporation event visible on the first derivative curve became more pronounced. It may be hypothesised that the distribution of water within the gels changes with polymer concentration with loosely bound water evaporating at higher temperatures

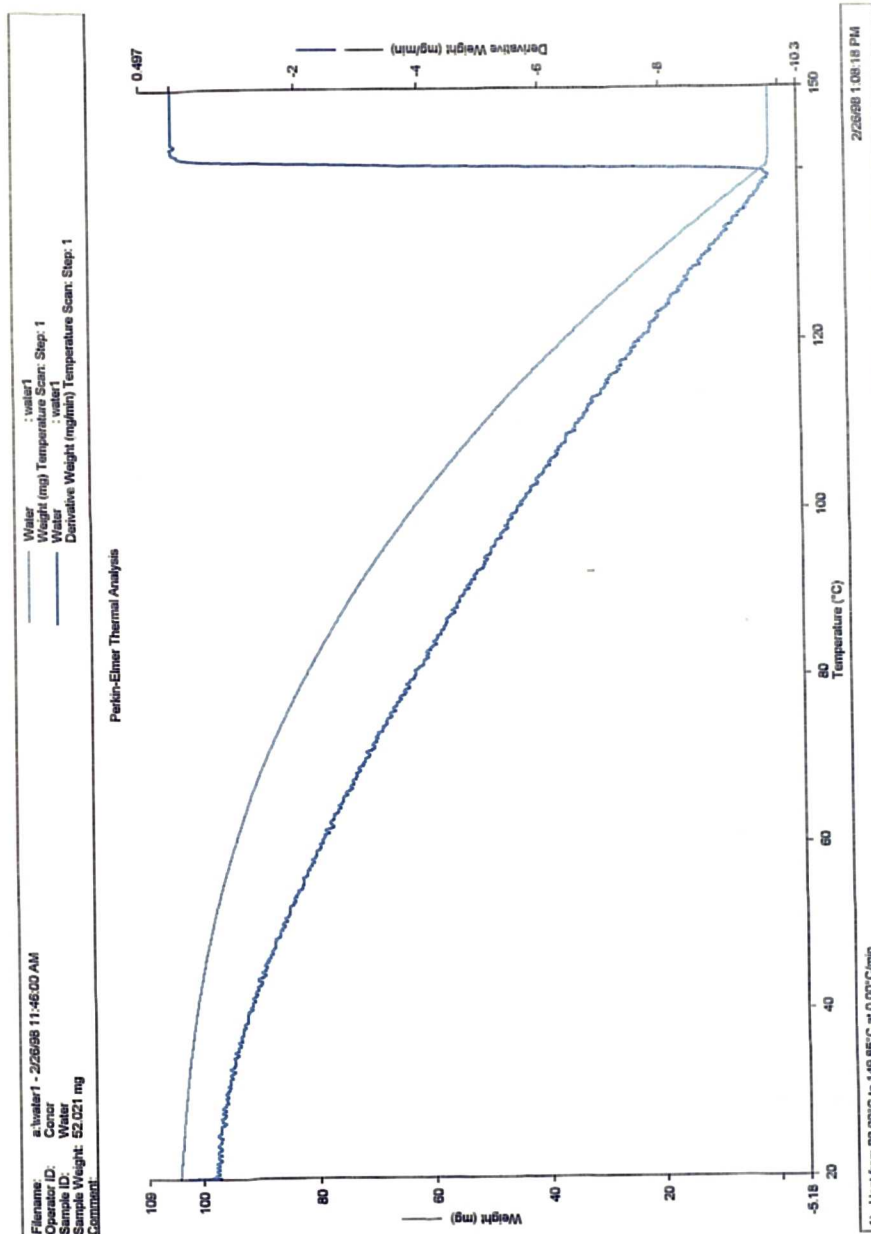


Figure 4.2 : TGA weight loss and first derivative curves for distilled water scanned at a heating rate of $+5^{\circ}\text{Cmin}^{-1}$ in an open sample pan

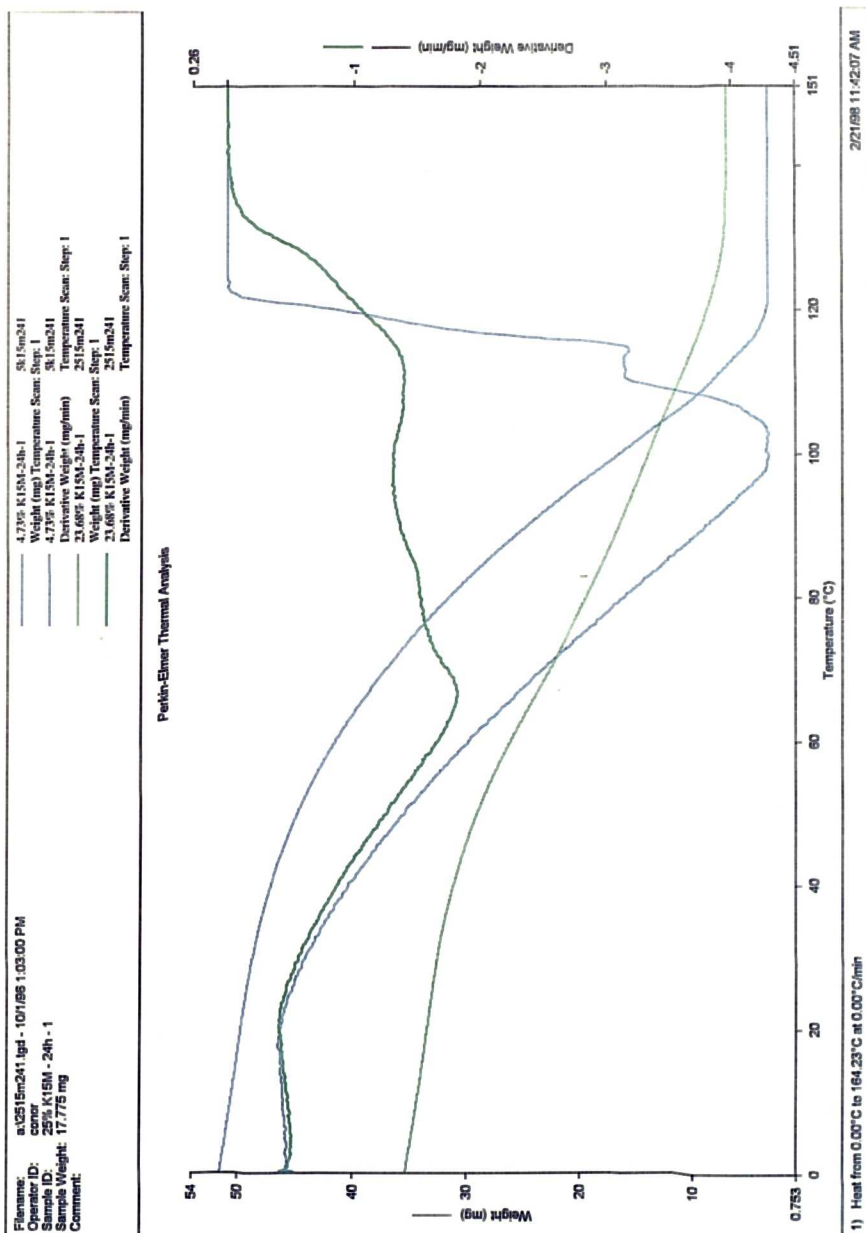


Figure 4.3 : TGA weight loss and first derivative curves of HPMC K15M (4.73 and 23.68% w/w) gels scanned at a heating rate of +5°Cmin⁻¹ in open sample pans

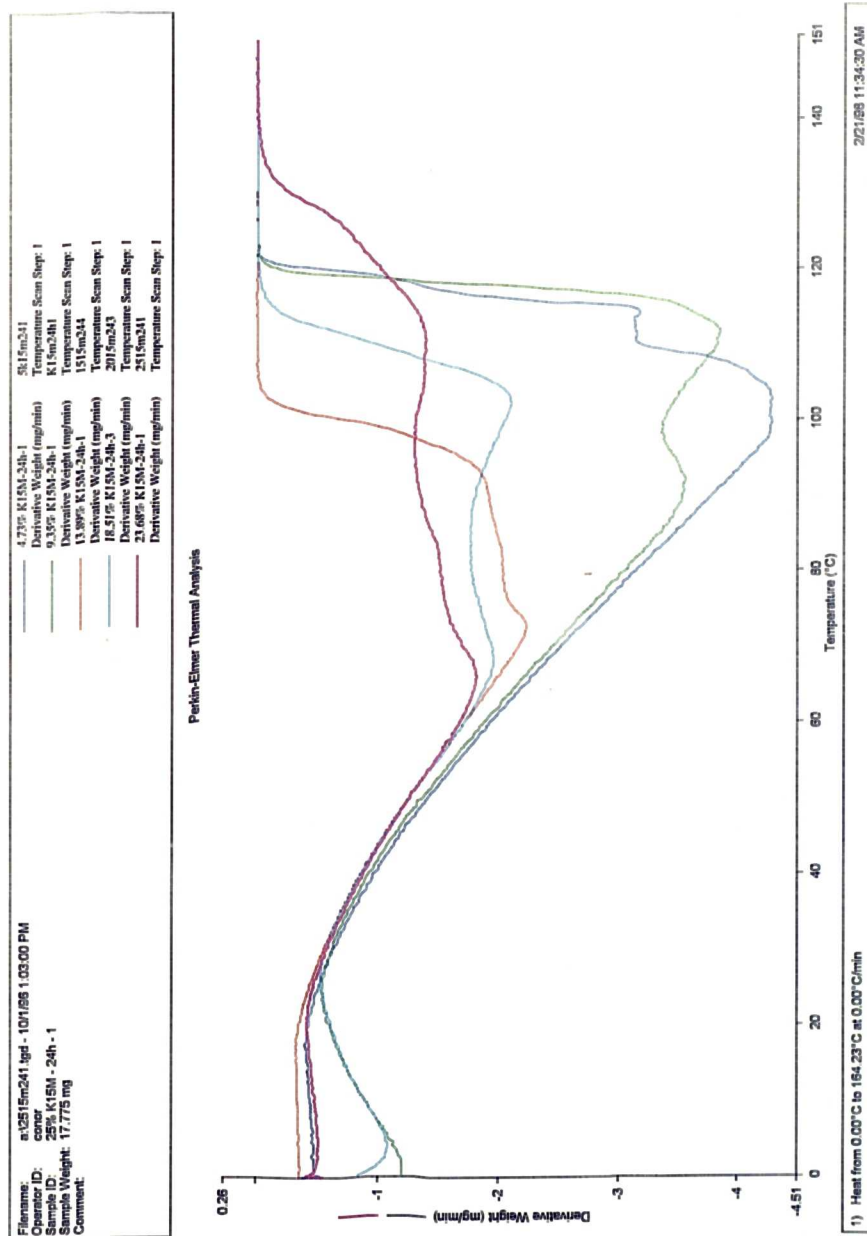


Figure 4.4 : TGA derivative curves of HPMC K15M (4.73 - 23.68% w/w) gels scanned at a heating rate of +5°Cmin⁻¹ in open sample pans

Table 4.1 : Thermogravimetric analysis data showing the temperature range over which moisture loss occurs and the mean percentage weight loss in a series of HPMC K15M gels scanned at $+5^{\circ}\text{Cmin}^{-1}$

HPMC K15M (% w/w)	Mean peak width ($^{\circ}\text{C}$) (n = 3) ($\pm\text{SD}$)	Mean weight loss(%) (n = 3) ($\pm\text{SD}$)
4.73	109.9 ± 11.2	93.4 ± 0.1
9.35	120.3 ± 1.9	90.5 ± 1.9
13.89	121.0 ± 17.0	86.0 ± 1.5
18.51	119.0 ± 4.6	83.7 ± 0.5
23.68	135.1 ± 12.3	79.4 ± 0.5

than free water. Table 4.1 shows the influence of polymer concentration on weight loss from their gels. The mean peak width is also shown which represents the temperature range over which evaporation of water from the gels occurred. As the polymer concentration increased, higher temperatures were required to remove all of the water from the gels. It may be hypothesised that with an increase in gel concentration there is an increased amount of closely associated or loosely bound water. It is assumed that loosely bound water evaporates at higher temperatures than free water because more energy is required to remove this type of water due to its association with the polymer and tightly bound water evaporates at even higher temperatures.

4.4.1.2 Effect of heating rate on moisture loss from HPMC K15M gels

The effect of heating rate on the nature of moisture loss from $\sim 15\%$ (w/w) HPMC K15M gels (10 mg approx.) in open sample pans was explored using a variety of

heating rates (+2, +5, +10, +15, +20°Cmin⁻¹). Two separate lots of HPMC K15M gels from the same batch were analysed. A further study was also carried out on HPMC K15M (~ 15% w/w) gels in which the gel samples were scanned in vented aluminium pans. These vented pans provided a controlled release of moisture from the gel samples and were employed to further explore the possible evaporation of different types of water.

Table 4.2 shows that as the heating rate was increased, the moisture was removed over a wider temperature range from gel samples in open sample pans. At heating rates of +10°Cmin⁻¹ and above, more than one evaporation event was visible on the derivative TGA curve (Figure 4.5). The appearance of such events only at the higher scanning rates, may indicate that bubbling of the gel occurred during heating at faster rates, providing a mechanism for release of loosely bound water from the gel. At lower heating rates, loosely bound water may be removed from the gels at lower temperatures and is not visible as a separate evaporation event on the first derivative curve.

When gels were scanned in vented aluminium pans, the water evaporated at higher temperatures (Figure 4.6) in comparison to open pans. At heating rates of 10°Cmin⁻¹ and above, more than one evaporation event was visible on the dTGA curve. Excellent separation of these evaporation events occurred. In vented aluminium pans, water vapour builds up inside the pan reaching equilibrium thus slowing down evaporation of water at lower temperatures from the gel. This explains why water evaporates at higher temperatures in vented pans in comparison to the temperature of water evaporation in open pans. Table 4.3 confirms that water evaporated over a much broader temperature range from gels analysed by vented pans when compared to gels analysed using open pans (Table 4.2).

Table 4.2 : Thermogravimetric analysis data showing the mean percentage weight loss and the temperature range over which moisture loss occurs in two HPMC K15M (15% w/w) gel samples scanned at a variety of heating rates in open sample pans

HPMC K15M (% w/w)	Heating rate (°Cmin ⁻¹)	Mean weight loss (%) (n = 2) (±SD)	Mean peak width (°C) (n = 2) (±SD)
14.10	+2	84.4 ± 1.8	45.2 ± 5.3
14.10	+5	85.3 ± 0.3	76.6 ± 2.4
14.10	+10	86.0 ± 0.04	96.2 ± 1.2
14.10	+15	86.2 ± 0.4	110.8 ± 5.9
14.10	+20	86.7 ± 0.03	128.1 ± 1.5
14.07	+2	81.3 ± 2.6	48.5 ± 7.9
14.07	+5	82.6 ± 0.3	80.8 ± 3.4
14.07	+10	84.4 ± 0.1	84.7 ± 2.2
14.07	+15	84.6 ± 1.3	114.0 ± 1.9
14.07	+20	84.7 ± 0.1	131.2 ± 1.9

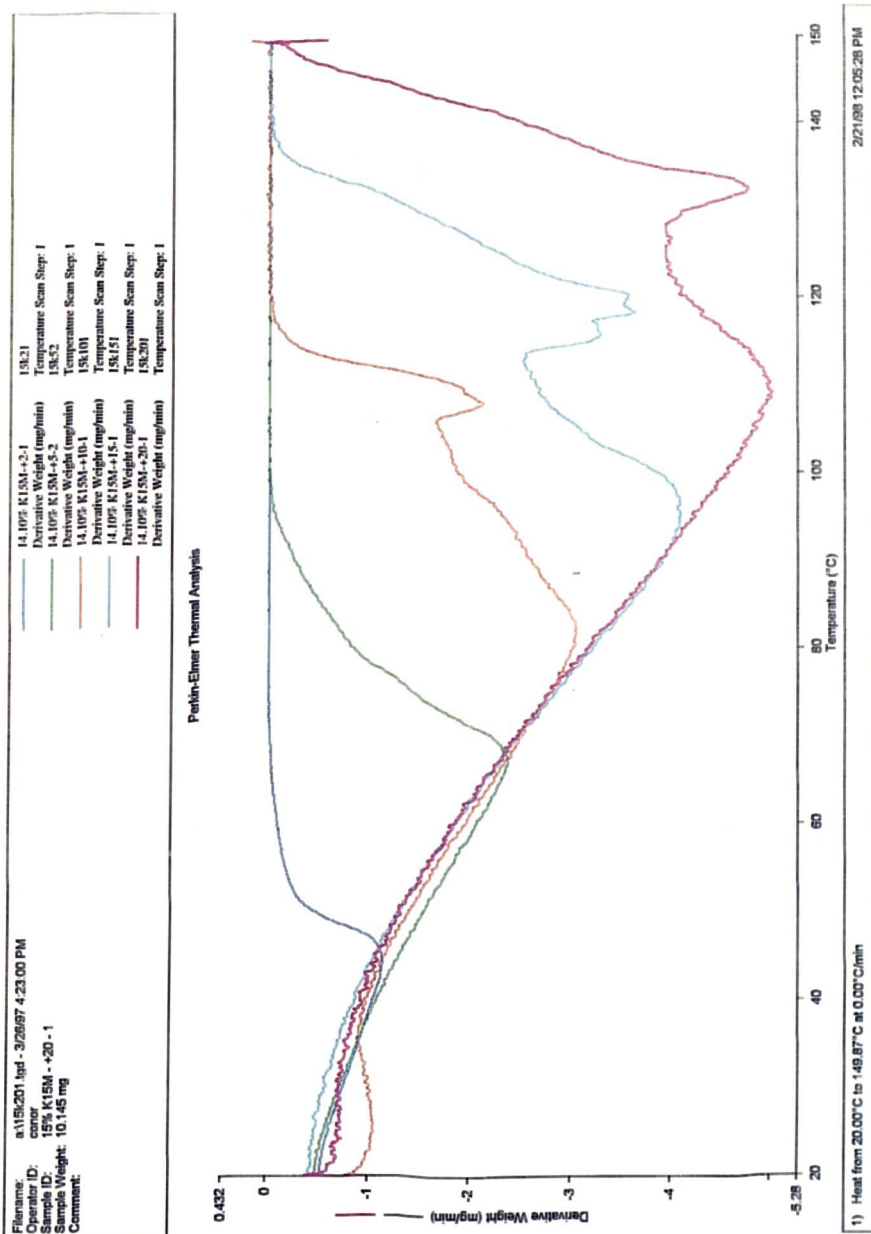


Figure 4.5 : TGA derivative curves of HPMC K15M (14.10% w/w) gels scanned at heating rates of +2, +5, +10, +15 and +20°Cmin⁻¹ in open sample pans

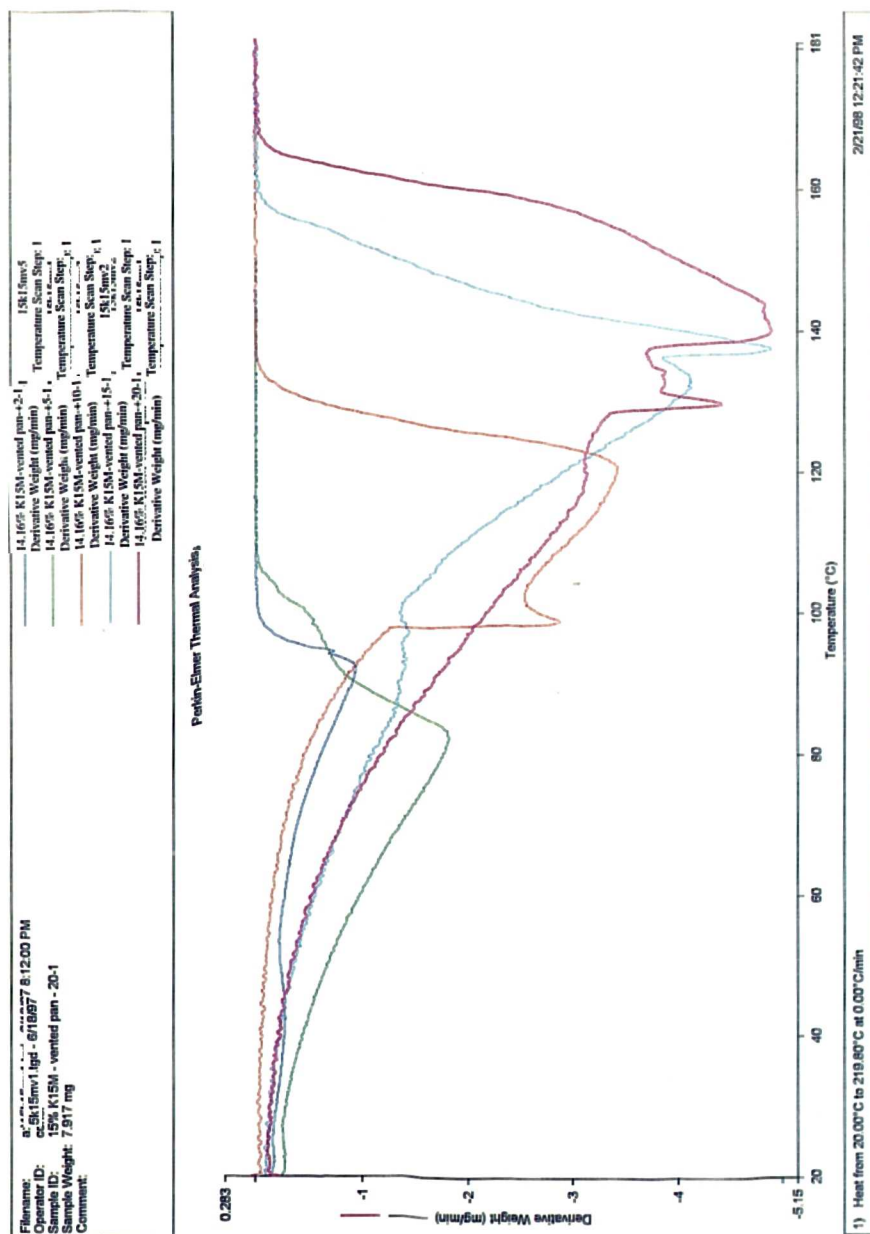


Figure 4.6 : TGA derivative curves of HPMC K15M (14.16% w/w) gels scanned at heating rates of +2, +5, +10, +15 and +20°Cmin⁻¹ in vented sample pans

Table 4.3 : Thermogravimetric analysis data indicating the mean percentage weight loss and the temperature range over which moisture loss occurs in HPMC K15M (14.16% w/w) gel samples scanned at a variety of heating rates in vented aluminium pans

HPMC K15M (% w/w)	Heating rate (°Cmin ⁻¹)	Mean weight loss (%)	Mean peak width (°C)
14.16	+2	86.6	80.6
14.16	+5	86.6	83.8
14.16	+10	86.8	109.6
14.16	+15	86.8	133.0
14.16	+20	85.3	143.3

4.4.1.3 Kinetic analysis of water loss from HPMC K15M gels

The velocity of the reaction in which HPMC K15M gel samples lose water is dependent on temperature. It has been previously detailed (section 4.1) how the activation energy (E_a) of a thermal event can be determined by applying the Arrhenius equation to a series of TGA runs made at different scanning rates. This was completed using the Perkin Elmer TGA 7 Decomposition Kinetics software program.

The data in section 4.4.1.2 (Table 4.2) was analysed using the Perkin Elmer TGA 7 Decomposition Kinetics software program. Five conversion (or weight loss %) values were chosen (2, 5, 10, 15 & 20), and the E_a values were calculated at each conversion and are shown in Table 4.4.

The highest E_a value was for the lowest conversion value, the point at which the reaction is in its early stages, i.e. the initial stages of moisture loss from the gel sample. At low conversion values, gels contain large quantities of bulk-like or free water and a lot of energy is required to remove this water. When a lot of free water is present in the gel system, the system is at its most dynamic and equilibrium has not been achieved. Hence, the standard deviation (SD) shows greatest spread in this region and reproducibility is at its poorest. As the reaction proceeds, less water is present in the gel, less energy is required to remove it, and as a result the activation energy shows a corresponding decrease. The SD spread and reproducibility are found to improve at higher conversion values. Unfortunately, such kinetic calculations may only be performed when the % conversion is relatively low i.e. 20% and below, as first order kinetics are assumed in the calculations (Perkin Elmer TGA 7 Decomposition Kinetics software program manual). Hence it is impossible to measure E_a in the later stages of dehydration when water which is more closely associated with the polymer is being removed.

The kinetic data from HPMC K15M gels scanned in vented aluminium pans is shown in Table 4.5. Clearly the E_a values are much lower than the values previously obtained from gels scanned in open sample pans (Table 4.4). It was shown in section 4.4.1.2 that water evaporated from gels at higher temperatures in vented pans in comparison to evaporation from open pans. This was due to build of water vapour pressure inside the pan inhibiting evaporation of water from the gel. This build up of water vapour pressure clearly causes a reduction in the energy required to cause removal of water from the gels. It is assumed that gels in vented pans reach equilibrium much faster than similar gels in open pans. As a result, more of the water in the gel is closely associated with the polymer and does not evaporate until higher temperatures are reached.

Table 4.4 : Activation energy (E_a) for two samples of HPMC K15M gel ($n = 2$; \pm SD) calculated at a number of different conversion values using the TGA 7 Decomposition Kinetics software program

HPMC K15M (% w/w)	conversion value (%)	E_a (KJ/mole) ($n = 2$; \pm SD)
14.10	2	138.55 \pm 14.64
14.10	5	70.9 \pm 9.05
14.10	10	51.15 \pm 3.61
14.10	15	44.15 \pm 2.19
14.10	20	40.2 \pm 1.84
14.07	2	121.4 \pm 18.81
14.07	5	68.1 \pm 6.22
14.07	10	50.25 \pm 2.62
14.07	15	43.5 \pm 1.70
14.07	20	39.8 \pm 1.27

Table 4.5 : Activation energy (E_a) of HPMC K15M gel samples scanned in vented aluminium pans calculated at a number of different conversion values using the TGA 7 Decomposition Kinetics software program

HPMC K15M (% w/w)	conversion value (%)	E_a (KJ/mole)
14.16	2	35.4
14.16	5	30.0
14.16	10	28.9
14.16	15	29.1
14.16	20	30.2

4.5 Conclusions

The existence of more than one type of water occurring within HPMC K15M polymer gels has previously been characterised using DSC (chapter 3). In this study, Thermogravimetric analysis (TGA) studies confirmed the findings of chapter 3 and provided evidence of the existence of more than one type of water within HPMC K15M polymer gels.

The evaporation of water from polymer gels has been shown to be affected by polymer concentration. The first derivative TGA curve which showed the rate of weight loss from gels, provided evidence of water evaporating at more than one temperature. At higher polymer concentrations the second evaporation event visible on the first derivative curve becomes gradually more pronounced. It may be hypothesised that the distribution of water within the gels and therefore the interaction of water with polymer changes with polymer concentration, with loosely bound water evaporating at higher temperatures than free water.

The evaporation of water from HPMC K15M gels was influenced by heating rate. As the heating rate was increased, moisture was removed over a wider temperature range. At heating rates of $+10^{\circ}\text{Cmin}^{-1}$ and above, more than one evaporation event was visible on the derivative TGA curve. It was hypothesised that at lower heating rates, loosely bound water is removed from the gels at lower temperatures, and was not visible as separate events on the first derivative curve.

When gels were scanned in vented aluminium pans, the water evaporated at higher temperatures in comparison to gels scanned in open pans. This was related to the build up of water vapour pressure within the vented aluminium pans inhibiting evaporation of water from the gel.

Kinetic studies were completed on the water evaporation process. The activation energy E_a of gels scanned in both open and vented pans was influenced by the conversion (or weight loss %) chosen. The activation energy E_a was further influenced by the build-up of water vapour pressure in gels scanned in vented pans.

CHAPTER 5

EFFECT OF MOLECULAR WEIGHT AND SUBSTITUTION TYPE ON WATER DISTRIBUTION WITHIN CELLULOSE ETHER POLYMERS

Chapter 5 Effect of molecular weight and substitution type on water distribution within cellulose ether polymers

5.1 Introduction

Different types of water were shown to exist in HPMC K15M gels by both differential scanning calorimetry (DSC) (Chapter 3) and thermogravimetric analysis (TGA) (Chapter 4). DSC studies, in this chapter, are extended to other cellulose ether polymers to examine the effects of molecular weight and substitution type on the different types of water, previously seen in studies on HPMC K15M gels.

Polymer viscosity grade depends primarily on the molecular weight of the polymer (Just and Majewicz, 1985). There have been many studies comparing the drug release from HPMCs of different molecular weights (and thus viscosity grades) with some debate existing within the literature regarding the influence of HPMC viscosity grade on drug release (Salomen et al, 1979; Nakano et al, 1983; Ford et al, 1985a, 1985b, 1985c; Liu et al, 1995). Similarly, many studies have been carried out on the influence of polymer substitution type on drug release (for example, Mitchell et al, 1993d; Bonferoni et al, 1996).

Nokhodchi et al (1997) characterised the water distribution in different viscosity grades of the HPMC K-series using DSC and concluded that viscosity grade had no significant effect on the amount of water bound to HPMC. The relationship between bound water content and HPMC substitution type has not previously been characterised.

5.1.1 Objectives

The objectives of the work in this chapter were to characterise the water distribution within HPMC K-series polymers of different molecular weights. In addition the water distribution in a range of HPMCs with different substitution types with similar molecular weights were characterised.

5.2 Materials

Methocel cellulose ethers were obtained from the DOW Chemical Company (section 2.1.1; Table 2.1). The batches of HPMC K100LV and HPMC K15M used were batches BN MM94051022K and BN MM94112811K respectively. HPMCs K4M, K100M, E4M, F4M and MC A4M are as described in Table 2.1. Hydroxypropylcellulose (HPC) MF EP (LOT 12187) was obtained from Hercules Limited, Aqualon Division, Salford, U.K. (section 2.1.1).

5.3 Methods

5.3.1 Gel preparation

Gels containing 5 - 25% (w/w) polymer were prepared as outlined in section 2.2.1. All gels were stored at 4-6°C for either 24 or 96h and water losses during both preparation and storage were taken into account when determining final polymer concentrations in the gels. Higher polymer concentrations of Methocel (HPMC) F4M gels (>25% w/w) and Klucel HPC gels (>25% w/w) were prepared from gels (15% w/w) by moisture extraction as outlined in section 2.2.1 and were stored for 24 to 96h at ambient temperatures to allow equilibration and uniform water distribution in the gels before analysis.

5.3.2 Thermal Analysis

A Perkin-Elmer DSC7 (Beaconsfield, UK) was employed as described in section 2.2.2.1. Gel samples were cooled from +20°C to -35°C at a cooling rate of -10°Cmin⁻¹ and heated from -35°C to +20°C at a heating rate of +10°Cmin⁻¹.

5.4 Results and Discussion

5.4.1 Effect of polymer molecular weight on the water distribution within cellulose ether polymers

Methocel (HPMC) K-series cellulose ether gels (5-25% w/w) i.e. HPMC K100LV, HPMC K4M, HPMC K15M and HPMC K100M were prepared and their DSC scans were recorded. Increasing the concentration of HPMC K15M (Table 5.1) resulted in a decrease in both exothermic and endothermic enthalpy (J/g) after gel storage for both 24 or 96h. The exothermic enthalpy is the energy released when water within the gels freezes and the endothermic enthalpy is the energy which is required for melting of frozen water within the gels to occur. Assuming that both exothermic (cooling) and endothermic (heating) peaks are attributable, in the main, to the crystallization and melting of free water respectively, it is apparent that there is a decrease in the amount of free water present with increase in HPMC concentration. As the concentration of the polymer increases, the amount of water required to hydrate the polymer increases and thus less free water is available. Increasing HPMC K15M concentration from 5 to 25% (w/w) caused a depression of both the endothermic melting peak and the endothermic melting peak onset. For example, Table 5.1 and Figure 5.1 show a depression of

Table 5.1a : Effect of HPMC K15M concentration (% w/w) on the exothermic peak onset/peak, the endothermic peak onset/peak and the exothermic and endothermic crystallization/melting enthalpies (Jg^{-1}) ($n = 3$; \pm SD) after 24h storage

HPMC K15M (% w/w)	Exothermic peak onset ($^{\circ}\text{C}$)	Exothermic peak ($^{\circ}\text{C}$)	Exothermic enthalpy (J/g)	Exothermic peak onset ($^{\circ}\text{C}$)	Exothermic peak ($^{\circ}\text{C}$)	Endothermic enthalpy (J/g)
5	-13.35 \pm 1.4	-13.85 \pm 1.5	259.90 \pm 13.9	3.43 \pm 0.2	8.90 \pm 0.4	334.72 \pm 8.0
10	-16.53 \pm 3.0	-16.87 \pm 3.0	213.40 \pm 21.1	2.89 \pm 0.2	7.29 \pm 0.8	289.80 \pm 11.3
15	-11.74 \pm 2.4	-12.36 \pm 2.2	248.20 \pm 12.1	2.81 \pm 0.3	8.33 \pm 0.3	289.71 \pm 14.0
20	-15.97 \pm 3.4	-16.47 \pm 3.4	208.21 \pm 31.7	2.37 \pm 0.3	7.10 \pm 0.8	263.56 \pm 15.8
25	-13.50 \pm 3.4	-14.35 \pm 3.2	205.00 \pm 18.1	1.82 \pm 0.5	6.17 \pm 0.5	228.28 \pm 15.4

Table 5.1b : Effect of HPMC K15M (% w/w) concentration on the exothermic peak onset/peak, the endothermic peak onset/peak and the exothermic and endothermic crystallization/melting enthalpies (Jg^{-1}) ($n = 3$; \pm SD) after 96h storage

HPMC K15M (% w/w)	Exothermic peak onset ($^{\circ}\text{C}$)	Exothermic peak ($^{\circ}\text{C}$)	Exothermic enthalpy (J/g)	Exothermic peak onset ($^{\circ}\text{C}$)	Exothermic peak ($^{\circ}\text{C}$)	Endothermic enthalpy (J/g)
5	-14.21 \pm 1.9	-14.69 \pm 2.0	218.15 \pm 78.3	3.60 \pm 0.9	8.76 \pm 3.4	343.29 \pm 12.5
10	-15.26 \pm 4.7	-15.60 \pm 4.6	217.02 \pm 33.7	2.81 \pm 0.3	7.51 \pm 1.4	304.00 \pm 13.9
15	-18.11 \pm 0.7	-18.68 \pm 0.8	216.74 \pm 8.4	2.64 \pm 0.2	7.43 \pm 0.5	281.62 \pm 15.5
20	-11.34 \pm 1.1	-12.06 \pm 0.9	209.20 \pm 26.8	2.02 \pm 0.4	6.94 \pm 1.0	246.32 \pm 13.7
25	-14.89 \pm 3.8	-15.80 \pm 3.5	202.25 \pm 9.1	1.52 \pm 0.1	6.38 \pm 0.5	231.06 \pm 6.6

endothermic melting peak ($8.9 \pm 0.35^\circ\text{C}$ to $6.17 \pm 0.53^\circ\text{C}$; 5 & 25% w/w gels respectively) and a depression in endothermic melting peak onset (3.43 ± 0.16 to $1.82 \pm 0.48^\circ\text{C}$; 5 & 25% w/w gels respectively) after a hydration time of 24h. The endothermic melting peak onset is defined as the temperature when the transition just leaves the baseline. The endothermic melting peak is the temperature at the apex of the melting peak (Ford and Timmins, 1989).

This temperature depression may be related to an increase in the quantity of loosely bound water which melts at a lower temperature than free water due to a stronger interaction with the polymer (Joshi and Wilson, 1993). This phenomena has previously been reported for HPMC K4M gels (Nokhodchi et al, 1997). Increasing HPMC K15M concentration has no quantifiable effect on the position of either the exothermic peak onset or the exothermic peak (Table 5.1). This may be because crystallization occurs via nucleation which is an uncontrolled phenomena. The process of crystallization occurs in three main stages i.e. production of a supersaturated solution, formation of crystal nuclei and finally by growth of the crystals. Prior to crystallization in a system, as well as the presence of a supersaturated solution, a number of nuclei or seeds that can act as the centre of crystallization must exist. Nucleation is defined as the production of the smallest possible particles or nuclei in a supersaturated solution of the crystallizing substance. Further agglomeration of the solute molecules or ions may then take place at these nuclei. This process may occur spontaneously (homogeneous nucleation) or alternatively may be induced by the presence of foreign particles (heterogeneous nucleation) (Mullin, 1993; Tanaka et al, 1995).

This lack of control during crystallisation was also apparent in HPMC K100, K4M and K100M gels (DSC scans not shown), where increase in polymer concentration had no effect on the position of either the exothermic peak onset or the exothermic peak.

Depression of melting point with increasing concentration of polymer is evident with variation in polymer molecular weight. HPMC K100, HPMC K4M and HPMC K100M

(Tables 5.2a and b, 5.3a and b, 5.4a and b) all display this depression in melting point. However, there is no apparent trend between polymer molecular weight and extent of melting point depression with increase in polymer concentration.

The existence of events present on the left of the main endotherm for the melting of free water in DSC scans for HPMC K15M was discussed in section 3.4. Such pre-endothermic events (visible in 20 and 25% w/w gels in Figure 5.1 and Figure 5.2) were dependent on HPMC K15M concentration, storage time and scanning rates during DSC analysis. Similar events were also visible prior to the main DSC melting endotherm in gels containing HPMC K100, HPMC K4M or HPMC K100M. Their appearance was dependent on both polymer molecular weight and gel storage time. In HPMC K100LV and HPMC K15M, pre-endothermic events were only visible in 20% (w/w) and 25% (w/w) gels after storage for 24 and 96h (Figure 5.1 and Figure 5.2). In the case of HPMC K15M, pre-endothermic events were more pronounced after 96h storage.

Gels of HPMC K4M or HPMC K100M showed pre-endothermic events at 15, 20 or 25% polymer content after storage for both 24 and 96h (Figure 5.4 and Figure 5.5). In both these cases, the appearance of such events were unaffected by storage time.

It appears that the appearance of endothermic events varied between HPMCs of different molecular weights.

Table 5.2a : Effect of HPMC K100 concentration (% w/w) on the endothermic peak onset/peak and the endothermic melting enthalpy (Jg^{-1}) ($n = 3$; \pm SD) after 24h storage

HPMC K100 (% w/w)	Endothermic peak onset ($^{\circ}C$)	Endothermic peak ($^{\circ}C$)	Endothermic enthalpy (J/g)
5	-0.22 ± 0.3	4.56 ± 0.9	309.50 ± 17.9
10	-0.82 ± 0.3	3.86 ± 0.6	290.11 ± 1.3
15	-1.26 ± 0.1	3.13 ± 0.4	272.96 ± 14.6
20	-1.90 ± 0.2	2.64 ± 0.3	248.02 ± 9.4
25	-1.96 ± 0.1	2.22 ± 0.03	234.28 ± 13.3

Table 5.2b : Effect of HPMC K100 concentration (% w/w) on the endothermic peak onset/peak and the endothermic melting enthalpy (Jg^{-1}) ($n = 3$; \pm SD) after 96h storage

HPMC K100 (% w/w)	Endothermic peak onset ($^{\circ}C$)	Endothermic peak ($^{\circ}C$)	Endothermic enthalpy (J/g)
5	-1.18 ± 0.1	3.63 ± 0.8	285.79 ± 6.8
10	-1.59 ± 0.2	3.34 ± 0.6	257.75 ± 8.4
15	-1.52 ± 0.5	3.51 ± 1.5	239.93 ± 7.9
20	-2.42 ± 0.3	2.48 ± 0.8	212.67 ± 6.8
25	-2.57 ± 0.03	2.63 ± 0.5	208.63 ± 2.3

Table 5.3a : Effect of HPMC K4M concentration (% w/w) on the endothermic peak onset/peak and the endothermic melting enthalpy (Jg^{-1}) (n = 3; \pm SD) after 24h storage

HPMC K4M (% w/w)	Endothermic peak onset ($^{\circ}C$)	Endothermic peak ($^{\circ}C$)	Endothermic enthalpy (J/g)
5	-2.58 \pm 0.1	2.76 \pm 0.6	331.33 \pm 2.5
10	-2.96 \pm 0.5	1.95 \pm 0.8	302.17 \pm 10.6
15	-3.46 \pm 0.1	0.85 \pm 0.7	268.28 \pm 16.5
20	-3.76 \pm 0.3	1.32 \pm 0.5	245.24 \pm 15.4
25	-3.36 \pm 1.2	0.64 \pm 0.2	217.23 \pm 6.9

Table 5.3b : Effect of HPMC K4M concentration (% w/w) on the endothermic peak onset/peak and the endothermic melting enthalpy (Jg^{-1}) (n = 3; \pm SD) after 96h storage

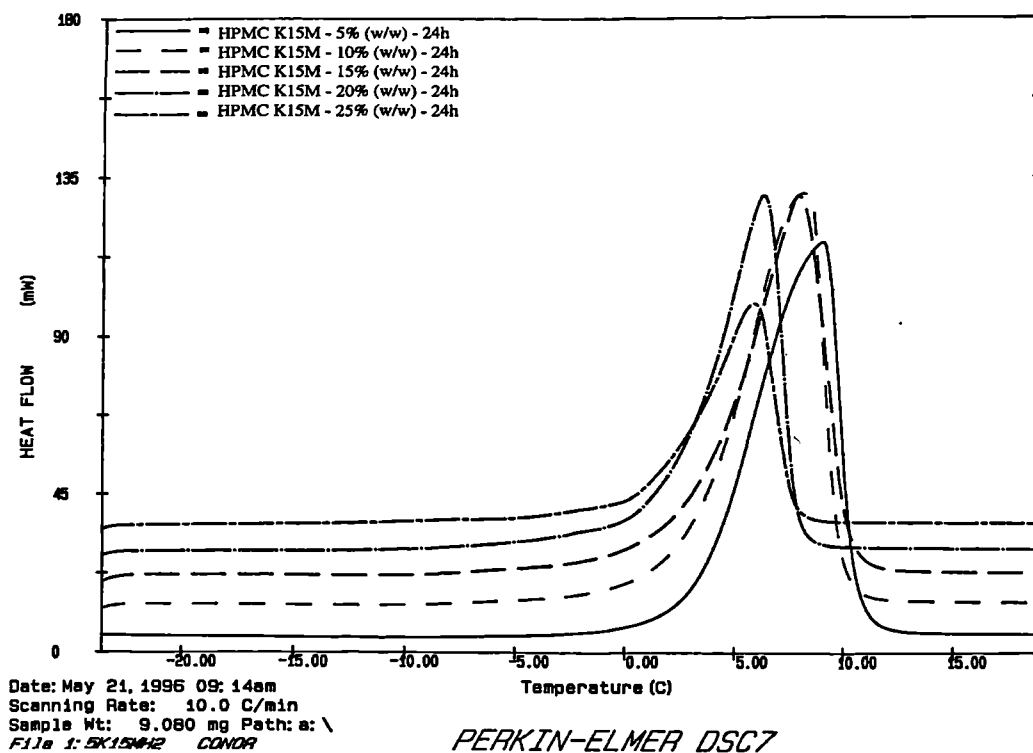
HPMC K4M (% w/w)	Endothermic peak onset ($^{\circ}C$)	Endothermic peak ($^{\circ}C$)	Endothermic enthalpy (J/g)
5	-2.70 \pm 0.2	2.33 \pm 0.5	326.14 \pm 6.3
10	-2.88 \pm 0.2	1.11 \pm 0.6	290.32 \pm 6.7
15	-2.88 \pm 0.2	1.11 \pm 0.6	290.32 \pm 6.7
20	-3.69 \pm 0.1	0.88 \pm 0.4	255.62 \pm 2.6
25	-4.22 \pm 0.3	0.43 \pm 0.4	227.09 \pm 12.7

Table 5.4a : Effect of HPMC K100M concentration (% w/w) on the endothermic peak onset/peak and the endothermic melting enthalpy (Jg^{-1}) (n = 3; \pm SD) after 24h storage

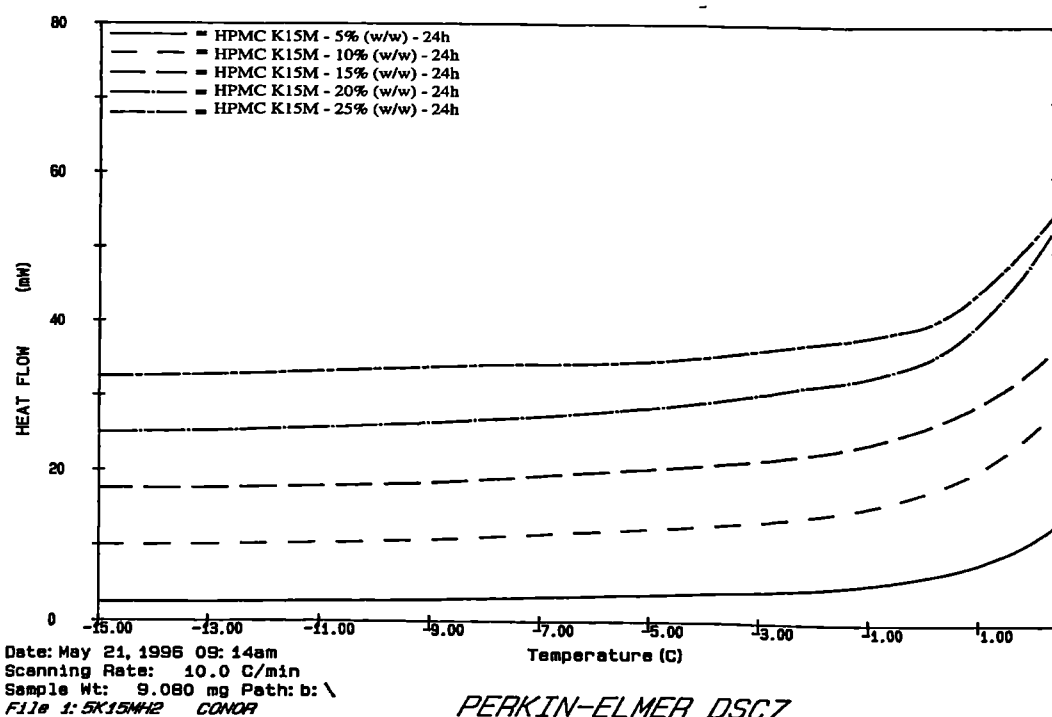
HPMC K100M (% w/w)	Endothermic peak onset ($^{\circ}\text{C}$)	Endothermic peak ($^{\circ}\text{C}$)	Endothermic enthalpy (J/g)
5	-0.23 ± 0.3	4.79 ± 0.8	218.06 ± 11.9
10	-0.76 ± 0.2	5.20 ± 0.8	209.48 ± 8.1
15	-1.55 ± 0.3	4.15 ± 0.6	182.01 ± 12.1
20	-1.69 ± 0.1	3.19 ± 0.4	172.96 ± 4.7
25	-2.01 ± 0.4	3.38 ± 1.4	147.17 ± 3.7

Table 5.4b : Effect of HPMC K100M concentration (% w/w) on the endothermic peak onset/peak and the endothermic melting enthalpy (Jg^{-1}) (n = 3; \pm SD) after 96h storage

HPMC K100M (% w/w)	Endothermic peak onset ($^{\circ}\text{C}$)	Endothermic peak ($^{\circ}\text{C}$)	Endothermic enthalpy (J/g)
5	-0.62 ± 0.3	5.09 ± 1.7	287.04 ± 3.4
10	-0.88 ± 0.3	5.59 ± 0.6	269.03 ± 4.1
15	-2.19 ± 0.1	3.04 ± 0.3	223.56 ± 8.1
20	-2.14 ± 0.2	3.75 ± 0.2	209.73 ± 3.1
25	-2.35 ± 0.4	2.93 ± 0.9	191.36 ± 6.4



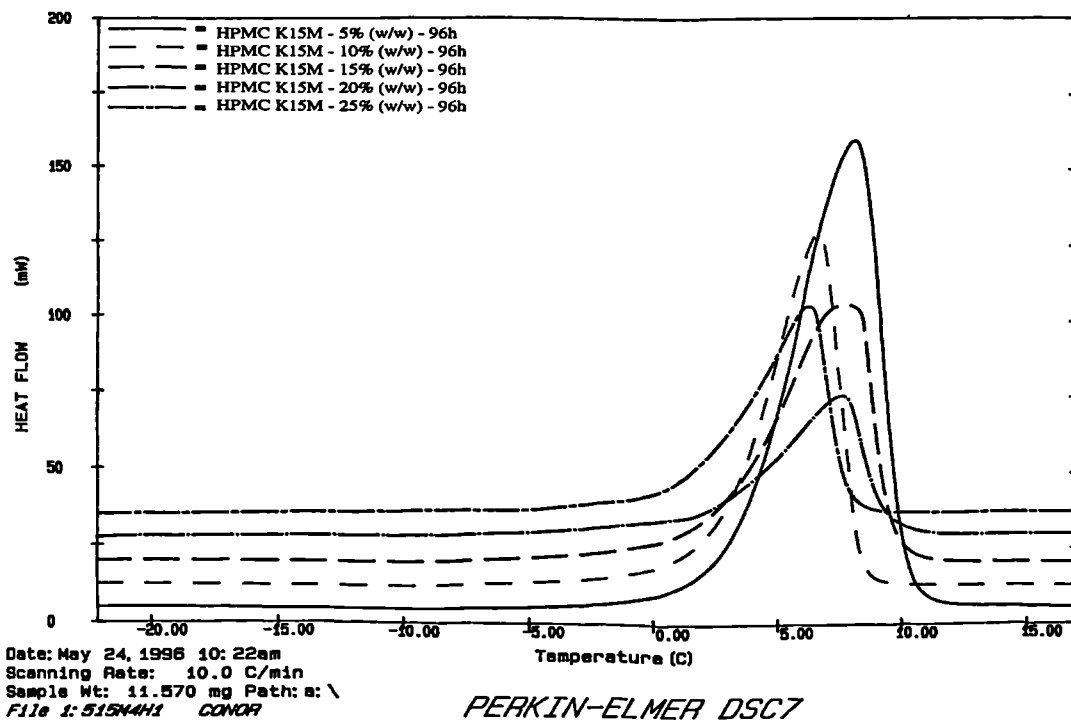
(a)



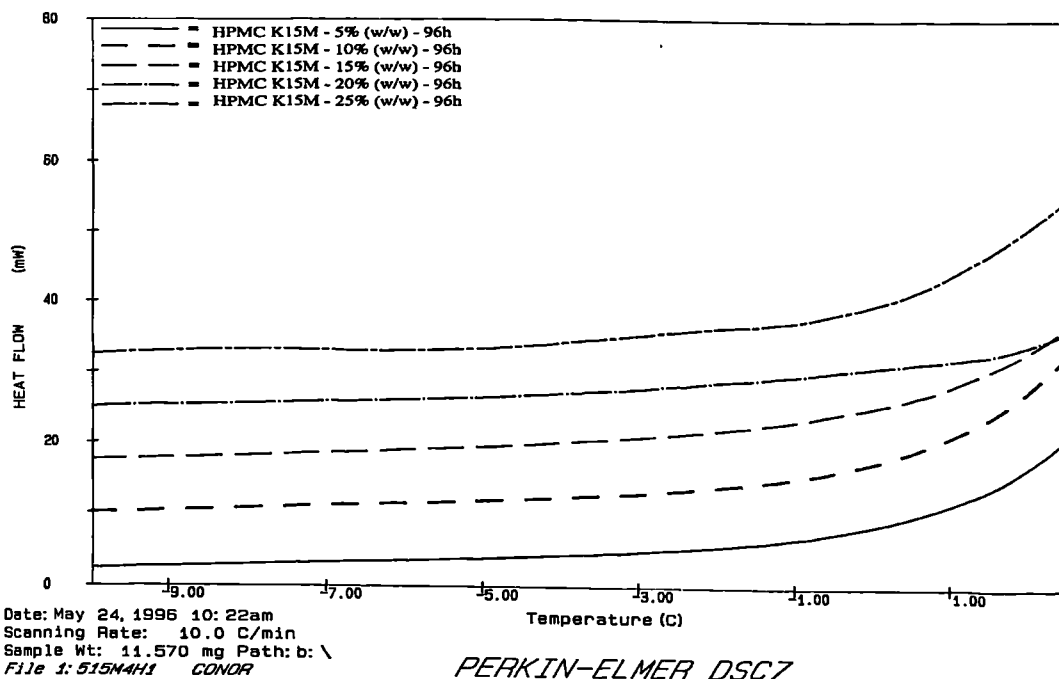
(b)

Figure 5.1 : DSC scans of HPMC K15M (5 - 25% w/w) gels cooled at $-10^{\circ}\text{Cmin}^{-1}$ and heated at $+10^{\circ}\text{Cmin}^{-1}$ after 24h storage

(a) from -22.5 to $+20^{\circ}\text{C}$ (b) from -15 to 0°C



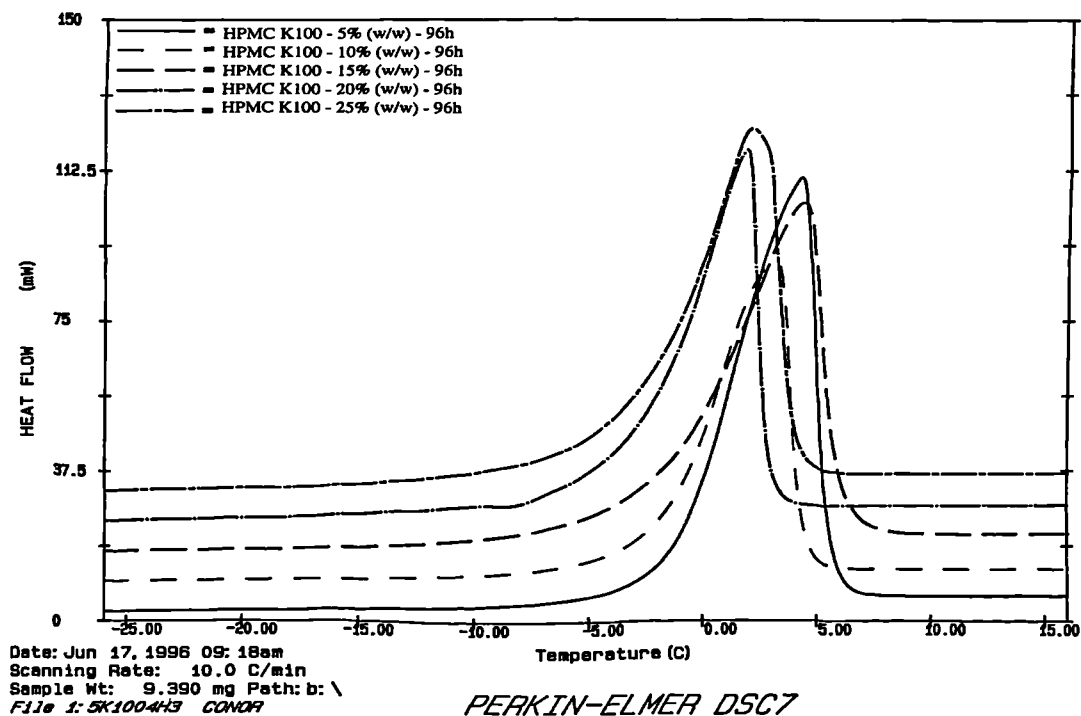
(a)



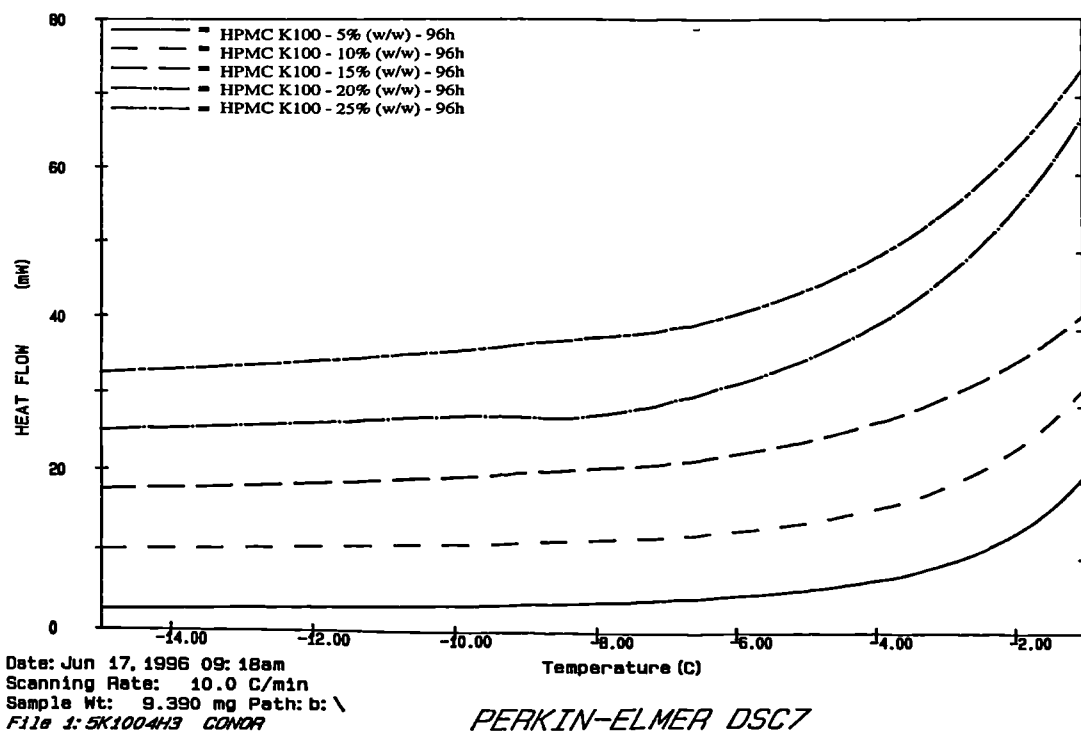
(b)

Figure 5.2 : DSC scans of HPMC K15M (5 - 25% w/w) gels cooled at $-10^{\circ}\text{Cmin}^{-1}$ and heated at $+10^{\circ}\text{Cmin}^{-1}$ after 96h storage

(a) from -22 to $+17^{\circ}\text{C}$ (b) from -10 to 0°C



(a)

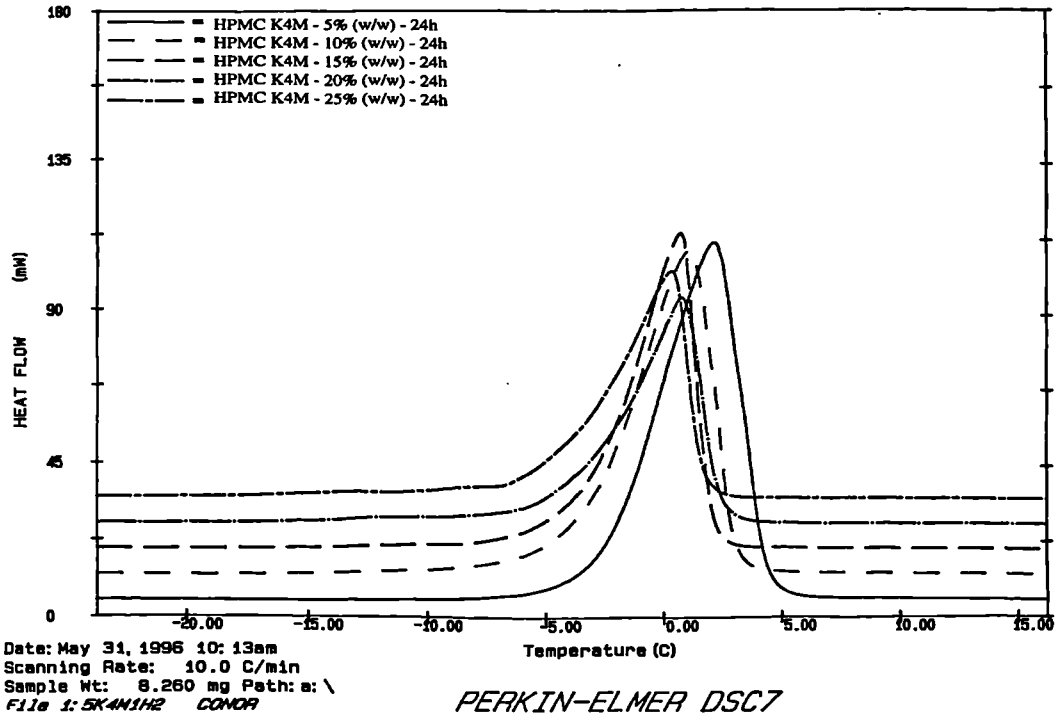


(b)

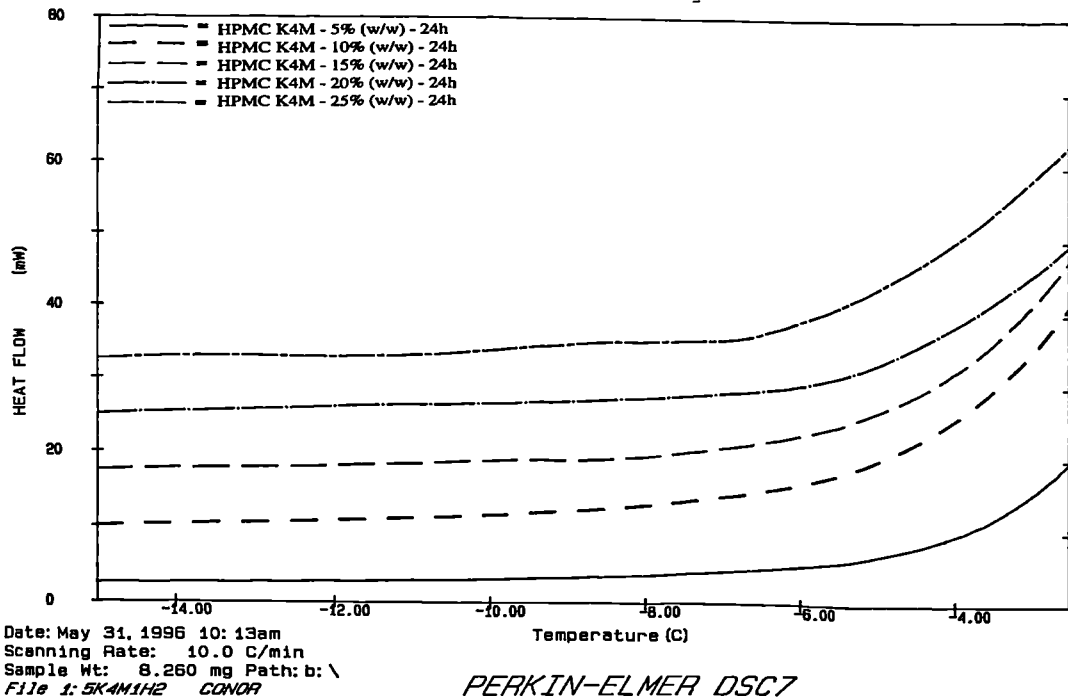
Figure 5.3 : DSC scans of HPMC K100LV (5 - 25% w/w) gels cooled at $-10^{\circ}\text{Cmin}^{-1}$ and heated at $+10^{\circ}\text{Cmin}^{-1}$ after 96h storage

(a) from -26 to $+16^{\circ}\text{C}$

(b) from -15 to -1°C



(a)

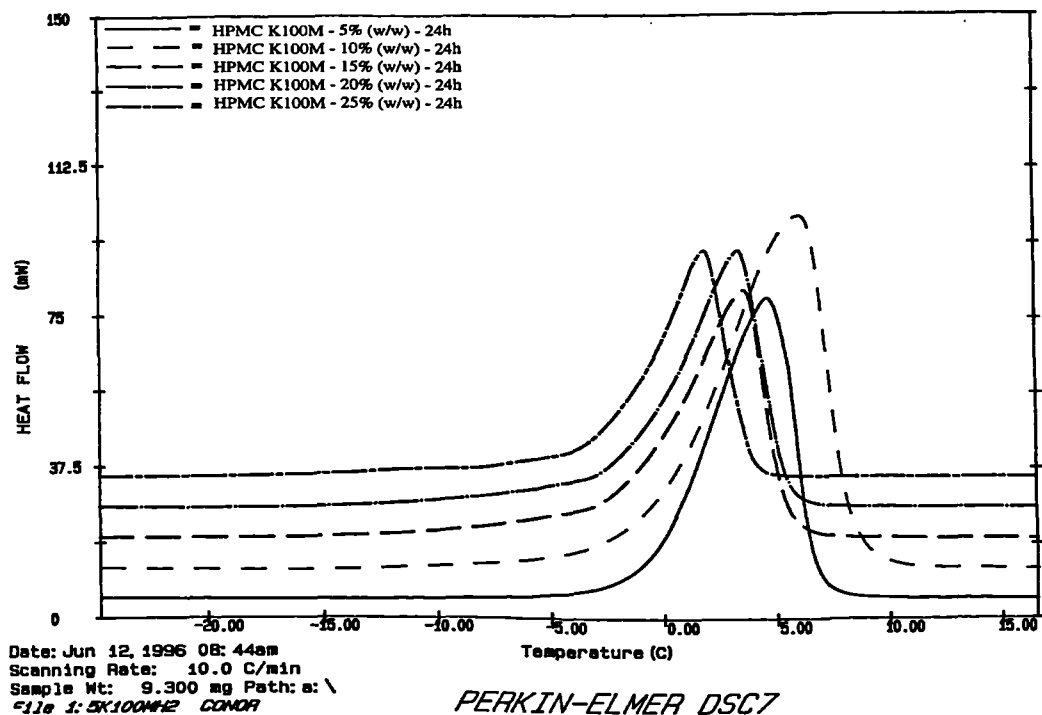


(b)

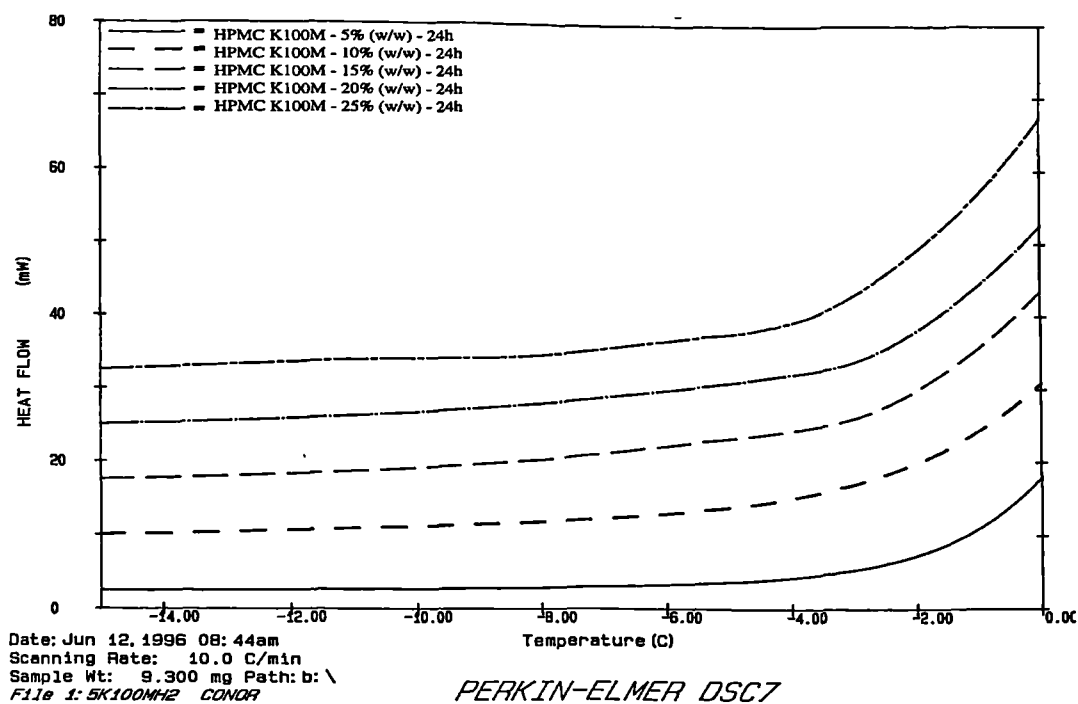
Figure 5.4 : DSC scans of HPMC K4M (5 - 25% w/w) gels cooled at $-10^{\circ}\text{Cmin}^{-1}$ and heated at $+10^{\circ}\text{Cmin}^{-1}$ after 24h storage

(a) from -25 to $+16^{\circ}\text{C}$

(b) from -15 to -3°C



(a)



(b)

Figure 5.5 : DSC scans of HPMC K100M (5 - 25% w/w) gels cooled at $-10^{\circ}\text{Cmin}^{-1}$ and heated at $+10^{\circ}\text{Cmin}^{-1}$ after 24h storage

(a) from -25 to $+16^{\circ}\text{C}$ (b) from -15 to 0°C

5.4.2 Effect of polymer substituent type on the nature of water distribution within cellulose ether polymers

HPMC E4M and HPMC F4M both have a higher percentage of hydrophobic methoxyl substituents (about 29%) compared to HPMC K4M (22.2%). HPMC E4M has a similar percentage of hydrophilic hydroxypropoxyl substituents to HPMC K4M (about 8%), unlike HPMC F4M which has a lower hydroxypropoxyl percentage content (6.1%) (Table 2.1). Methylcellulose (MC A4M) possesses no hydrophilic hydroxypropoxyl substituents whereas hydroxypropylcellulose (HPC) possesses no methoxyl substituents. Therefore, cellulose ether polymers of different substitution types and levels were used.

Tables 5.5a and b, 5.6a and b, 5.7a and b and 5.8a and b show the DSC data for HPMC E4M, HPMC F4M, MC A4M and HPC. In all cases, increasing the concentration of the polymer from 5-25% (w/w) resulted in a decrease in both the endothermic peak onset temperature and the endothermic peak. A decrease in the endothermic melting enthalpy with increasing polymer concentration was also observed. These trends are similar to those observed for the HPMC K-series (section 5.4.1).

There was no specific trend between polymer substitution type and extent of melting peak depression with increase in polymer concentration.

The presence of thermal events occurring to the left of the main endotherm for the melting of free water were found to be dependent on polymer substitution type. In HPMC F4M gels, such events were barely visible after 24h storage, but became more pronounced in 20 and 25 % w/w gels after 96h storage. In HPMC E4M, pre-endothermic events were visible in both 20 and 25 % w/w gels after 24 and 96h storage. In the case of methylcellulose, these events were visible in both 20 and 25 % w/w gels after 24h storage, however, they were only visible in 25 % w/w gels after 96h storage. Finally, in all HPC gels, there were no pre-endothermic events visible after either 24 or

Table 5.5a : Effect of HPMC E4M concentration (% w/w) on the endothermic peak onset/peak and the endothermic melting enthalpy (Jg^{-1}) (n = 3; \pm SD) after 24h storage

HPMC E4M (% w/w)	Endothermic peak onset ($^{\circ}C$)	Endothermic peak ($^{\circ}C$)	Endothermic enthalpy (J/g)
5	3.77 \pm 0.5	10.26 \pm 1.2	237.19 \pm 1.4
10	3.23 \pm 0.4	8.50 \pm 1.6	210.12 \pm 3.6
15	2.86 \pm 0.3	9.33 \pm 0.5	184.76 \pm 5.1
20	2.49 \pm 0.3	8.48 \pm 0.6	174.22 \pm 4.0
25	1.91 \pm 0.1	7.31 \pm 0.1	160.92 \pm 4.8

Table 5.5b : Effect of HPMC E4M concentration (% w/w) on the endothermic peak onset/peak and the endothermic melting enthalpy (Jg^{-1}) (n = 3; \pm SD) after 96h storage

HPMC E4M (% w/w)	Endothermic peak onset ($^{\circ}C$)	Endothermic peak ($^{\circ}C$)	Endothermic enthalpy (J/g)
5	-2.05 \pm 0.3	3.73 \pm 1.1	306.78 \pm 8.2
10	-2.03 \pm 0.2	4.01 \pm 0.4	278.37 \pm 6.5
15	-2.59 \pm 0.5	3.95 \pm 1.2	256.61 \pm 6.6
20	-2.67 \pm 0.1	4.99 \pm 0.3	248.02 \pm 3.5
25	-3.81 \pm 0.3	1.91 \pm 1.6	204.53 \pm 1.9

Table 5.6a : Effect of HPMC F4M concentration (% w/w) on the endothermic peak onset/peak and the endothermic melting enthalpy (Jg^{-1}) (n = 3; \pm SD) after 24h storage

HPMC F4M (% w/w)	Endothermic peak onset ($^{\circ}\text{C}$)	Endothermic peak ($^{\circ}\text{C}$)	Endothermic enthalpy (J/g)
5	-3.19 ± 0.4	3.43 ± 0.7	303.53 ± 2.6
10	-4.00 ± 0.5	1.14 ± 1.7	271.22 ± 8.3
15	-4.10 ± 0.1	2.68 ± 0.7	251.57 ± 7.1
20	-5.08 ± 0.3	0.60 ± 1.0	235.74 ± 5.8
25	-5.27 ± 0.2	1.18 ± 0.8	223.99 ± 4.5

Table 5.6b : Effect of HPMC F4M concentration (% w/w) on the endothermic peak onset/peak and the endothermic melting enthalpy (Jg^{-1}) (n = 3; \pm SD) after 96h storage

HPMC F4M (% w/w)	Endothermic peak onset ($^{\circ}\text{C}$)	Endothermic peak ($^{\circ}\text{C}$)	Endothermic enthalpy (J/g)
5	-3.13 ± 0.6	2.79 ± 1.1	300.52 ± 3.6
10	-3.90 ± 0.4	2.44 ± 1.4	274.57 ± 6.1
15	-4.51 ± 0.6	2.66 ± 1.8	244.38 ± 18.1
20	-5.10 ± 0.0	0.02 ± 0.5	230.18 ± 4.8
25	-5.53 ± 0.3	0.29 ± 0.5	206.46 ± 10.1

Table 5.7a : Effect of MC A4M concentration (% w/w) on the endothermic peak onset/peak and the endothermic melting enthalpy (Jg^{-1}) (n = 3; \pm SD) after 24h storage

MC A4M (% w/w)	Endothermic peak onset ($^{\circ}C$)	Endothermic peak ($^{\circ}C$)	Endothermic enthalpy (J/g)
5	-3.58 \pm 0.5	2.05 \pm 1.0	302.72 \pm 4.8
10	-4.27 \pm 0.4	1.79 \pm 1.3	276.28 \pm 1.1
15	-4.79 \pm 0.6	1.71 \pm 2.0	254.36 \pm 4.5
20	-5.17 \pm 0.1	1.10 \pm 1.0	234.83 \pm 4.0
25	-5.75 \pm 0.2	0.57 \pm 1.4	208.97 \pm 6.3

Table 5.7b : Effect of MC A4M concentration (% w/w) on the endothermic peak onset/peak and the endothermic melting enthalpy (Jg^{-1}) (n = 3; \pm SD) after 96h storage

MC A4M (% w/w)	Endothermic peak onset ($^{\circ}C$)	Endothermic peak ($^{\circ}C$)	Endothermic enthalpy (J/g)
5	-2.03 \pm 0.5	4.89 \pm 1.1	299.71 \pm 9.5
10	-2.37 \pm 0.3	4.23 \pm 0.9	277.04 \pm 4.1
15	-3.05 \pm 0.1	2.97 \pm 0.7	264.40 \pm 1.7
20	-3.11 \pm 0.5	3.61 \pm 1.8	241.75 \pm 0.3
25	-4.18 \pm 0.4	1.53 \pm 0.8	212.90 \pm 10.9

Table 5.8a : Effect of Klucel HPC concentration (% w/w) on the endothermic peak onset/peak and the endothermic melting enthalpy (Jg^{-1}) (n = 3; \pm SD) after 24h storage

HPC (% w/w)	Endothermic peak onset ($^{\circ}C$)	Endothermic peak ($^{\circ}C$)	Endothermic enthalpy (J/g)
5	-2.83 \pm 0.5	5.35 \pm 1.4	303.73 \pm 0.9
10	-4.20 \pm 0.1	1.37 \pm 0.4	274.39 \pm 3.9
15	-4.26 \pm 0.3	1.81 \pm 1.2	251.76 \pm 7.4
20	-5.05 \pm 0.1	0.57 \pm 0.6	218.07 \pm 6.7
25	-5.00 \pm 0.2	-0.03 \pm 0.7	208.55 \pm 8.4

Table 5.8b : Effect of Klucel HPC concentration (% w/w) on the endothermic peak onset/peak and the endothermic melting enthalpy (Jg^{-1}) (n = 3; \pm SD) after 96h storage

HPC (% w/w)	Endothermic peak onset ($^{\circ}C$)	Endothermic peak ($^{\circ}C$)	Endothermic enthalpy (J/g)
5	-1.49 \pm 0.6	5.73 \pm 1.9	294.64 \pm 13.9
10	-1.76 \pm 0.7	5.65 \pm 1.8	270.88 \pm 2.7
15	-2.11 \pm 0.1	4.86 \pm 1.0	255.3 \pm 14.7
20	-3.07 \pm 0.1	3.06 \pm 0.7	220.53 \pm 9.6
25	-3.73 \pm 0.5	2.19 \pm 0.9	195.59 \pm 8.3

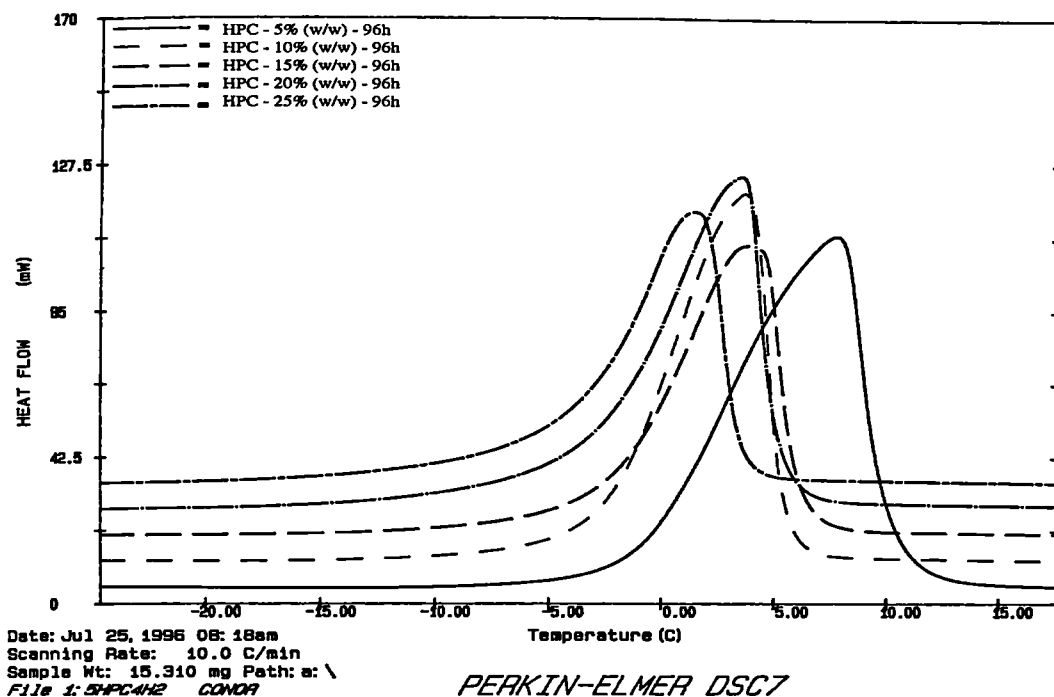
96h (Figure 5.6). These results indicate that the nature of water distribution within polymer gels is dependent on substitution type and substitution level. The DSC scans of HPMC F4M in which no pre-endothermic events are visible after 24h and HPC gels in which no pre-endothermic events are visible after either 24 or 96h storage are investigated further.

Previously, the pre-endothermic events in HPMC K15M gels were found to be exaggerated by an increase in polymer concentration (section 3.4.1.1). Therefore, the presence of pre-endothermic events was examined for gels of HPC and HPMC F4M of higher concentration.

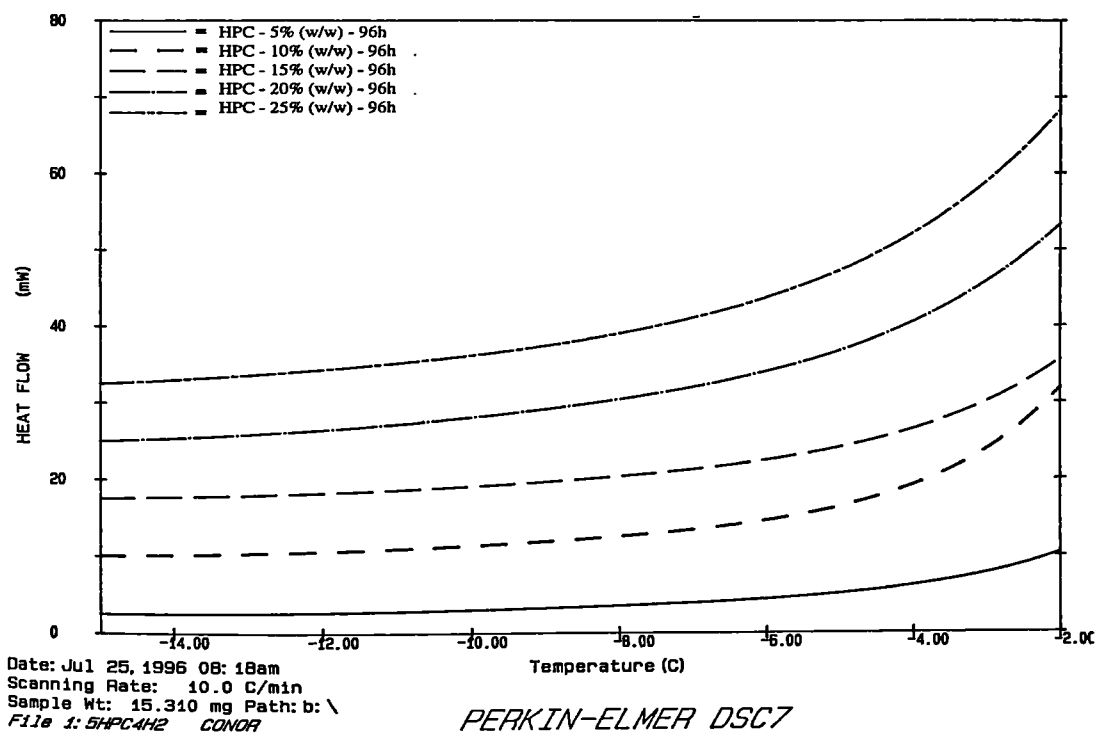
A series of HPMC F4M (19.10 - 37.8% w/w) and HPC (27.3 - 48.2% w/w) gels were prepared according to the method outlined in section 2.2.1 for gels (>25% w/w) and were subjected to DSC after 24h storage.

Pre-endothermic events were visible in HPMC F4M at the higher concentrations studied (Figure 5.7). Events were visible at concentrations < 25(% w/w), unlike previous analysis, after 24h storage. This may be explained by considering the gel preparation method used in this analysis, where gel samples were analysed effectively 48h after the initial gel had been made up. Appearance of pre-endothermic events may be due to the additional 24h equilibration time, which allowed more time for water to become bound to the polymer making it visible as pre-endothermic events on the DSC trace. In contrast, in HPC gels, only a small secondary event became visible at concentrations > 30 % (w/w) (Figure 5.8).

Hydroxypropylcellulose gels clearly behaved differently in comparison to the HPMC/MC gels studied. HPC contains a high percentage of hydrophilic hydroxypropoxyl groups and therefore may be expected to have a lot of bound water due to binding site availability. If water is binding to these groups, it is not visible as pre-endothermic events on DSC scans. It is possible that water attached to the polymer, in this case,



(a)

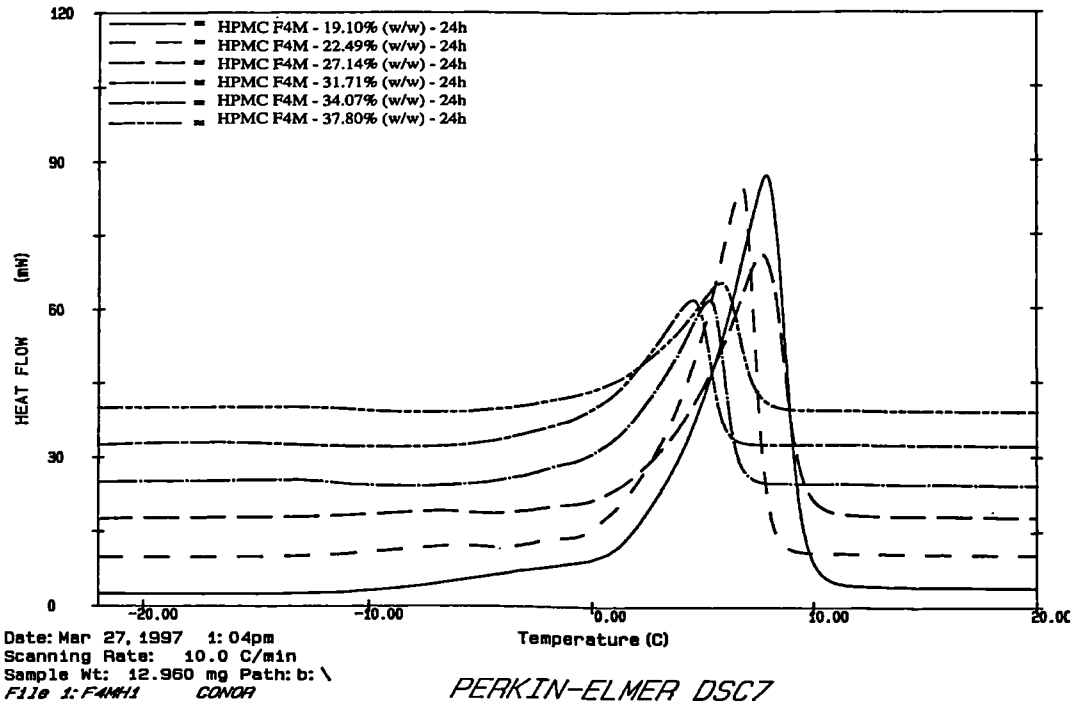


(b)

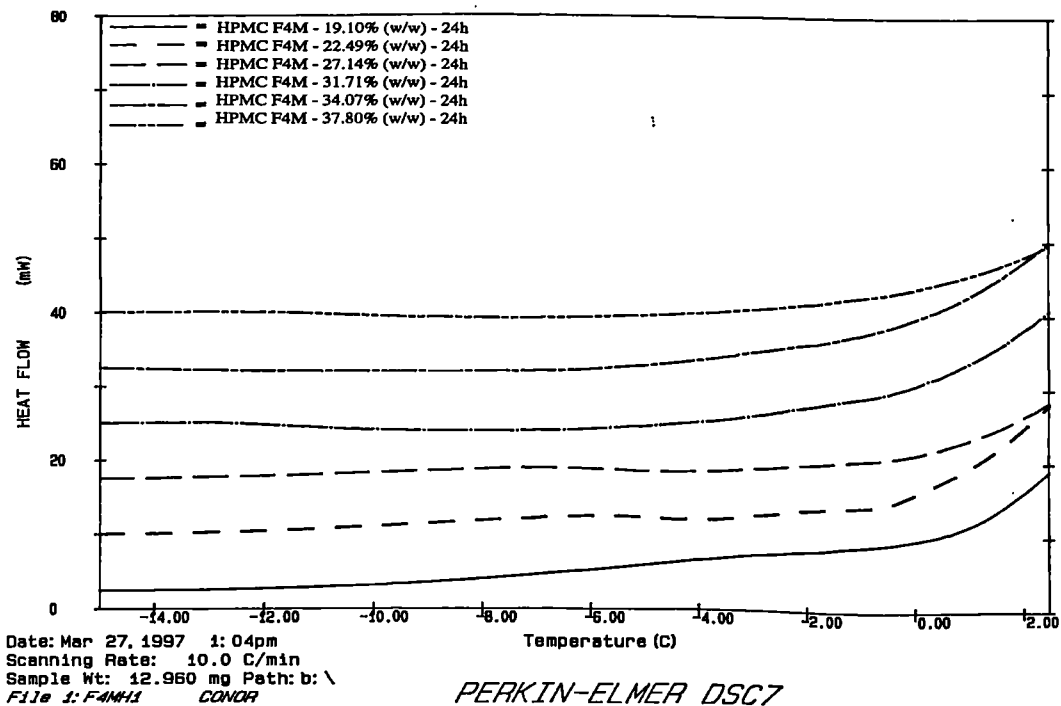
Figure 5.6 : DSC scans of HPC (5 - 25% w/w) gels cooled at $-10^{\circ}\text{Cmin}^{-1}$ and heated at $+10^{\circ}\text{Cmin}^{-1}$ after 96h storage

(a) from -25 to $+17.5^{\circ}\text{C}$

(b) from -15 to -2°C



(a)



(b)

Figure 5.7 : DSC scans of HPMC F4M (19.10 - 37.8% w/w) gels cooled at $-10^{\circ}\text{Cmin}^{-1}$ and heated at $+10^{\circ}\text{Cmin}^{-1}$ after 24h storage

(a) from -22 to $+20^{\circ}\text{C}$ (b) from -15 to $+2.5^{\circ}\text{C}$

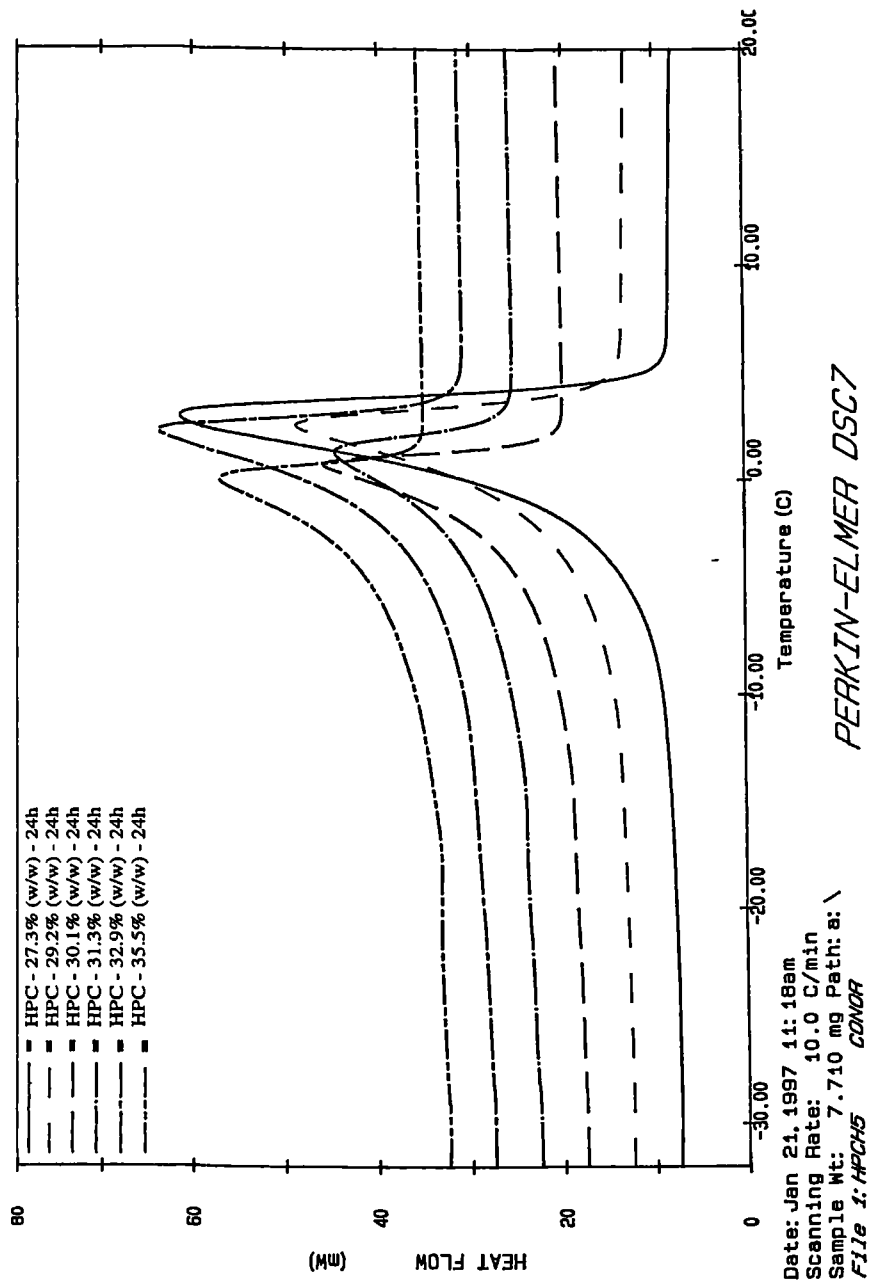


Figure 5.8 : DSC scans of HPC (27.3 - 35.5% w/w) gels cooled at $-10^{\circ}\text{Cmin}^{-1}$ and heated at $+10^{\circ}\text{Cmin}^{-1}$ after 96h storage

binds so tightly that it does not freeze upon cooling. This would explain the non-appearance of pre-endothermic events which have been attributed to water loosely attached to the polymer and is capable of freezing. If this theory is indeed correct, the amount of non-freezing bound water in HPC gels, should be quite high as shown in Table 5.9. This idea is explored further in section 5.4.3.2.

5.4.3 Quantitative analysis of the effect of molecular weight and substitution type on water distribution within cellulose ether polymers

5.4.3.1 Water distribution within cellulose ether polymers as calculated by the method proposed by Ford and Mitchell

The number of moles of bound (non-freezing) water per polymer repeating unit (PRU) was calculated for HPMC K100LV, HPMC K4M, HPMC K15M, HPMC K100M, HPMC E4M, HPMC F4M, MC A4M and HPC from the data in Tables 5.1 - 5.8, according to the method outlined by Ford and Mitchell (1995) (section 3.4.1.3.1) and are listed in Table 5.9. The bound water content was calculated using values for the PRU as indicated in Table 5.9. The values for PRU were calculated according to the % methoxyl and % hydroxypropoxyl substitution on the cellulose ether backbone (Table 2.1).

HPMC K4M, HPMC E4M and MC A4M all showed a decrease in their bound water content from 24 to 96h storage, whereas all other polymers showed an increase in their bound water content during this equilibration period (Table 5.9). The largest change in bound water content occurs in HPMC K100LV (the lowest viscosity polymer within the K-series), which shows a 58% increase in the bound water content from 24 to 96h. Allowing 96h equilibration, which should be ample time for uniform equilibration in all gel samples, an increase in the bound water content is apparent with an increase in polymer viscosity within the K-series.

Table 5.9 : Effect of cellulose ether molecular weight, substitution type and equilibration time on the bound (non-freezing) water (BW) content per polymer repeating unit (PRU) as calculated by the method proposed by Ford and Mitchell (1995)

Polymer	Viscosity (cP)	PRU Value	Moles BW per		R ²	
			PRU (24h)	PRU (96h)	(24h)	(96h)
HPMC K100	93	189	2.4	4.4	0.994	0.973
HPMC K4M	4, 196	188	7.1	4.5	0.996	0.973
HPMC K15M	15, 825	189	4.5	6.5	0.978	0.934
HPMC K100M	119, 768	192	6.0	6.6	0.970	0.963
HPMC F4M	5, 218	187	3.2	5.4	0.968	0.993
HPMC E4M	3, 970	190	6.2	5.6	0.974	0.966
MC A4M	3, 811	177	5.3	3.8	0.999	0.988
HPC	5, 950	171	5.5	6.1	0.983	0.990

R² = correlation coefficient

Considering the bound water content after 96h to be a more accurate reflection of the water distribution within gel systems, MC A4M has the lowest bound water content of all other substitution types. This may be explained by considering the structure of MC A4M, which has a high hydrophobic methoxyl content (29.9%) (Table 2.1) with no hydrophilic hydroxypropoxyl substitution.

A high methoxyl substituent content will not favour large amounts of water binding to the polymer. Previous studies have shown that methoxyl substituent levels are the major factor in causing an apparent decrease in cellulose ether solubility and causing precipitation of polymers in cloud-point studies (Mitchell et al, 1993a). Reduced cellulose ether solubility will result in lower amounts of water binding to the polymer.

After 96h equilibration time, HPC has a high bound water content. HPC contains no methoxyl substitution and only hydroxypropoxyl substituents and a large value for bound water content after equilibration would be expected. This was considered to explain the non-appearance of pre-endothermic events in the DSC scans of HPC gels (section 5.4.2), indicating that only tightly bound water was present.

It is reported that HPMC K4M, having a similar hydroxypropoxyl constituent to HPMC E4M, but with smaller methoxyl substituent levels than either HPMC E4M, HPMC F4M or MC A4M, is more water soluble and undergoes precipitation at higher temperatures than polymers of other substitution types (Mitchell et al, 1993a). This may explain the high value for bound water content (7.1 moles BW per PRU) after 24h in the case of HPMC K4M. However, this high bound water content is not reflected after 96h. HPMC E4M and HPMC F4M have similar bound water contents after 96h which may be a reflection of similar percentages of methoxyl substituents.

5.4.3.2 Comparison of two methods used to estimate bound water content of hydrophilic polymers using DSC

Characterisation of bound water content, within HPMC polymers, using DSC data has been described by two methods. In section 3.4.1.3.1 and section 5.4.3.1, the number of moles of non-freezing water per PRU was determined according to the procedure reported by Ford and Mitchell (1995). They have reported that a linear relationship exists between the melting enthalpy (J/g, of gel) and the percentage water or polymer content in a HPMC gel. By extrapolating such plots to zero enthalpy through the lines of best fit, the concentration of the minimum water required to occupy the binding sites of the polymer, giving complete hydration is calculated. All water present at this point is regarded as bound water. Alternatively, Sung (1978) has described a linear relationship between enthalpy calculated as J/g dry polymer and the water : polymer ratio calculated as gram of water per gram of polymer. In this case, extrapolation to zero enthalpy gives the total amount of water which may be bound to a polymer. Examples of both methods are depicted in Figure 5.9 and Figure 5.10 for MC A4M gels stored for 24h.

For comparison purposes, the calculation method proposed by Sung (1986) was applied to the enthalpy data for all polymers after both 24 and 96h storage and the quantity of bound water was calculated as the number of moles of BW per PRU using the PRU values listed in Table 5.9. Table 5.10 shows the calculated data and the associated regression coefficients (R^2).

The number of moles of BW per PRU varied according to the calculation method. In general, the amount of BW calculated using the Sung method was greater after both 24 and 96h than that calculated using the Ford and Mitchell method. The regression coefficient values also indicate that the fit of a straight line through the data is much better when employing the Sung method of calculation.

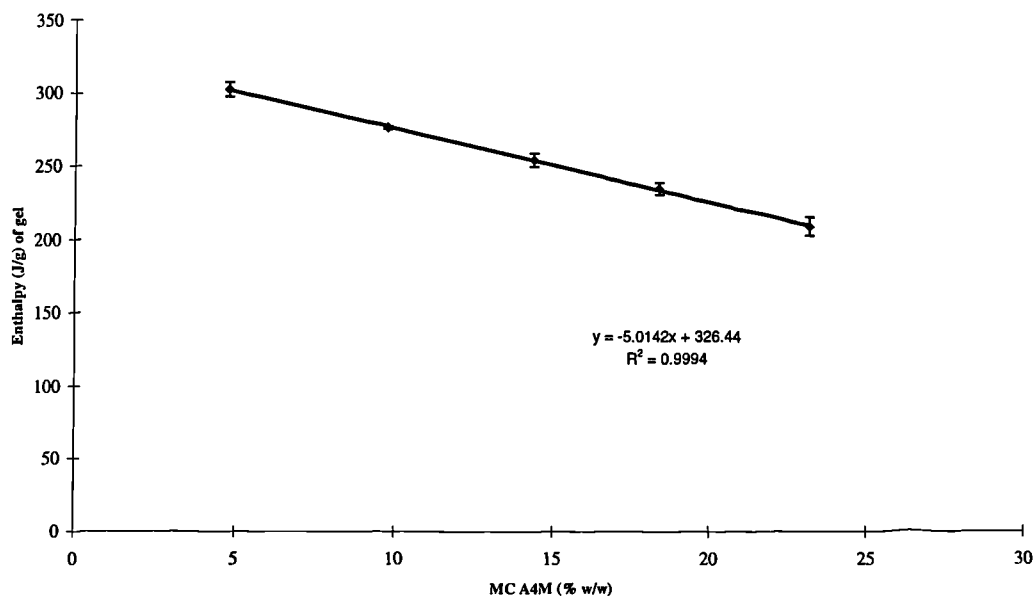


Figure 5.9 : Effect of MC A4M concentration (% w/w) on melting enthalpy (J/g of gel) after 24h storage time ($n = 3 \pm SD$)

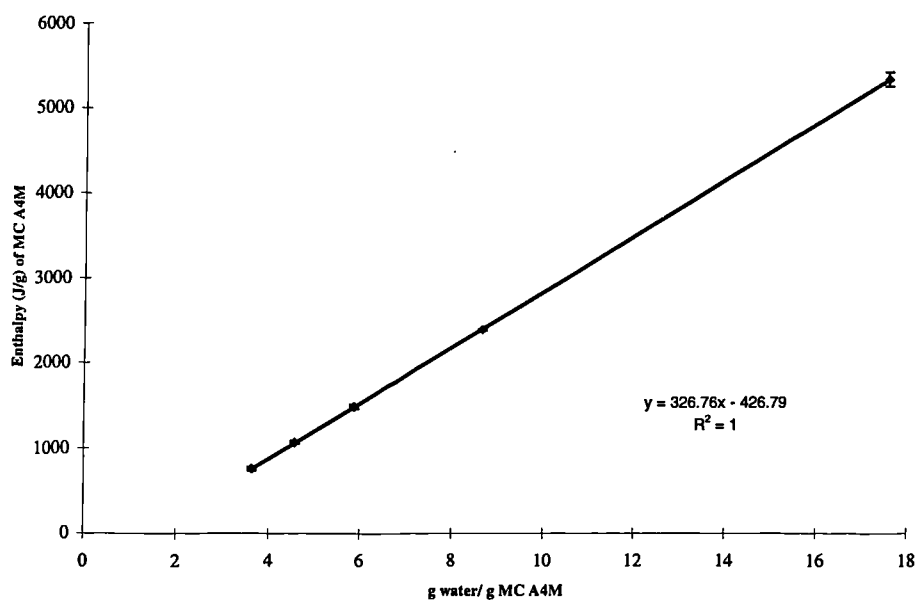


Figure 5.10 : Effect of MC A4M concentration (water/polymer content; g/g) on melting enthalpy (J/ g of polymer) after 24h storage time ($n = 3 \pm SD$)

A much closer comparison of BW values, calculated using both methods, has previously been described for the HPMC K-series (not for methylcellulose) (Nokhodchi et al, 1997). The values reported varied between 6 and 7 (method of Sung) or 5 and 6 (method of Ford and Mitchell) for gels stored for 4 days. A value of 6.6 moles per PRU was also reported by Ford and Mitchell (1995) for HPMC K15M gels. The high BW values obtained using the method of Sung in this work may be explained by considering the sample preparation method employed. Nokhodchi et al (1997) added different weights of distilled water to DSC pans containing HPMC powders compressed as wafers enabling direct calculation of the water : polymer ratio (g water / g HPMC). All samples were held at room temperature for 4 days before DSC analysis. Preparation of samples in this way, enables a much broader range of water : polymer ratios to be prepared and analysed. However these are not gel samples and uniform and full hydration may not occur. On the other hand, sample preparation by initial extemporaneous gel preparation, enables only a limited range of gel concentrations (low polymer concentrations) to be prepared and analysed, but uniform and full hydration of the polymer is ensured. Extrapolation through these points, as in the Ford and Mitchell method (Figure 5.9), involves a long extrapolation to the intercept on the x - axis. The relationship between melting enthalpy and percentage polymer may not be a straight line and construction of a line of best fit through these points introduces a possible source of error in this method which is magnified due to extended extrapolation to the x - axis.

Table 5.10 : Effect of cellulose ether molecular weight, substitution type and equilibration time on the bound (non-freezing) water (BW) content per polymer repeating unit (PRU) as calculated by the method proposed by Sung (1978)

Polymer	Moles BW per	R ² (24h)	Moles BW per	R ² (96h)
	PRU (24h)		PRU (96h)	
HPMC K100	10.7	1	13.7	0.999
HPMC K4M	15.2	0.999	13.9	0.999
HPMC K15M	13.7	0.998	17.4	0.997
HPMC K100M	13.0	0.999	15.0	0.999
HPMC F4M	13.1	0.999	13.8	0.999
HPMC E4M	15.6	0.999	13.5	0.999
MC A4M	12.9	1	11.22	0.999
HPC	13.7	0.999	12.6	0.999

R² = correlation coefficient

5.5 Conclusions

The water distribution within cellulose ether polymer gels was found to be dependent on polymer molecular weight and gel equilibration (or storage) time. The presence of loosely bound water was characterised as pre-endothermic events occurring to the left of the main melting endotherm of free water. The occurrence and magnitude of these pre-endothermic events were affected by polymer molecular weight, substitution type and substitution levels. As the concentration of polymer increased, the amount of water required to hydrate the polymer also increased resulting in less free water being available. This was reflected in a decrease in both exothermic and endothermic enthalpies with increase in polymer concentration, irrespective of molecular weight or substitution type.

The amount of water tightly bound to the polymer, as calculated by the method proposed by Ford and Mitchell (1995), was dependent on polymer molecular weight, substituent type and substitution level. It was thought that the amount of bound water present in gel systems after 96h gave a truer reflection of the water distribution within gels due to an increased equilibration time. A number of conclusions were drawn regarding the amount of bound water within selected polymers based on the degree of substitution of hydrophilic and hydrophobic substituents on the polymer backbone. Calculation of the bound water content of the gels using an alternative method (Sung, 1978) has identified possible problems in the assumptions made when analysing bound water content by the Ford and Mitchell method, using gels of only low polymer concentration.

HPC gels did not exhibit any pre-endothermic events at gel concentrations of 5-30% w/w and after 96h storage, HPC had a relatively high bound water content. It was thought, because HPC contains no methoxyl substitution and only hydroxypropoxyl substituents, that a lot of bound water would be present in such systems. It is possible that water attached to the polymer in this case binds so tightly that it does not freeze

upon cooling, thus explaining the non-appearance of pre-endothermic events which have been attributed to water loosely attached to the polymer and is capable of freezing.

Methylcellulose (MC A4M) gels were found to contain the lowest amount of bound water of all the polymers studied after 96h storage time. This may be explained by consideration of the structure of methylcellulose which has a high hydrophobic methoxyl content with no hydrophilic hydroxypropoxyl substitution. A high methoxyl substituent content will not favour large amounts of water binding to the polymer.

CHAPTER 6

DYNAMIC WATER VAPOUR SORPTION/DESORPTION STUDIES ON CELLULOSE ETHER POLYMERS

Chapter 6 Dynamic water vapour sorption/desorption studies on cellulose ether polymers

6.1 Introduction

Polymers in the solid state containing residual moisture, experience significant changes in their physico-chemical properties. For example, their crystal structure, powder flow, chemical stability, compaction, lubricity, polymer film permeability, dissolution rate and glass transition temperature (T_g) are influenced (Zografi, 1988). Such water may be present due to storage conditions or alternatively may be due to processing conditions which involve the use of water.

Water sorption to cellulose and starch based excipients has been studied, and at least three thermodynamic states of water have been identified (Zografi and Kontny, 1986). These include water which is tightly bound to anhydroglucose units on the cellulose backbone, unrestricted water which has properties similar to bulk water, and water having properties intermediate between the two extremes.

Moisture sorption isotherms are constructed by measuring the mass of moisture taken up per unit mass of dry solid as a function of the relative humidity at constant temperature. It is possible to apply a number of mathematical formulae to such isotherms in an attempt to characterise the process of vapour uptake. Brunauer, Emmett and Teller (1938) suggested that water only exists in two states according to their BET equation (section 2.2.3.2; equation 2.6). It is assumed that the influence of the solid on the adsorbed species extends only to the first layer and the remainder of the molecules making up the multilayered portion have similar properties to those within the bulk phase. This equation, however, generally fails to provide a good data fit with relative humidities of 35% and above, which may suggest that more than two thermodynamic states are present. Particle surface area has been calculated from this equation (Hollenbeck et al, 1978; Zografi et al, 1984; Faroongsarng and Peck, 1994b; Matsumoto et al, 1994).

The BET equation was subsequently modified (Anderson, 1946; Pickett, 1958) to be applicable over a wider range of relative humidities. Svetlik and Pouchly (1976) have applied the Anderson equation to copolymers of hydroxyethyl methacrylate and hydroxyethoxyethyl methacrylate. Independently, the GAB (Guggenheim, Anderson, and DeBoer) equation (DeBoer, 1968) was developed (equation 6.1):

$$\text{Equation 6.1} \quad W = \frac{C_G \cdot K \cdot W_m \frac{p}{p_0}}{(1 - K \frac{p}{p_0}) (1 - K \frac{p}{p_0} + C_G K \frac{p}{p_0})}$$

where W is the weight of water absorbed, C_G and K are parameters related to the heat of sorption, W_m is the weight of water in the form of a monolayer and p/p_0 is the relative humidity. This equation is essentially an extension of the BET equation assuming three thermodynamic states for the adsorbed species by introduction of a state with properties intermediate to those assumed in the original BET model represented by the parameter K . This GAB theory has been successfully applied to water sorption of celluloses (Sadeghnejad et al, 1986; Faroongsarng and Peck, 1994a) and to wheat gluten samples (De Jong et al, 1996). The BET model assumes adsorption onto the surfaces of a crystalline solid, however, water interactions with amorphous solids e.g. celluloses are different due to water absorption. Young and Nelson (1967a, 1967b) have hypothesised that condensed moisture on top of the monomolecular layer may develop a concentration gradient driving moisture into the sorbent bulk. They proposed the Young-Nelson equations which were later applied to maize starch and its mixtures with various drugs (York, 1981); selected disintegrants (Faroongsarng and Peck, 1994a) and hydroxypropylmethylcelluloses (Nokhodchi et al, 1997).

The construction of moisture sorption/desorption isotherms has traditionally been achieved employing desiccators and saturated solutions to produce the required relative humidity in combination with gravimetric techniques to measure mass change (Khan and Pilpel, 1986, 1987; Ahlneck and Alderborn, 1989). Sadek and Olsen (1981) employed an oscillating quartz crystal which functions as a highly sensitive microbalance to construct sorption/ desorption isotherms. The resonating

quartz crystal was coated with a range of polymers, including cellulose derivatives, which change the resonating frequency of the crystal. The resonating frequency, which is a function of mass deposited on the crystal surface, was monitored before and after exposure to water vapour. A twin heat conduction microcalorimeter, made up of a sample and reference calorimeters each consisting of two calorimetric vessels, has been employed (Wadso and Wadso, 1996). The calorimetric vessels include a vaporisation chamber from which vaporized liquid diffuses into a sorption chamber during measurements. A new method for the measurement of water sorption by biological materials known as single particle levitation (SPL) was applied to the measurement of water vapour sorption by bacterial spores (Rubel, 1997). This method had been previously used to measure water adsorption by microparticles of carbon (Rubel, 1992).

The dynamic measurement of water uptake by solids has been achieved by employing gravimetric methods with electronic microbalances. Such on-line gravimetric methods have traditionally used vacuum systems to achieve the required relative humidity (Rasmussen and Akinc, 1983; Astill et al, 1987). Alternatives to vacuum based measurements include systems where moisture uptake can be measured dynamically in atmospheres of controlled composition. Such systems rely on an inert carrier gas to transport moisture to the sample (Bergren, 1994). Such a system was employed to examine the solid phases of delavirdine mesylate and the technique has been called dynamic moisture sorption gravimetry (DMSG) (Bergren et al, 1996). A similar technique, employing a temperature and humidity controlled microbalance system, is that of Dynamic Vapour Sorption (DVS). Again, this is a relatively new technique, in which relative humidities are achieved by dry nitrogen gas flow through switching valves which in turn determine the amount of total flow to pass through a humidification stage (Figure 6.1). Such an apparatus was used in studies by Buckton and Darcy (1995, 1996).

Constant Temperature Incubator

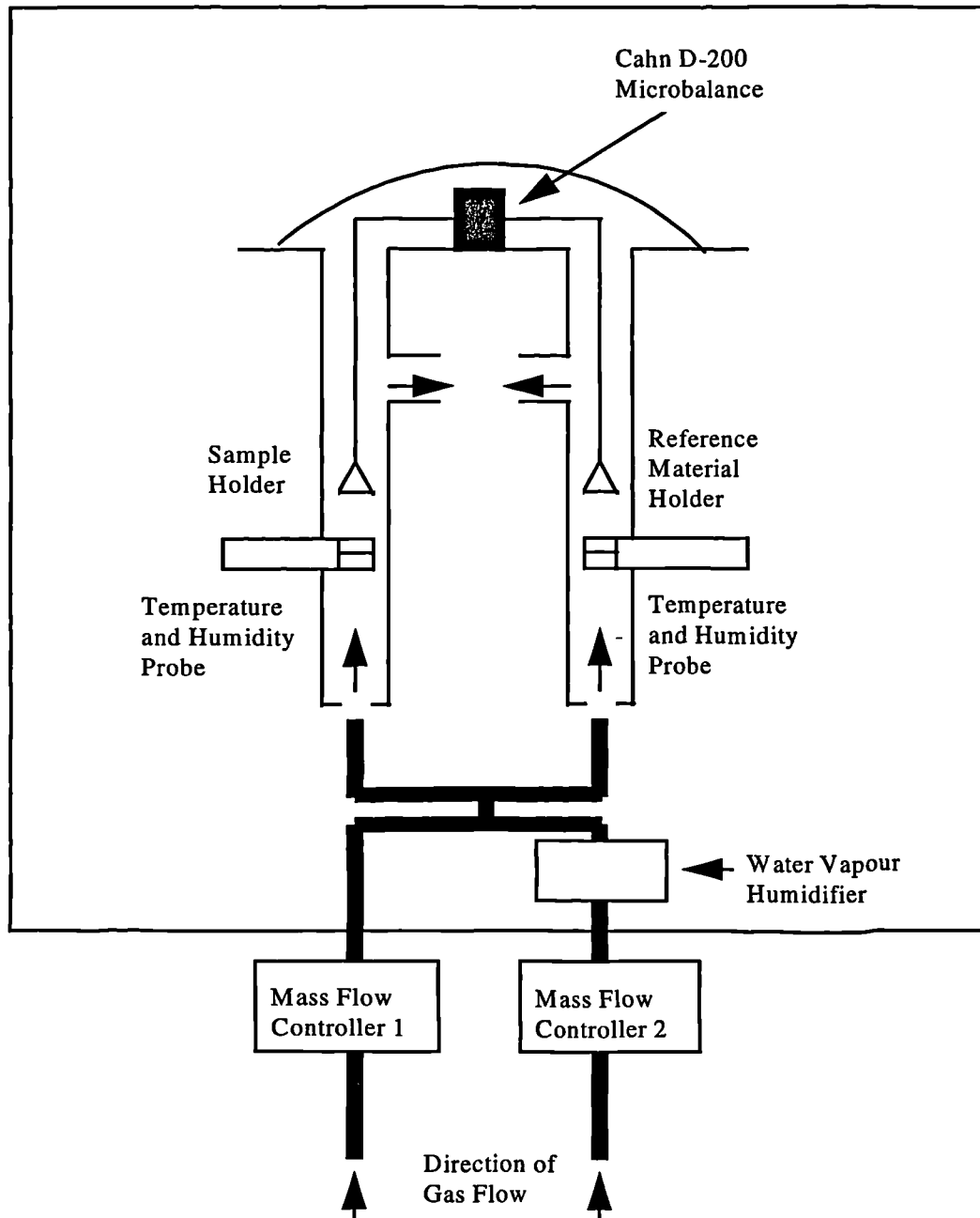


Figure 6.1 : Schematic layout of DVS-1 apparatus (adapted from, DVS Automated Water Sorption Analyser, Operations Manual)

6.1.1 Objectives

In this study, the influence of molecular weight and substitution levels of cellulose ethers on their vapour sorption/desorption characteristics was investigated using 'dynamic vapour sorption.' Subsequently, Young & Nelson (Young and Nelson, 1967a, 1967b) and BET (Brunauer, Emmett and Teller, 1938) theories were applied to the moisture sorption/ desorption data to obtain information on the moisture distribution and specific surface area of HPMC polymers, respectively.

6.2 Materials

Methocel cellulose ethers were obtained from the DOW Chemical Company (section 2.1.1; Table 2.1). The batches of HPMC K100LV and HPMC K15M used were batches BN MM94051022K and BN MM94112811K respectively. HPMCs K4M, K100M, E4M, F4M and MC A4M are as described in Table 2.1.

6.3 Methods

6.3.1 Sample preparation

Size fractions of 90 - 125 μ m for all samples were obtained by sieving 30g aliquots of each sample through test sieves (Endecotts Ltd., London, UK) on a Pascal sieve shaker (Pascal Ltd., Sussex, UK) for a period of 45 min.

6.3.2 Dynamic Vapour Sorption

The water sorption/desorption properties of the powder samples (20.83 ± 1.73 mg), were studied gravimetrically in a temperature and humidity controlled microbalance system [Dynamic Vapour Sorption (DVS) apparatus, Surface Measurement Systems, U.K.]. The Relative Humidity (RH) was raised from 0% to 90% during the sorption

cycle and lowered from 90% to 0% during the desorption cycle, at a temperature of 25°C. Each sample remained at the same RH until either six hours had passed or equilibrium had been reached (± 0.002 mg).

6.4 Results and Discussion

6.4.1 Water sorption characteristics of HPMC's with different molecular weights

The vapour sorption/ desorption properties of HPMC K100LV, HPMC K4M, HPMC K15M & HPMC K100M with similar substitution levels but increasing molecular weight were examined by dynamic vapour sorption. A typical sorption/ desorption cycle is illustrated in Figure 6.2 which shows the step by step change in the RH and the corresponding mass change as a function of time (min) for HPMC K4M. Initially, there is a rapid gain (or loss) of moisture with change in RH. This is followed by a very slow change in sample weight as a steady-state value is approached and the RH changes. This two-stage behaviour of the moisture sorption was reported previously by Chatterjee et al (1997) in their studies on the hysteresis region in cellulose based paperboard. Wadso (1994) reported similar sorption/ desorption patterns during measurements of moisture adsorption in wood and attributed the first stage to fast Fickian diffusion and the second stage to non-Fickian diffusion into the cell wall.

Moisture sorption isotherms were constructed by plotting the mass of moisture taken up per unit mass of dry powder against the relative humidity at 25°C. A typical moisture sorption/ desorption isotherm for HPMC K4M is illustrated in Figure 6.3. A hysteresis loop is present between the sorption and desorption cycles. This phenomena and its implications are discussed later in section 6.4.1.2.

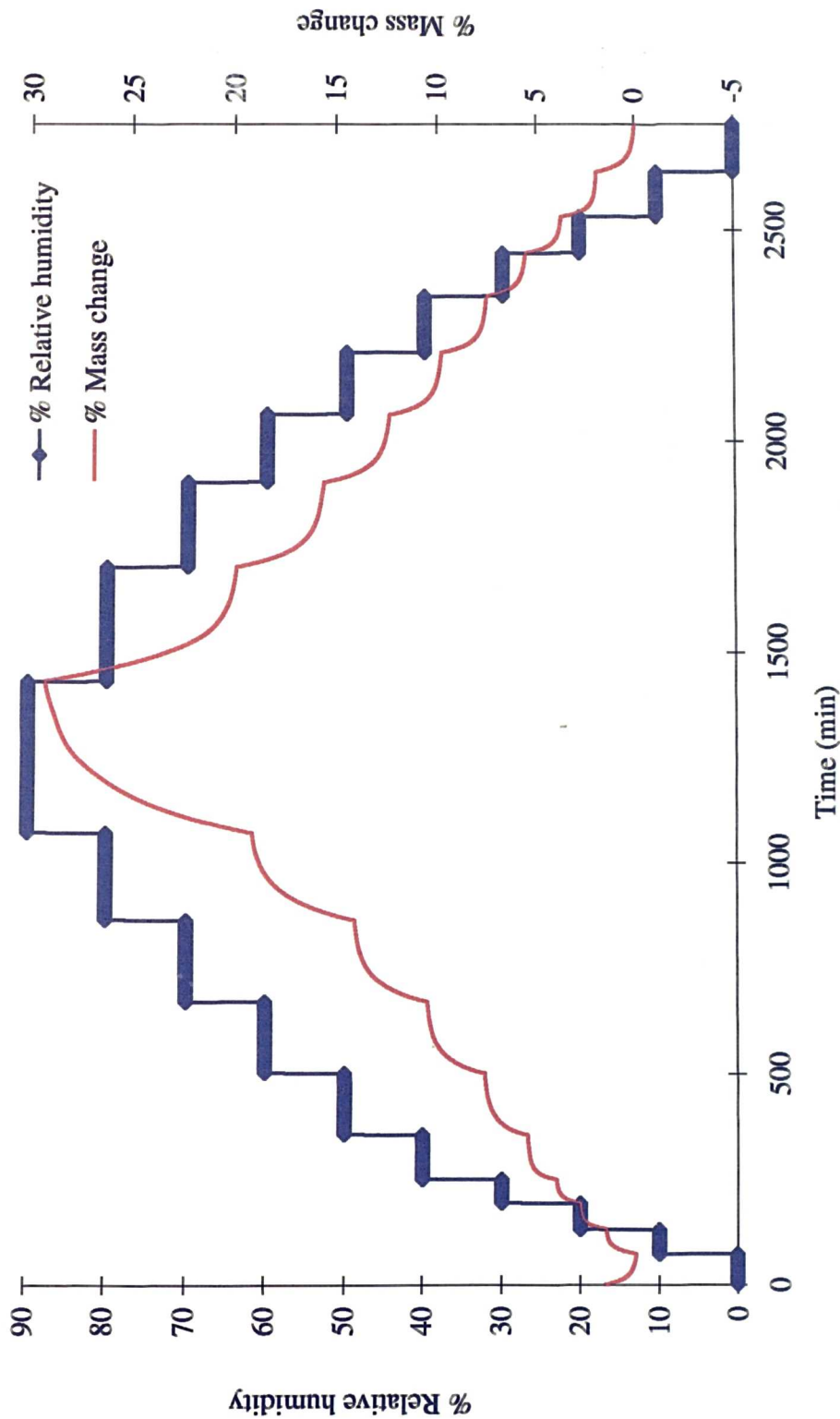


Figure 6.2: Mass change (%) and relative humidity change (%) in a typical dynamic vapour sorption cycle for HPMC K4M (90 - 125mm)

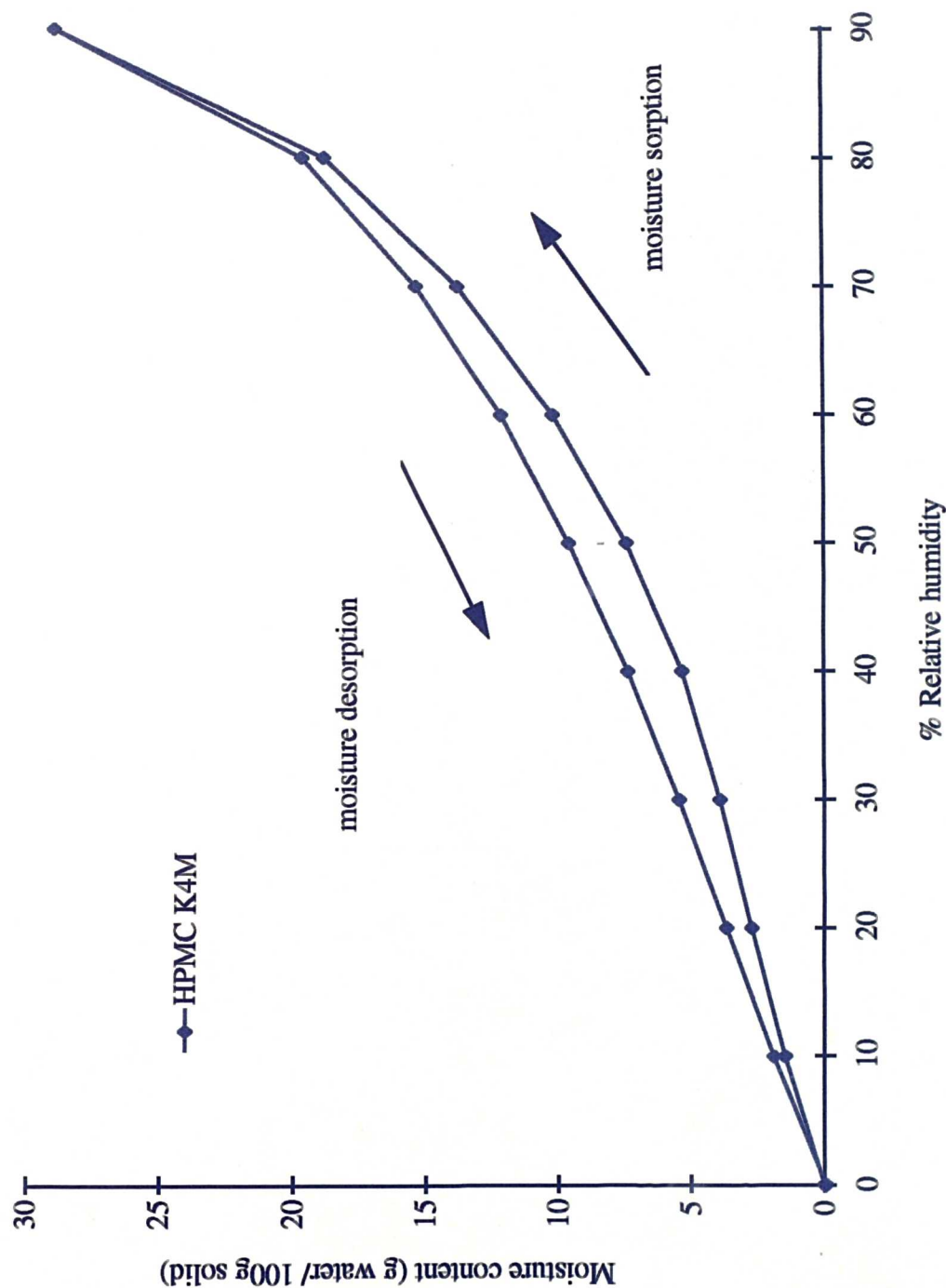


Figure 6.3: Moisture sorption/ desorption isotherm for HPMC K4M at a temperature of 25°C

Brunauer (Shaw, 1992) classified adsorption isotherms into five characteristic types (Figure 6.4). Type 1 isotherms are referred to as Langmuir-type isotherms and are obtained when adsorption is restricted to a monolayer. Type II isotherms, typical of those shown here, represent multilayer physical adsorption on non-porous solids and are referred to as sigmoid isotherms. Point B represents the formation of an adsorbed monolayer in this case. Adsorption on microporous solids may also result in Type II isotherms and, in this case, point B is equivalent to condensation in the fine pores as well as monolayer adsorption on the surface. Type IV isotherms level off near the saturation vapour pressure and reflect capillary condensation in porous solids. Types III and V show no rapid initial uptake of gas and occur when the forces of adsorption in the first monolayer are small. The shape of the moisture sorption/ desorption isotherms for all the polymer samples analysed here were similar to that illustrated for HPMC K4M. All samples showed Type II isotherms irrespective of molecular weight and substitution levels.

Figure 6.5 and Figure 6.6 show the moisture sorption and desorption behaviour of the HPMC K-series respectively. Polymer molecular weight had no effect on the moisture sorption behaviour. However, it appears that HPMC K100LV and HPMC K4M retain slightly more water vapour during the desorption cycle than HPMC K15M and HPMC K100M. This may be due to the phenomenon of hysteresis (section 6.4.1.1) which according to one theory is due to water being transferred into the polymer and being retained (York, 1981). Polymers within the HPMC K-series are thought to be similar in terms of surface and particulate morphology. In addition these polymers have similar methoxyl and hydroxypropoxyl substitution levels. Therefore, no major differences in the moisture sorption and desorption properties of these polymers were expected.

6.4.1.1 The influence of polymer molecular weight on hysteresis area

The area between the sorption and the desorption isotherm curves is known as the hysteresis area. 'Sorption hysteresis' commonly occurs in amorphous solids but is less prevalent in crystalline materials which often show reversible sorption/ desorption isotherms because the absorbate is adsorbed onto the solid surfaces and

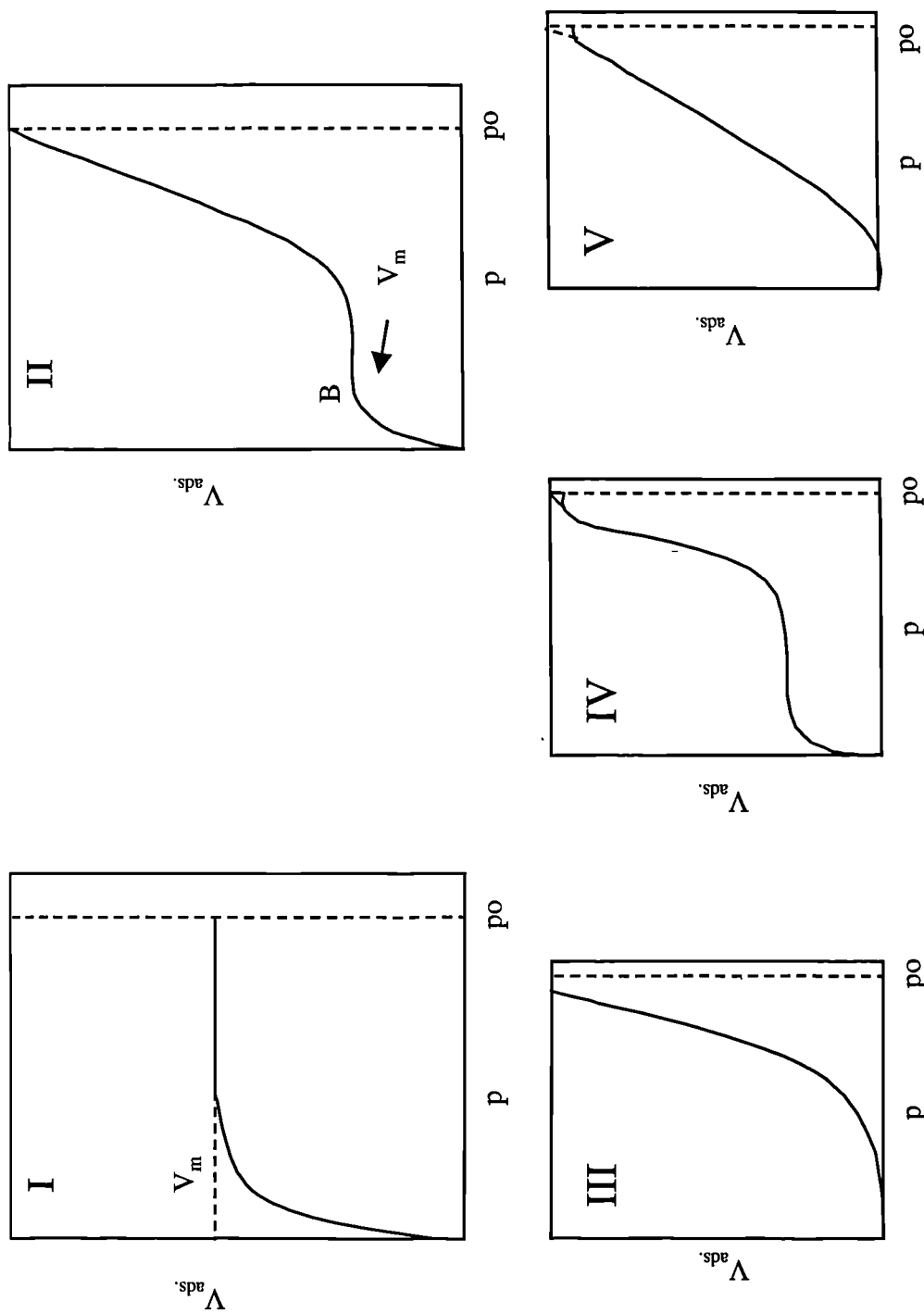


Figure 6.4 : Classification of adsorption isotherms, where V_{ads} is the amount of gas adsorbed; p is vapour pressure; p_0 is saturated vapour pressure and V_m represents formation of an adsorbed monolayer (after Shaw, 1992)

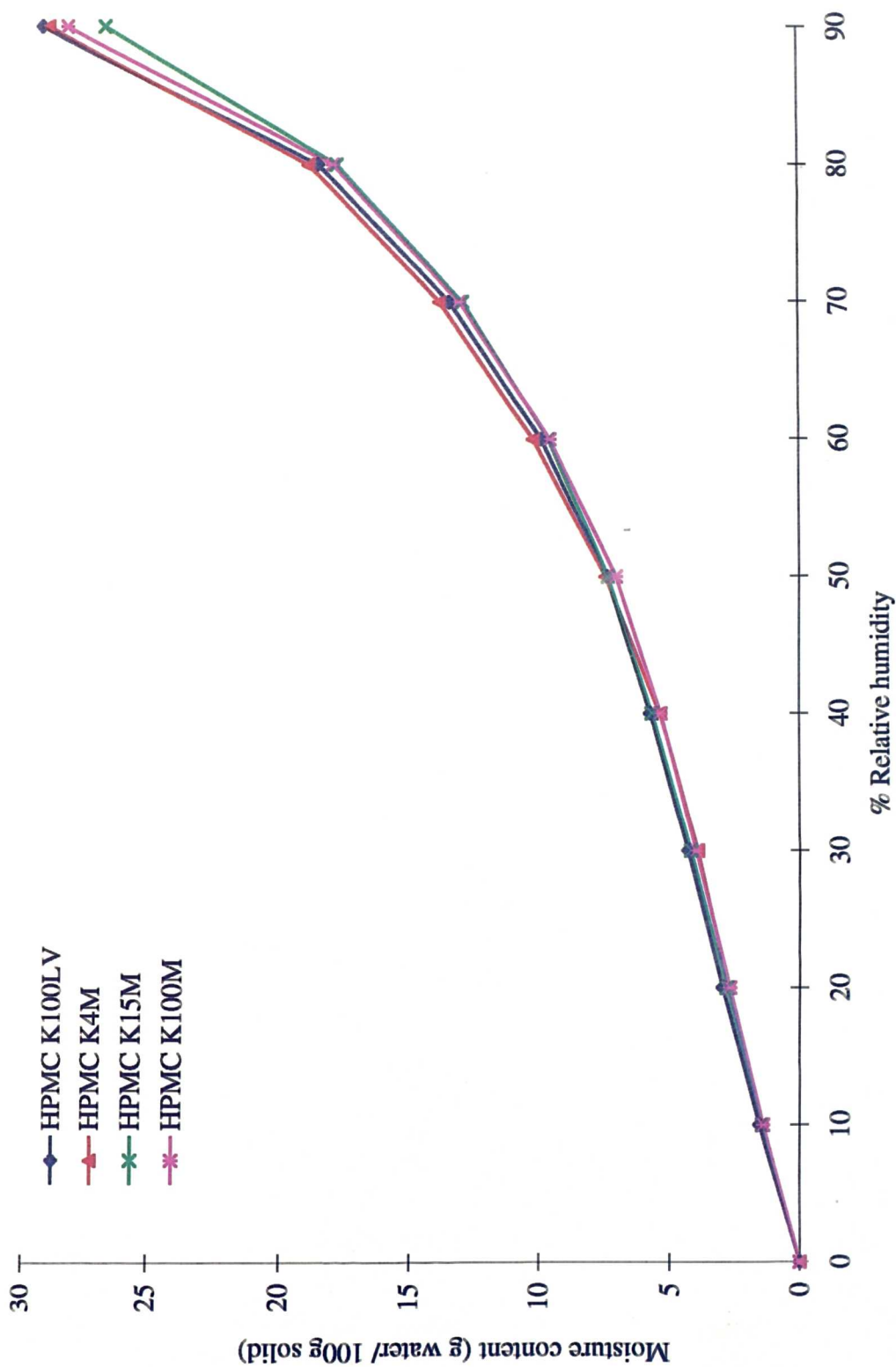


Figure 6.5: Moisture sorption profiles for HPMC K100LV, K4M, K15M and K100M

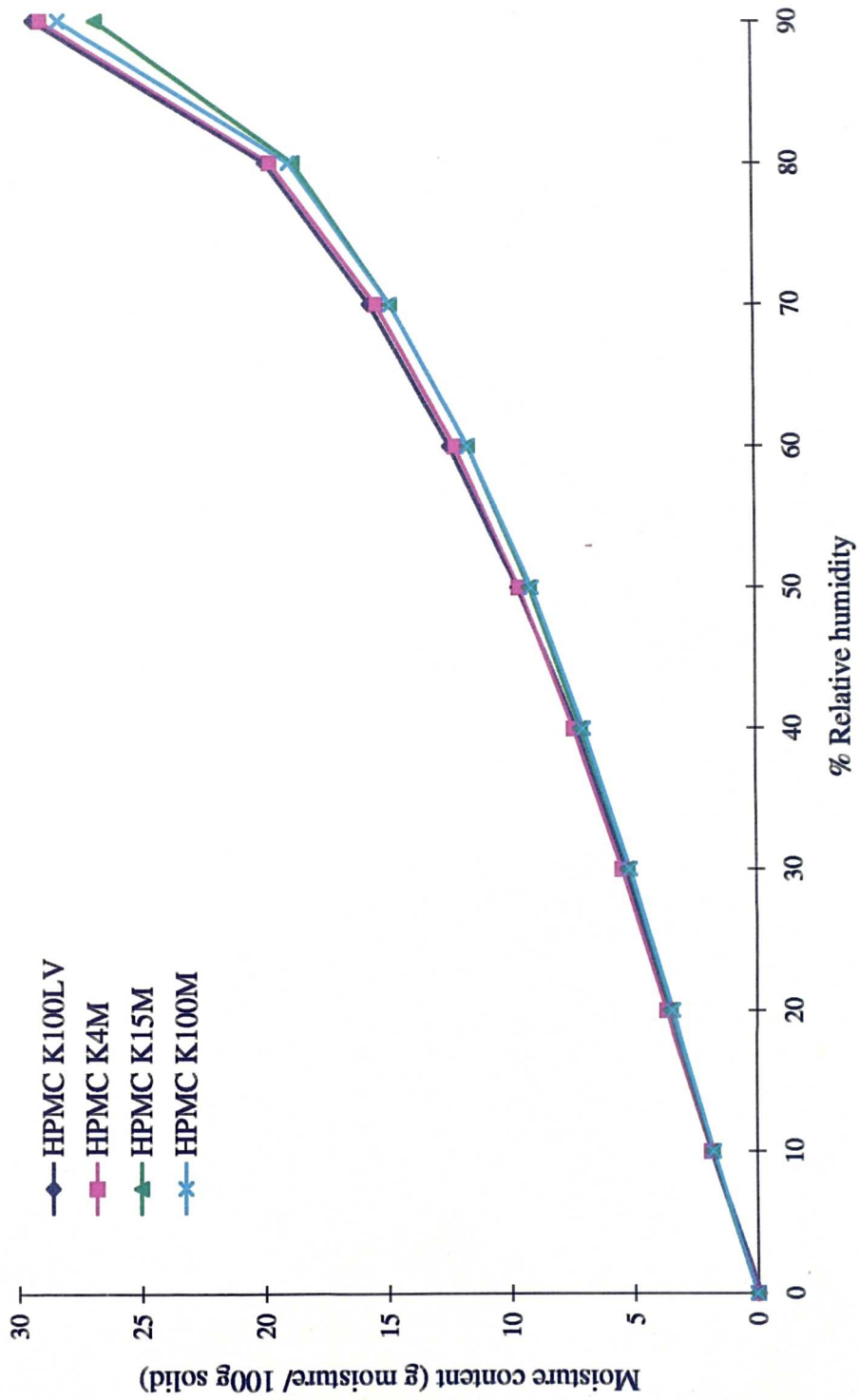


Figure 6.6: Moisture desorption profiles for HPMC K100LV, K4M, K15M and K100M

fails to penetrate the material (Kontny et al, 1987). The sorption hysteresis shown here for hydroxypropylmethylcelluloses (HPMCs) is typical of that seen for celluloses (Morrison and Dzieciuch, 1959). Hysteresis has been widely discussed and a number of different explanations have been put forward to explain this phenomenon. The phenomenon was originally thought to represent an artefact caused by a very slow rate of equilibrium attainment during desorption (Gregg, 1951). Thermodynamic evidence has indicated that hysteresis may be real, and represents differences in free energies of the two systems at the same relative humidity (Hollenbeck et al, 1978). Thus, from this, hysteresis may be due to a difference in specific surface area (irreversible swelling), solid-liquid bonding strengths (enthalpy effect), molecular ordering (entropy) or a combination of these effects (Hollenbeck et al, 1978).

Multilayer adsorption followed by capillary condensation in cylindrical pores which are at pressures lower than the normal saturation vapour pressure have been considered by Shaw (1989) as a suitable explanation for hysteresis. Factors such as differences in the contact angle, which is usually greater on adsorption than on desorption and contributions due to differing pore shape and volume, have been discussed (Shaw, 1989). It has been hypothesised that two types of pores may be present. The first type is V-shaped and fills and empties reversibly. The second type, having a wide interior and a narrow neck which fills but fails to release its contents until the partial pressure is reduced to a value corresponding to the width of the narrow pore neck.

York (1981) has explained moisture hysteresis according to the Young and Nelson theory (Young and Nelson, 1967a, 1967b), as when a dry material exposed to moisture, adsorbs water as a monomolecular layer. This layer is subjected to both surface binding and diffusional forces. When the diffusional forces exceed the binding forces as more water binds to the surfaces, water is transferred into the material. If the moisture vapour pressure is reduced on the desorption cycle, water molecules at the surface must be removed before diffusional forces pull moisture out of the interior of the material (Young and Nelson, 1967a, 1967b).

It may be hypothesised that if the hysteresis area is due to water being transferred into the polymer, this area may be related to the capability of a particular polymer to absorb water. The area of the hysteresis curves were calculated by calculating the area under the desorption and sorption curves respectively and subtracting one from the other. Table 6.1 shows the hysteresis areas for the HPMC K-series. HPMC K100LV and HPMC K4M have slightly larger hysteresis areas than HPMC K15M and HPMC K100M indicating that more water is transferred into these polymers and remained there. This was expected according to the trend seen in Figure 6.6 which indicated that HPMC K100LV and HPMC K4M retain slightly more moisture during desorption than HPMC K15M and HPMC K100M.

6.4.2 Water sorption characteristics of HPMC's with different substitution levels

The vapour sorption/ desorption properties of HPMC E4M, HPMC F4M, HPMC K4M and MC A4M with similar molecular weight but different substitution levels were examined by dynamic vapour sorption. Figure 6.7 and Figure 6.8 show the moisture sorption and desorption behaviour of cellulose ether polymers with different substitution levels respectively. HPMC K4M sorbed more moisture at all RH values than the other polymers studied here. This may be related to the low percentage methoxyl substitution level (22.2%) of this polymer in combination with a high percentage hydroxypropoxyl level (8.4%).

6.4.2.1 The influence of polymer substitution level on hysteresis area

Table 6.2 shows the hysteresis areas for HPMC E4M, HPMC F4M, HPMC K4M and MC A4M. The hysteresis area is quite similar for HPMC K4M, HPMC F4M and methylcellulose (MC) A4M. However, that for HPMC E4M is larger than the others.

The water sorption/ desorption characteristics of HPMC K4M in the current study may be related to its particle surface morphology and also its low hydrophobic methoxyl substituent level. HPMC K4M has the lowest methoxyl substitution level

Table 6.1 : Hysteresis area calculated from moisture sorption/ desorption profiles of the HPMC K-series of polymers

Polymer	Hysteresis Area
HPMC K100LV	120.01
HPMC K4M	115.04
HPMC K15M	103.20
HPMC K100M	109.44

Table 6.2 : Hysteresis area calculated from moisture sorption/ desorption profiles for cellulose ethers with different substitution levels

Polymer	Hysteresis Area
HPMC K4M	115.04
MC A4M	111.81
HPMC E4M	153.44
HPMC F4M	118.46

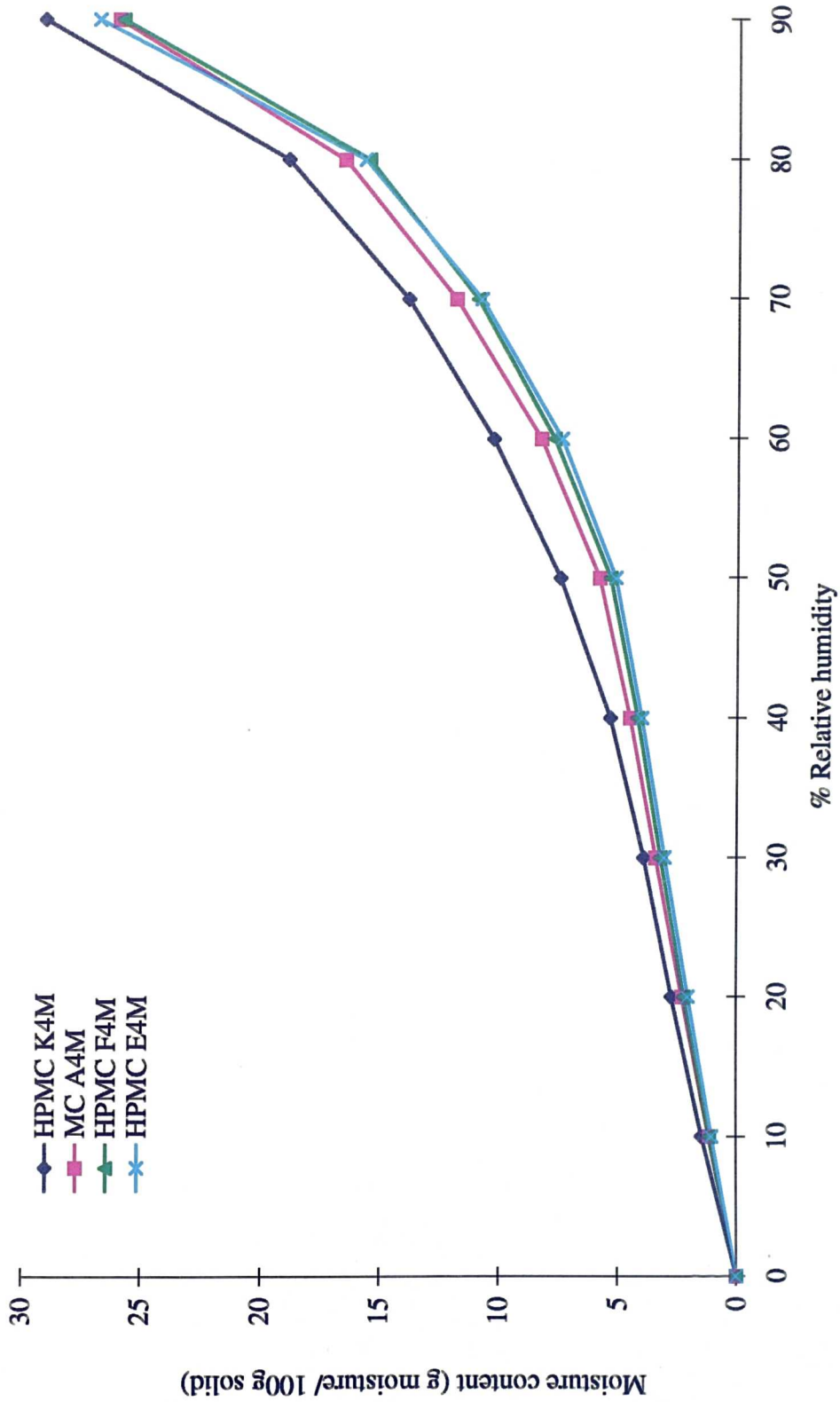


Figure 6.7: Moisture sorption profiles for HPMC K4M, MC A4M, HPMC F4M and HPMC E4M

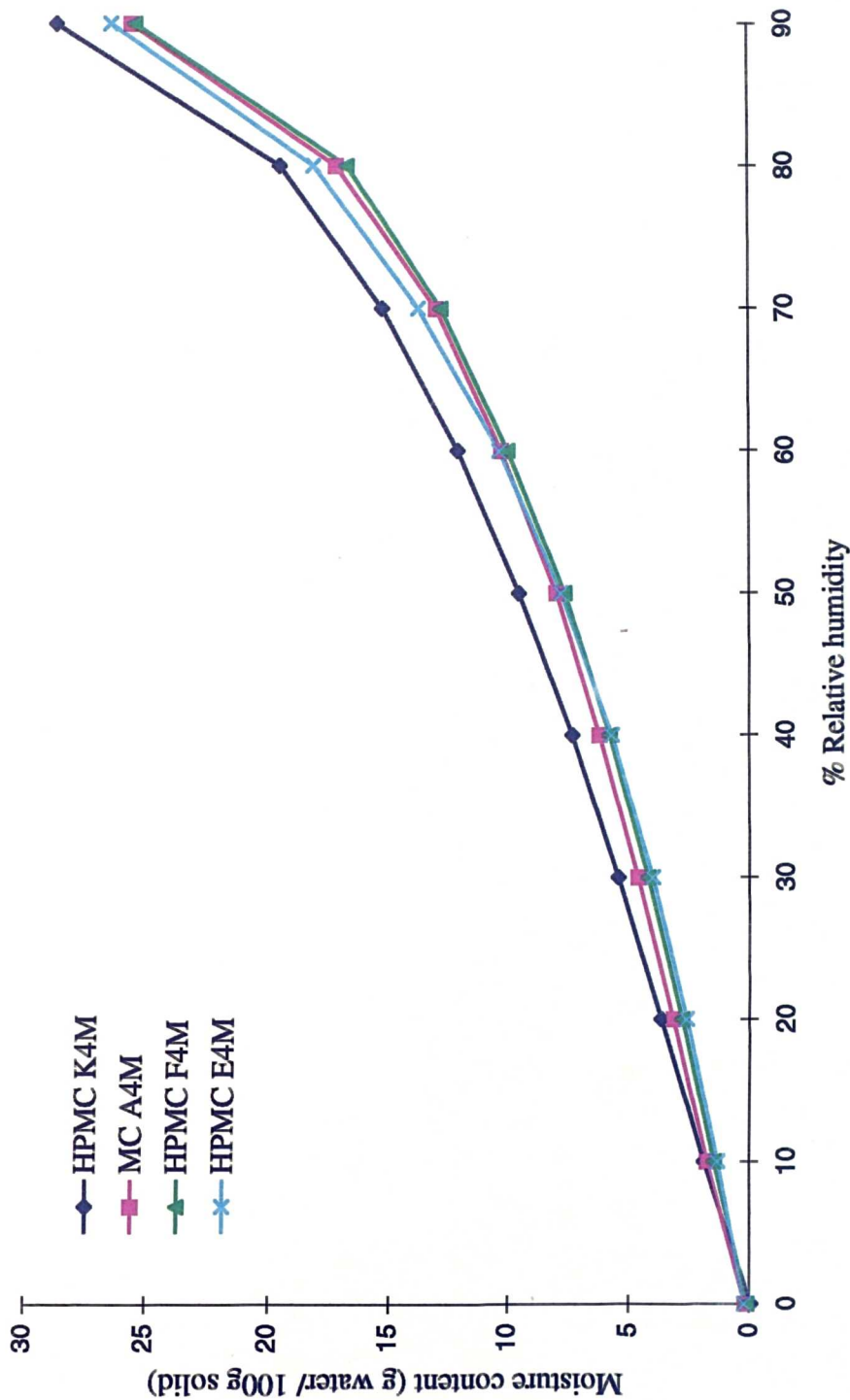


Figure 6.8: Moisture desorption profiles for HPMC K4M, MC A4M, HPMC F4M and HPMC E4M

(22.2%) compared to HPMC E4M (29.1%) and HPMC F4M (28.9%). Differences in substitution levels have been reported to result in different drug release characteristics which had previously been thought to be due to differing rates of polymer hydration (Alderman, 1984). This has been since found not to be the case (Ford and Mitchell, 1995) with no differences existing in the rates at which these polymers take up water. Rajabi-Siahboomi et al (1996) have shown that the water mobility in the 'gel layer' of HPMC K4M is reduced in comparison with that in other HPMCs. This has been proposed to explain slower drug release from HPMC K4M matrices. The results in this study also show that the total amount of moisture taken up and retained by HPMC K4M remained higher than other HPMCs at all RH values during sorption/desorption cycles.

6.4.3 Application of the Young-Nelson Theory to moisture sorption/ desorption of cellulose ether polymers

Young and Nelson (1967a, 1967b) hypothesised three mechanisms by which water can associate to biological materials. A dry material, when exposed to moisture, adsorbs water as a monomolecular layer. Secondly, multimolecular layers of water molecules can form on top of the first layer. These layers are subjected to both surface binding and diffusional forces. When the diffusional forces exceed the binding forces as more water binds to the surfaces, water is transferred into the material. This moisture is known as absorbed moisture and is clearly different to the monomolecular and multimolecular water which may be considered as adsorbed moisture. If the moisture vapour pressure is reduced, water molecules at the surface must be removed before diffusional forces pull moisture out of the interior of the material (Young and Nelson, 1967a, 1967b). The relevant equations of Young & Nelson, from the kinetic theory of gases are as follows:

Equation 6.2
$$\theta = \frac{RH}{RH + (1 - RH)E}$$

where θ is the fraction of the surface of the powder covered by a monomolecular layer, RH is the relative humidity (expressed as a fraction and not as a percentage), and E is a variable, unique to each material. E may be represented by equation 6.3:

$$\text{Equation 6.3} \quad E = \exp [-(q_1 - q_L) / k_B T_e]$$

where q_1 (J mol^{-1}) is the heat of adsorption of water, q_L (J mol^{-1}) is the normal heat of condensation of water molecules, k_B is Boltzmann's constant ($1.381 \times 10^{-23} \text{ J K}^{-1}$), and T_e (K) is the temperature of the experimental conditions.

$$\text{Equation 6.4} \quad \psi = \text{RH} \cdot \theta$$

where ψ is the fraction of surface covered by at least one or more layers of water. Equation 6.5 may be used to determine the fractional amount of externally adsorbed moisture:

Equation 6.5:

$$\beta = -\frac{E \cdot \text{RH}}{E - (E - 1) \cdot \text{RH}} + \frac{E^2}{E - 1} \log_e \frac{E - (E - 1) \cdot \text{RH}}{E} - (E + 1) \cdot \log_e (1 - \text{RH})$$

where β is the fraction of total amount of adsorbed moisture in a multilayer.

Using calculated values of θ , ψ and β , the pattern of moisture distribution may be determined. The total amount of moisture held by a material may be obtained by adding together the internally absorbed and the externally adsorbed moisture:

$$\text{Equation 6.6} \quad M_s = A \cdot (\theta + \beta) + B \cdot \psi$$

$$\text{Equation 6.7} \quad M_d = A \cdot (\theta + \beta) + B \cdot \theta \cdot \text{RH}_{\max}$$

where M_s and M_d are the total moisture contents (% w/w) held by the material during sorption and desorption respectively, and RH and RH_{\max} are the relative humidity and

the maximum relative humidity used in the particular study in question. In equations 6.6 and 6.7, $A = \frac{(\rho_w V_m)}{W_m}$ and $B = \frac{\rho_w V_a}{W_m}$, where V_m (cm³) and V_a (cm³) are the volumes of the adsorbed and absorbed moisture, ρ_w (g/cm³) is the density of water and W_m (g) is the mass of dry material. The distribution of water may be further calculated as, $A.\theta$ which is the amount of water present as a monolayer, $A.(\theta+\beta)$ is the externally adsorbed moisture, and $\beta.\psi$ is the amount of the internally absorbed moisture during the sorption cycle.

Due to the fact that q_1 , V_m and V_a are not known, a combination of iteration and multiple regression techniques were used to fit the experimental data to these equations. This involved the following operations. A value of E was assumed, and was used to calculate θ , ψ and β , from equations 6.2, 6.4 and 6.5. Using the experimental values of M_s and M_d , and a multiple regression technique, the values of θ , ψ and β at various RHs were substituted into equations 6.6 and 6.7 to obtain the values of M_s and M_d .

Multiple regression took place between M_s , $(\theta+\beta)$ and ψ . The correlation coefficients were calculated (equation 6.8) for the computed against the observed values of equilibrium moisture content using the best values of A , B and E , and excellent correlations were found (Table 6.3 and Table 6.4). The experimental and theoretical values of M_s and M_d were subjected to an error analysis in which the sums of squares of deviation between them were estimated. Using other values of E , the calculations were repeated, and again the sums of squares of deviation between M_s and M_d were estimated. Values of E which gave the highest correlation coefficient were chosen as the optimum values.

$$\text{Equation 6.8} \quad r = \left(1 - \frac{ESS}{EMS}\right)^{1/2}$$

where r is the correlation coefficient, ESS is the sums of squares of deviation of the theoretical values from experimental values and EMS is the sums of squares of deviation of the experimental values from their mean.

All calculations were carried out using a Minitab (version 10) programme specially written for this work. The results of this work show that if values for E, A and B are correctly estimated, the calculated values give a good fit for the experimental values. Table 6.5 lists the calculated and experimental water uptake data for HPMC K15M during both the sorption and desorption cycles for an assumed E value of 0.64. Values of θ , ψ and β are also shown. Such calculated water uptake data may be plotted against the experimental data to indicate graphically how good a fit the calculated data is to the experimental data. Such plots are illustrated in Figures 6.9 (a-d) and Figures 6.10 (a-c) for each of the polymers studied. The calculated data fit closely to the experimental data as expected from the correlation values listed in Table 6.4. This indicates that the Young-Nelson theory which assumes a three state approach to the attachment of water to a biological material may be correctly applied to investigate the water sorption/desorption characteristics of the polymers studied here.

6.4.3.1 Influence of polymer molecular weight and substitution levels on the water distribution within cellulose ether polymers

The distribution of water within cellulose ether polymers may be calculated as: $A \cdot \theta$ is the amount of water present as a monolayer, $A \cdot (\theta + \beta)$ is the externally adsorbed moisture, and $\beta \cdot \psi$ is the amount of the internally absorbed moisture during the sorption cycle. Table 6.6 shows the influence of polymer molecular weight and substitution level on the distribution of water within cellulose ether polymers at representative relative humidities of 50 and 90%. The percentage values are considered as the moisture in each location which is expressed as a percentage of the total moisture content at that relative humidity. Within the HPMC K-series, the internally absorbed moisture was highest for HPMC K100LV (24.8 & 21.0% at 50 and 90% RH) and lowest for HPMC K4M (13.9 & 11.4% at 50 and 90% RH) respectively. The amount of externally adsorbed moisture, reflecting monolayer and multilayer contributions, was highest for HPMC K4M (86.1 & 88.6% at 50 and 90% RH) and was lowest for HPMC K100LV (75.2 & 79.0% at 50 and 90% RH)

Table 6.3 : Values of A & B (equation 6.6) and correlation coefficients (equation 6.8) obtained from analysis of HPMC K15M moisture sorption/ desorption data using assumed values of E

E	A	B	R
0.50	0.102	0.112	0.9698
0.60	0.094	0.085	0.9890
0.61	0.093	0.083	0.9897
0.62	0.092	0.080	0.9904
0.63	0.092	0.077	0.9909
0.64	0.091	0.074	0.9910
0.65	0.090	0.072	0.9908
0.69	0.087	0.060	0.9875
0.70	0.086	0.058	0.9864

Table 6.4 : Values of A, B and E (equation 6.6) and correlation coefficients (equation 6.8) from analysis of moisture sorption/ desorption data of cellulose ether polymers

Polymer	E	A	B	R
HPMC K100LV	0.70	0.109	0.127	0.9879
HPMC K4M	0.79	0.091	0.052	0.9827
HPMC K15M	0.64	0.091	0.074	0.9910
HPMC K100M	0.75	0.099	0.098	0.9866
HPMC E4M	1.06	0.103	0.139	0.9805
HPMC F4M	0.95	0.096	0.121	0.9781
MC A4M	0.92	0.085	0.065	0.9743

Table 6.5 : Values of θ , ψ and β (equations 6.2, 6.4 & 6.5) calculated for HPMC K15M using an assumed value of $E= 0.64$

Relative humidity (fraction)	θ	ψ	β	Experimental water uptake (g water/100g solid)	Theoretical water uptake (g water/100g solid)
0.1	0.148	0.015	0.016	0.014	0.014
0.2	0.281	0.056	0.065	0.028	0.028
0.3	0.401	0.120	0.151	0.042	0.042
0.4	0.510	0.204	0.280	0.057	0.057
0.5	0.610	0.305	0.465	0.074	0.075
0.6	0.701	0.421	0.723	0.097	0.098
0.7	0.785	0.549	1.095	0.131	0.130
0.8	0.862	0.690	1.665	0.180	0.179
0.9	0.934	0.840	2.713	0.269	0.269
0.9	0.957	0.862	2.613	0.269	0.268
0.8	0.909	0.727	1.680	0.189	0.192
0.7	0.854	0.598	1.153	0.149	0.148
0.6	0.789	0.474	0.796	0.118	0.117
0.5	0.714	0.357	0.535	0.093	0.092
0.4	0.625	0.250	0.340	0.072	0.072
0.3	0.517	0.155	0.193	0.053	0.053
0.2	0.385	0.077	0.089	0.035	0.036
0.1	0.217	0.022	0.023	0.018	0.019

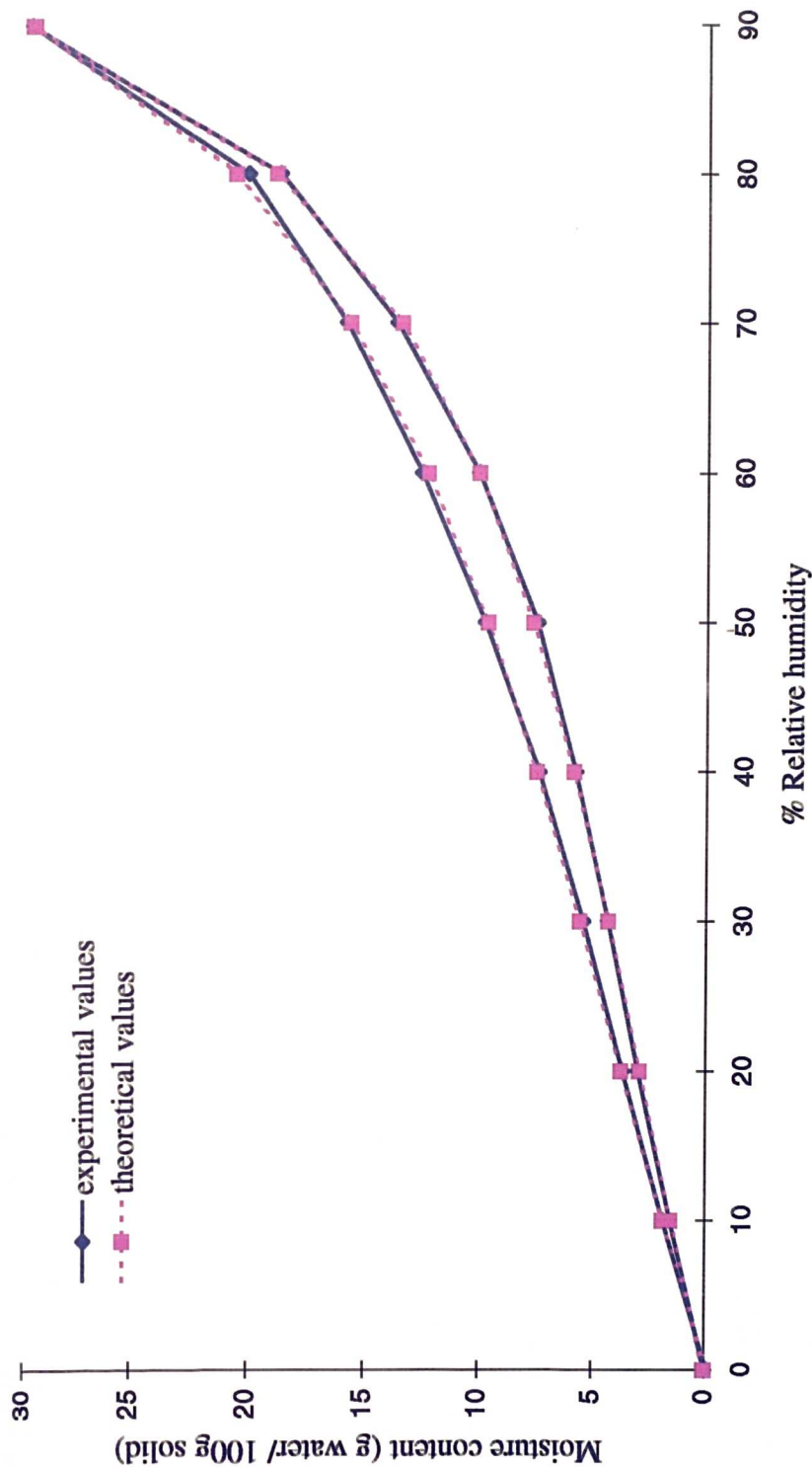


Figure 6.9a: Moisture sorption/ desorption isotherms of HPMC K100LV showing the experimental and theoretical data

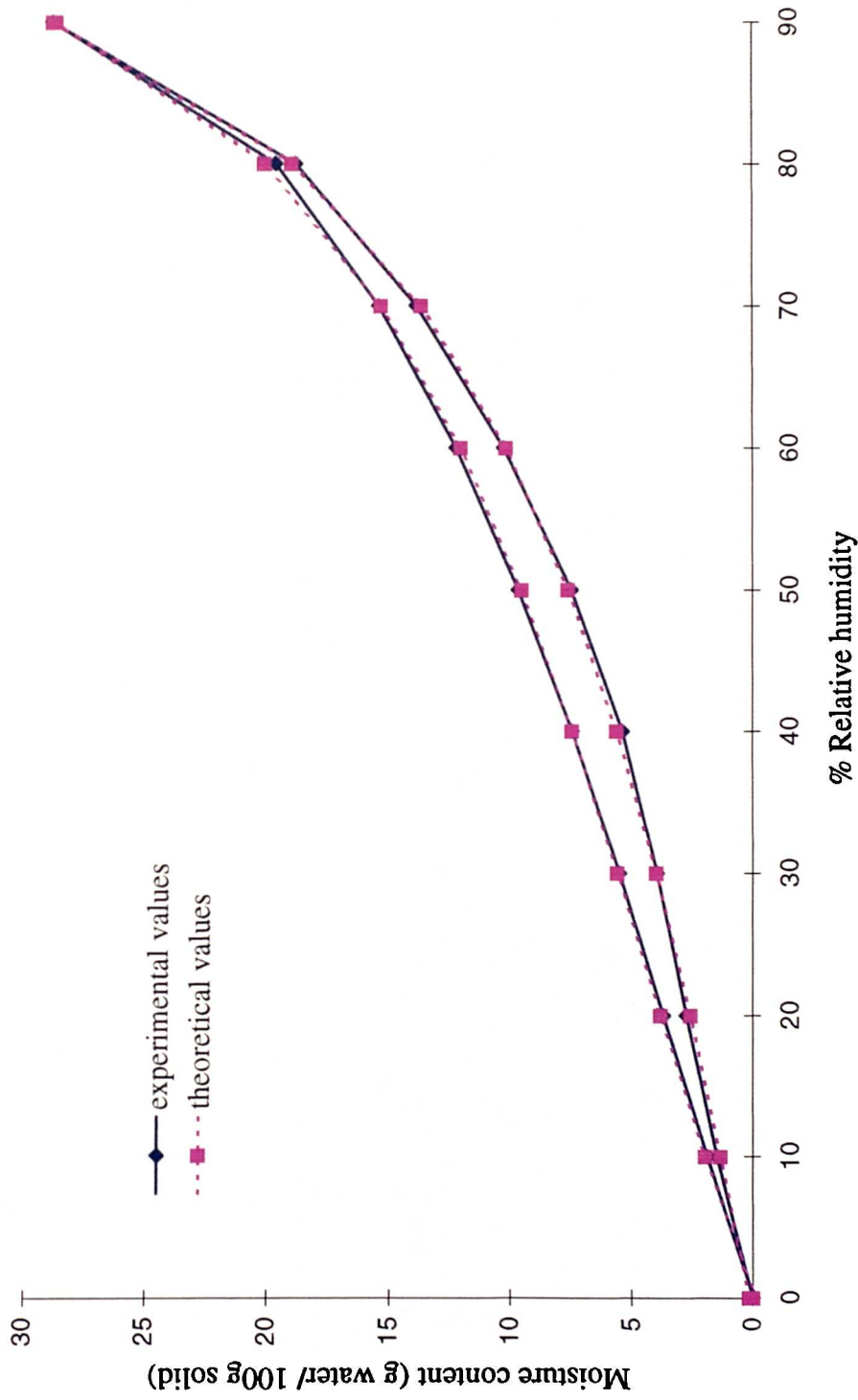


Figure 6.9b: Moisture sorption/ desorption isotherms of HPMC K4M showing the experimental and theoretical data

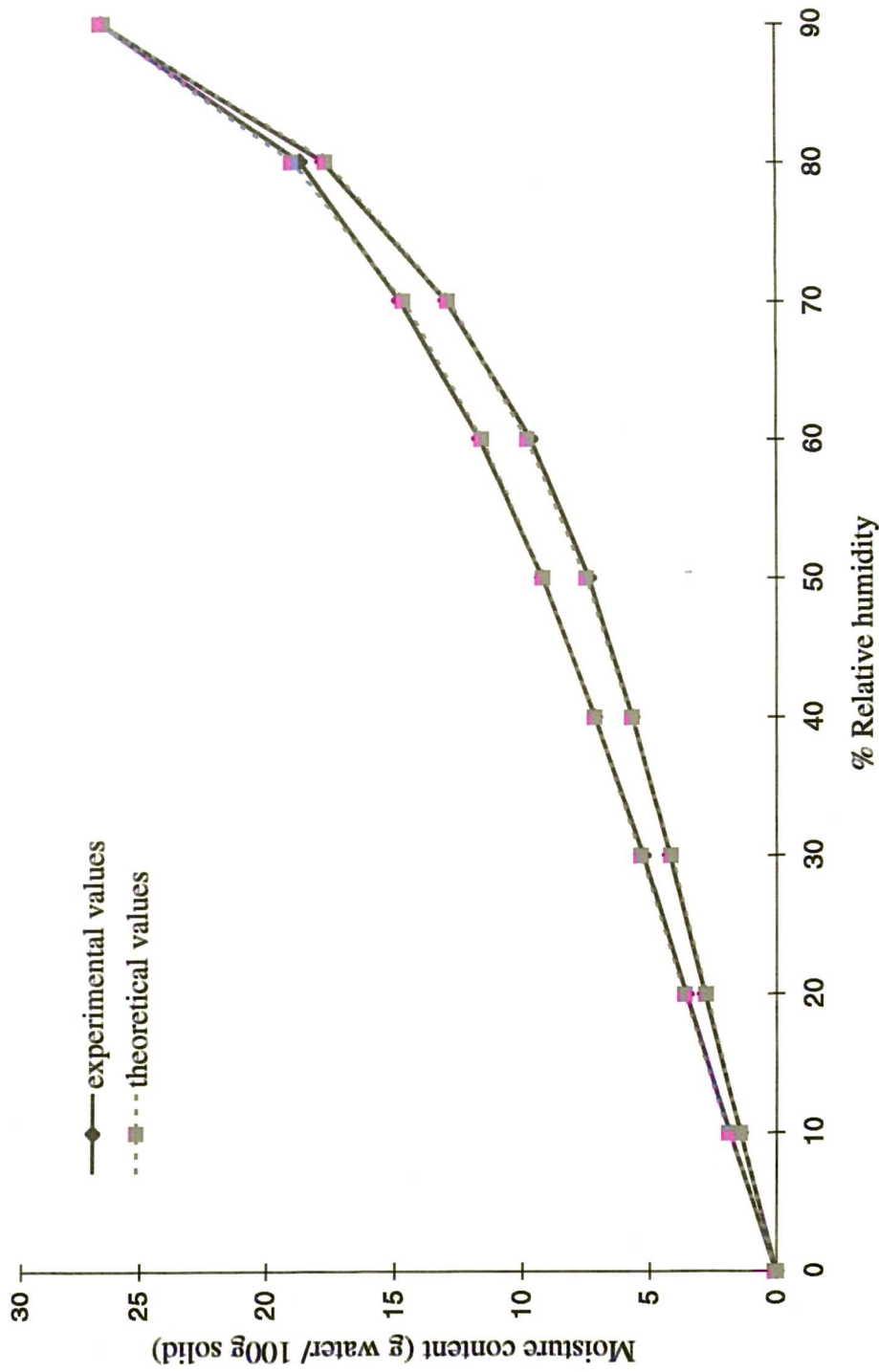


Figure 6.9c: Moisture sorption/ desorption isotherms of HPMC K15M showing the experimental and theoretical data

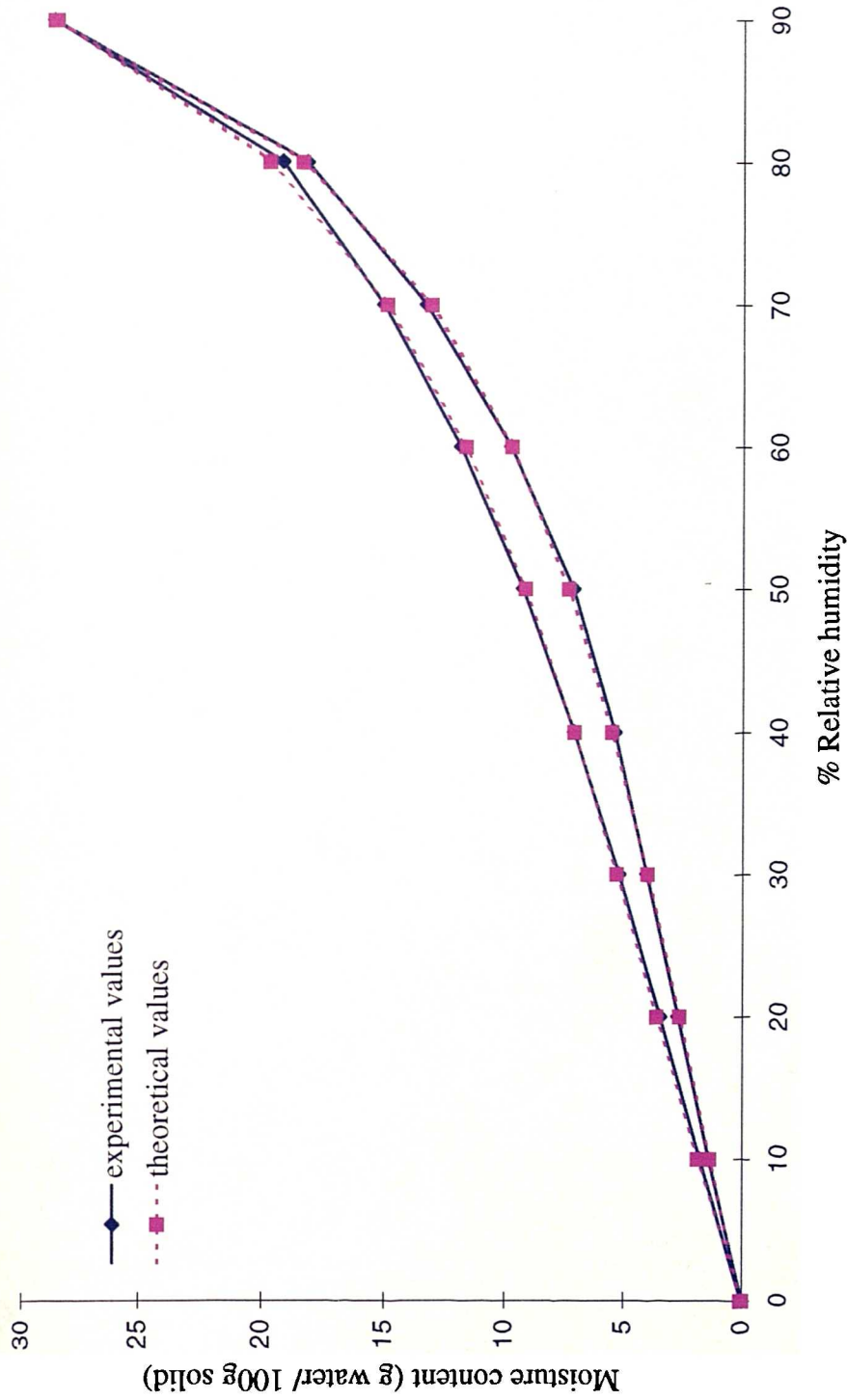


Figure 6.9d: Moisture sorption/ desorption isotherms of HPMC K100M showing the experimental and theoretical data

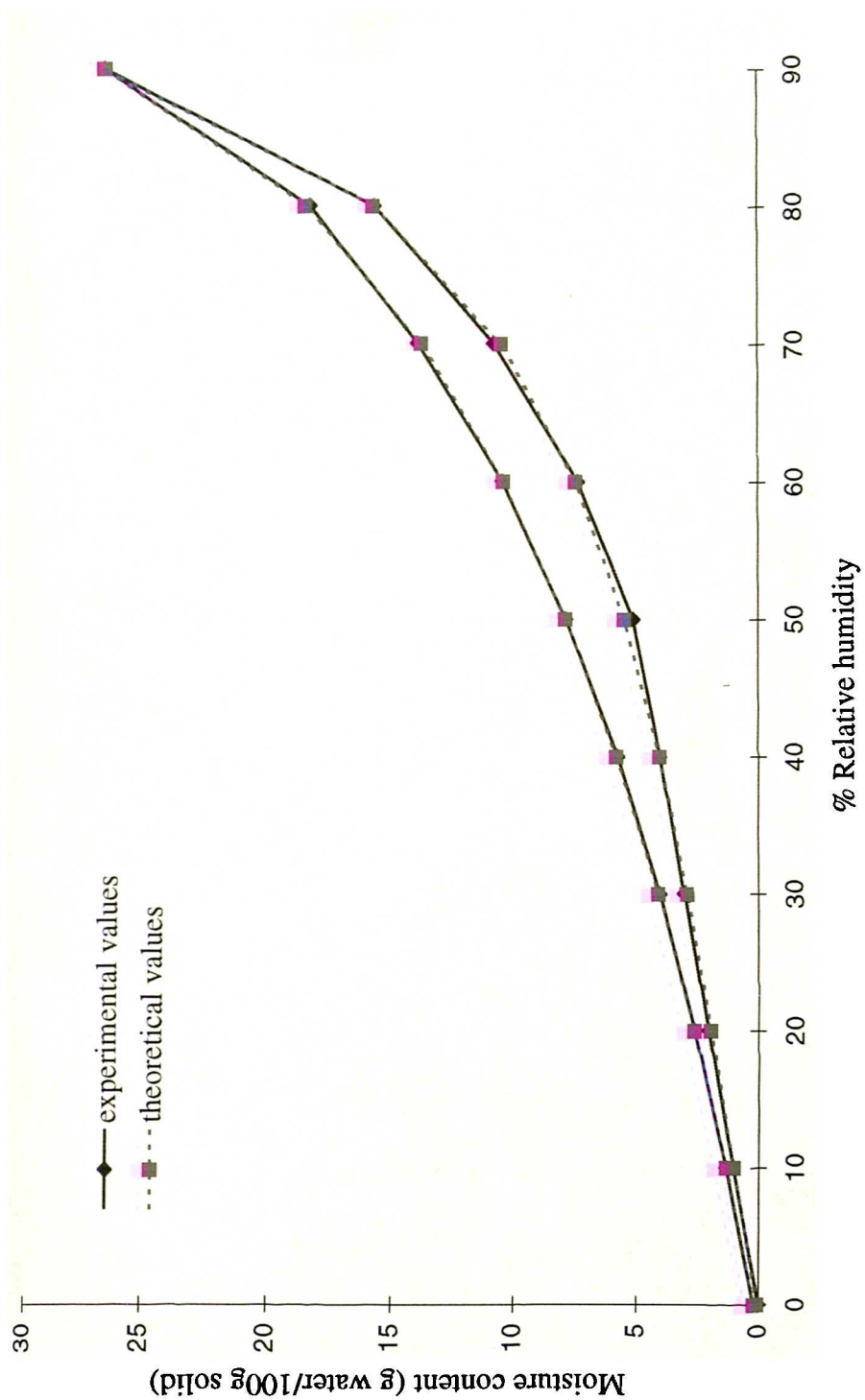


Figure 6.10a: Moisture sorption/ desorption isotherms of HPMC E4M showing the experimental and theoretical data

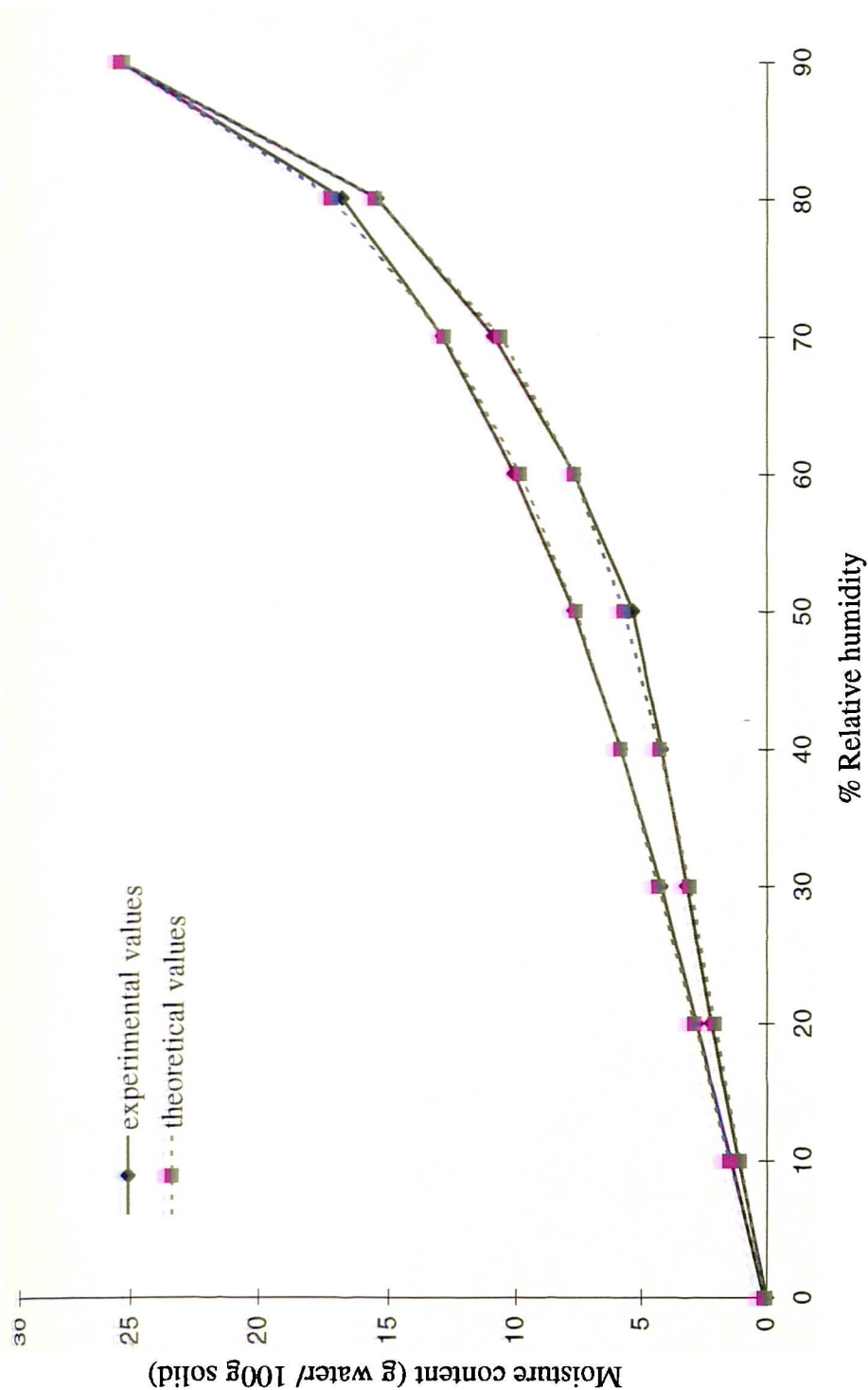


Figure 6.10b: Moisture sorption/ desorption isotherms of HPMC F4M showing the experimental and theoretical data

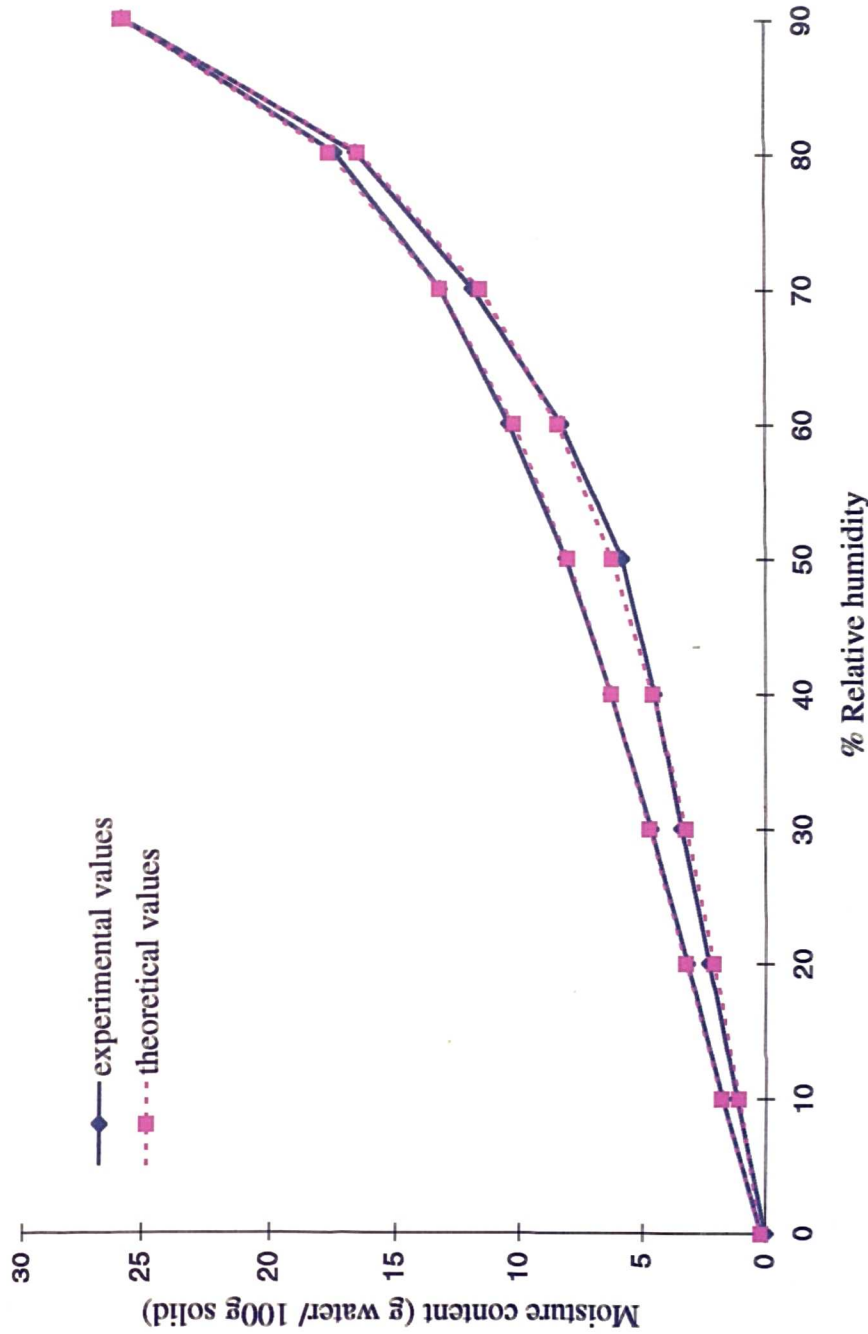


Figure 6.10c: Moisture sorption/ desorption isotherms of MC A4M showing the experimental and theoretical data

Table 6.6 : Influence of polymer molecular weight and substitution type on water distribution at 50% and 90% RH

Polymer	50% RH		50% RH		90% RH		90% RH	
	A. θ^a	A. ($\theta+\beta$) ^b	B. ψ^c	A. ($\theta+\beta$) ^b	A. θ	A. ($\theta+\beta$)	B. ψ	
HPMC K100LV	6.41 (42.6) ^d	11.31 (75.2)	3.74 (24.8)	10.11 (20.0)	39.89 (79.0)	10.61 (21.0)		
HPMC K4M	5.06 (48.7)	8.93 (86.1)	1.45 (13.9)	8.32 (22.1)	33.28 (88.6)	4.29 (11.4)		
HPMC K15M	5.54 (46.1)	9.75 (81.2)	2.26 (18.8)	8.48 (21.5)	33.11 (84.2)	6.23 (15.8)		
HPMC K100M	5.67 (44.3)	10.02 (78.1)	2.80 (21.9)	9.17 (20.6)	36.44 (81.7)	8.15 (18.3)		
HPMC K4M	5.06 (48.7)	8.93 (86.1)	1.45 (13.9)	8.32 (22.1)	33.28 (88.6)	4.29 (11.4)		
HPMC E4M	5.00 (40.8)	8.87 (72.4)	3.37 (27.6)	9.21 (18.6)	38.22 (77.3)	11.19 (22.7)		
HPMC F4M	4.94 (41.7)	8.76 (73.8)	3.10 (26.2)	8.72 (19.2)	35.67 (78.4)	9.85 (21.6)		
MC A4M	4.40 (46.4)	7.79 (82.2)	1.69 (17.8)	7.67 (21.0)	31.23 (85.5)	5.30 (14.5)		

^amonomolecular adsorbed moisture^bexternally adsorbed moisture (monolayer + multilayer)^cinternally adsorbed moisture^dpercentage of moisture expressed as a percentage of the total moisture content at that relative humidity

respectively. Figure 6.11 shows that HPMC K100LV clearly has the highest amount of internally absorbed moisture and HPMC K4M the lowest. However, if values are taken as absolute instead of % of the total moisture content, then Figure 6.11 shows that HPMC K100LV has the greatest and HPMC K4M has the least amount of externally adsorbed moisture. Values in the graph represent absolute values of water distribution in each location and they do not show the water distribution as a percentage of the total moisture content at that relative humidity. Differences between the amounts of monomolecular adsorbed moisture were slight for polymers of different molecular weight.

Table 6.6 also shows the variation in moisture distribution with changes in polymer substituents. Considering the percentage values, HPMC E4M has the highest amount of internally absorbed moisture (27.6 & 22.7% at 50 and 90% RH) while HPMC K4M has the lowest (13.9 & 11.4% at 50 and 90% RH). This is reflected in Figure 6.12, where the effect of polymer substitution level on the distribution of water is shown. Again, considering the percentage values in Table 6.6, HPMC K4M has the highest amount of externally adsorbed moisture (86.1 & 88.6% at 50 and 90% RH), while HPMC E4M has the lowest amount (72.4 & 77.3% at 50 and 90% RH), respectively. This is not reflected in Figure 6.12 where HPMC E4M clearly has the highest absolute value of externally adsorbed moisture while MC A4M has the lowest. Very small differences in monomolecular adsorbed moisture occurred in polymers of different substitution levels.

The methoxyl/ hydroxypropoxyl substitution ratio in cellulose ether polymers has previously been related to the distribution of water as calculated using the Young-Nelson theory (Malamataris et al, 1994 and Malamataris and Karidas, 1994). Malamataris et al (1994) have indicated that values of monomolecular adsorbed moisture and externally adsorbed moisture decrease with an increase in the methoxyl/ hydroxypropoxyl substitution ratio. However, the ratio had very little influence on the internally absorbed moisture. Table 6.6 indicates that a similar trend occurs in the current study with the absolute values of external moisture ($A.\theta$, $A.(\theta+\beta)$) decreasing as the methoxyl/ hydroxypropoxyl substitution ratio increases from HPMC K4M (ratio = 2.6) to HPMC E4M (ratio = 3.6) and HPMC F4M (ratio = 4.7).

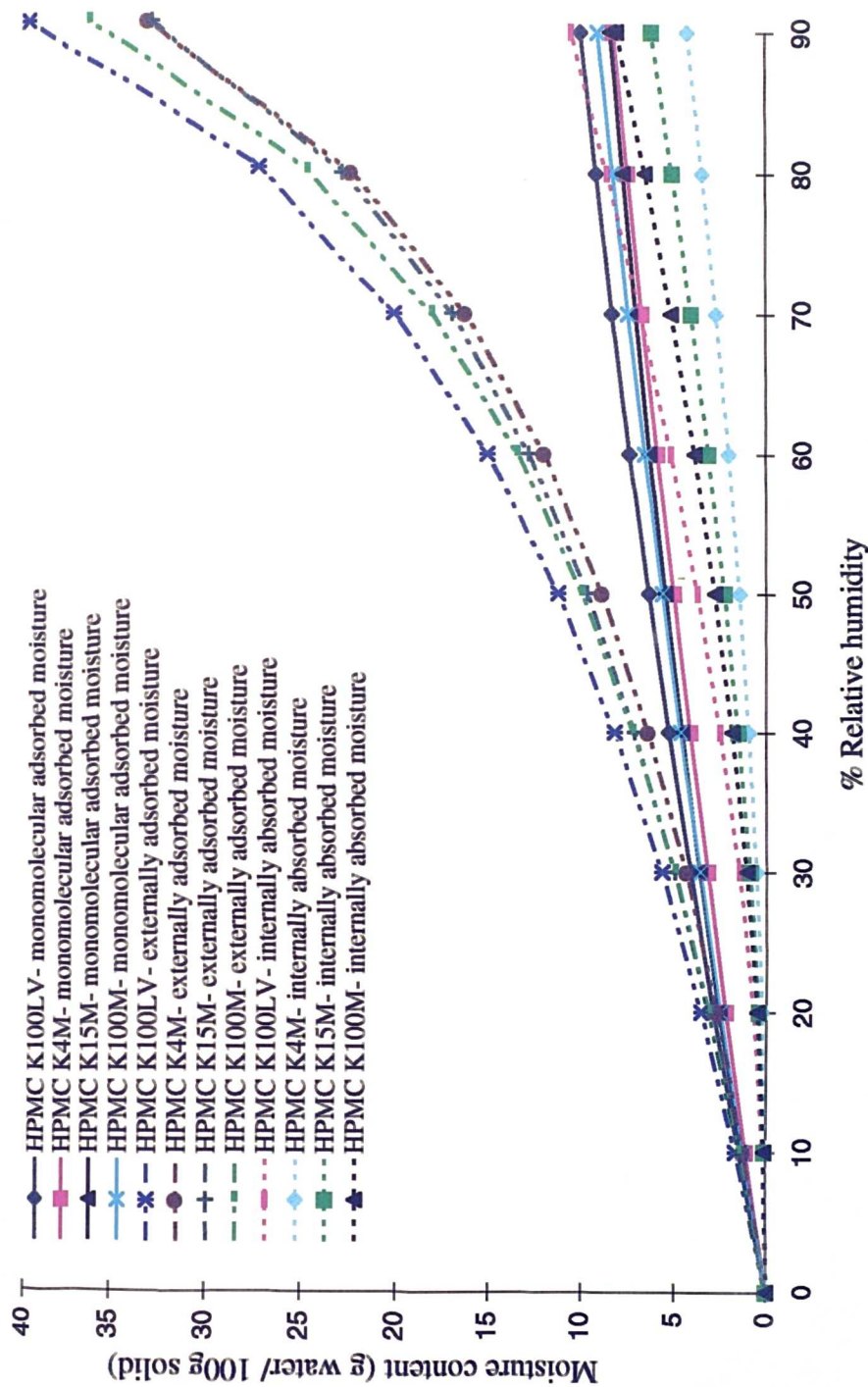


Figure 6.11: Influence of relative humidity on the distribution of water for a series of cellulose ether polymers of similar substitution type but varying molecular weight at 25°C

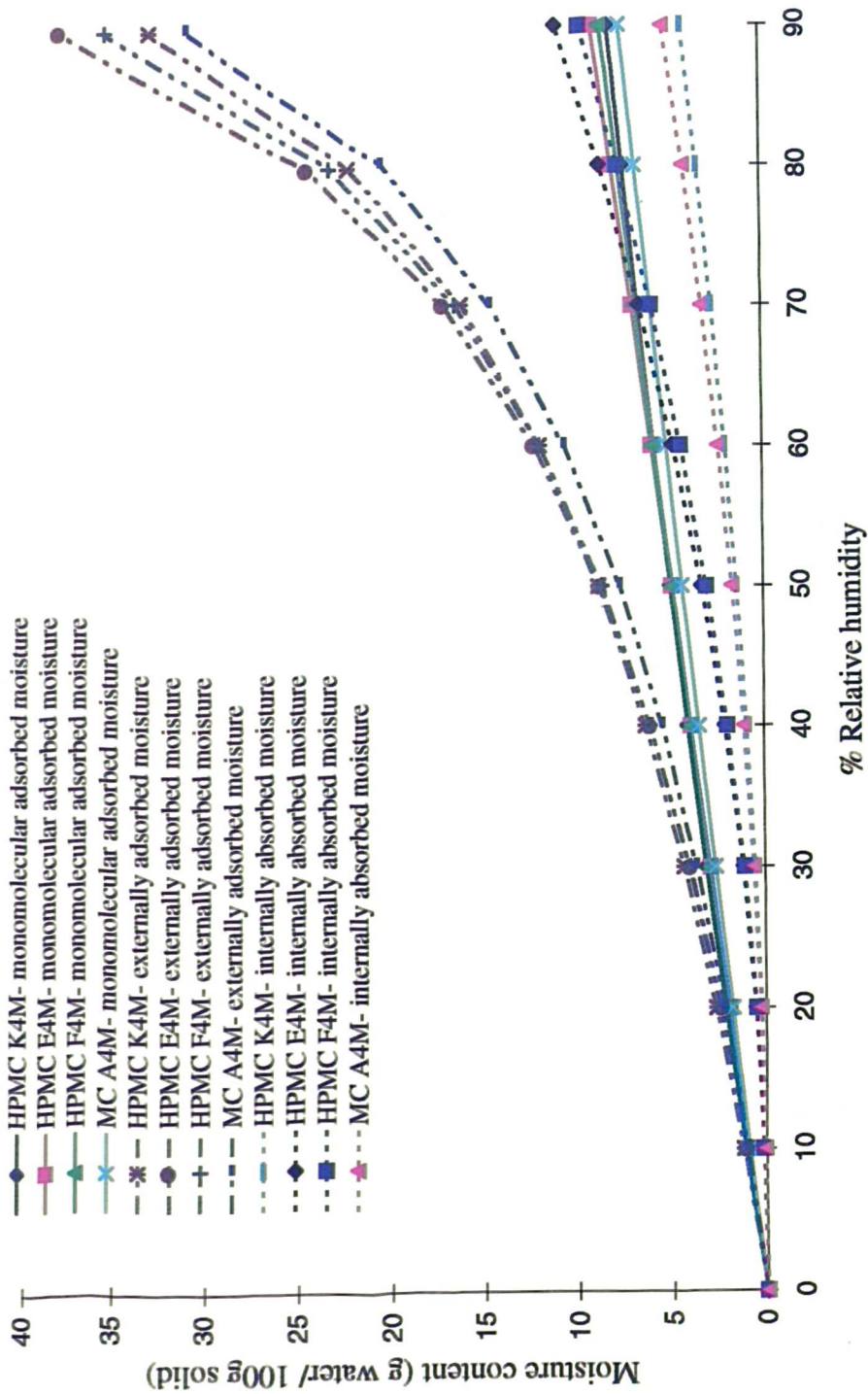


Figure 6.12: Influence of relative humidity on the distribution of water for a series of cellulose ether polymers of varying substitution type but similar molecular weight at 25°C

The E values previously reported for the HPMC K-series by Malamataris et al (1994) are less than 0.472, while Nokhodchi et al (1997) reported values greater than 0.64. In the current study, the E values for the HPMC K-series of polymers are above 0.64. The different values reported by Malamataris et al (1994) may be due to batch to batch variation in the methoxyl/ hydroxypropoxyl substitution ratio.

6.4.4 BET analysis of dynamic vapour sorption data for cellulose ether polymers

The Brunauer, Emmett and Teller (BET) (1938) equation (equation 2.6) has been applied to sorption isotherm data. The equation (and related equations) are shown in section 2.2.3.2 together with an explanation of how the equation may be used to obtain the weight of a monolayer of adsorbate W_m and the BET constant C. The latter is related to the energy of adsorption in the first adsorbed layer and indicates the magnitude of the adsorbent/adsorbate interactions. Surface area and specific surface area of the adsorbate may also be subsequently calculated. Although use of the BET equation has no theoretical basis for water absorption into amorphous solids (Oksanen and Zografis, 1993), some physical significance has been attributed to the W_m value. Direct compression properties of microcrystalline cellulose are lost below the W_m value and it has been suggested that below W_m , water molecules are not available to aid compression because they are tightly bound to the polymer (Zografis and Kontny, 1986).

The specific surface areas of cellulose ether powders (90 - 125 μ m) were found previously using a NOVA-2000 Gas Sorption Analyzer (section 2.2.3.2). This apparatus calculates specific surface area by applying the BET principle based on nitrogen gas sorption by the adsorbent. The BET equation was applied to the sorption of water vapour onto cellulose ether polymers in an attempt to compare the specific surface area of a range of cellulose ether polymers as calculated by water sorption as opposed to the values obtained when nitrogen gas is employed as the sorption gas. The calculations were carried out using a DVS BET Analysis software programme as supplied by Surface Measurement Systems Ltd., U.K. in which the molecular weight of water was taken as 18 g/mol and the effective molecular area of a water molecule

was taken as 12.5 \AA^2 . Calculations were carried out on the sorption data only and the results are shown in Table 6.7.

The values for specific surface area (SSA) obtained when water vapour was used as the adsorbate gas, are much larger than those obtained when nitrogen gas was employed, for example, for MC A4M, SSA (nitrogen) = $0.344 \text{ m}^2/\text{g}$; SSA (water) = $183.77 \text{ m}^2/\text{g}$.

Such differences have been reported previously in the measurement of specific surface area of microcrystalline cellulose (MCC). Hollenbeck et al (1978) have explained such differences by assuming that residual water in the polymer freezes when liquid nitrogen is used during nitrogen sorption analysis which blocks access to the porous polymer structure and as a result less nitrogen is adsorbed. This theory has since been refuted by Zografí et al (1984) who have considered that water interacts with the anhydroglucose molecule in the cellulose polymer chain. If this is indeed the case, the surface area obtained by water sorption is not indicative of a true surface area due to the effects of sorption into cavities within the particles. Using nitrogen as the adsorbent gas, the accessible internal and external surfaces are measured by physical adsorption and a truer estimate of specific surface area may be obtained (Sadeghnejad et al, 1986). No trends were visible between the SSA data for each individual polymer, calculated from water and nitrogen sorption data. This may be due to the highly amorphous nature of these polymers and indeed it may be due to the inconsistencies that may arise when water is used as the sorption gas.

Table 6.7 : Specific surface area and related parameters obtained from BET analysis of DVS water vapour sorption data (included are specific surface area values obtained using nitrogen gas as the adsorbate gas for comparison purposes)

Polymer	V_m (cm ³ /g)	C- value	specific surface area (m ² /g) (water sorption)	R ² (water sorption)	specific surface area (m ² /g) (N ₂ sorption)	R ² (N ₂ sorption)
HPMC K100LV	64.39	3.32	216.29	0.996	-	-
HPMC K4M	56.03	3.76	188.21	0.997	-	-
HPMC K15M	67.75	2.79	227.58	0.996	-	-
HPMC K100M	62.02	3.03	208.31	0.998	-	-
HPMC K4M	56.03	3.76	188.21	0.997	0.284	0.987
HPMC E4M	49.03	2.80	164.68	0.997	0.246	0.992
HPMC F4M	48.66	3.22	163.46	0.997	0.429	0.983
MC A4M	54.71	2.83	183.77	0.996	0.344	0.978

V_m is volume of monolayer coverage of adsorbate by adsorbent gas

C is the BET adsorption constant

R² is the correlation coefficient

- not determined

6.5 Conclusions

The influence of molecular weight and substitution levels on the vapour sorption/desorption characteristics of HPMC polymers were investigated using 'dynamic vapour sorption.'

All samples analysed showed Type II isotherms irrespective of molecular weight and substitution levels. Polymer molecular weight had no effect on moisture sorption behaviour, however HPMC K100LV and HPMC K4M retained slightly more water during desorption than other members of the HPMC K-series. HPMC K4M sorbed more moisture at all RH values than the polymers of other substitution levels studied. This may be related to the low percentage methoxyl substitution level (22.2%) of this polymer in combination with a high percentage hydroxypropoxyl level (8.4%).

The phenomenon of sorption hysteresis was studied and the hysteresis area for each of the polymers was calculated. HPMC K100LV and HPMC K4M had slightly larger hysteresis areas than HPMC K15M and HPMC K100M indicating that more water was taken up and retained by these polymers. HPMC E4M was found to have the largest hysteresis area in comparison with polymers of all other substitution levels studied.

The Young and Nelson theory which hypothesises three mechanisms by which water can associate to biological materials was applied to the water vapour sorption data. The calculated data fitted closely to the experimental data indicating that the Young-Nelson theory may be correctly applied to investigate the water sorption/desorption characteristics of HPMC polymers. The distribution of water as calculated using the Young-Nelson theory was related to the methoxyl/ hydroxypropoxyl substitution ratio in cellulose ether polymers.

The BET equation, for calculation of surface area, was applied to the sorption of water vapour onto cellulose ether polymers in an attempt to compare the specific surface area of a range of cellulose ether polymers as calculated by water sorption as opposed to the values obtained when nitrogen gas is employed as the sorption gas.

The values for SSA obtained when water vapour was used as the adsorbate gas, were much larger than those obtained when nitrogen gas was employed. These results were explained as being due to the effects of sorption of water vapour into the polymer.

Dynamic vapour sorption has proven a useful technique in examining the sorption and desorption characteristics of HPMC polymers at both high and low relative humidities and it has provided information on the distribution of water within these polymers.

CHAPTER 7

DIELECTRIC PROPERTIES OF CELLULOSE ETHER GELS

Chapter 7 Dielectric properties of cellulose ether gels

7.1 Introduction

Dielectric spectroscopy has been used to study a wide variety of pharmaceutical systems over a large range of frequencies. Low frequency dielectric spectroscopy (LFDS) involves measurement of dielectric behaviour over the frequency range of 10^{-4} to 10^7 Hz and in simple terms it measures the electrical properties of a material from which information related to the structure and behaviour of the material may be elucidated (Craig, 1992). A dielectric material is a material which contains dipoles and the majority of pharmaceutical systems may thus be classified as dielectrics. When an alternating field is applied to such a material the dipoles will try to reorientate themselves in the direction of the field in an attempt to maintain overall neutrality. At low field strengths, the polarisation (P) is given by:

$$\text{Equation 7.1} \quad P = \chi_0 E = \epsilon_0 (\epsilon - 1) E$$

where E is the field strength, χ_0 is the static susceptibility, ϵ_0 is the permittivity of free space and ϵ is the relative permittivity of the sample. On application of an alternating field, a phase lag develops between the field and the polarisation as the dipoles attempt to relax at the same rate as the changes in field direction. Thus the response of the sample may be described by two parameters; the magnitude of the response and the phase relationship between the stimulus (field) and the response. The susceptibility becomes vectorial (χ^*) and is hence more conveniently described as:

$$\text{Equation 7.2} \quad \chi^* = \chi' - i\chi''$$

where χ' and χ'' are the real (energy storage) and imaginary (energy loss) components of the susceptibility respectively and i is $\sqrt{-1}$. These components may be measured in terms of real and imaginary permittivities (permittivity is a measure

of the ease with which a sample polarises and is an intrinsic property of a particular sample). In practice, the response is measured in terms of the capacitance (C) and dielectric loss (G/ω) where G is the conductance and ω is the frequency. Capacitance is considered to be the real component and dielectric loss as the imaginary component of the response. These may be related to the real and imaginary permittivities by:

$$\text{Equation 7.3} \quad C(\omega) = \frac{\epsilon_0 A}{d} (\chi'(\omega) + \epsilon_\varphi)$$

$$\text{Equation 7.4} \quad \frac{G(\omega)}{\omega} = \frac{\epsilon_0 A \chi''(\omega)}{d}$$

where A and d are the area and separation distance of the electrodes respectively and ϵ_φ is the permittivity at infinite frequencies. In some systems, free charges exist which may generate a direct current by moving from one electrode to the other. This may be accounted for by rewriting equation 7.4 to include a direct current conductivity (G_{dc}) term.

$$\text{Equation 7.5} \quad \frac{G(\omega)}{\omega} = \frac{\epsilon_0 A \chi''(\omega)}{d} + \frac{G_{dc}}{\omega}$$

The values of capacitance and dielectric loss are measured over a range of frequencies and examination of both their absolute magnitudes and also the relationship between the two parameters may lead to information regarding the structure of the sample under study. More detail about the theory of dielectric spectroscopy may be found in the texts of Hill & Jonscher (1983) and Craig (1995).

LFDS has been used to characterise many pharmaceutical systems. The dielectric response of polyethylene glycols (PEGs) in both the molten and solid state (Craig and Newton, 1993) and the structure of drug dispersions within PEGs have been characterised (Craig et al, 1993b). It was found that the low frequency response of molten PEGs consists of a conduction process in series with a barrier layer of PEG

molecules which are adsorbed onto the electrodes. In the solid state, the low frequency response, which is considered to correspond to a d.c. conductivity process, showed a decrease in conductivity with increasing PEG chain length. Upon addition of nortriptyline HCl, it was found that in the molten state, the barrier layer of PEG molecules located at the electrodes was disrupted by the drug. In the solid state, the low frequency response is associated with the amorphous fraction of the PEG. Multi-component solid systems have been studied by LFDS using β -Cyclodextrin/acetotoluide (ACT) systems where evidence for the existence of an inclusion complex between para (p) - ACT and β -Cyclodextrin was found (Craig et al, 1992a).

A theory regarding barrier effects in dispersive media on the measurement of dielectric properties has been proposed by Hill and Pickup (1985). This theory suggests that for many aqueous dispersed systems, the conducting bulk (aqueous) phase of the sample is seen at high frequencies ($10^2 - 10^4$ Hz) in series with a thin barrier layer located at the electrodes and seen at low frequencies. This theory has been applied to studies on liposome suspensions containing dipalmitoylphosphatidylcholine (DPPC). It was found that the low frequency response was associated with a layer of liposomes absorbed onto the electrode surface thus providing a potential method of characterising liposomal suspensions (Barker et al, 1994).

The dielectric properties of gels such as sodium alginate gels have been characterised (Binns et al, 1992) and the treatment proposed by Hill and Pickup (1985) has been successfully applied. The high frequency capacitance and dielectric loss showed linear and logarithmic relationships with alginate concentration and the effects of calcium sulfate and diclofenac sodium addition were characterised in association with gel viscosity measurements. Craig et al (1992b, 1994) studied the effects of a number of variables on the dielectric and rheological behaviour of Carbopol 934 gels using LFDS and oscillatory rheometry. They found that both methods in conjunction were capable of characterising the effect of additives such as propylene glycol and chlorhexidine gluconate on the gel structure. The study was extended to other associated poly (acrylic acid) gel systems in which the mucoadhesive properties of the gel systems were also assessed by means of a force detachment test (Tamburic & Craig, 1995). The three techniques were found to provide information on the effect of

ageing on the gel structure in which it was found that significant changes in structure occurred upon storage (Tamburic & Craig, 1996).

The behaviour of water in polymeric systems has been previously characterised by analysis of the dielectric response. The relaxation and crystallization of water in a terpolymer hydrogel have been characterised in terms of their dielectric response (Pathmanathan and Johari, 1994). It was found that on cooling, a fraction of the total amount of water crystallizes to ice and this is detectable by the appearance of a relaxation peak. Water and ice were found to coexist at temperatures up to 270°C which may indicate the existence of crystallizable and non-crystallizable water in the polymer. Non-crystallizable water is thought to be that water stored in the cavities of hydrogels which may be considered as bound and is not readily evaporated on heating.

The dielectric response of polymer-water interactions in poly (hydroxyethyl acrylate) hydrogels have been studied and compared to studies carried out using DSC and sorption isotherm measurements on similar hydrogels (Kyritsis et al, 1995). In this case, low frequency dielectric measurements were carried out using thermally stimulated depolarisation current (TSDC) techniques. The TSDC method consists of recording the thermally activated release of frozen-in polarisation and is equivalent to measuring dielectric losses against temperature. The sample is polarised by a d.c. electric field for a certain time t and this polarisation is stopped by cooling to low temperatures. When the sample is warmed, the polarisation decays, and for each relaxation mechanism a current peak is recorded which provides information on polymer-water structure. While sorption/ desorption isotherm measurements suggest that no water is tightly bound to the polymer, dielectric relaxation and DSC studies have indicated that certain water contents exist in the systems studied, above which more than one type of water may be identified.

In this chapter, the dielectric properties of cellulose ether gels were investigated using LFDS. The dielectric response of the gels over a range of frequencies (10^{-2} to 10^{+7} Hz) at constant temperature and also a range of temperatures (-30°C to +20°C) at frequencies of 1 and 100Hz were measured.

7.1.1 Objectives

The objectives of this work were to characterise the dielectric response of cellulose ether gels over a temperature range of -30°C to $+22^{\circ}\text{C}$. Cellulose ether gels have been previously characterised in a similar temperature range using DSC (Chapter 3 and Chapter 5). The influences of polymer concentration, molecular weight and substitution levels on their dielectric responses were investigated.

7.2 Materials

Methocel cellulose ethers were obtained from the DOW Chemical Company (section 2.1.1; Table 2.1). HPMC K100LV (BN MM94051022K) and HPMC K15M (BN MM94112811K) were used. HPMCs K4M, K100M, E4M, F4M and MC A4M were as described in Table 2.1.

Hydroxypropylcellulose (HPC) MF EP (LOT 12187) was obtained from Hercules Limited, Aqualon Division, Salford, U.K. (section 2.1.1).

Propranolol hydrochloride and diclofenac sodium were as outlined in section 2.1.2.

7.3 Methods

7.3.1 Gel preparation

Polymer gels containing 2 - 25% (w/w) polymer were prepared in the absence and presence of 50mM of diclofenac sodium or propranolol hydrochloride with deionised water (Elgastat), and stored at $4-6^{\circ}\text{C}$ as outlined in section 2.2.1.

7.3.2 Dielectric Spectroscopy Analysis

A Novocontrol Broadband Dielectric Converter BDC (Hundsangen, Germany) with an attached QUATRO temperature controller was employed. This apparatus has the capability of carrying out dielectric analysis in the frequency range of 10^{-5} - 10^{+7} Hz at temperatures between -150°C to $+400^{\circ}\text{C}$.

Gel samples were transferred to a round plate electrode dielectric cell (diameter (d) = 20mm; thickness = 0.5mm). The Novocontrol BDC was used to apply an alternating voltage of 0.5V across the sample. Dielectric spectra for HPMC K15M gels were obtained over frequency sweeps from 10^{-2} to 10^7 Hz at a constant temperature of 22°C . From this work, two frequencies (1 and 100Hz) were chosen and gels were subjected to temperature sweeps from -30°C to $+20^{\circ}\text{C}$ at a scanning rate of $+1^{\circ}\text{C min}^{-1}$, and their dielectric responses were recorded. In addition, their dielectric response at constant temperatures of -30 , 0 or $+22^{\circ}\text{C}$ were recorded over a frequency range of 10^{-2} to 10^7 Hz. Each dielectric response at a particular temperature or frequency represents an average of at least two measurements with each set of measurements being repeated at least twice.

7.4 Results and Discussion

7.4.1 Dielectric response of HPMC K15M gels

7.4.1.1 Effect of temperature on the nature of the dielectric response

Figure 7.1 shows the dielectric response of HPMC K15M (25% w/w) gels and deionised water over a frequency range of 10^{-2} to 10^{+7} Hz at a constant temperature of 22°C . The overall dielectric response of the HPMC K15M gels follows the same pattern as that of the deionised water. However, an increase in magnitude of both the capacitance ($\text{Log } C_p'$) and dielectric loss ($\text{Log } C_p''$) values occurs in the presence of HPMC K15M. This may be due to the presence of the polymer or indeed due to the

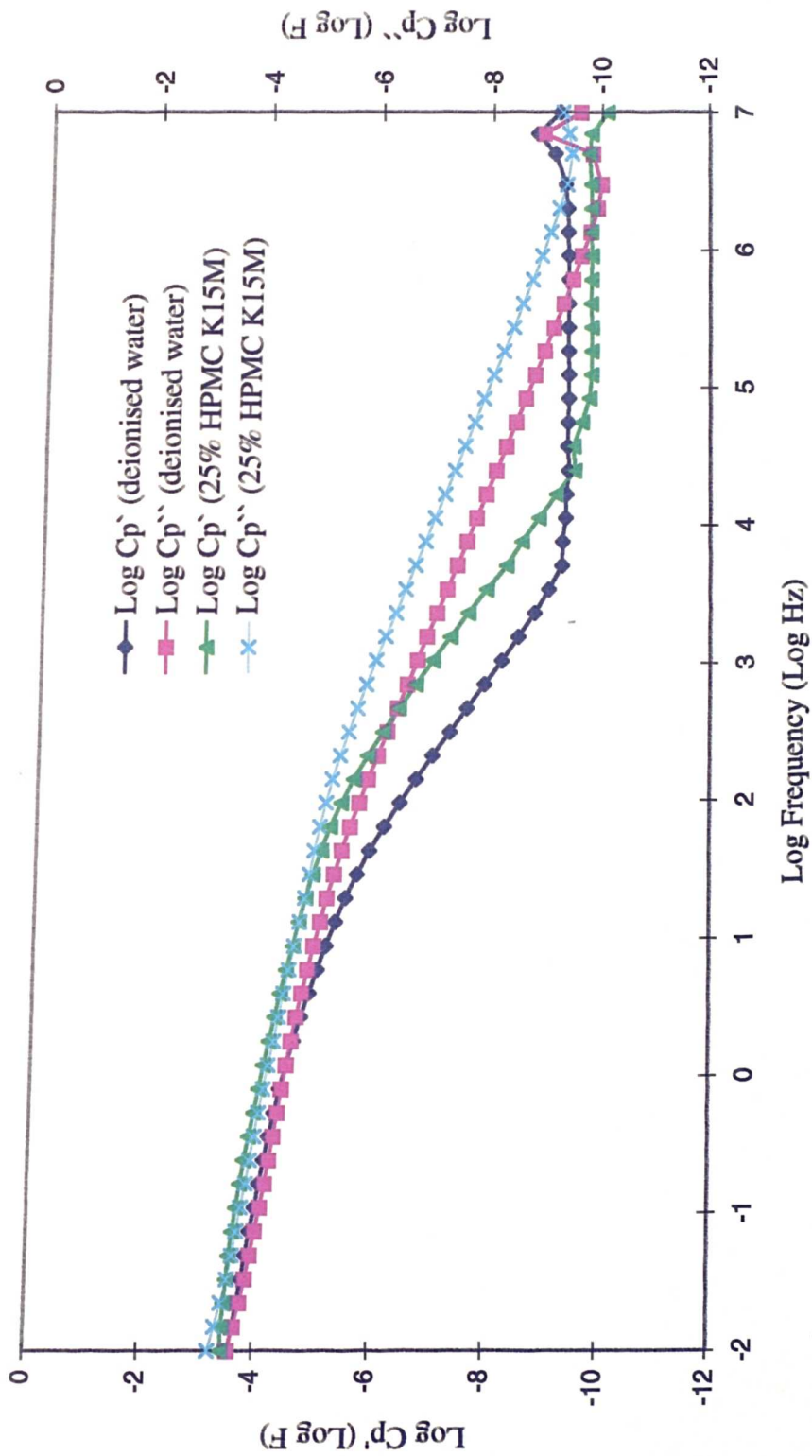


Figure 7.1 : Log Capacitance (Log Cp') (Log F) and Log Dielectric loss (Log Cp'') (Log F) against Log Frequency (Log Hz) for deionised water and 25% (w/w) HPMC K15M gels at 22°C

effect of contaminants in HPMC K15M, which includes ionic species such as Na^+ and Cl^- (see Table 2.1).

Figure 7.2 and Figure 7.3 illustrate the dielectric response of 25% (w/w) HPMC K15M gels and deionised water over the same frequency range at temperatures of 0 and -30°C respectively. At 0°C , the dielectric response shows a quite similar pattern to that observed at 22°C . However, deionised water and gel samples scanned at -30°C show very different dielectric behaviour compared to the response at higher temperatures. The capacitance of deionised water decreased from -3.5 (Log F) at 22°C to -8.75 (Log F) at -30°C . Similarly, the capacitance of 25% (w/w) HPMC K15M gels decreased from -3.5 (Log F) at 22°C to -6 (Log F) at -30°C approximately. The decrease in magnitude of the dielectric response, which occurs with a decrease in temperature, is related to the reduction in mobility of dipoles in the system as the sample freezes. At 22°C , the system is liquid and water and other ionic species possess kinetic energy and are mobile. Dipoles within the system can easily respond to an alternating current and the dielectric response is therefore large in magnitude. With a reduction in temperature, the kinetic energy of the dipoles is correspondingly reduced until freezing occurs and thus a dielectric response typical of a solid is apparent. In essence, at -30°C , water is frozen and the response of the dipoles are typical of those recorded for solids (Craig et al, 1993a).

The dielectric response of 25% (w/w) HPMC K15M gel samples and that of deionised water were recorded as the temperature of the samples was varied from -30°C to $+20^\circ\text{C}$ at frequencies of 1 and 100Hz. The capacitance and dielectric loss of the samples are shown in Figures 7.4 & 7.5 respectively. The dielectric response of the deionised water is characterised by a sharp increase in both the capacitance and dielectric loss at the melting point of ice (0°C). Figure 7.4 shows that deionised water showed no change in capacitance over a temperature range of -30°C to 0°C . However, at about 0°C , a sudden increase in capacitance from -9 to -6.5 at 100Hz, an increase in capacitance in the order of 1.5, was observed. In the presence of 25% (w/w) HPMC K15M, the dielectric response of the system is different to that observed for deionised water. Figure 7.4 shows that at 100Hz, the value of Log C_p

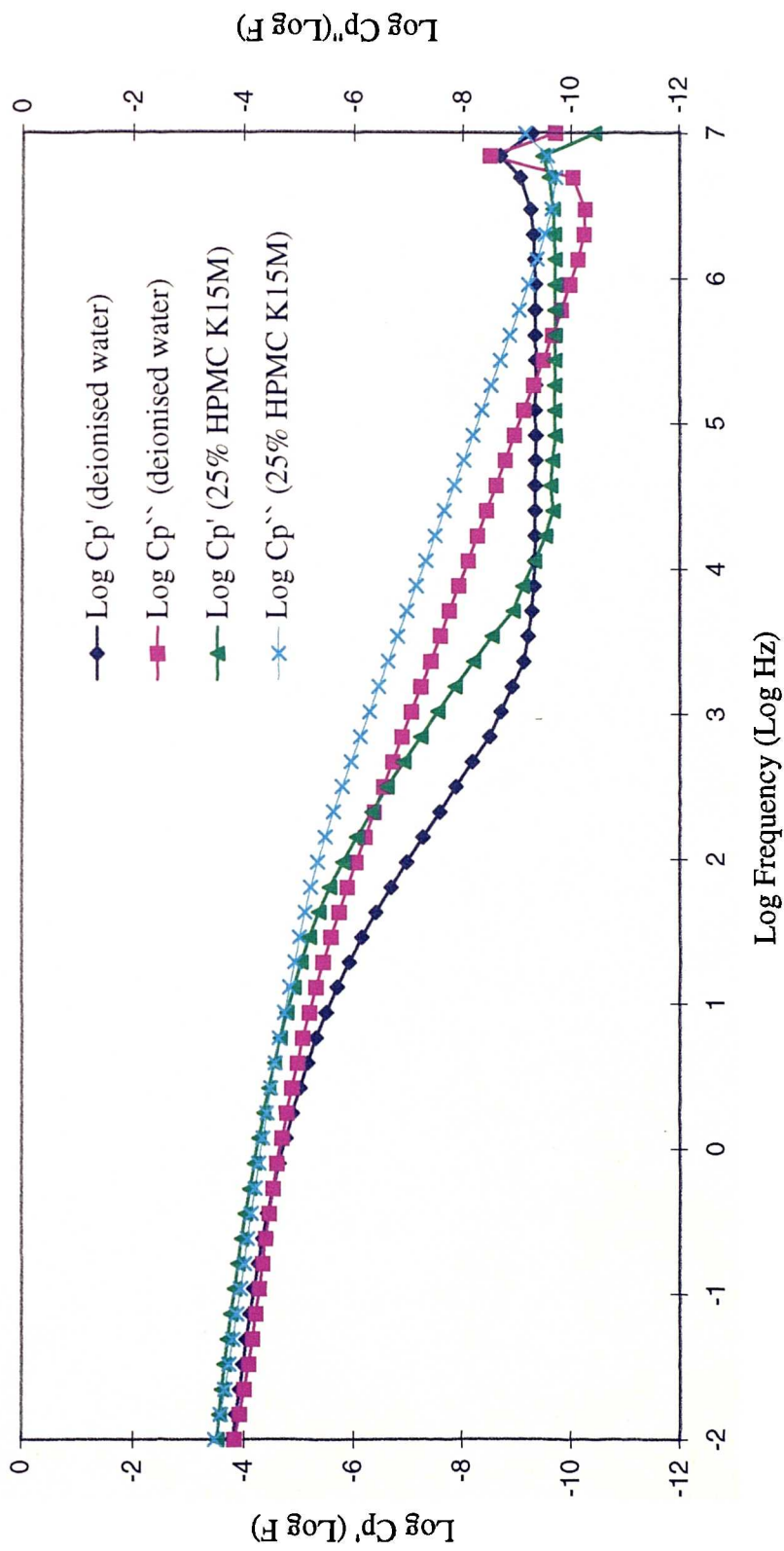


Figure 7.2 : Log Capacitance (Log Cp') (Log F) and Log Dielectric loss (Log Cp'') (Log F) against Log Freq (Log Hz) for deionised water and 25% (w/w) HPMC K15M gels at 0°C

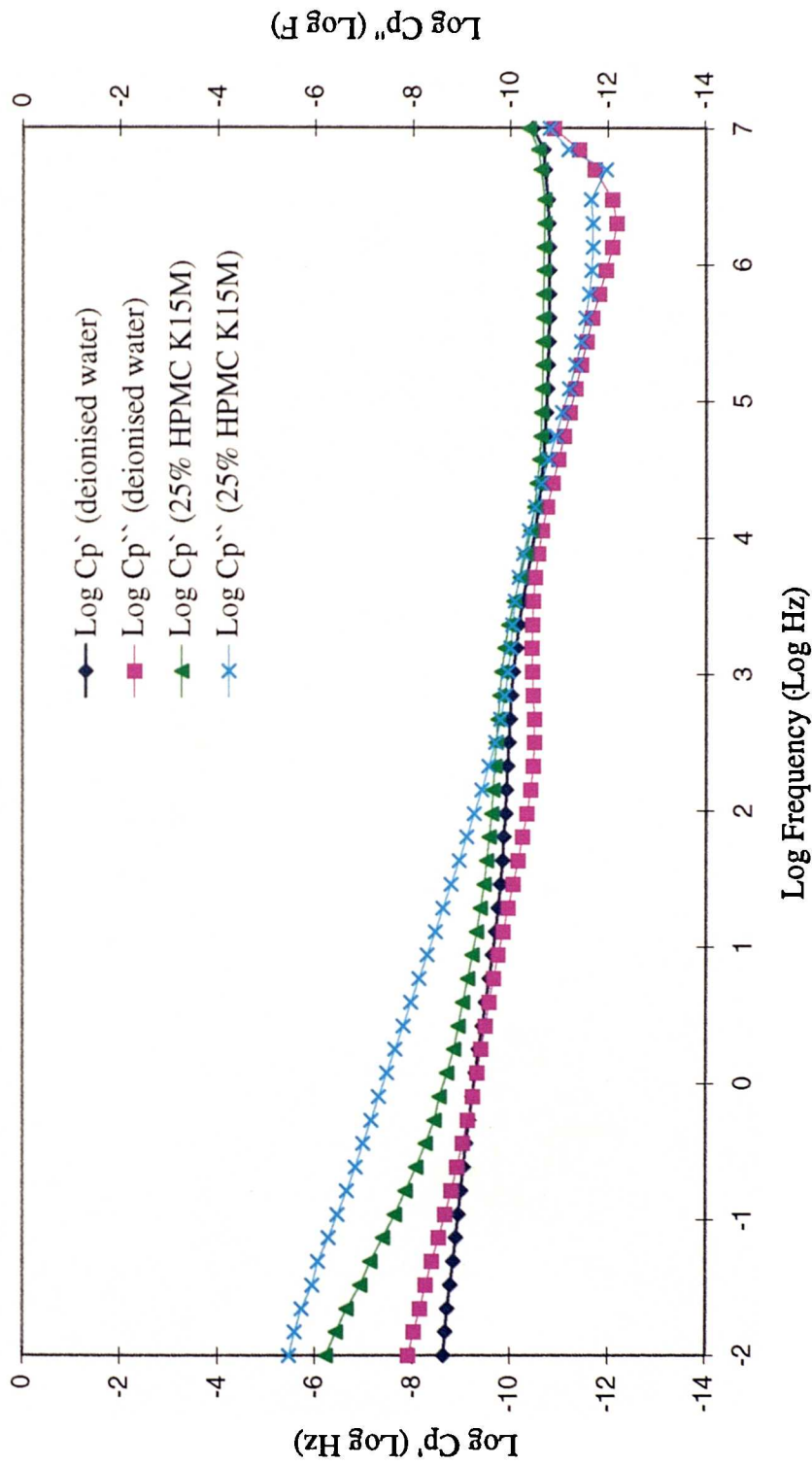


Figure 7.3 : Log Capacitance (Log Cp') (Log F) and Log Dielectric loss (Log Cp'') against Log Frequency (Log Hz) for deionised water and 25% (w/w) HPMC K15M gels at -30°C

increases from -9.5 to -6 (Log F), which is quite similar in magnitude to the increase for deionised water. However, the increase in capacitance begins at about -12°C and continues to +4°C. This may be related to a depression in the melting point of ice which appears to occur at about -22°C and -12°C in the presence of HPMC K15M at frequencies of 1 and 100Hz respectively. Similar trends are observed from the Log Cp'' data (Figure 7.5). As well as the melting of free water, a number of other processes seem to be occurring as indicated by the shape of the dielectric response curves. These data are in agreement with the findings by DSC (section 3.4.1) which have identified more than one event occurring during the melting of ice in HPMC K15M gels of a similar concentration. It is hypothesised that these events may be indicative of the presence of more than one type of water in HPMC K15M gels. Alternatively, these events may be due to the occurrence of a glass transition in this region or due to cold crystallization occurring (section 3.4.1.1). TGA analysis of similar gel samples (section 4.4.1) has shown that on heating, more than one event is visible on the TGA derivative curves, indicating the existence of a type (types) of loosely bound water which evaporates at higher temperatures than free water.

7.4.1.2 Effect of HPMC K15M concentration on the dielectric response

The effect of HPMC K15M concentration on the behaviour of water in gel systems has previously been characterised using thermal methods (section 3.4.1.1) which showed that events occurring on the leading edge of the main endotherm for the melting of free water in HPMC K15M gel systems are polymer concentration dependent. Such events, attributed to the presence of loosely bound water, are present in 20% (w/w) gels but are absent in 10% (w/w) gels. Further studies using TGA (section 4.4.1.1) showed that, at higher polymer concentrations, the secondary evaporation event visible on the first derivative curve becomes gradually more pronounced. It was hypothesised that the distribution of water within the gels changes with polymer concentration with loosely bound water evaporating at higher temperatures than free water.

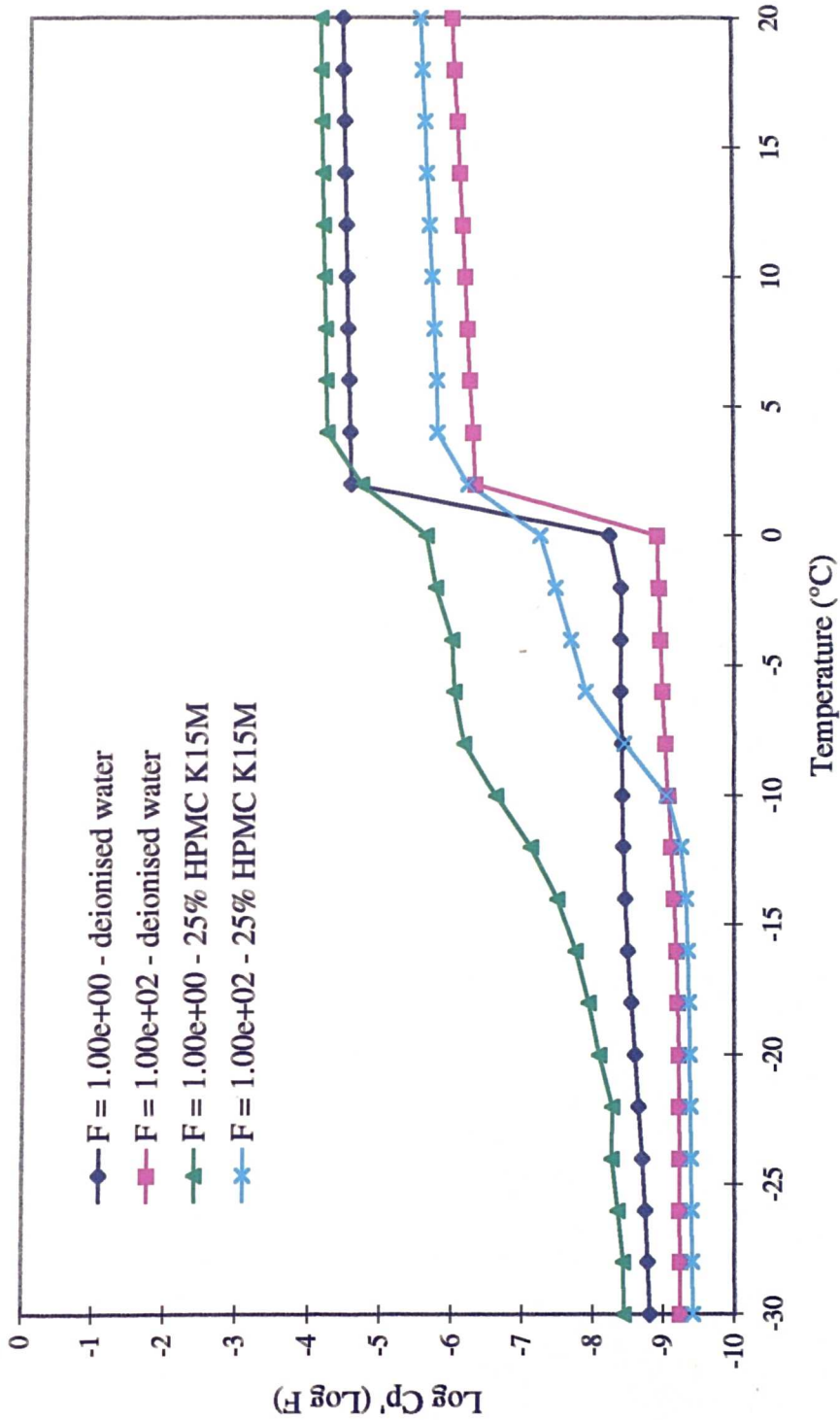


Figure 7.4 : Log Capacitance (Log Cp') (Log F) against Temperature (°C) for 25% (w/w) HPMC K15M gels and deionised water at frequencies of 1 and 100 Hz

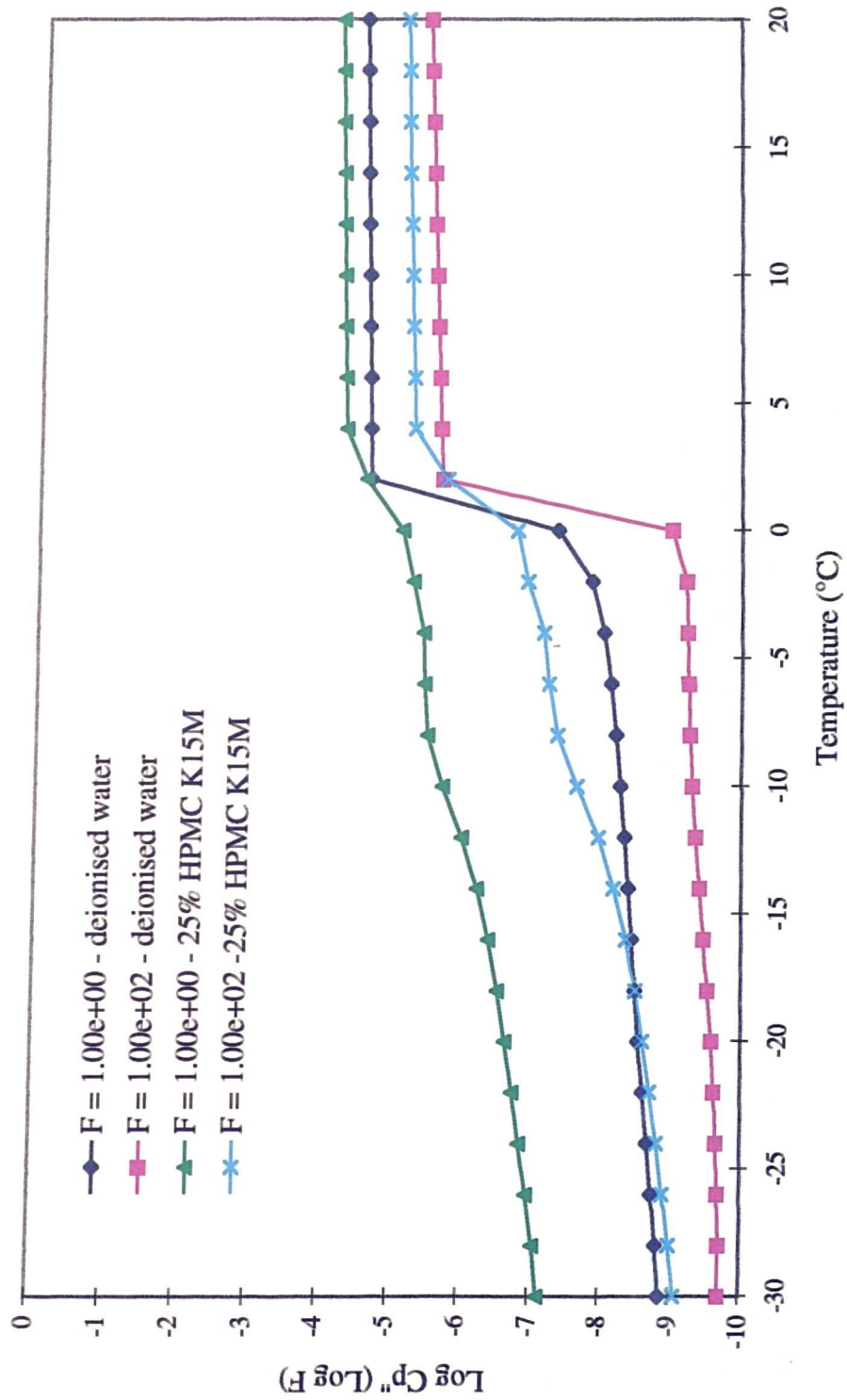


Figure 7.5 : Log Dielectric loss (Log Cp'') (Log F) against Temperature (°C) for 25% (w/w) HPMC K15M gels and deionised water at frequencies of 1 and 100 Hz

Figures 7.6-7.9 show the dielectric response of deionised water and HPMC K15M (2-25% w/w) gels scanned at 1 and 100Hz respectively. The dielectric response of the gels clearly changes with increase in polymer concentration. Figure 7.6 shows that a transition beginning at approximately -8.5°C becomes more pronounced with increase in polymer concentration. Such a response is also visible in the dielectric loss response at 1Hz (Figure 7.7) and in the capacitance and dielectric loss responses at 100Hz (Figure 7.8 and Figure 7.9). Such transitions may be related to events seen on the leading edge of the main endotherm in DSC data in HPMC K15M gels of greater than 15% (w/w) concentration. These are in agreement with DSC and TGA studies in showing that more than one type of water exists in HPMC K15M polymer gels. A linear relationship exists between $\text{Log } C_p''$ and polymer concentration (Fig 7.10). This may suggest that the increase in dielectric response ($\text{Log } C_p''$) may be due to the ionic species in the gel samples.

7.4.1.3 Effect of polymer molecular weight on the dielectric response of cellulose ether gels

The dielectric spectra of HPMC K-series polymers of similar substitution levels but with increasing molecular weight at frequencies of 1 and 100Hz are shown in Figures 7.11-7.14. Both the capacitance and dielectric loss of the gel samples studied indicate that, in addition to the melting of free water, other processes seem to be occurring. This is similar to those previously seen in HPMC K15M gels which may indicate the presence of different types of water. The dielectric response of the gels at these frequencies over a temperature range of -30°C to $+20^{\circ}\text{C}$ seems to vary with polymer molecular weight. The temperature at which melting of frozen water appears to begin in the gels varies with polymer molecular weight. Additionally, the pattern of melting as observed by the dielectric response, is somewhat different for HPMC K100LV in comparison to the three other K-series polymers studied. Similarly, in DSC studies, the appearance of endothermic events varied between HPMCs of different molecular weights, however no specific trend was apparent.

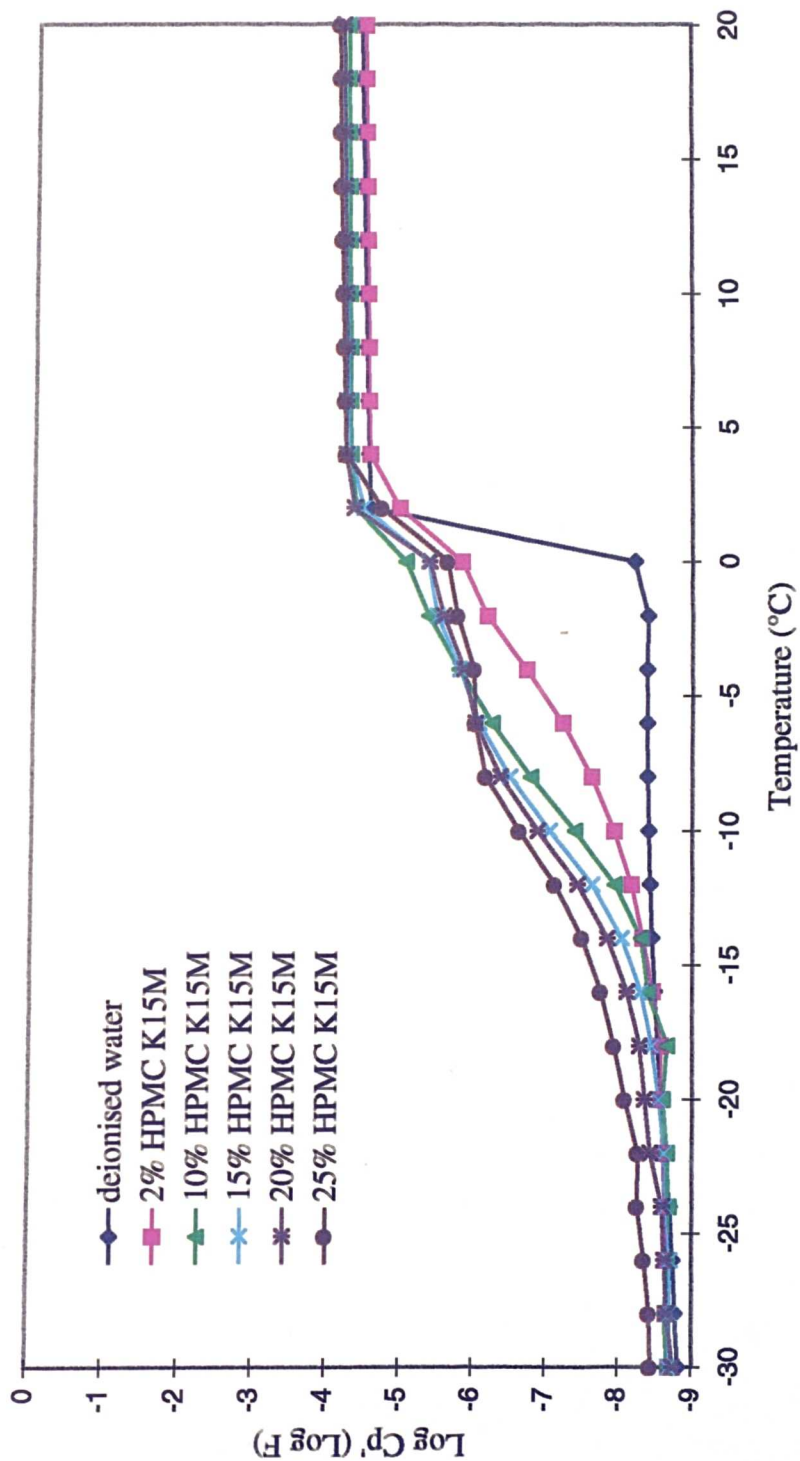


Figure 7.6 : Log Capacitance (Log Cp') (Log F) against Temperature (°C) for 2-25% (w/w) HPMC K15M gels and deionised water at a frequency of 1 Hz

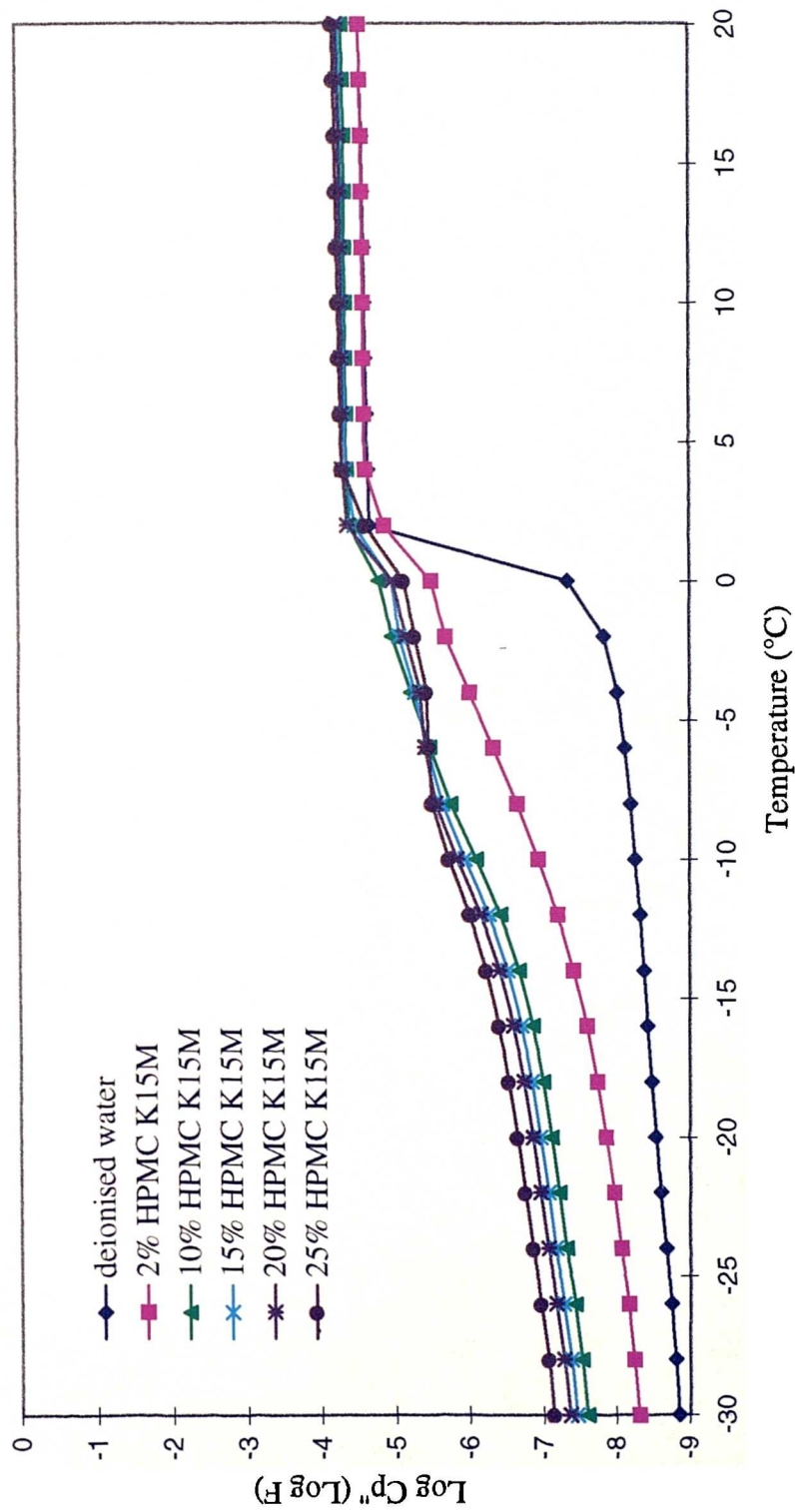


Figure 7.7 : Log Dielectric loss (Log Cp'') (Log F) against Temperature (°C) for 2-25% (w/w) HPMC K15M gels and deionised water at a frequency of 1 Hz

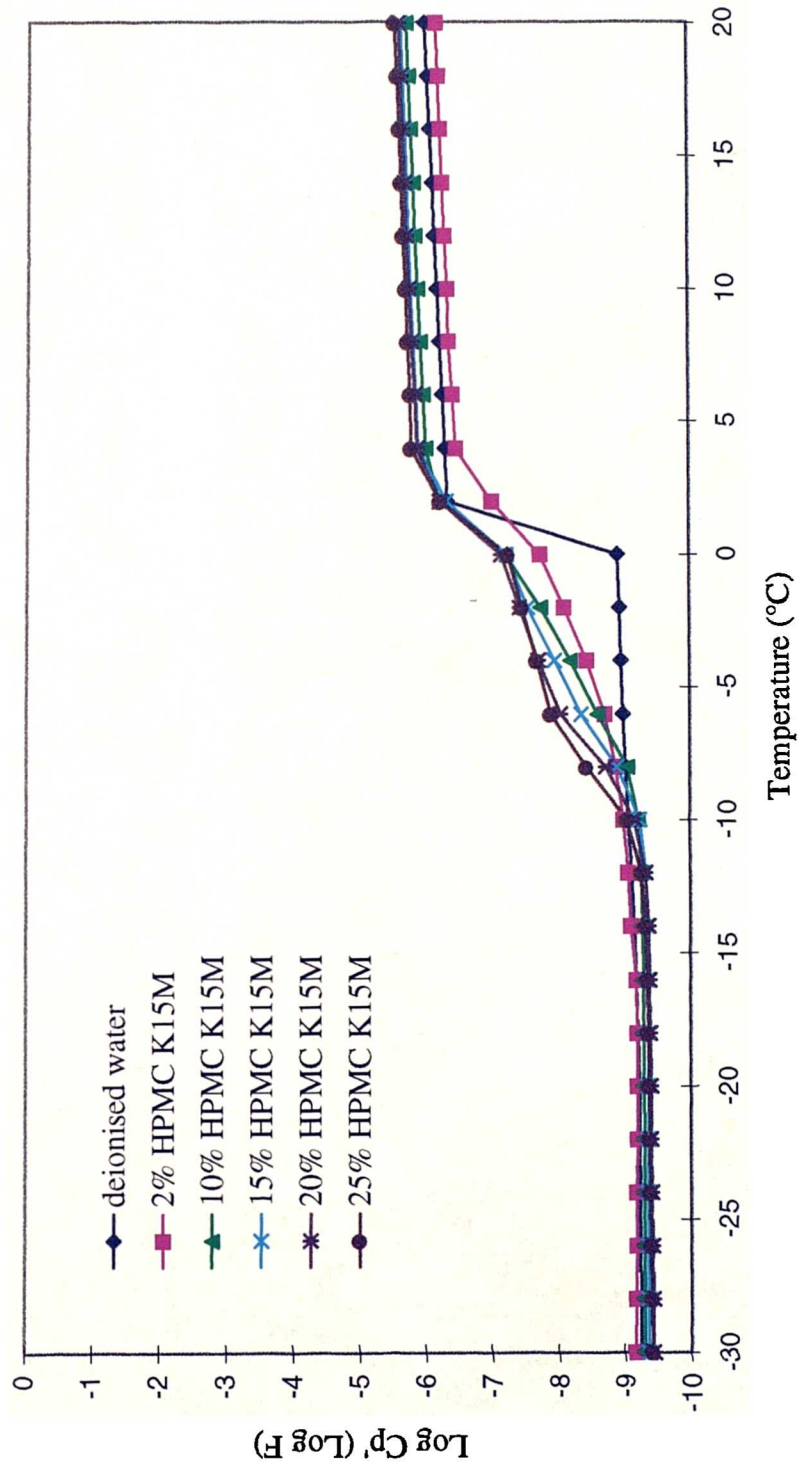


Figure 7.8 : Log Capacitance (Log Cp') (Log F) against Temperature (°C) for (2-25% w/w) HPMC K15M gels and deionised water at a frequency of 100Hz

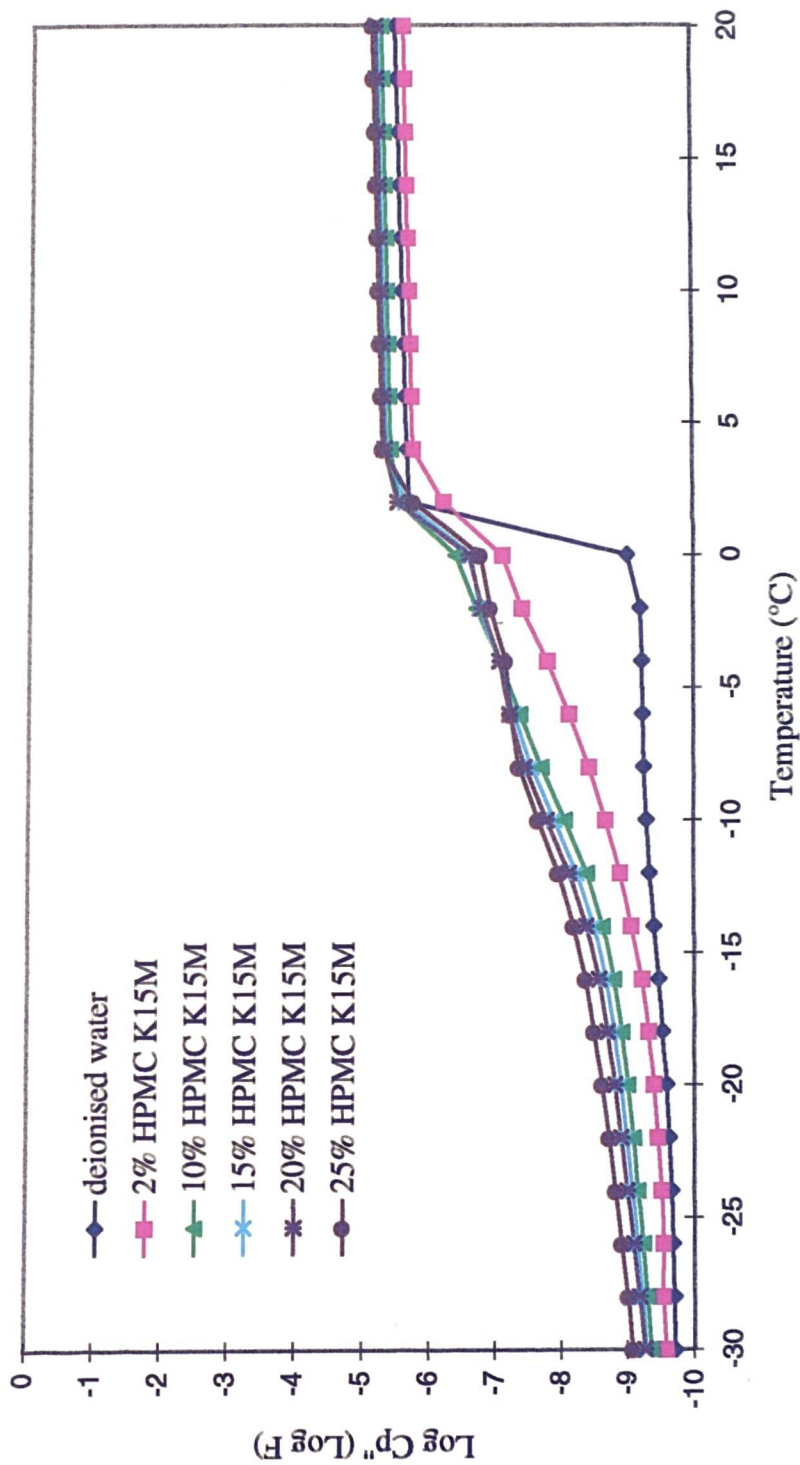


Figure 7.9 : Log Dielectric loss (Log Cp'') (Log F) against Temperature (°C) for (2-25% w/w) HPMC K15M gels and deionised water at a frequency of 100Hz

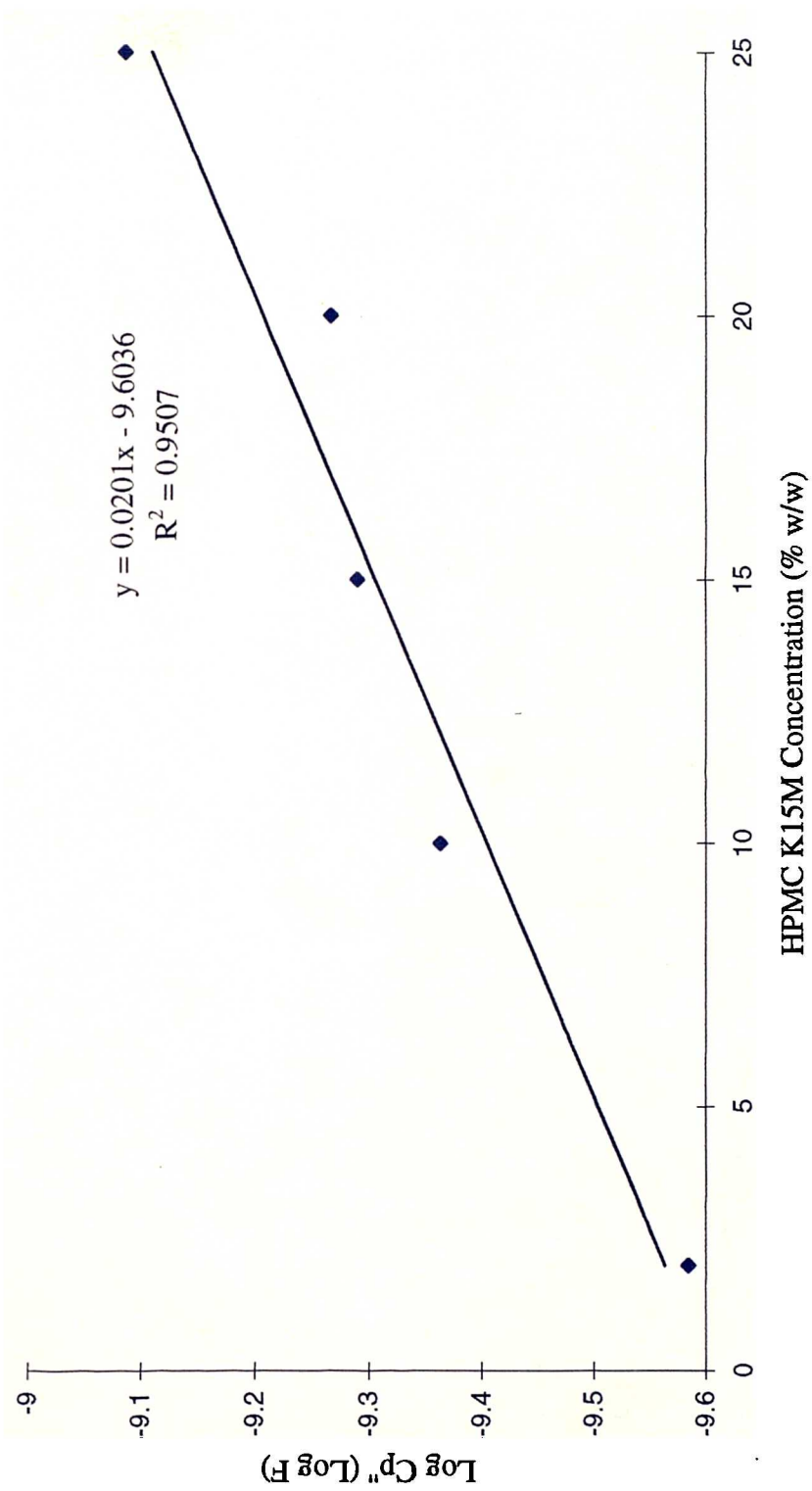


Figure 7.10 : Log Dielectric loss (Log Cp'') (Log F) as a function of concentration for HPMC K15M gels at a frequency of 100 Hz at -30°C (n=2)

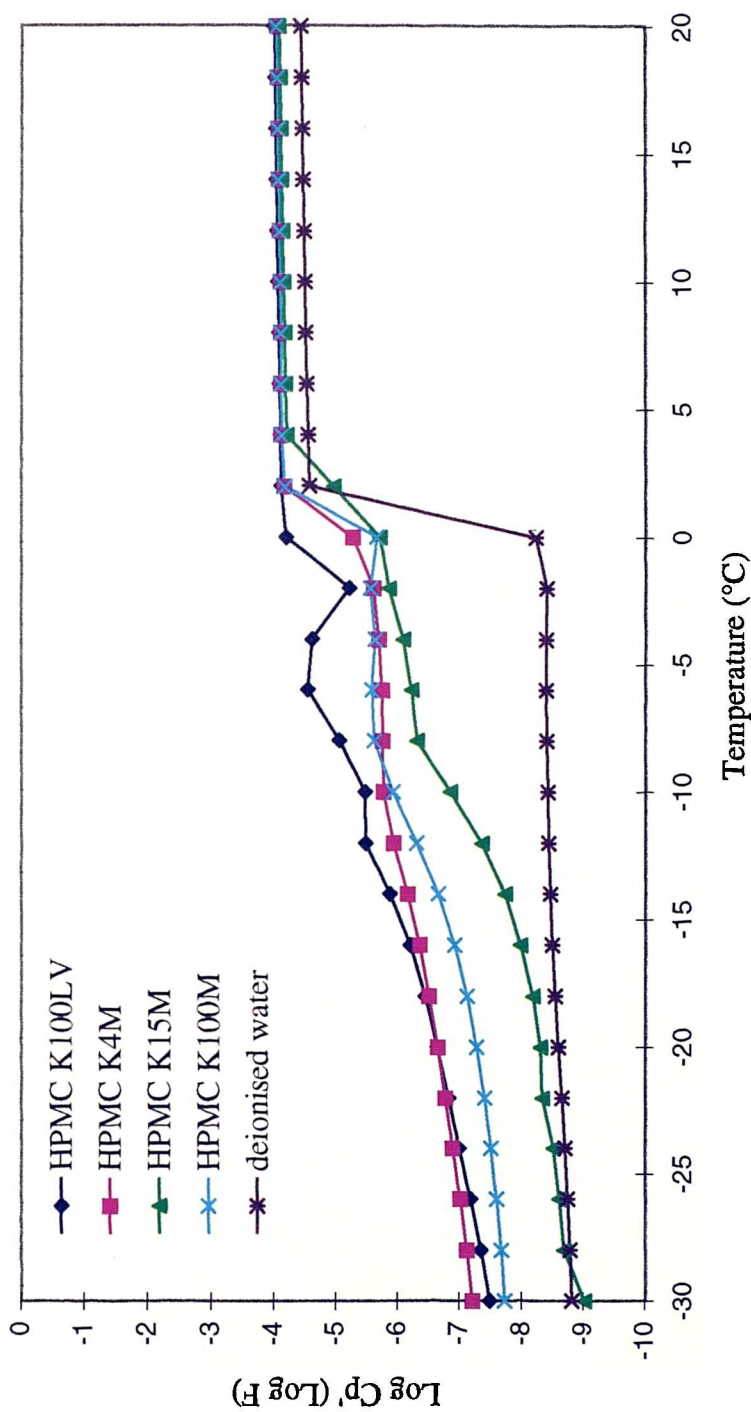


Figure 7.11 : Log Capacitance (Log Cp') (Log F) against Temperature (°C) for 25% (w/w) HPMC K100LV, K4M, K15M & K100M gels and deionised water at a frequency of 1 Hz

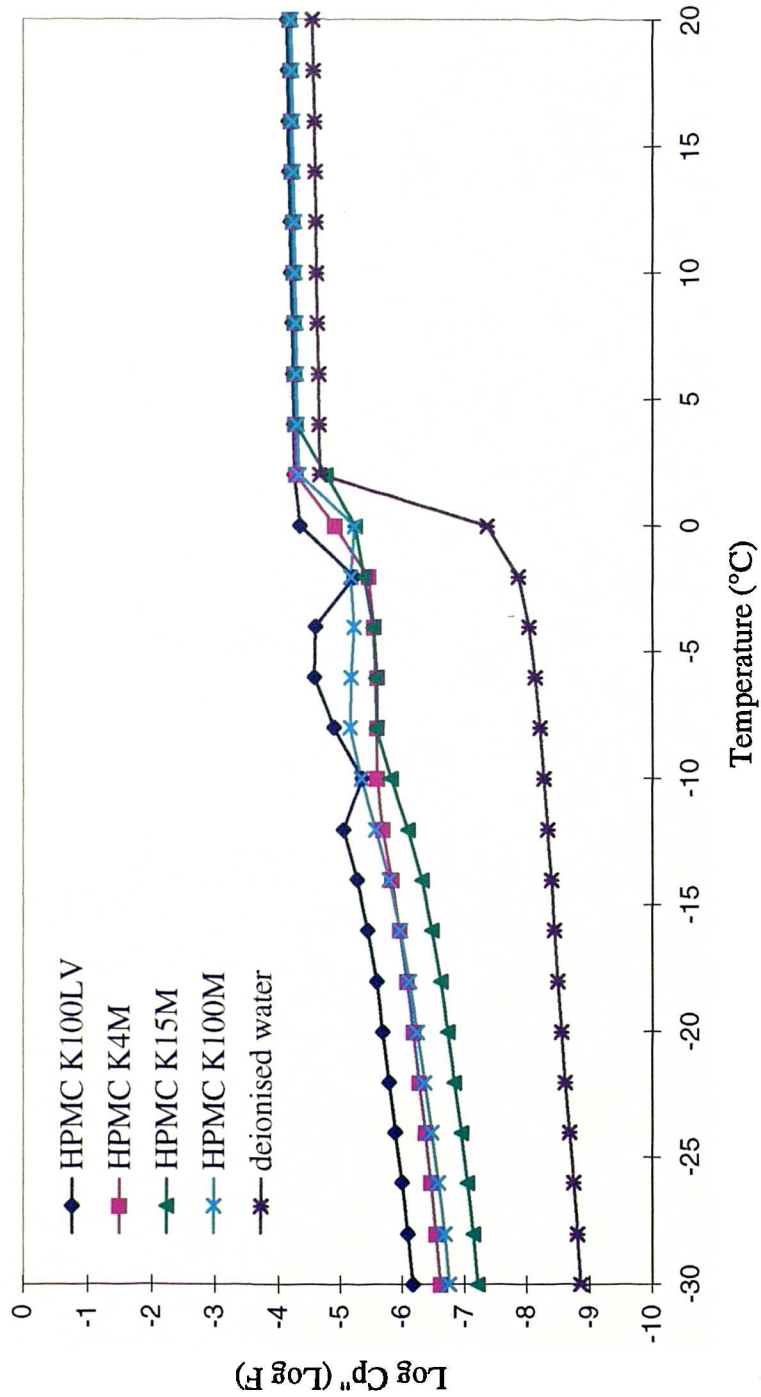


Figure 7.12 : Log Dielectric loss (Log Cp'') (Log F) against Temperature (°C) for 25% (w/w) HPMC K100LV, K4M, K15M & K100M gels and deionised water at a frequency of 1 Hz

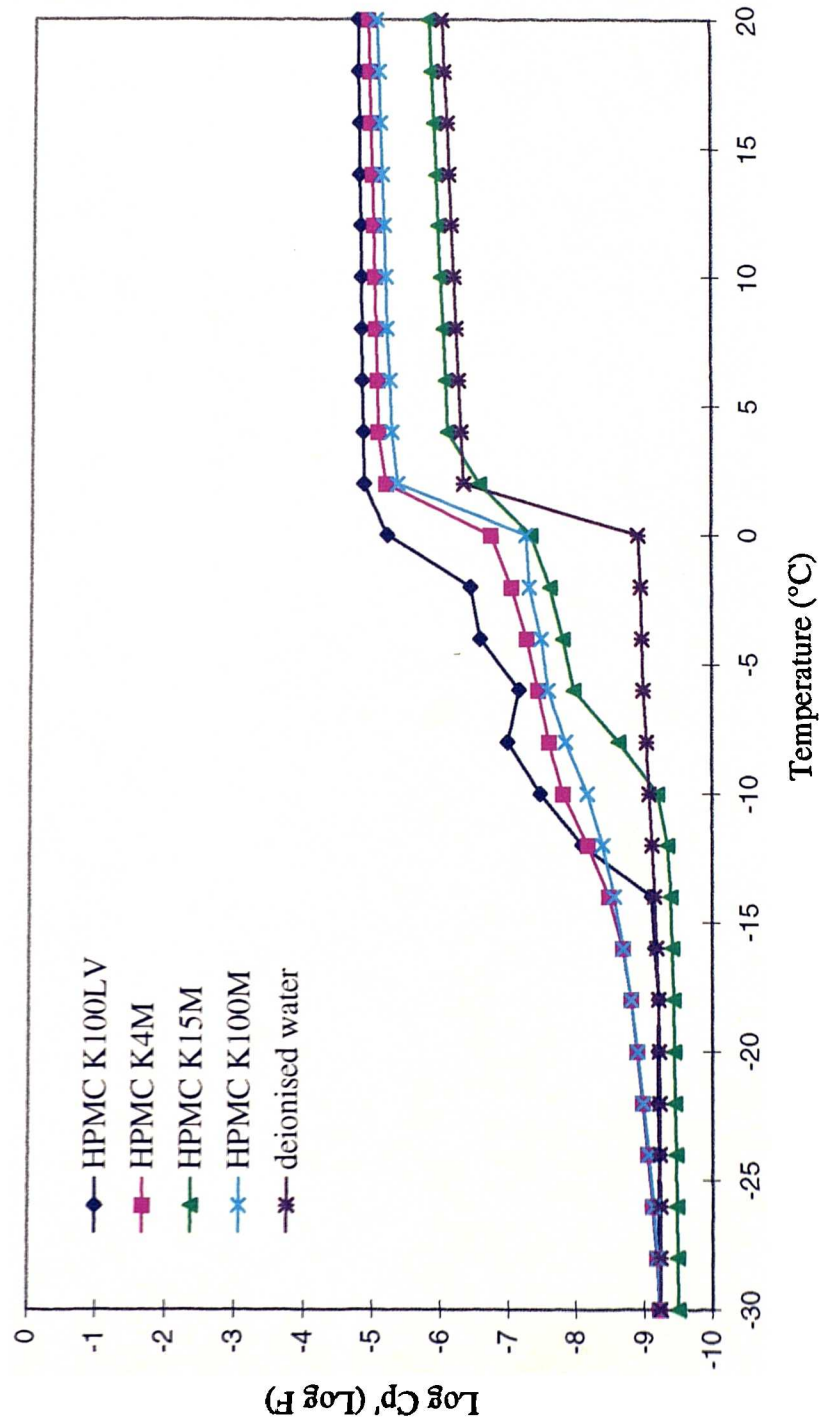


Figure 7.13 : Log Capacitance (Log Cp') (Log F) against Temperature (°C) for 25% (w/w) HPMC K100LV, K4M, K15M & K100M gels and deionised water at a frequency of 100Hz

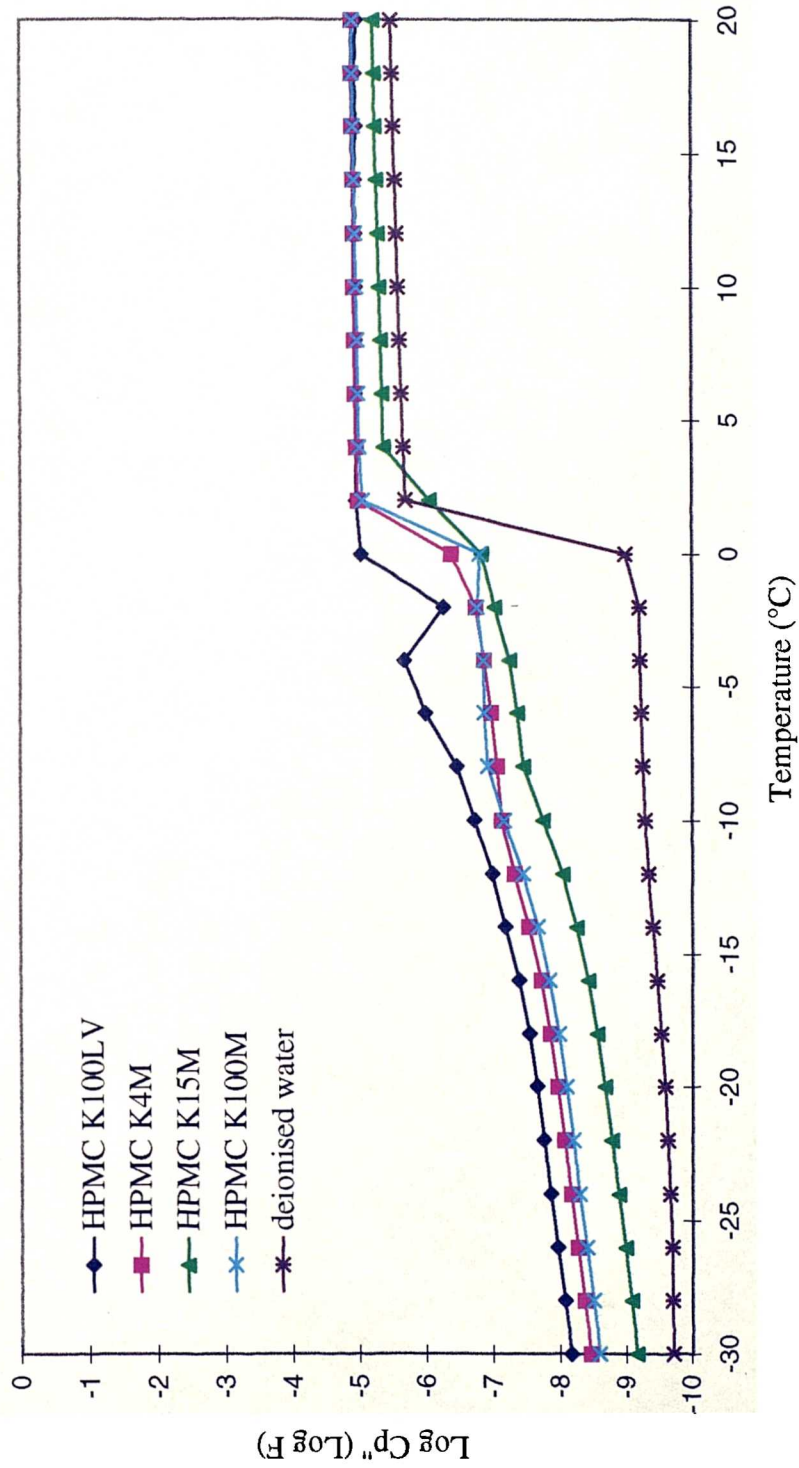


Figure 7.14 : Log Dielectric loss (Log Cp'') (Log F) against Temperature (°C) for 25% (w/w) HPMC K100LV, K4M, K15M & K100M gels and deionised water at a frequency of 100Hz

HPMC K100LV gels show a series of transitions during the melting process which are quite exaggerated in comparison with such transitions in other gels. The magnitude of the dielectric response in the gels studied vary to a large extent, but these may be related to the presence of different concentrations of ionic contaminants. For example, the increased magnitude of the responses for HPMC K100LV may be explained by the higher percentage of NaCl contamination (0.49%) than HPMC K4M (0.36%), HPMC K15M (0.16%) or HPMC K100M (0.28%) respectively (Table 2.1).

7.4.1.4 The influence of polymer substitution level on the dielectric response of cellulose ether gels

Figures 7.15-7.18 show the dielectric spectra of a series of polymers of similar molecular weight but with different substitution types and levels at frequencies of 1 and 100Hz. Their dielectric response over a temperature range of -30°C to +20°C clearly varies with polymer substitution level. The magnitude of both the capacitance and dielectric loss responses vary in a similar pattern within the polymer range studied at both frequencies. This may be related to the level of ionic contaminants in the polymers. Methylcellulose (MC) A4M has the highest level of NaCl contamination (0.75%), while HPC has no reported NaCl contamination. The magnitude of the dielectric response follows the level of NaCl contamination for each of the polymers sequentially (Table 2.1).

DSC studies on 25% (w/w) HPC gels showed that the melting of ice occurs as a single event with no evidence of any loosely bound water (section 5.4.2). The dielectric response in the region where ice melts in HPC gels shows a gradual transition in comparison with the other polymers analysed which show a two stage transition. This is well illustrated in the capacitance response at 100Hz (Figure 7.17). This may indicate, similar to DSC studies, that the distribution of water in 25% (w/w) HPC gels is different in comparison to the water distribution in gels of other substitution types studied.

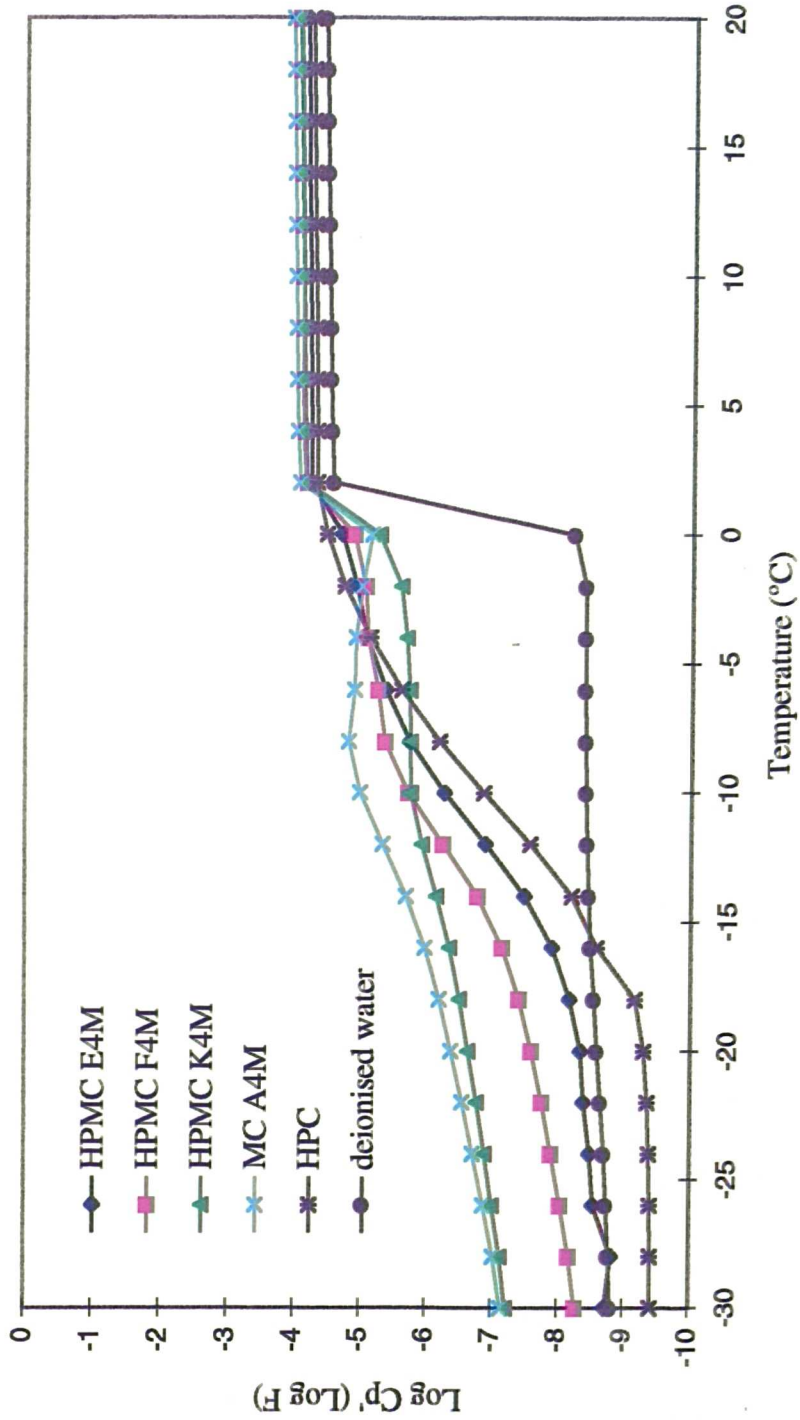


Figure 7.15 : Log Capacitance (Log Cp') (Log F) against Temperature (°C) for 25% (w/w) HPMC E4M, F4M, K4M, MC A4M & HPC gels and deionised water at a frequency of 1 Hz

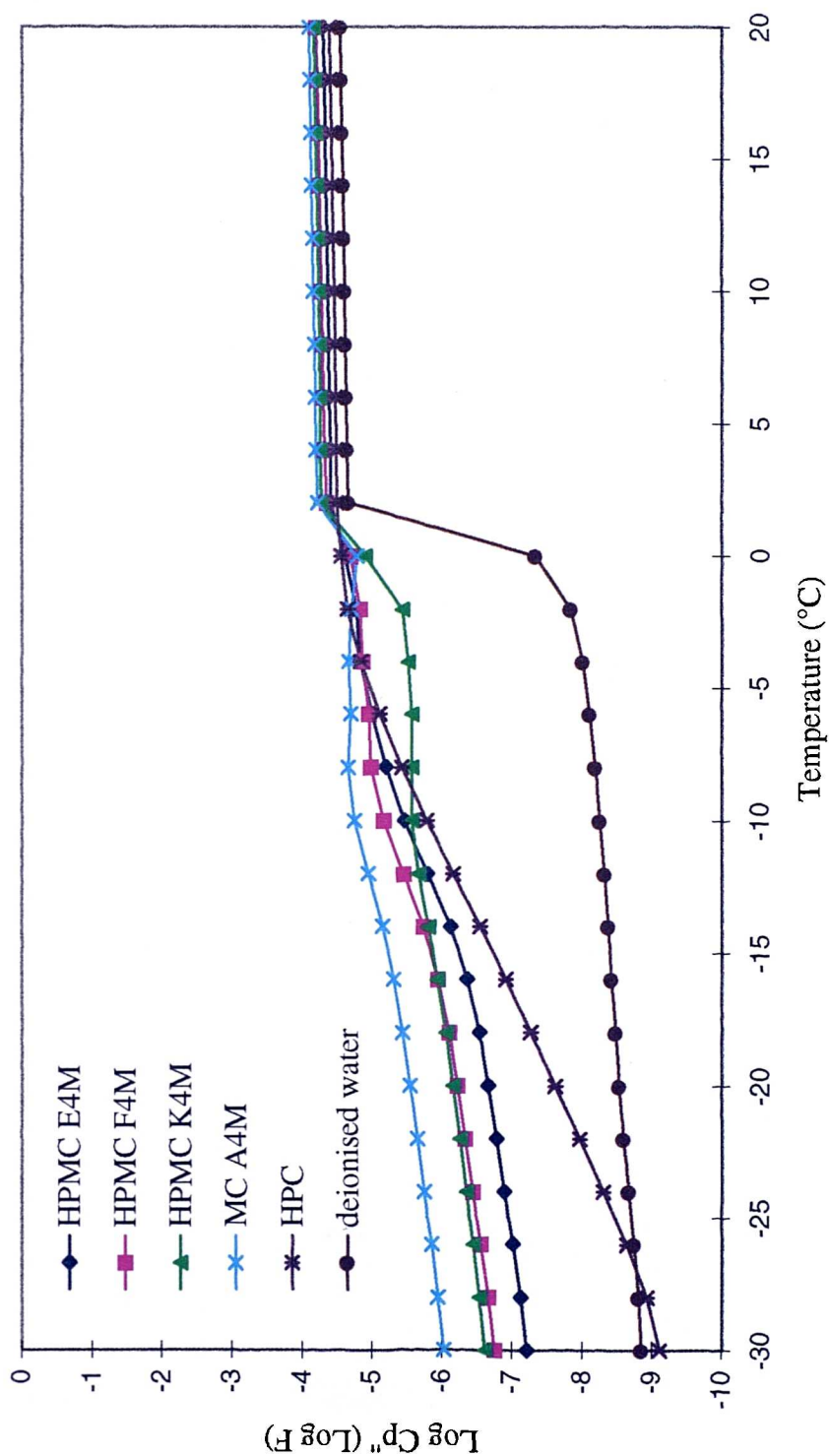


Figure 7.16 : Log Dielectric loss (Log Cp'') (Log F) against Temperature (°C) for 25% (w/w) HPMC E4M, F4M, K4M, MC A4M & HPC gels and deionised water at a frequency of 1 Hz

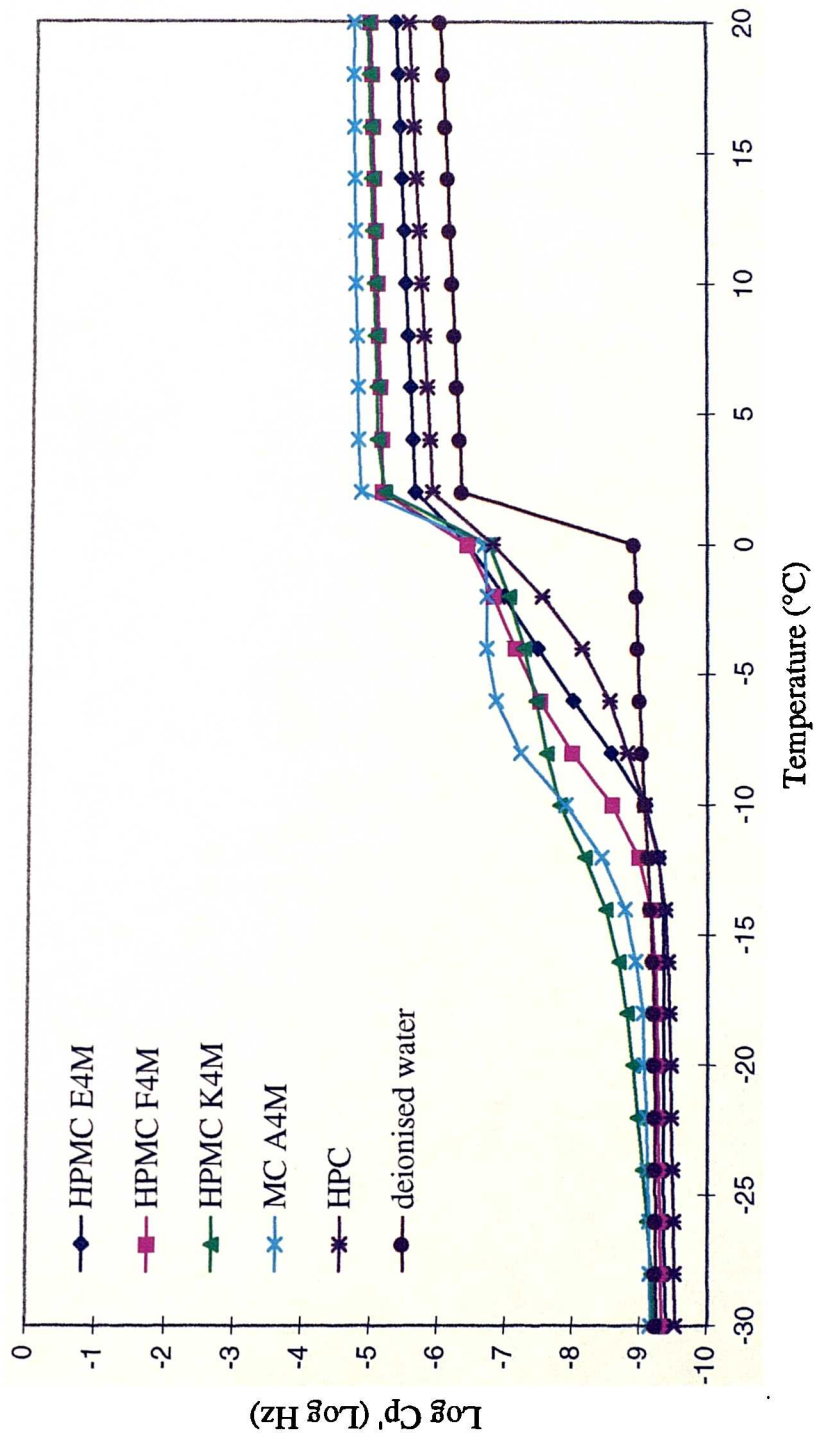


Figure 7.17 : Log Capacitance (Log Cp') (Log F) against Temperature (°C) for 25% (w/w) HPMC E4M, F4M, K4M, MC A4M & HPC gels and deionised water at a frequency of 100 Hz

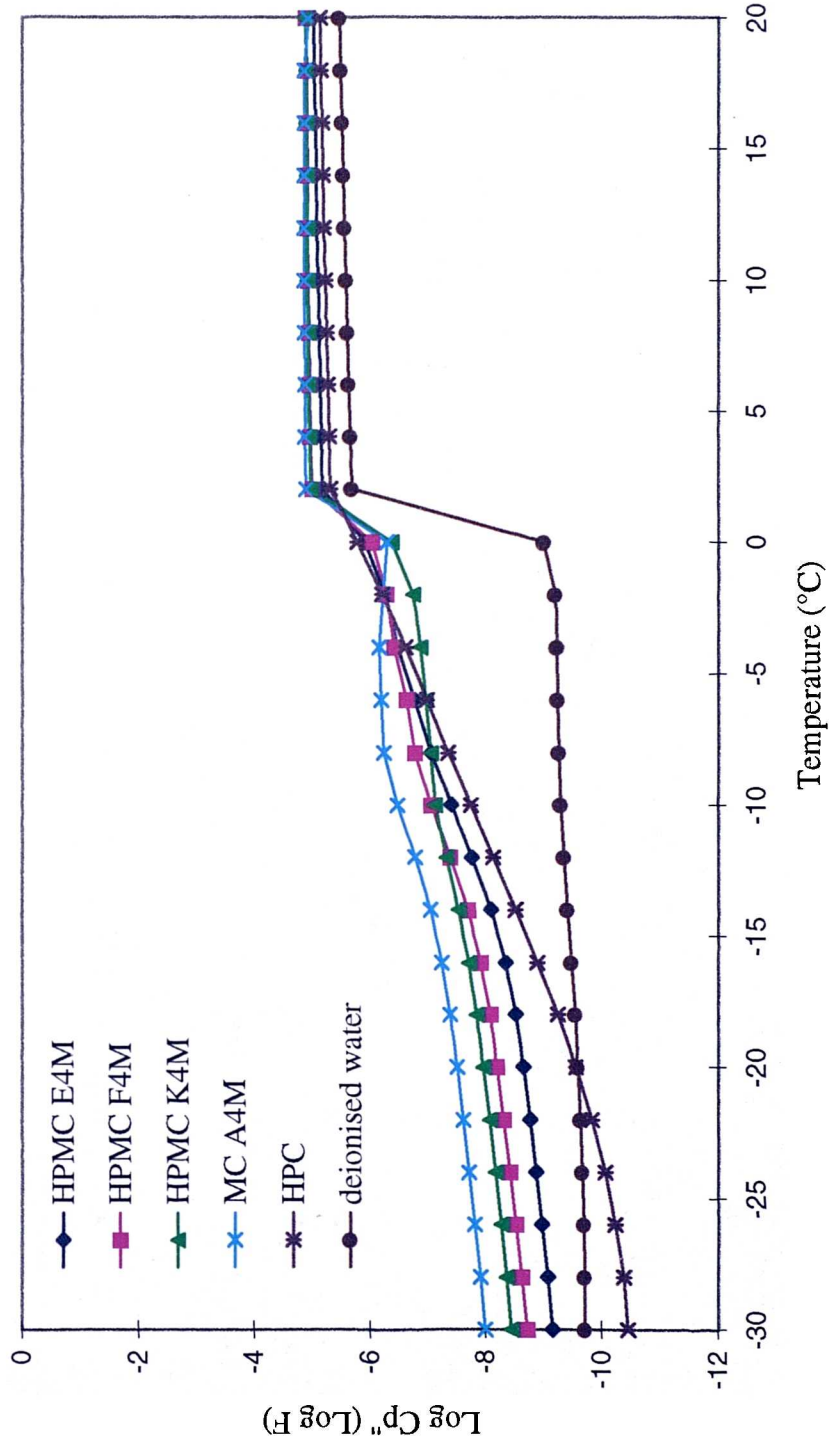


Figure 7.18 : Log Dielectric loss (Log Cp") (Log F) against Temperature (°C) for 25% (w/w) HPMC E4M, F4M, K4M, MC A4M & HPC gels and deionised water at a frequency of 100 Hz

The temperature of the sodium chloride : water eutectic is -21.2°C (Partington, 1954). It is possible that one or more of the transitions occurring below 0°C in cellulose ether gels may be due to this eutectic temperature. This is a possible explanation for the gradual dielectric response visible in the region of ice melting for HPC gels which have no reported NaCl contamination.

7.4.1.5 Effect of drug addition on the nature of the dielectric response in HPMC K15M gels

DSC studies (section 8.4.1) have shown that addition of both propranolol hydrochloride and diclofenac sodium affects the distribution of bound water within HPMC K15M gels. Addition of these drugs affected the nature of the transitions visible on the leading edge of the main endotherm for the melting of free water. Figures 7.19-7.22 show the dielectric response of deionised water and HPMC K15M gels in the absence or presence of propranolol hydrochloride (P.H.) and diclofenac sodium (DIC Na) at frequencies of 1 and 100Hz over a temperature range of -30°C to $+20^{\circ}\text{C}$. Drug addition clearly has an effect on the transitions occurring during the melting of ice in the gels. The magnitude of the dielectric response is increased in gels containing propranolol hydrochloride in comparison to the response seen in gels containing diclofenac sodium in both the capacitance and dielectric loss spectra at both frequencies studied. It is possible that the molar ratio of ionic species released upon dissociation of each drug may differ with diclofenac sodium releasing less ionic species and showing a reduced dielectric response. Figure 7.23 shows the effect of drug addition on the capacitance and dielectric loss of 25% (w/w) HPMC K15M gels in the frequency range of 10^{-2} to 10^{+7}Hz at 22°C . The nature of the dielectric response in HPMC K15M gels, which include either propranolol hydrochloride or diclofenac sodium is different, when compared to the dielectric response of deionised water or HPMC K15M gels in the absence of drug. An increase in magnitude of both the capacitance ($\text{Log } C_p'$) and dielectric loss ($\text{Log } C_p''$) values occurs in the presence of added drugs. This increase in magnitude is greater in HPMC K15M gels

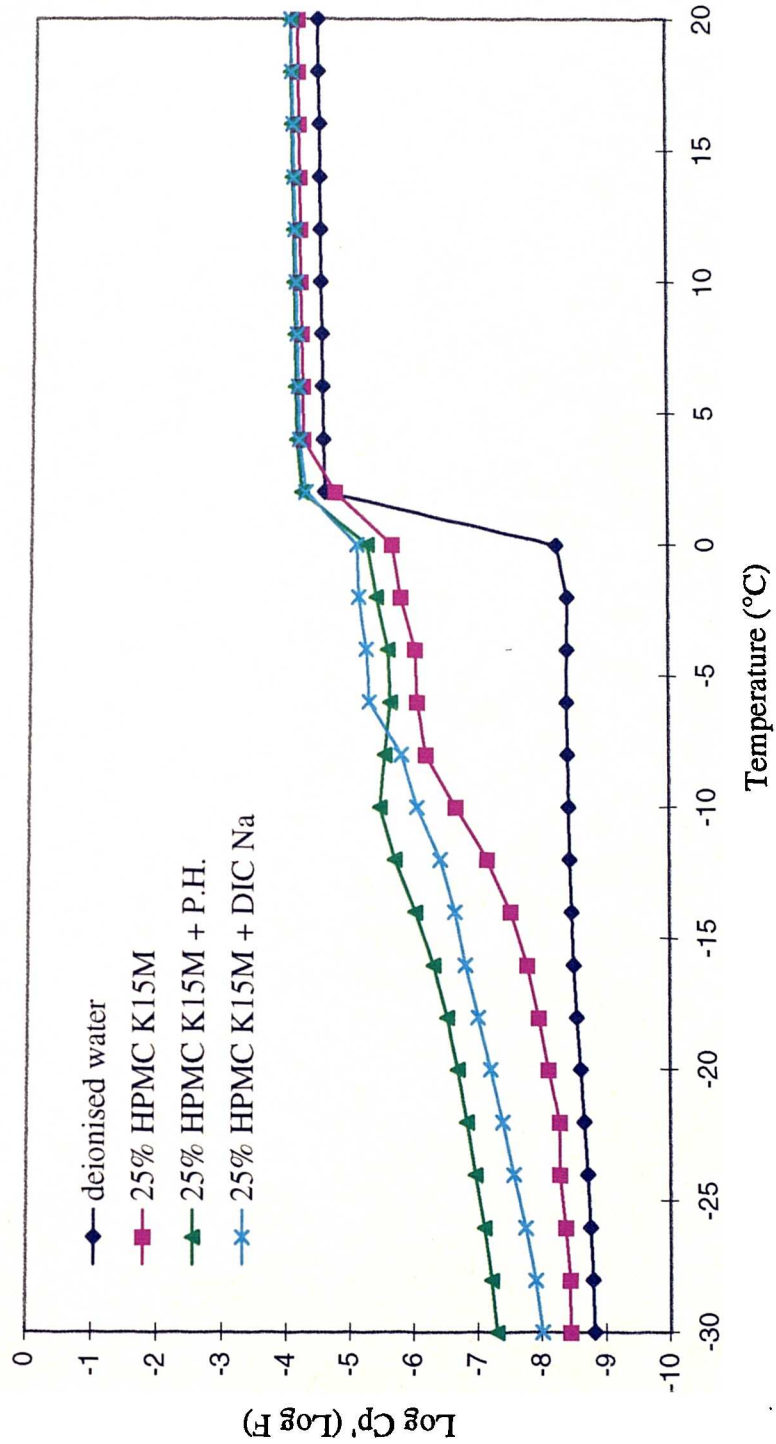


Figure 7.19 : Log Capacitance (Log Cp) (Log F) against Temperature (°C) for HPMC K15M gels alone and in the presence of propranolol hydrochloride (50mM) and diclofenac sodium (50mM) at a frequency of 1 Hz

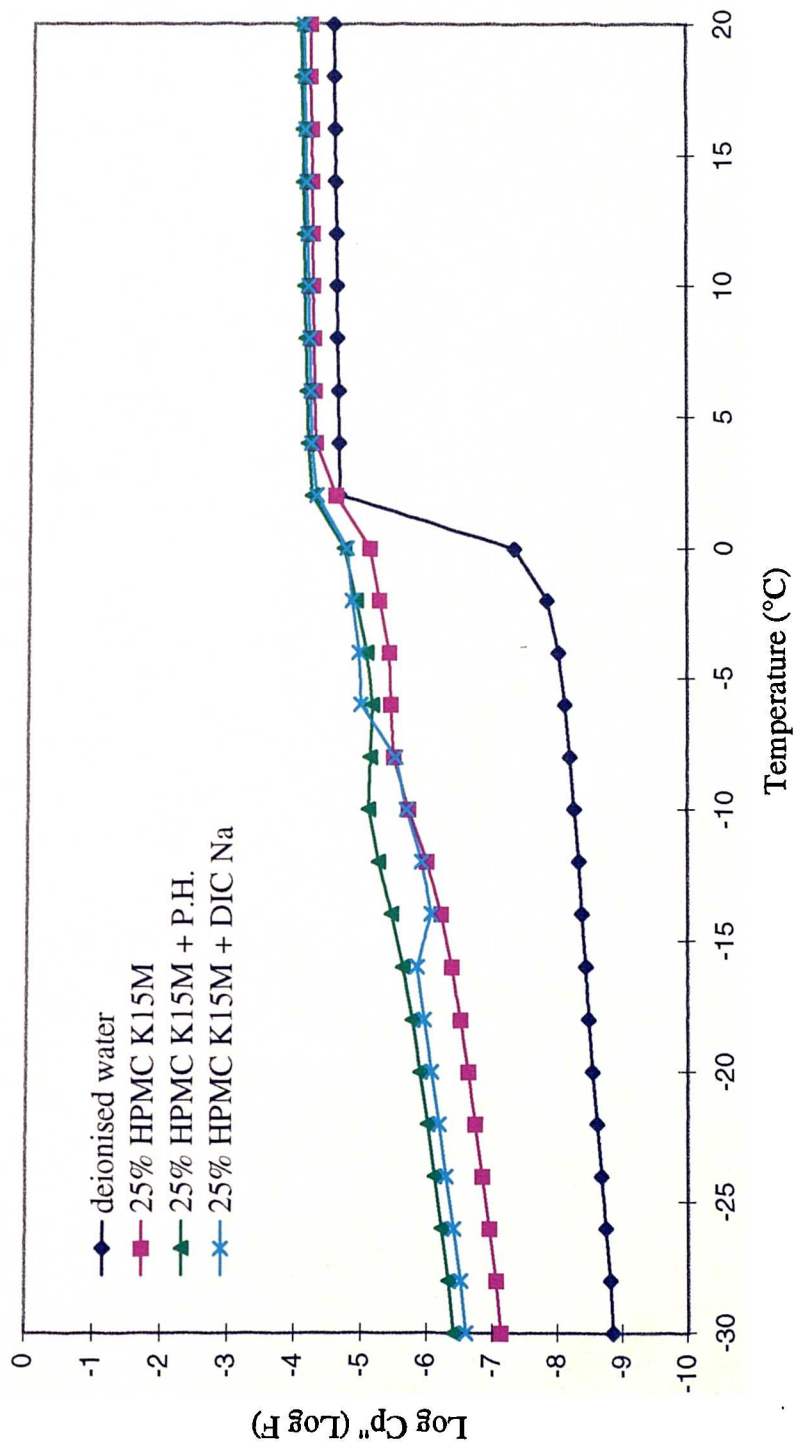


Figure 7.20 : Log Dielectric loss (Log Cp") (Log F) against Temperature (°C) for HPMC K15M gels alone and in the presence of propranolol hydrochloride (50mM) and diclofenac sodium (50mM) at a frequency of 1 Hz

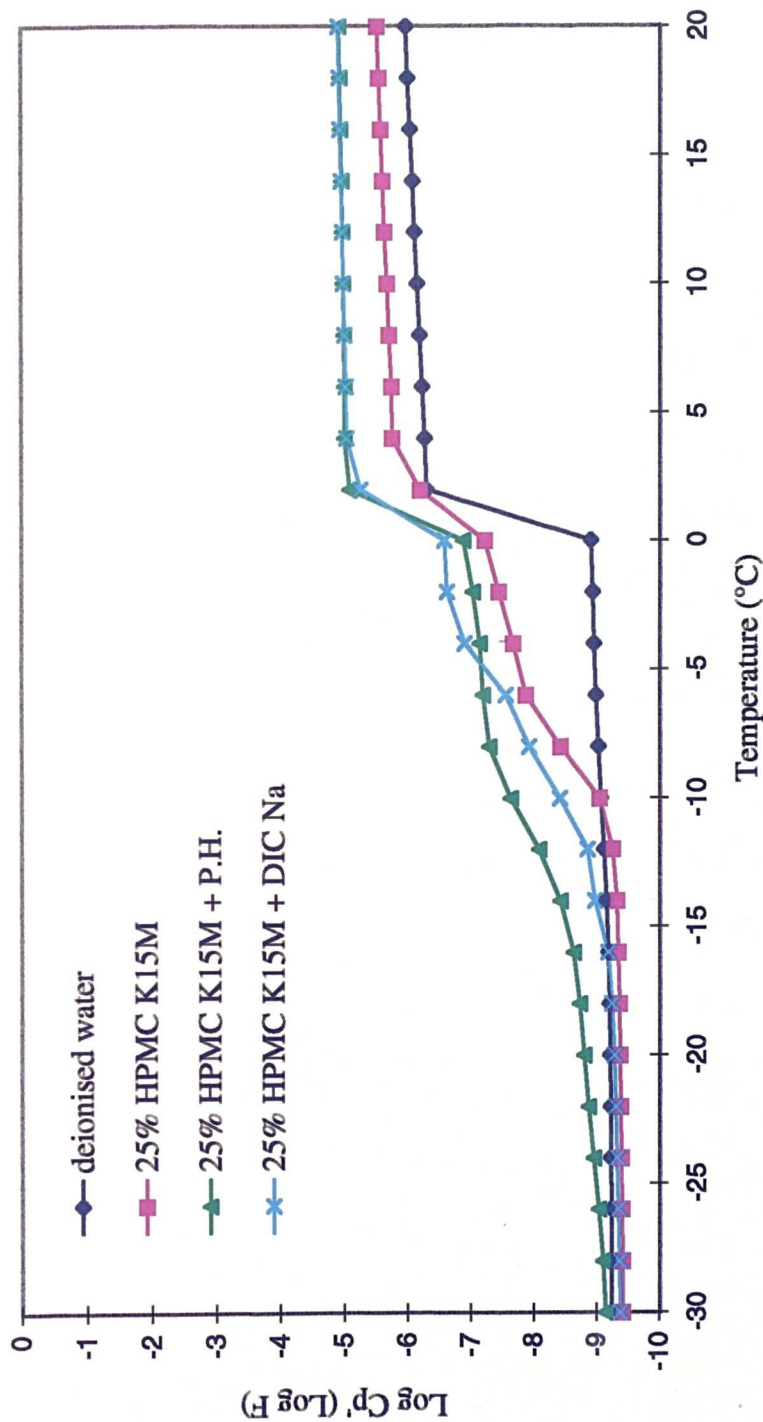


Figure 7.21 : Log Capacitance (Log Cp') (Log F) against Temperature (°C) for HPMC K15M gels alone and in the presence of propranolol hydrochloride (50mM) and diclofenac sodium (50mM) at a frequency of 100Hz

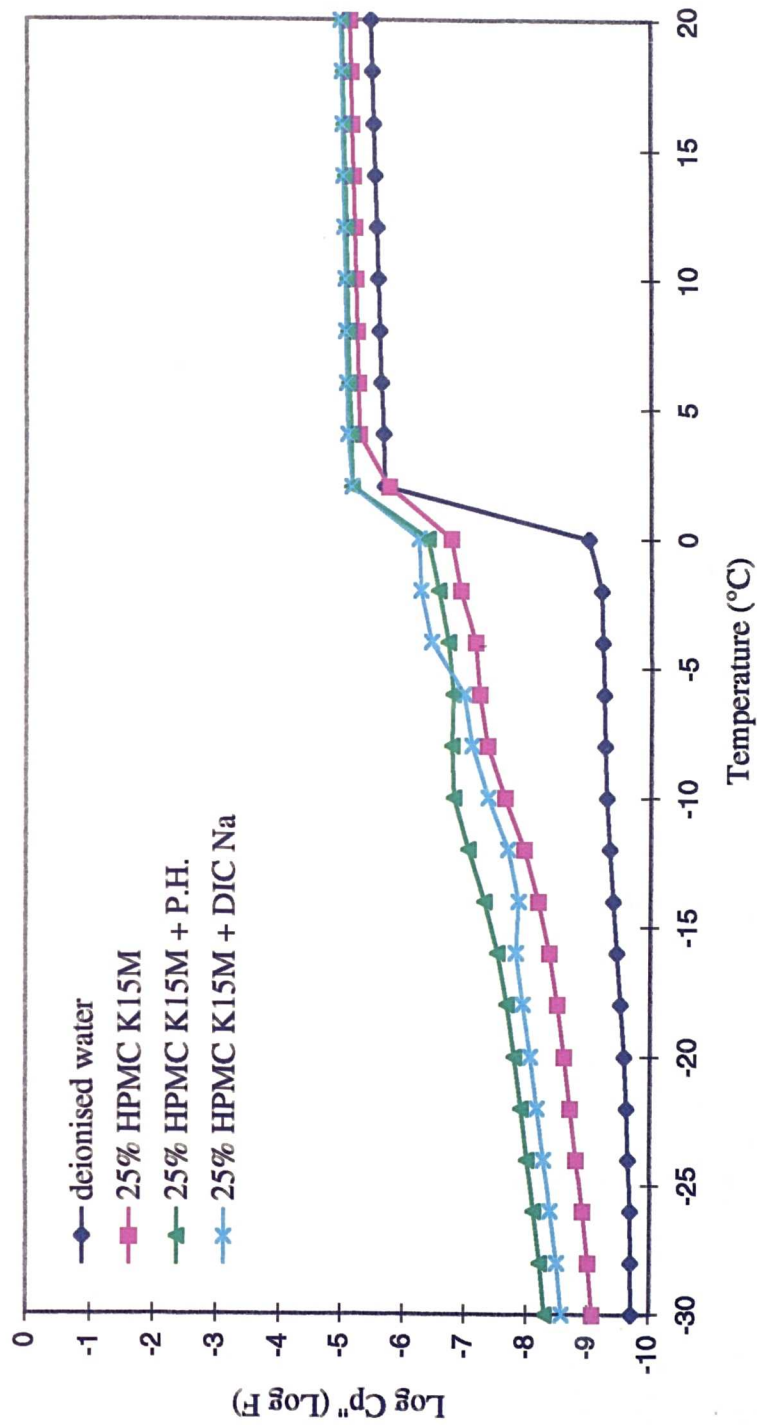


Figure 7.22 : Log Dielectric loss (Log Cp'') (Log F) against Temperature (°C) for HPMC K15M gels alone and in the presence of propranolol hydrochloride (50mM) and diclofenac sodium (50mM) at a frequency of 100Hz

containing propranolol hydrochloride which is consistent with the response previously seen in temperature scans at constant frequencies. A similar pattern is seen in Figure 7.24 which shows the effect of drug addition on the dielectric response of 25% (w/w) HPMC K15M gels in the frequency range of 10^{-2} to 10^{+7} Hz at 0°C . However, when such gel systems are analysed at -30°C as shown in Figure 7.25, the magnitude and nature of the dielectric response both changed. The magnitude of the dielectric response is reduced which is consistent with a reduction in the mobility of dipoles in the system with reduction in temperature. A peak is present at 10^3 Hz in the capacitance response of HPMC K15M gels in the presence of propranolol hydrochloride at -30°C .

Considerable potential has been highlighted in these preliminary studies on the effect of drug addition on the dielectric response of HPMC polymers and further work is required in order to comment on the patterns and transitions that occur.

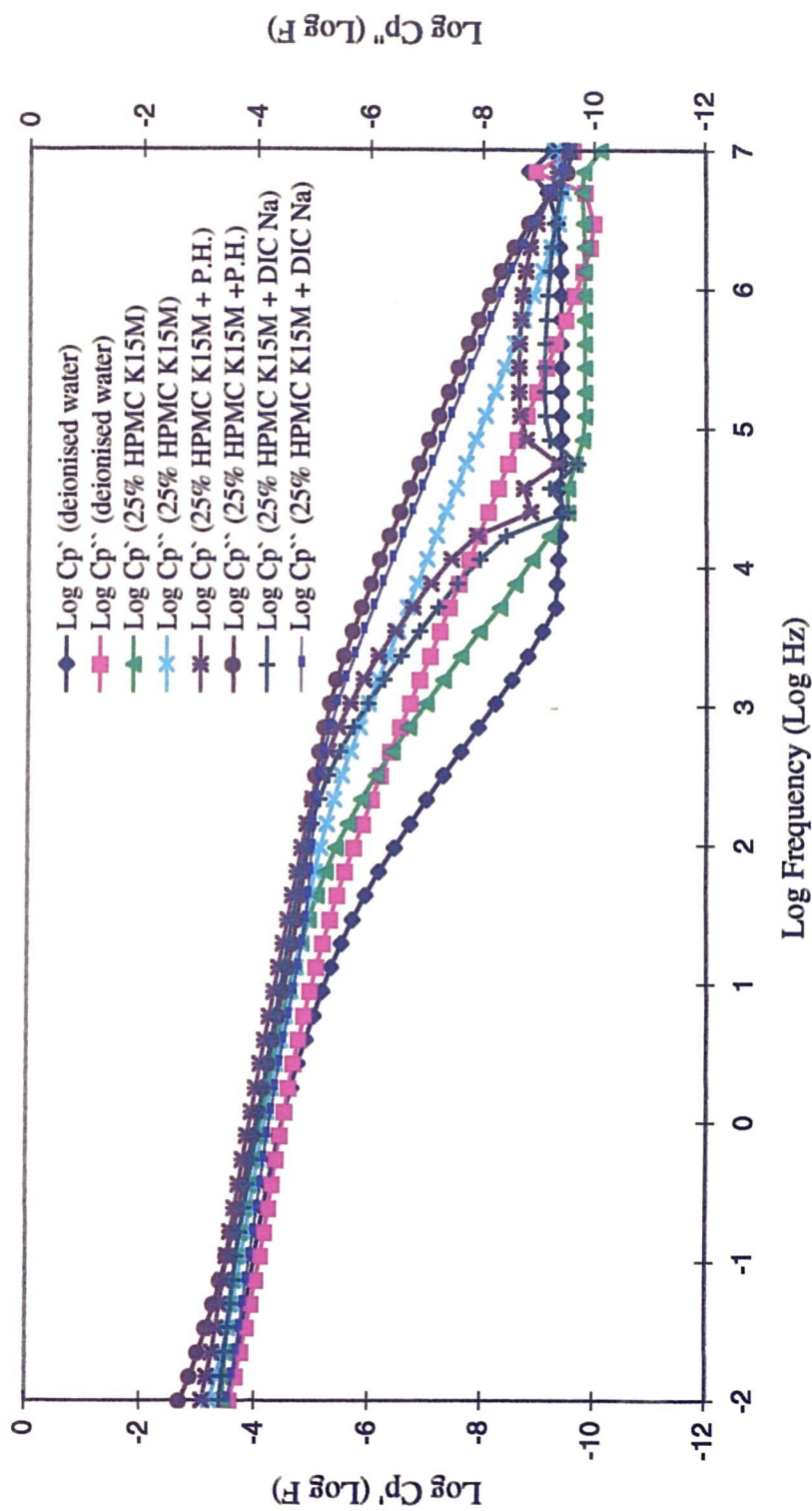


Figure 7.23 : Log Capacitance (Log Cp') and Log Dielectric loss (Log Cp'') against Log Frequency (Log Hz) for deionised water and 25% (w/w) HPMC K15M gels in the absence and presence of propranolol hydrochloride and diclofenac sodium at 22°C

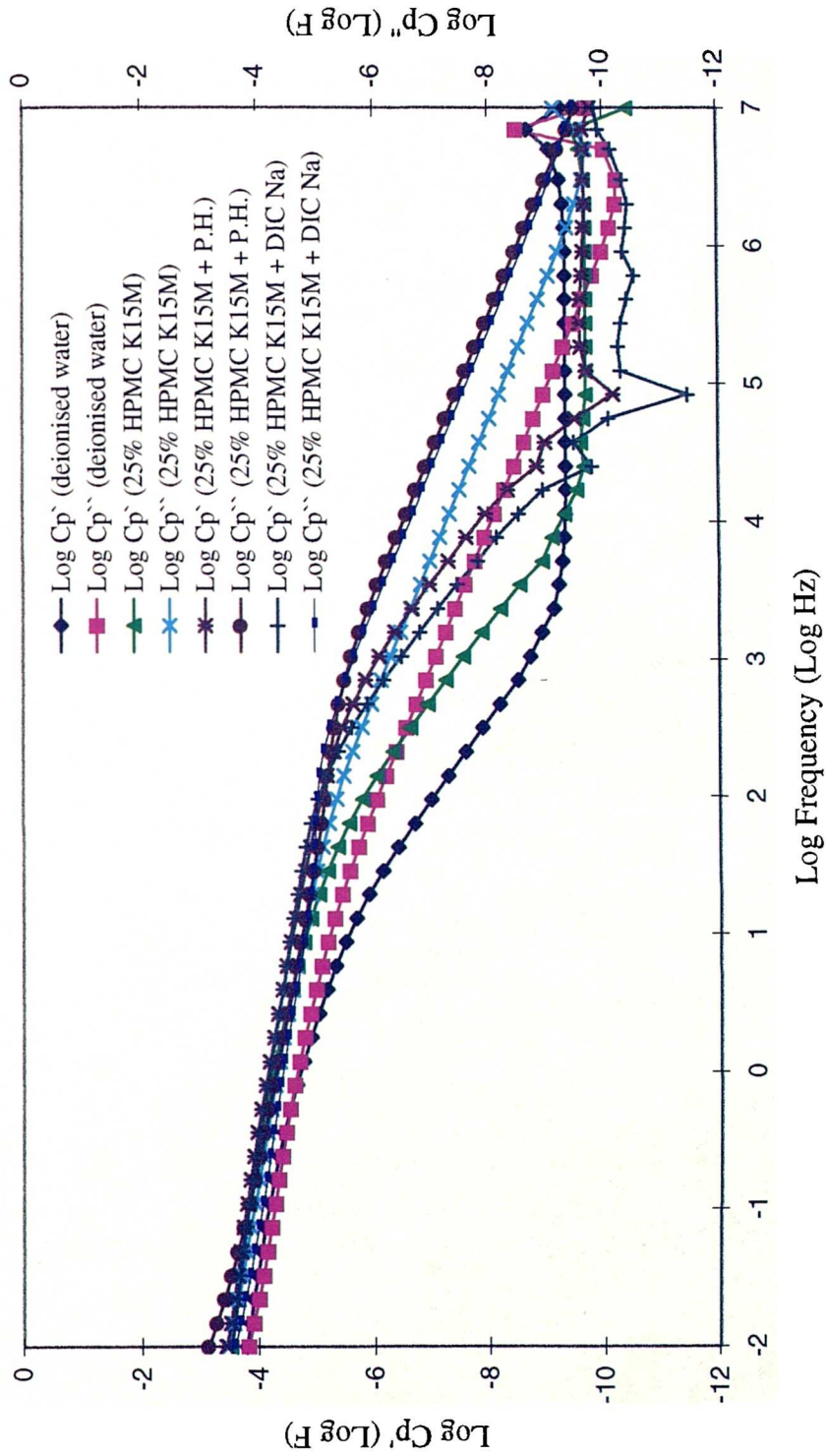


Figure 7.24 : Log Capacitance (Log Cp') and Log Dielectric loss (Log Cp'') against Log Frequency (Log Hz) for deionised water and 25% (w/w) HPMC K15M gels in the absence and presence of propranolol hydrochloride and diclofenac sodium at 0°C

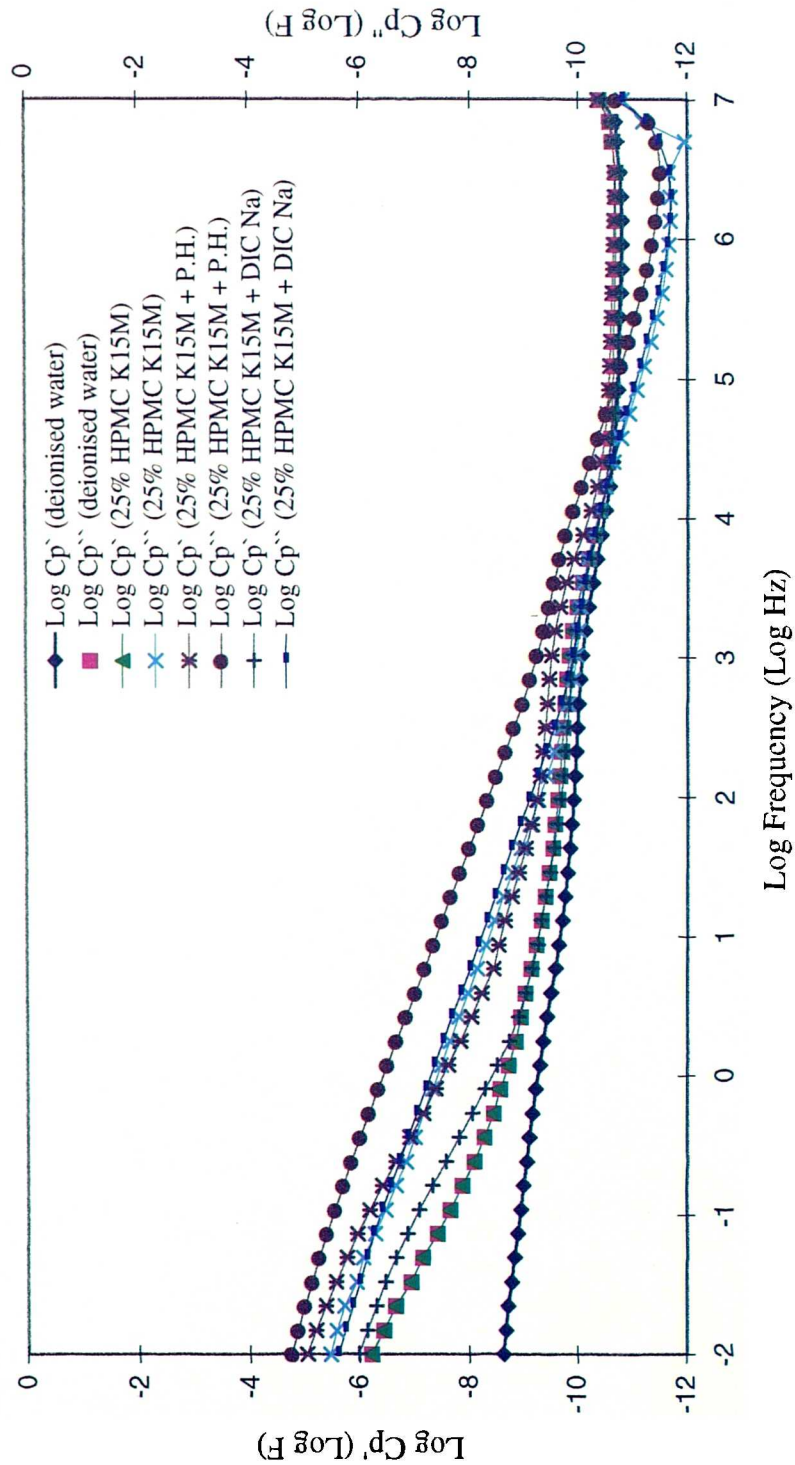


Figure 7.25 : Log Capacitance (Log Cp') and Log Dielectric loss (Log Cp'') against Log Frequency (Log Hz) for deionised water and 25% (w/w) HPMC K15M gels in the absence and presence of propranolol hydrochloride and diclofenac sodium at -30°C

7.5 Conclusions

The dielectric response of deionised water was found to be characterised by a sharp increase in both capacitance and dielectric loss at the melting point of ice (0°C) in temperature scans from -30°C to +20°C at frequencies of 1 and 100Hz. In comparison, in the presence of 25% (w/w) HPMC K15M, the dielectric response of the system was quite different. A depression in the melting point of ice seemed to occur in the presence of polymer which was reduced to -22°C and -12°C as seen in Figure 7.2 which shows the capacitance data for 25% (w/w) HPMC K15M gels at 1 and 100Hz respectively. Similar trends were observed in dielectric loss data. In DSC studies on 25% (w/w) HPMC K15M gels, water was observed to commence melting at approximately -12.5°C (Figure 5.1) for gels after 24h storage.

As well as the melting of free water, a number of other processes seemed to be occurring as indicated by the shape of the dielectric response curves. These data were found to be in agreement with findings by DSC which have identified more than one event occurring during the melting of ice in HPMC K15M gels of a similar concentration. TGA analysis of similar gel samples has shown that on heating, more than one event is visible on the TGA derivative curves. The results from all three techniques indicate the presence of more than one type of water in HPMC K15M gels.

Frequency scans from 10^{-2} to 10^{+7} Hz at temperatures of +22, 0 and -30°C showed that deionised water and gel samples scanned at -30°C gave very different dielectric behaviour compared to the response at higher temperatures. The decrease in magnitude of the dielectric response which occurs at -30°C was related to the reduction in mobility of dipoles in the system as the sample freezes.

The dielectric response of HPMC K15M gels with variation in polymer concentration was studied. A transition beginning at approximately -8.5°C became more pronounced with increase in polymer concentration. Such transitions may be related to events seen on the leading edge of the main endotherm in DSC data only in higher

concentrations of HPMC K15M gels and to events seen in TGA studies which become more pronounced with increase in polymer concentration.

The dielectric response of HPMC K-series of similar substitution levels but with increasing molecular weight at frequencies of 1 and 100Hz was studied. Both the capacitance and dielectric loss of the gel samples studied indicated that in addition to the melting of free water, other processes occurred, predicting the presence of different types of water. The dielectric response of the gels at the temperature range studied, varied with polymer molecular weight in terms of both the temperature at which melting begins in the gels and the pattern of melting. As in DSC studies where the appearance of endothermic events varied between HPMCs of different molecular weights, no specific trend was evident.

The dielectric responses of a series of polymers of similar molecular weights (4, 000-6,000 cP) but with different substitution types and levels were also found to vary.

The magnitude of the dielectric response varied according to the levels of NaCl contamination in polymers of different molecular weights and substitution levels.

Drug addition clearly has an effect on the melting of water within HPMC K15M gels as seen by the nature of the dielectric response over the low temperature range where ice melts within the gels.

Low Frequency Dielectric Spectroscopy (LFDS) studies on cellulose ether gels have provided some interesting evidence for the existence of more than one type of water within such gel systems. The results are in good agreement with thermal analysis findings on similar gel systems.

CHAPTER 8

INFLUENCE OF DRUGS ON WATER DISTRIBUTION WITHIN CELLULOSE ETHER POLYMER GELS

Chapter 8 Influence of drugs on water distribution within cellulose ether polymer gels

8.1 Introduction

The simplest form of a hydrophilic matrix (HM) tablet is made up of polymer and drug. In previous chapters, the interaction of water with cellulose ethers was studied. In this chapter, the influence of added drug on the interaction of water and cellulose ethers of different viscosity grades and substitution levels is investigated using thermal methods.

The presence of a drug in a matrix tablet may influence the way water is bound to, or taken up by the cellulose ether. The influence of drugs such as propranolol hydrochloride (a water soluble drug) on the interaction of water with polymer has been studied by DSC (Mitchell et al, 1989) and in thermal gelation or cloud-point studies (Mitchell et al, 1990a). The availability of water within the barrier gel layer plays an important part in drug movement across this barrier. Increased availability of free water (i.e. not bound to the polymer) may lead to increased drug diffusion across the gel layer.

The effect of diclofenac sodium (a sparingly water soluble drug) on polymer hydration within hydrophilic polymer matrices has been studied using cryogenic scanning electron microscopy (SEM) and has revealed that internal gel structure is modified by drug addition (Binns et al, 1990; Melia et al, 1990). In addition, it has been reported that diclofenac sodium decreases the hydration of HPMC polymers, causing the polymers to precipitate at elevated temperatures (Rajabi-Siahboomi et al, 1994).

8.1.1 Objectives

In the present study the effects of drug addition on the water distribution within a series of cellulose ethers are characterised. Initially, the nature of the interaction between propranolol hydrochloride and HPMC K15M gels was studied using a range of drug concentrations by differential scanning calorimetry (DSC). The influence of a single concentration of propranolol hydrochloride on water distribution in a series of cellulose ether polymers was similarly studied. This study was then repeated with diclofenac sodium.

Thermogravimetric analysis (TGA) was employed as a complementary thermal analysis technique to further explore the effect of both propranolol hydrochloride and diclofenac sodium on the water distribution within HPMC K15M gels.

8.2 Materials

Methocel cellulose ethers were obtained from DOW Chemical Company (see section 2.2.1; Table 2.1). The batches of HPMC K100LV (BN MM94051022K) and HPMC K15M (BN MM94112811K) were characterised. Klucel Hydroxypropylcellulose (HPC) was obtained from Hercules Limited, Aqualon Division (see section 2.1.1).

Propranolol hydrochloride and diclofenac sodium used, were as outlined in section 2.1.2.

8.3 Methods

8.3.1 Gel and solution preparation

Polymer gels containing 5-25% (w/w) polymer were prepared as outlined in section 2.2.1 to contain propranolol hydrochloride (0, 1.479 (50mM), 10, 20 and 30% w/v) or diclofenac sodium (1.59% w/v (50mM)). All gels were stored at 4-6°C for either 24 or 96h and water losses during both preparation and storage were taken into account when determining final polymer concentrations in the gels.

HPMC K15M (26.7 - 34.6% w/w) gels without any drug, HPMC K15M (29.0 - 54.0% w/w) gels containing 50mM propranolol hydrochloride and HPMC K15M (22.0 - 46.2% w/w) gels containing 50mM diclofenac sodium were prepared as outlined in section 2.2.1. HPC (21.2 - 46.5% w/w) gels containing 50mM propranolol hydrochloride and HPC (23.1 - 38.4% w/w) gels containing 50mM diclofenac sodium were prepared in a similar manner. The gels were stored overnight in sealed DSC sample pans at ambient temperatures, prior to DSC analysis.

Propranolol hydrochloride control solutions (10-30 % w/v) were prepared with gentle heat to aid dissolution. It was shown that propranolol hydrochloride was not thermolabile under such heating conditions (section 2.2.1). The solutions were stored in volumetric flasks at ambient temperatures for either 24 or 96h. After 96h, some evidence of propranolol hydrochloride recrystallization was apparent in 20 & 30% (w/v) solutions which were gently warmed to resolubilise before use. DSC analysis was carried out on these solutions (section 8.3.2).

8.3.2 Thermal Analysis

A Perkin-Elmer DSC7 (Beaconsfield, UK) with an attached liquid nitrogen based cooling accessory, controlled by a Perkin-Elmer TAC-7 was employed as described in section 2.2.2.2. Gel samples were cooled from +20°C to -60°C at a cooling rate of -10°Cmin⁻¹ and heated from -60°C to +20°C at a heating rate of +10°Cmin⁻¹ and their DSC scans were recorded.

Thermogravimetric studies were carried out on HPMC K15M gel samples (5-25% w/w; 10mg approx.) in the absence and presence of drugs on a Perkin Elmer TGA 7 as described in section 2.2.2.3. Samples were scanned at five scanning rates (+2, +5, +10, +15 & +20°Cmin⁻¹) using an open sample pan. In addition, some of the samples were analysed in vented aluminium sample pans (20µl, Perkin-Elmer). These vented pans provided a controlled release of moisture from the gel samples and were employed to further explore the evaporation of different types of water.

8.4 Results and Discussion

8.4.1 Determination of the eutectic point for the propranolol hydrochloride : water system

Figure 8.1 shows typical DSC scans of propranolol hydrochloride (P.H.) solutions and distilled water and the resultant enthalpies are listed in Table 8.1a and Table 8.1b.

Propranolol hydrochloride addition depressed the onset of the melting point of free water from $-3.2 \pm 0.26^\circ\text{C}$ (no P.H.) to $-4.35 \pm 0.38^\circ\text{C}$ (10% w/v), $-5.02 \pm 0.22^\circ\text{C}$ (20% w/v) and $-5.09 \pm 0.31^\circ\text{C}$ (30% w/v) ($n = 3$; \pm SD) after 24h storage. The reduced depression of melting point observed between 20 and 30% (w/v) propranolol hydrochloride solutions may be because solution saturation levels were approached.

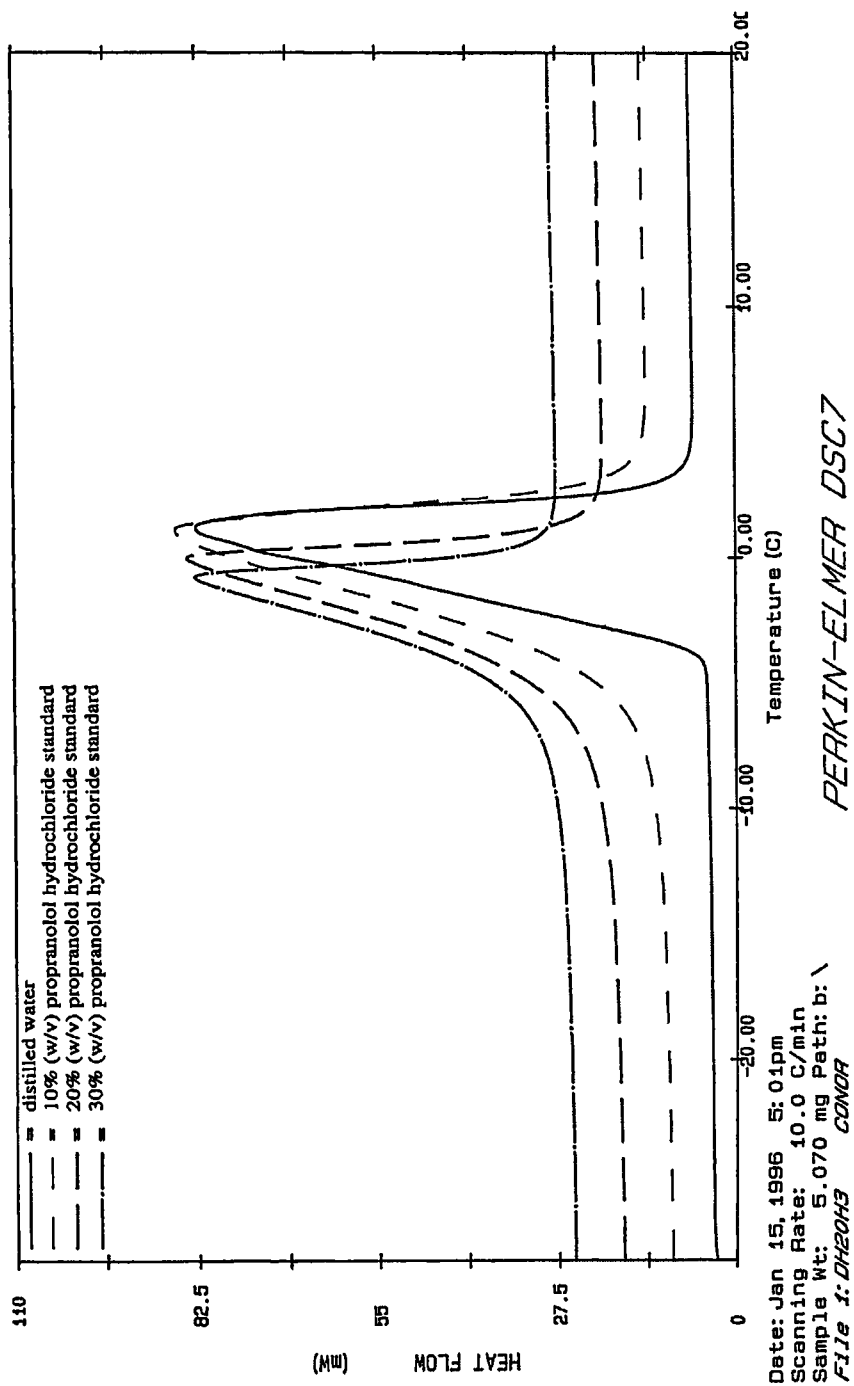


Figure 8.1 : DSC scans of distilled water and 10 - 30% (w/v) propranolol hydrochloride solutions cooled at $-10^{\circ}\text{Cmin}^{-1}$ and heated at $+10^{\circ}\text{Cmin}^{-1}$ after 24h storage

Tables 8.1a and 8.1b show that as the concentration of propranolol hydrochloride was increased, the enthalpy of melting of free water decreased after both 24 and 96h equilibration. It appears that propranolol hydrochloride addition resulted in a disruption of water distribution within the system.

An estimation of the composition of the eutectic of the propranolol hydrochloride : water system is achieved by plotting melting enthalpy (J/g) against propranolol hydrochloride concentration (% w/w) and extrapolating to zero enthalpy. In this case, the eutectic point is the lowest temperature at which a liquid phase can exist in the system; below this point, no liquid phase exists and hence zero enthalpy is achieved. By extrapolation (Figure 8.2):

t = 24h, eutectic point = 89.6% propranolol hydrochloride : 10.4% water

t = 96h, eutectic point = 60.5% propranolol hydrochloride : 39.5% water

The position of the eutectic changes between 24 and 96h storage indicating a change in equilibrium of the system during this period. Between 24h and 96h, the solutions containing higher concentrations of P.H. visibly show signs of precipitation of the drug from the solution. This undoubtedly will affect the eutectic point of the system. The propranolol hydrochloride : water system acts as a control for the propranolol hydrochloride : HPMC K15M system studied in section 8.4.2.

Ford and Mitchell (1995) have reported a value of 61.9% propranolol hydrochloride : 38.1% water for 2h old solutions and Dabbagh (1995) has reported a value of $57.8 \pm 3.1\%$ propranolol hydrochloride : 42.2% water for 24h old solutions.

Table 8.1a : Endothermic melting enthalpies (J/g) ($n = 3; \pm SD$) of polymer gels containing 0 - 30% w/w propranolol hydrochloride (P.H.) and 0 - 25% w/w HPMC K15M after storage for 24h

HPMC K15M (% w/w)	Melting Enthalpy (J/g) ($n = 3 \pm SD^a$)			
	P. H. ^b (0% w/v)	P. H. (10% w/v)	P. H. (20% w/v)	P.H. (30% w/v)
0	333 \pm 18	275 \pm 25	246 \pm 1	222 \pm 32
5	297 \pm 28	267 \pm 12	233 \pm 6	181 \pm 3
10	259 \pm 5	253 \pm 5	215 \pm 13	168 \pm 5
15	254 \pm 8	223 \pm 6	215 \pm 4	162 \pm 9
20	226 \pm 13	210 \pm 18	193 \pm 37	139 \pm 4
25	219 \pm 21	206 \pm 2	170 \pm 11	136 \pm 1

^a SD = standard deviation

^b P.H. = propranolol hydrochloride

Table 8.1b : Endothermic melting enthalpies (J/g) ($n = 3; \pm SD$) of polymer gels containing 0 - 30% w/w propranolol hydrochloride (P.H.) and 0 - 25% w/w HPMC K15M after storage for 96h

HPMC K15M (% w/w)	Melting Enthalpy (J/g) ($n = 3 \pm SD$)			
	P.H. (0% w/v)	P.H. (10% w/v)	P.H. (20% w/v)	P.H. (30% w/v)
0	333 \pm 18	261 \pm 22	236 \pm 4	160 \pm 34
5	295 \pm 7	255 \pm 7	237 \pm 13	236 \pm 22
10	278 \pm 5	248 \pm 13	209 \pm 26	198 \pm 6
15	241 \pm 14	220 \pm 3	192 \pm 18	170 \pm 20
20	199 \pm 16	201 \pm 17	182 \pm 10	157 \pm 10
25	204 \pm 7	160 \pm 3	145 \pm 25	127 \pm 25

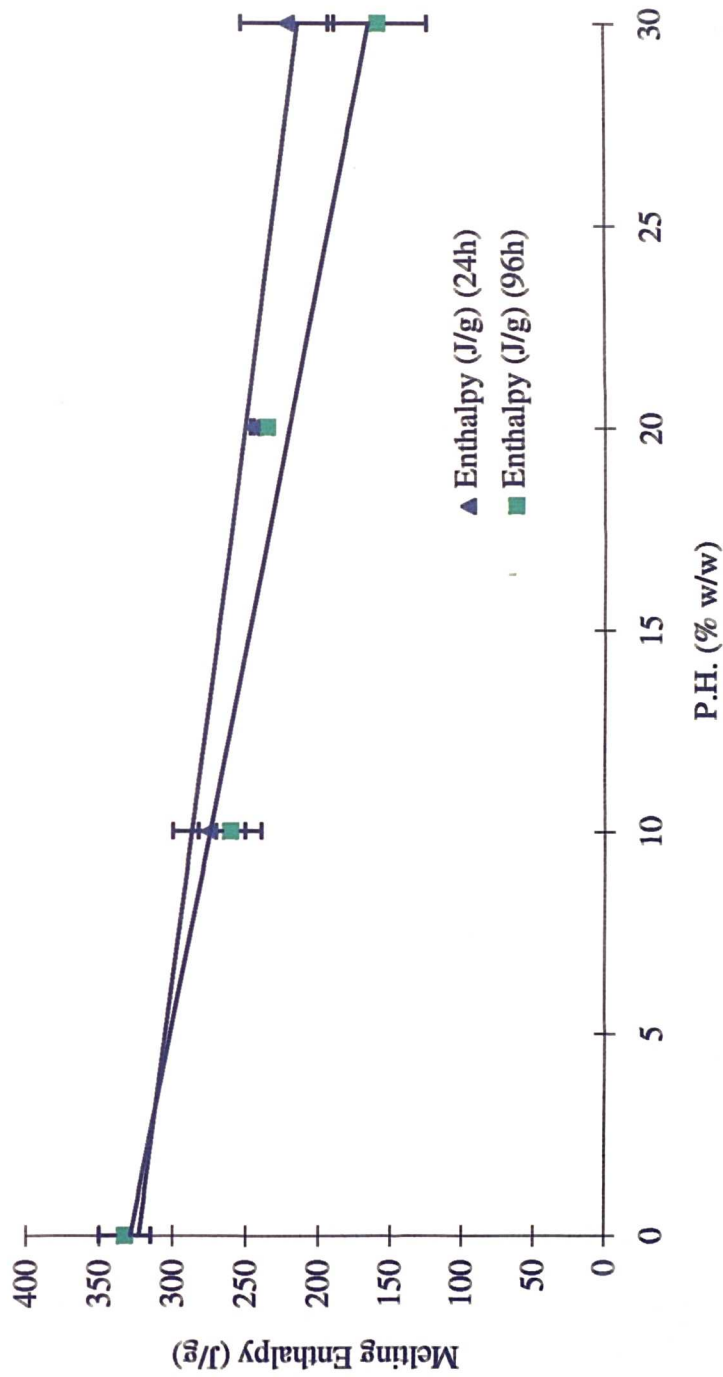
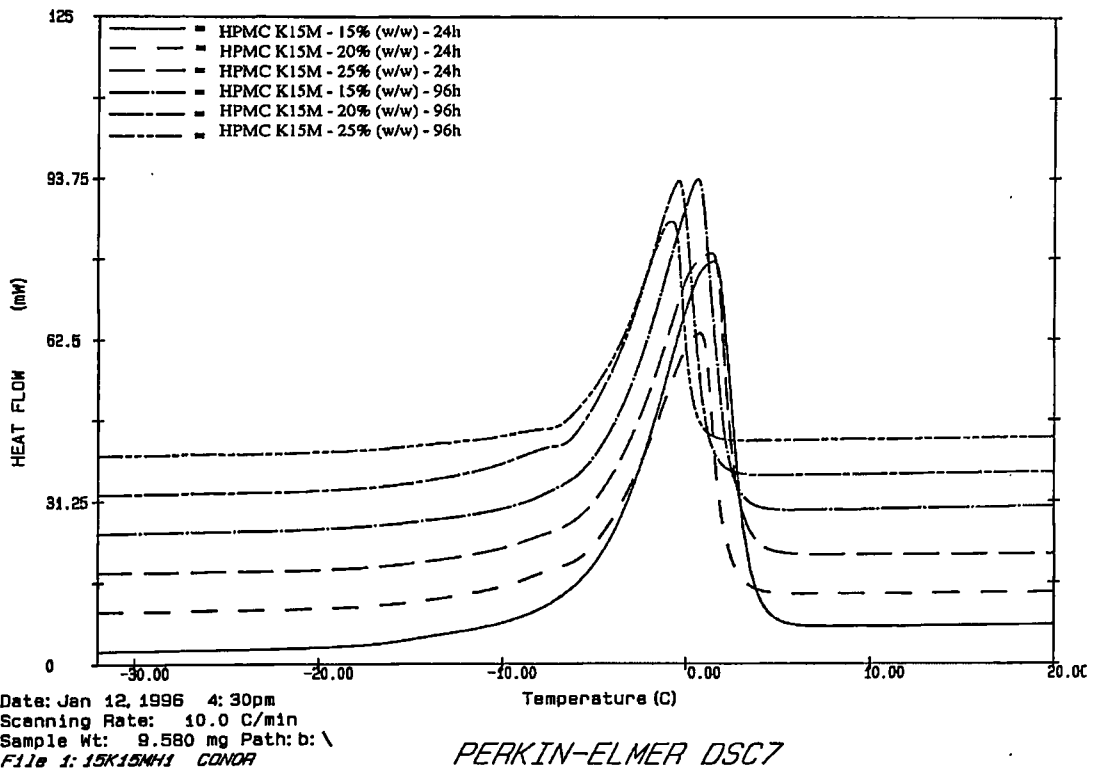


Figure 8.2 : Effect of propranolol hydrochloride concentration (P.H.) (% w/v) on the melting enthalpy (J/g) of solutions stored for 24h and 96h ($n = 3 \pm SD$)

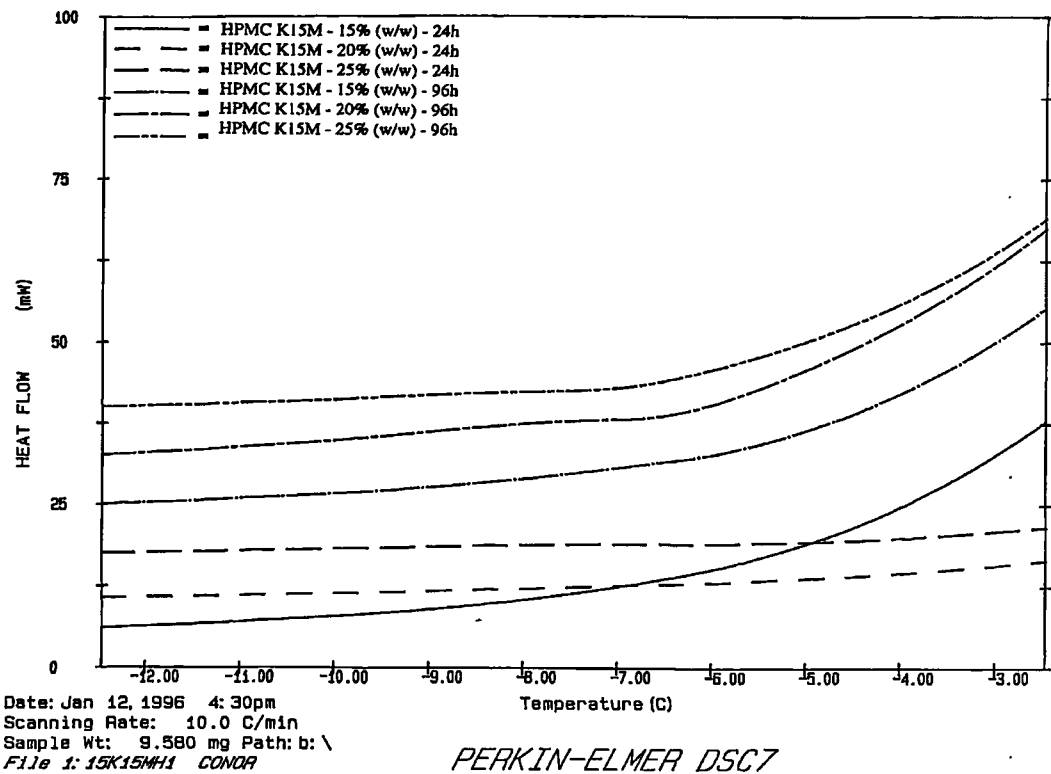
8.4.2 The influence of propranolol hydrochloride concentration on the water distribution in HPMC K15M gels

The existence of certain pre-endothermic events in HPMC K15M gels was shown in section 3.4.1. Their presence was dependent on gel concentration, gel storage time and heating and cooling rates during DSC analysis. Such events were probably related to the existence of a type of loosely bound water within HPMC K15M gels. If propranolol hydrochloride affects the water distribution within HPMC gels, it is possible that this effect may be reflected in the appearance of these pre-endothermic events.

The pre-endothermic events appeared initially in HPMC K15M gels somewhere between gel concentrations of 15 and 16.73% (w/w) polymer (section 3.4.1). Figure 8.3 shows that in HPMC K15M gels with no drug present, pre-endothermic events are not visible in 15% (w/w) gels but are visible in 20 and 25% (w/w) gels with the effect being more exaggerated after 96h storage. This may be due to increasing amounts of water binding to the polymer over an increased equilibration period. Previously (see section 3.4.1.5; table 3.4), the number of moles of bound water (BW) per polymer repeating unit (PRU) for HPMC K15M gels increased on storage from 24h (4.5) to 96h (6.5). With the addition of propranolol hydrochloride, such events are equally likely to appear after both 24 or 96h equilibration (Figures 8.4a and 8.4b) and indeed became apparent in gels containing $\geq 15\%$ (w/w) HPMC K15M and various concentrations of propranolol hydrochloride (20% propranolol hydrochloride only shown). Figure 8.5 shows much broader pre-endothermic events appearing after propranolol hydrochloride was added to HPMC K15M (25% w/w) gels. Increase in propranolol hydrochloride concentration from 10 to 30% (w/w) caused a shift of the broad pre-endothermic peak to higher temperatures.

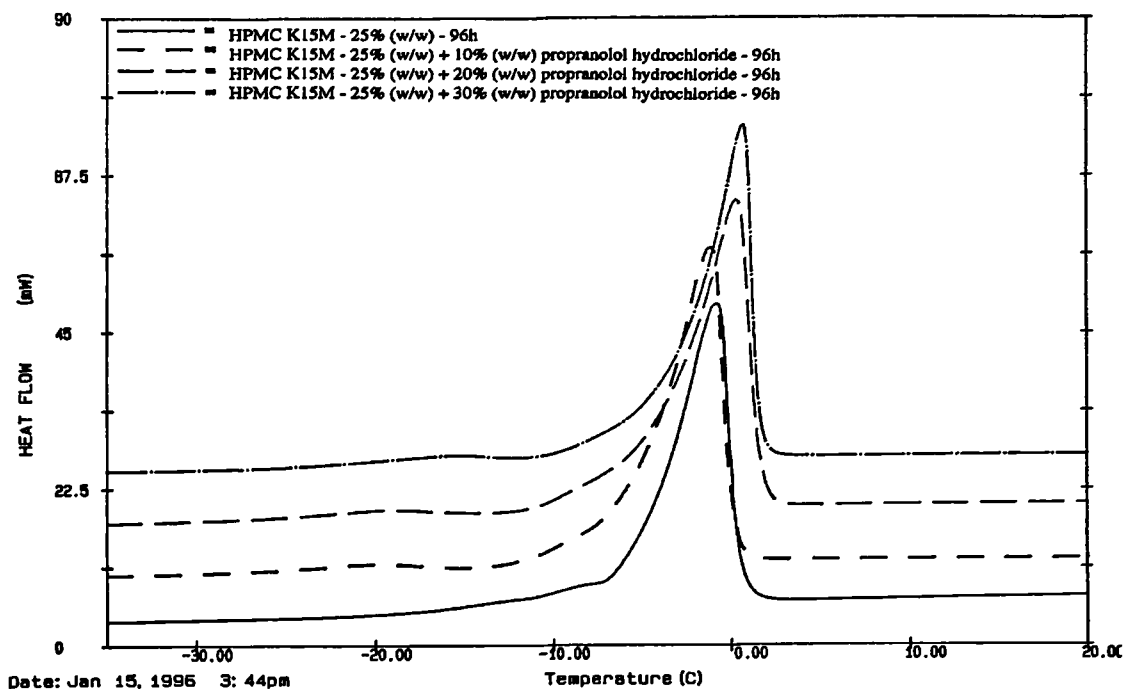


(a)



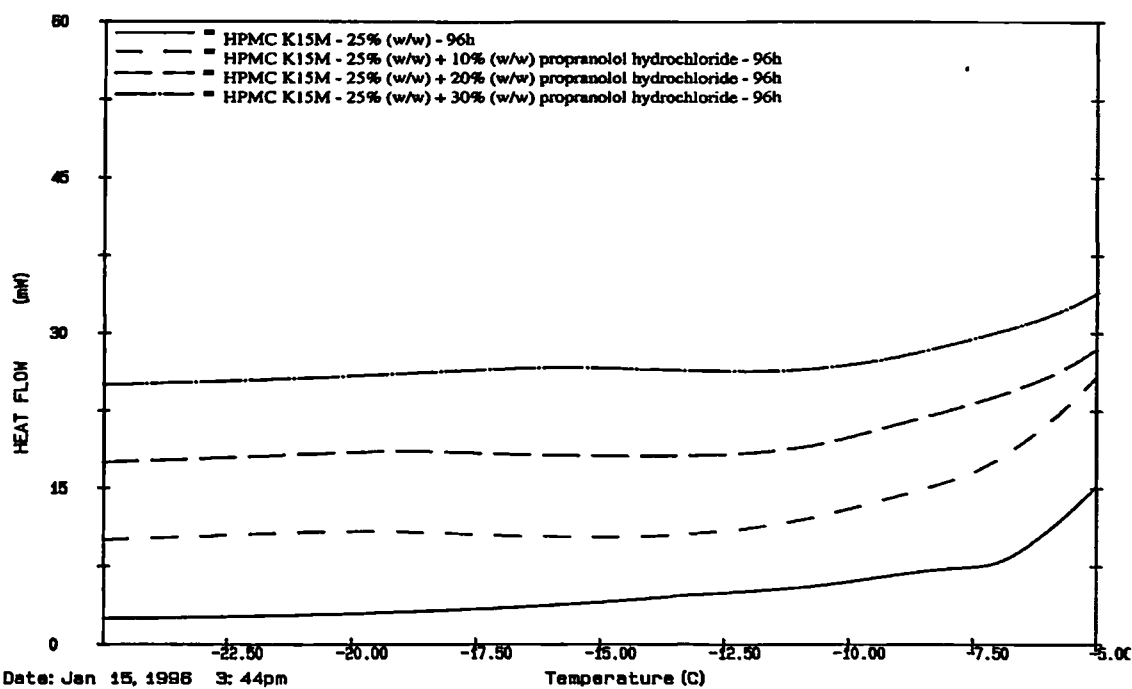
(b)

Figure 8.3 : DSC scans of 15 - 25% (w/w) HPMC K15M gels cooled at $-10^{\circ}\text{Cmin}^{-1}$ and heated at $+10^{\circ}\text{Cmin}^{-1}$ after either 24 or 96h storage
 (a) from -32.5 to $+20^{\circ}\text{C}$ (b) from -20 to -2.5°C



PERKIN-ELMER DSC7

(a)



PERKIN-ELMER DSC7

(b)

Figure 8.5 : DSC scans of 25% (w/w) HPMC K15M gels containing 0 to 30% (w/w) propranolol hydrochloride cooled at $-10^{\circ}\text{Cmin}^{-1}$ and heated at $+10^{\circ}\text{Cmin}^{-1}$ after 96h storage

(a) from -35 to $+20^{\circ}\text{C}$

(b) from -25 to -5°C

8.4.3 Quantitative analysis on the effect of propranolol hydrochloride concentration on water distribution within HPMC K15M gels

Melting enthalpies (J/g) (Table 8.1a and Table 8.1b) were plotted against concentration of HPMC K15M as previously described in section 3.4.1.3.1. Extrapolation to zero enthalpy enabled estimation of the minimum water content required to form fully hydrated gels in the presence of different concentrations of propranolol hydrochloride. The number of moles of non-freezing water per PRU were calculated using these data and the previously calculated PRU value of 189 for HPMC K15M (section 5.4.3.1; Table 5.9). Table 8.2 shows the water and polymer concentrations at zero enthalpy and the number of moles of bound water per PRU. No corrections were made for the effect of propranolol hydrochloride on the ratio of water within the gels.

Figures 8.6 and 8.7 show the effect of propranolol hydrochloride addition on the melting enthalpies of HPMC K15M gels after either 24 or 96h equilibration. As concentration of propranolol hydrochloride increases, the melting enthalpy (J/g) i.e. the amount of free water, tends to decrease. A straight line relationship is assumed between propranolol hydrochloride concentration and melting enthalpy at all concentrations. However, this is clearly not the case for 30% (w/v) propranolol hydrochloride solution after 96h storage. For propranolol hydrochloride solution (30% w/v, 96h), the amount of free water was reduced (Table 8.1b). This may have been linked to the previously mentioned precipitation of the drug at this concentration after 96h storage. This point was omitted from Figure 8.7 with extrapolation to zero enthalpy taking place through the linear portion. At other concentrations of propranolol hydrochloride studied, acceptable linear relationships were observed between melting enthalpy (J/g) and % HPMC K15M ($R^2 > 0.9$). Ford and Mitchell (1995) have previously observed a similar low enthalpy value for 30% (w/v) propranolol hydrochloride solution. Table 8.2 shows that less water is required to fully hydrate gels containing 10 and 20% w/w propranolol hydrochloride when compared with gels containing 0 or 30% w/w drug. The ability of propranolol

Table 8.2 : The effect of propranolol hydrochloride (P.H.) (0 - 30% w/w) on the distribution of water within HPMC K15M gels after 24 or 96h equilibration time

P.H. (% w/w)	Water	HPMC K15M	Moles of bound
t = 24h	(% w/w)	(% w/w)	water per PRU
0	33.6	66.4	5.3
10	13.3	86.7	1.6
20	16.0	84.0	2.0
30	38.7	61.3	6.6

P.H. (% w/w)	Water	HPMC K15M	Moles of bound
t = 96h	(% w/w)	(% w/w)	water per PRU
0	43.8	56.2	8.2
10	29.2	70.8	4.3
20	33.9	66.1	5.4
30	52.7	47.3	11.7

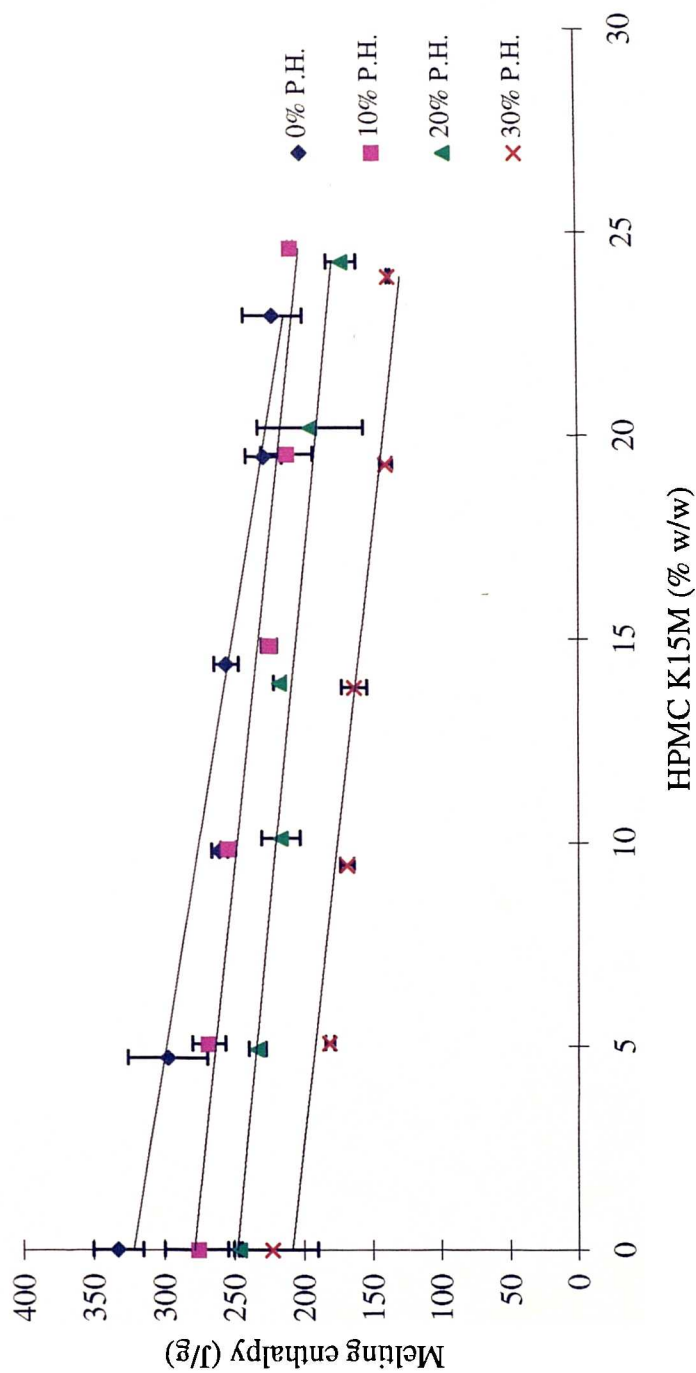


Figure 8.6 : Effect of concentration of propranolol hydrochloride (P.H.) (0 - 30% w/w) on the melting enthalpies of HPMC K15M gels (0 - 25% w/w) stored for 24h (n = 3 ± SD)

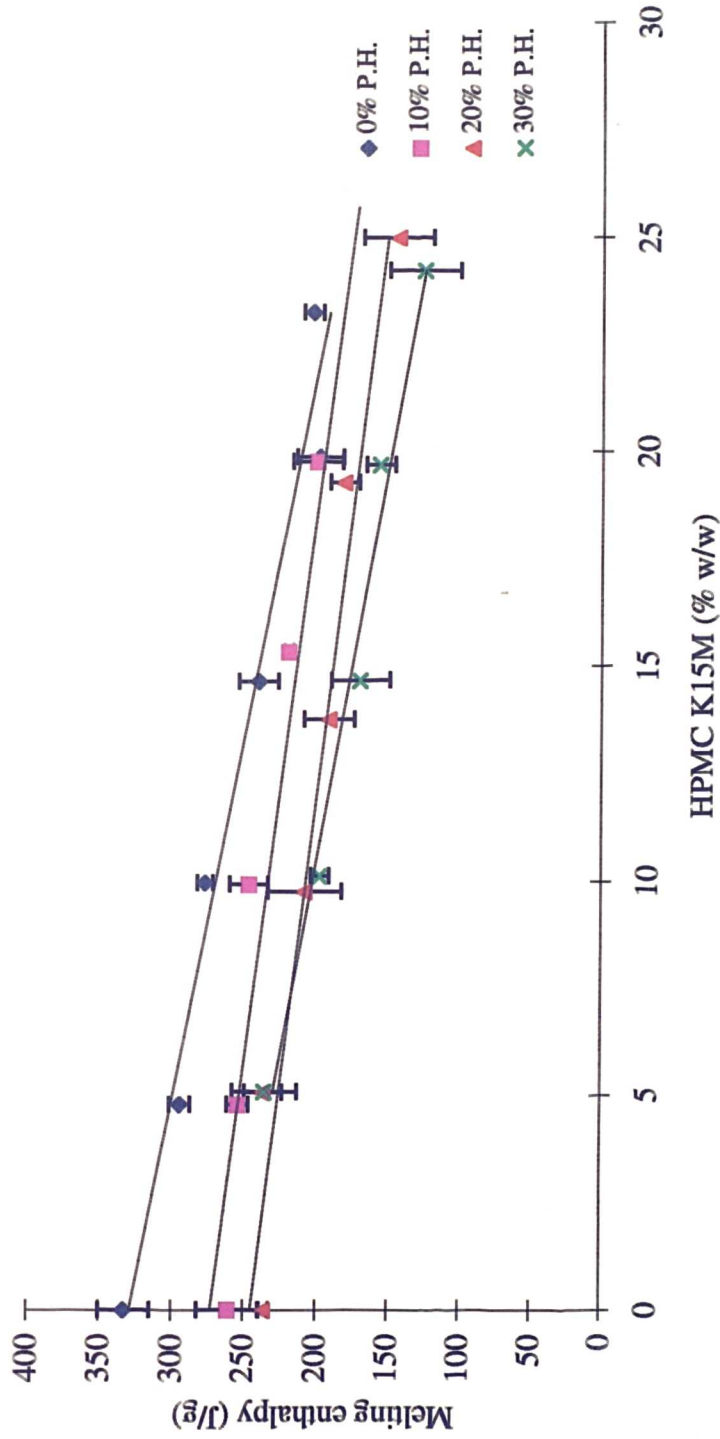


Figure 8.7 : Effect of concentration of propranolol hydrochloride (P.H.) on the melting enthalpies of HPMC K15M gels (0 - 25% w/w) stored for 96h (n = 3 ± SD)

hydrochloride to reduce the amount of water required to fully hydrate HPMC K15M gels has been previously reported (Mitchell et al, 1989). It has been suggested that propranolol hydrochloride 'salts in' the polymer i.e. makes it more soluble and therefore, the polymer requires less water to fully hydrate (Mitchell et al, 1993c).

8.4.4 Effect of propranolol hydrochloride (50mM) and diclofenac sodium (50mM) on water distribution in cellulose ether polymer gels

The effects of polymer molecular weight and substitution type on the nature of the thermal events occurring on the leading edge of the main endotherm for the melting of free water were described in sections 5.4.1 and 5.4.2. The effect of propranolol hydrochloride (10 - 30% w/w) on such events was described for HPMC K15M gels in section 8.4.2. The effect of 50mM of propranolol hydrochloride and diclofenac sodium on pre-endothermic events in a range of polymers of varying molecular weight (HPMC K-series) and a range of polymers with similar viscosity's (3,500 - 6,000 cP) but different substitution types (HPMC E4M, F4M, MC A4M and HPC), is examined in this section.

A single concentration of propranolol hydrochloride (50mM) was incorporated into cellulose ether gels as outlined in section 8.3.1. This concentration is equivalent to 1.479 (% w/w) drug and was chosen so that an equimolar amount of a poorly water soluble drug, diclofenac sodium, could be incorporated within polymer gels for comparison purposes. Diclofenac sodium (50mM) reaches its saturation solubility above 50mM concentration (1.59% w/w).

Thermal analysis was carried out after 24h equilibration time as described in section 8.3.2.

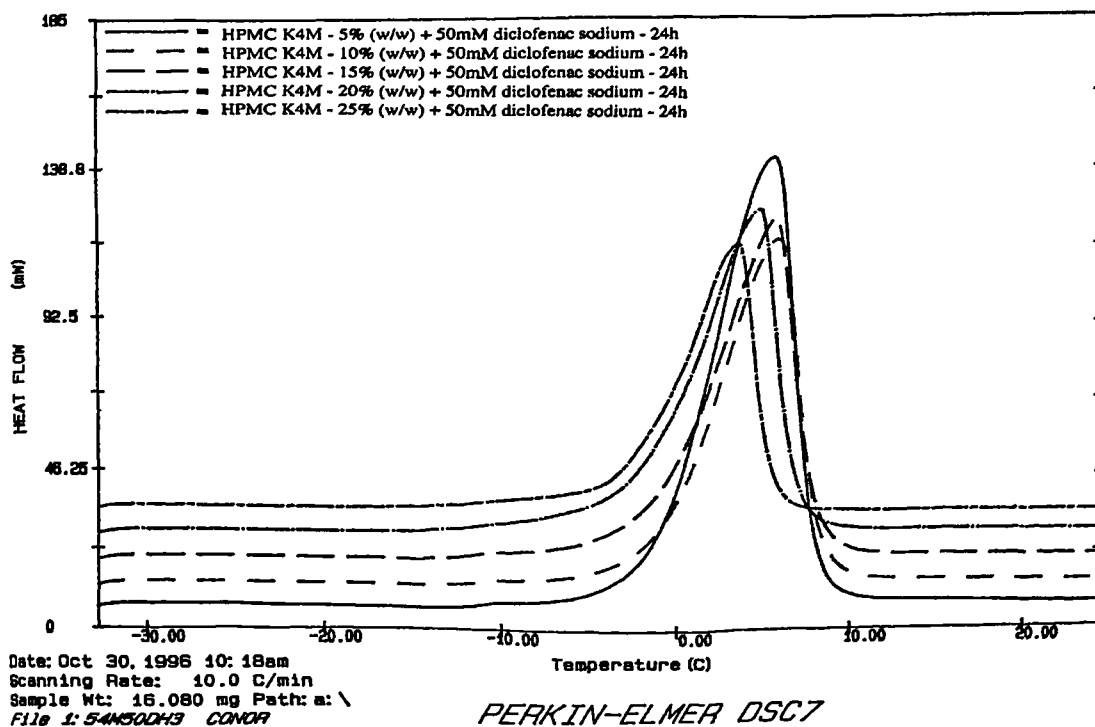
8.4.4.1 Influence of propranolol hydrochloride and diclofenac sodium on the thermal events occurring within a series of cellulose ether polymers of varying molecular weight

In the absence of drug, pre-endothemic events were present in HPMC K4M and HPMC K100M gels (15, 20 and 25% w/w) after 24h storage (section 5.4.1). Incorporation of 50mM of propranolol hydrochloride did not affect the appearance of such events in HPMC K4M gels. However, in HPMC K100M gels, pre-endothemic events were visible only in 20 and 25% w/w gels after 24h.

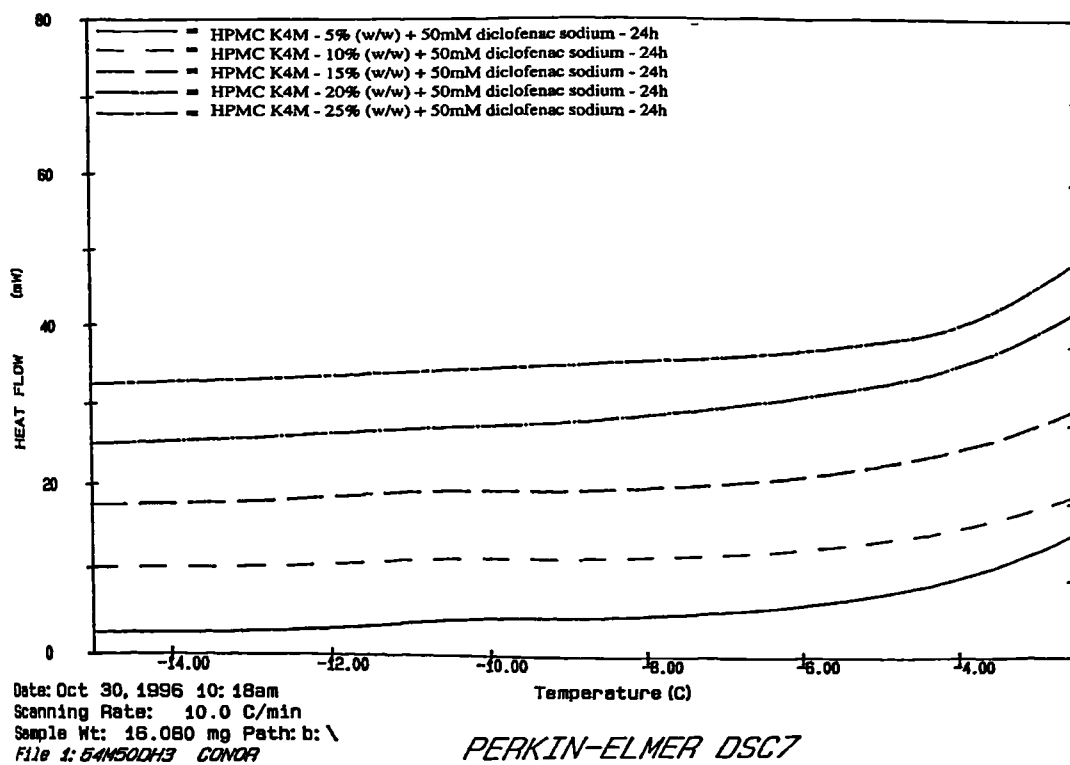
In the absence of drug, pre-endothemic events were present in 20 and 25% (w/w) HPMC K100LV and HPMC K15M gels after 24h storage (section 5.4.1). The addition of propranolol hydrochloride did not affect the appearance of such events in either HPMC K100LV and HPMC K15M gels after 24h, with pre-endothemic events remaining visible in both 20 and 25% (w/w) gels, for each polymer.

Propranolol hydrochloride concentration influenced the thermal events in HPMC K15M gels (section 8.4.1) where pre-endothemic events were visible in 15% (w/w) gels, as well as 20 and 25% (w/w) gels after 24h storage when 10, 20 or 30 % (w/w) propranolol hydrochloride was added to the gels. However, no pre-endothemic events were seen in 15% (w/w) gels after addition of 50mM of propranolol hydrochloride. This may have been related to the low concentration of the drug.

Figure 8.8 shows the influence of diclofenac sodium on the appearance of pre-endothemic events in 5 - 25% (w/w) HPMC K4M gels which is representative of other polymers studied. After 24h equilibration, pre-endothemic events were visible in all HPMC K-series studied here, at each concentration. It is hypothesised that diclofenac sodium causes the polymer to 'salt out,' making it less soluble and requiring more water to bind to the polymer to keep it in solution. Therefore there is more loosely bound water



(a)



(b)

Figure 8.8 : DSC scans of 5 - 25% (w/w) HPMC K4M gels containing 50mM of diclofenac sodium cooled at $-10^{\circ}\text{Cmin}^{-1}$ and heated at $+10^{\circ}\text{Cmin}^{-1}$ after 24h storage (a) from -32.5 to $+22.5^{\circ}\text{C}$ (b) from -15 to -2°C

in the system. It is possible that this loosely bound water appears in DSC scans and may explain the appearance of these pre-endothemic events.

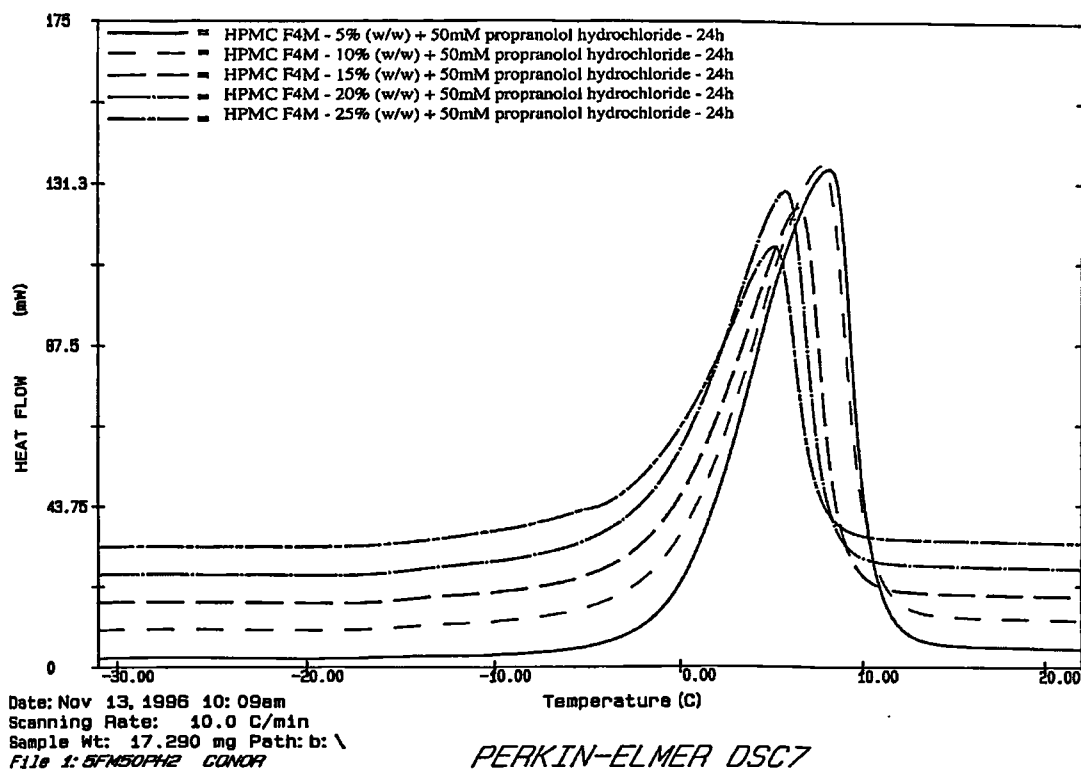
8.4.4.2 Influence of propranolol hydrochloride and diclofenac sodium on the thermal events occurring within a series of cellulose ether polymers of different substitution types

In the absence of drug, pre-endothemic events were very slight or not visible in 5 - 25% (w/w) HPMC F4M and HPC gels after 24h equilibration (section 5.4.2). Figure 8.9 shows that incorporation of propranolol hydrochloride (50mM) resulted in the appearance of such events in HPMC F4M gels at concentrations of 15, 20 and 25% (w/w). However, no pre-endothemic events were visible in 5 - 25% (w/w) HPC gels after incorporation of propranolol hydrochloride (50mM) (not shown).

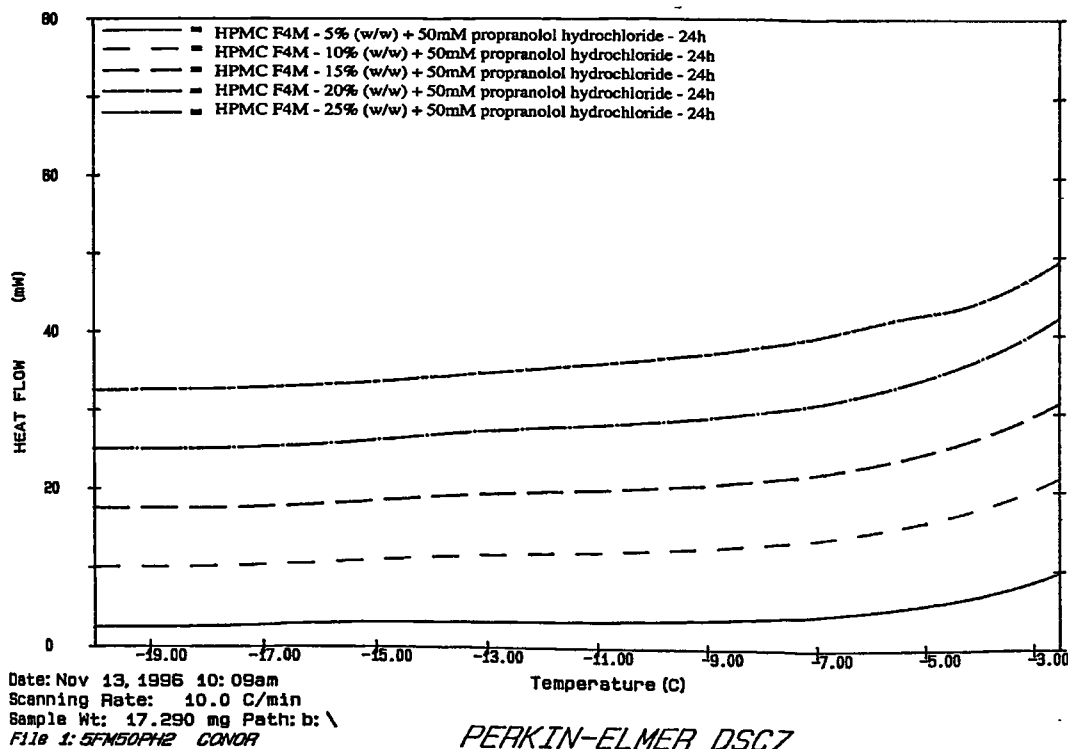
Propranolol hydrochloride addition had no effect on pre-endothemic events in HPMC E4M and MC A4M gels after 24h equilibration with such events being visible in 20 and 25% (w/w) gels both in the absence or presence of the drug.

Figure 8.10 illustrates how incorporation of diclofenac sodium into gels resulted in the appearance of pre-endothemic events in 5 - 25% (w/w) MC A4M gels. Pre-endothemic events were visible in 5 - 25% (w/w) HPMC E4M and HPMC F4M gels at all concentrations studied (not shown). In HPC gels, however, no pre-endothemic events were visible after addition of diclofenac sodium at any gel concentration (5 - 25% w/w) (not shown).

Pre-endothemic events in HPMC K15M gels were previously found to be exaggerated in the 25 - 35% (w/w) concentration range in comparison to the events observed with 20 and 25% w/w HPMC K15M gels (section 3.4.1). In addition, 5 - 25% (w/w) HPC gels failed to show the appearance of any pre-endothemic events either in the absence or



(a)

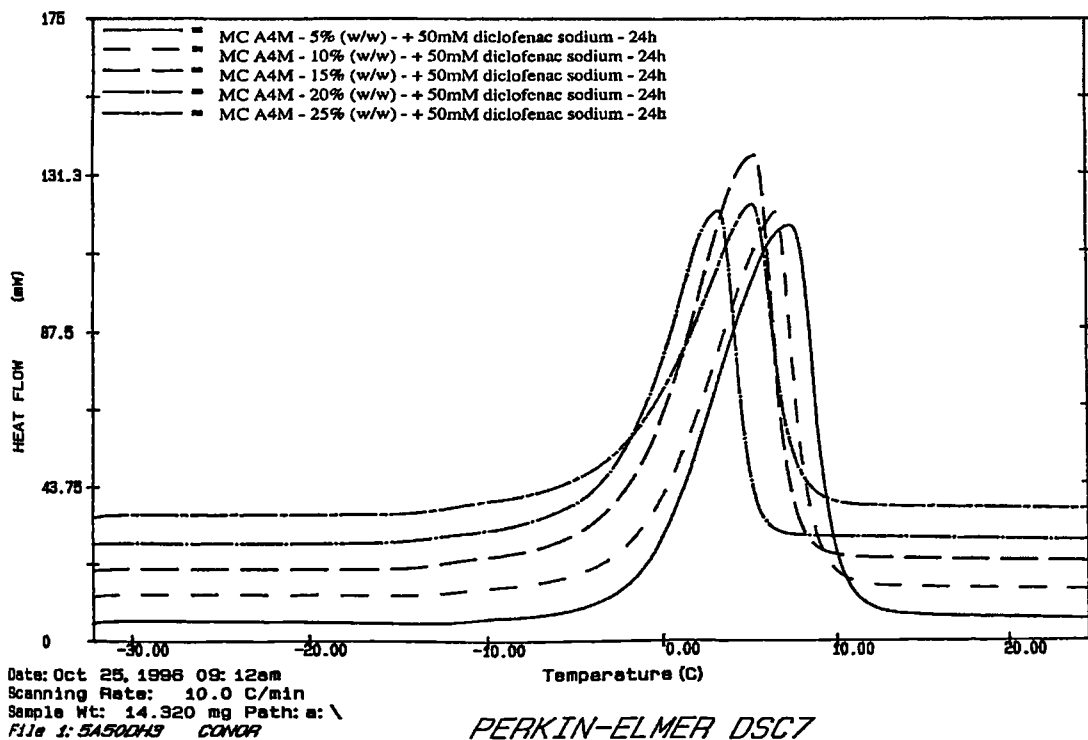


(b)

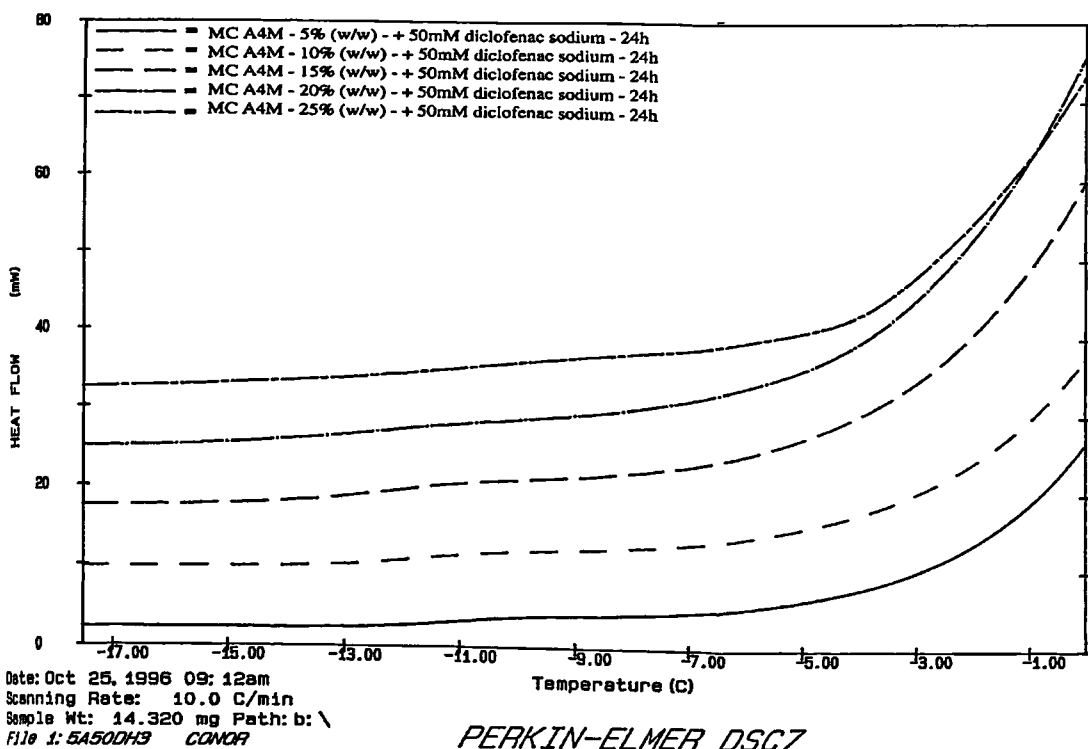
Figure 8.9 : DSC scans of 5 - 25% (w/w) HPMC F4M gels containing 50mM of propranolol hydrochloride cooled at $-10^{\circ}\text{Cmin}^{-1}$ and heated at $+10^{\circ}\text{Cmin}^{-1}$ after 24h storage

(a) from -30 to $+20^{\circ}\text{C}$

(b) from -20 to -2.5°C



(a)



(b)

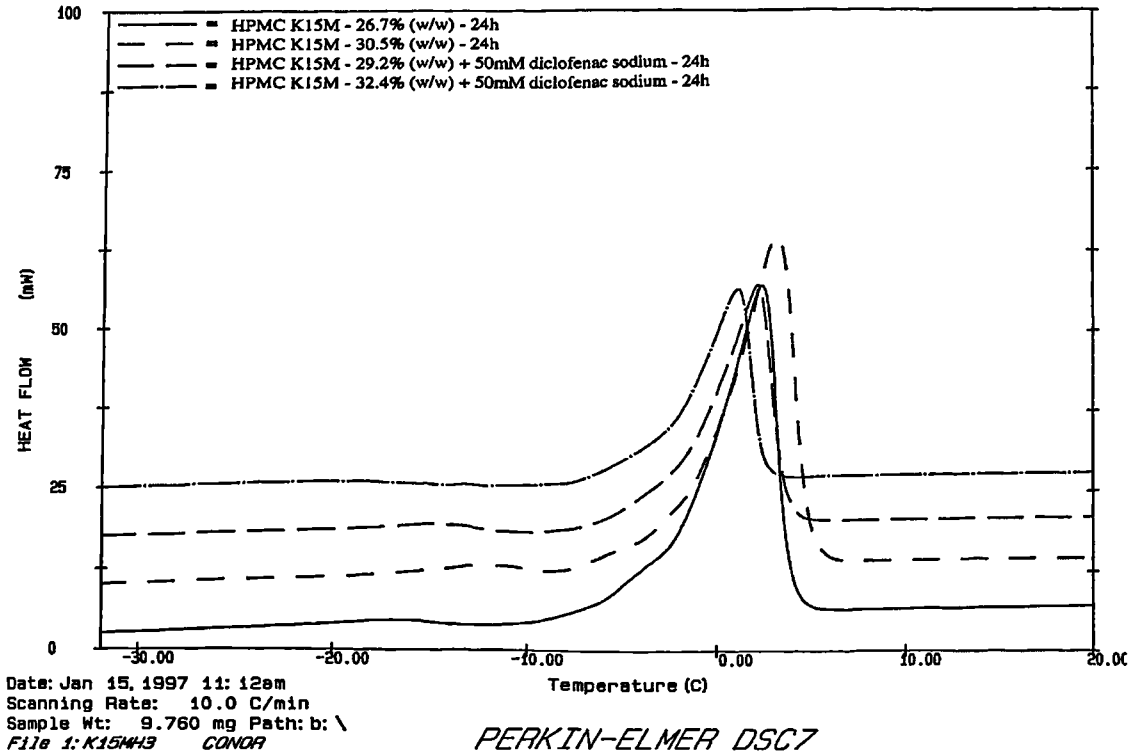
Figure 8.10 : DSC scans of 5 - 25% (w/w) MC A4M gels containing 50mM of diclofenac sodium cooled at $-10^{\circ}\text{Cmin}^{-1}$ and heated at $+10^{\circ}\text{Cmin}^{-1}$ after 24h storage
 (a) from -32 to $+22.5^{\circ}\text{C}$ (b) from -17.5 to -0.5°C

presence of drug. The influence of each drug on the DSC scans of gels containing 25 - 35% (w/w) HPMC K15M and 21 - 38% (w/w) HPC were examined.

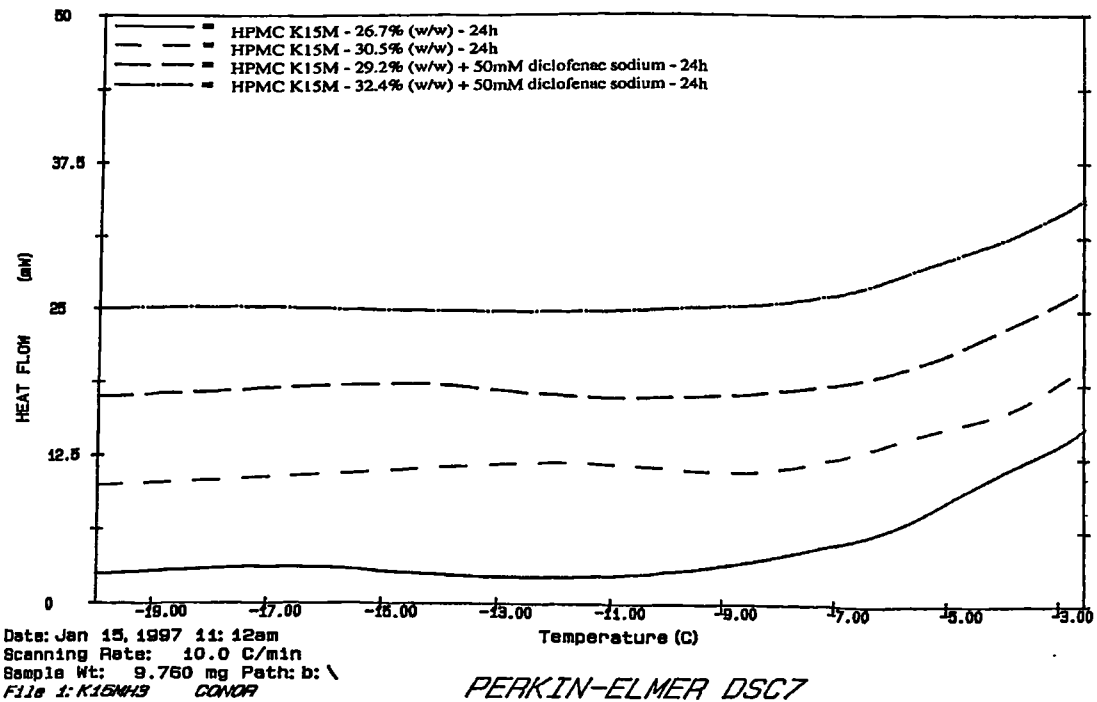
Following the inclusion of 50mM of propranolol hydrochloride into HPMC K15M gels, pre-endothemic events were visible at 29.0% (w/w) but were not present at the higher concentrations studied of 30.7 - 40.1% (w/w). The pre-endothemic events became quite pronounced at the HPMC K15M gels 25 - 35% (w/w) concentration range when diclofenac sodium (50mM) was added. However, they were not apparent in HPMC K15M gels at concentrations >35% (w/w). Figure 8.11 shows that in the HPMC K15M gels 25 - 33% (w/w) concentration range, secondary events were clearly visible in HPMC K15M gels both in the presence and absence of diclofenac sodium.

DSC analysis of 27.3 - 48.2% (w/w) HPC gels revealed that, even at high concentrations, only a small secondary event was visible at concentrations > 30% w/w (section 5.4.2). In HPC gels greater than 25% (w/w), containing 50mM of propranolol hydrochloride, pre-endothemic events were barely visible and were similar to the events observed in HPC gels in the absence of drug over a similar concentration range. Figures 8.12a and 8.12b show that, in contrast, pre-endothemic events are clearly visible in HPC gels containing diclofenac sodium in the 25 - 35% (w/w) concentration range.

HPC gels clearly behaved differently in comparison to the HPMC and MC gels studied. HPC contains a high percentage of hydrophilic hydroxypropoxyl groups and therefore may be expected to have a lot of bound water due to binding site availability. If water is binding to these groups, it is not visible as pre-endothemic events on DSC scans. It is possible that water attached to the polymer in this case binds so tightly that it does not freeze upon cooling. This would explain the non-appearance of pre-endothemic events which have been attributed to water loosely attached to the polymer and is capable of freezing. With addition of diclofenac sodium however, pre-endothemic events are visible in 25 - 35% (w/w) HPC gels. It is hypothesised that these pre-endothemic events may be related to the presence of loosely bound water as a result of the 'salting-out'



(a)

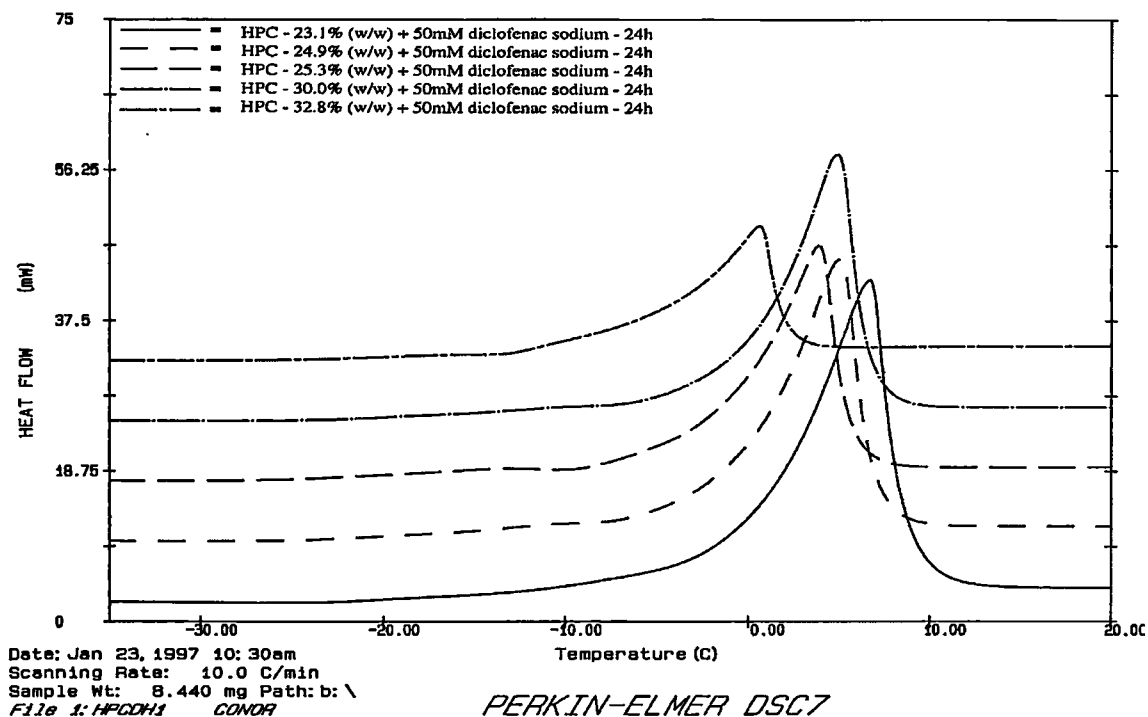


(b)

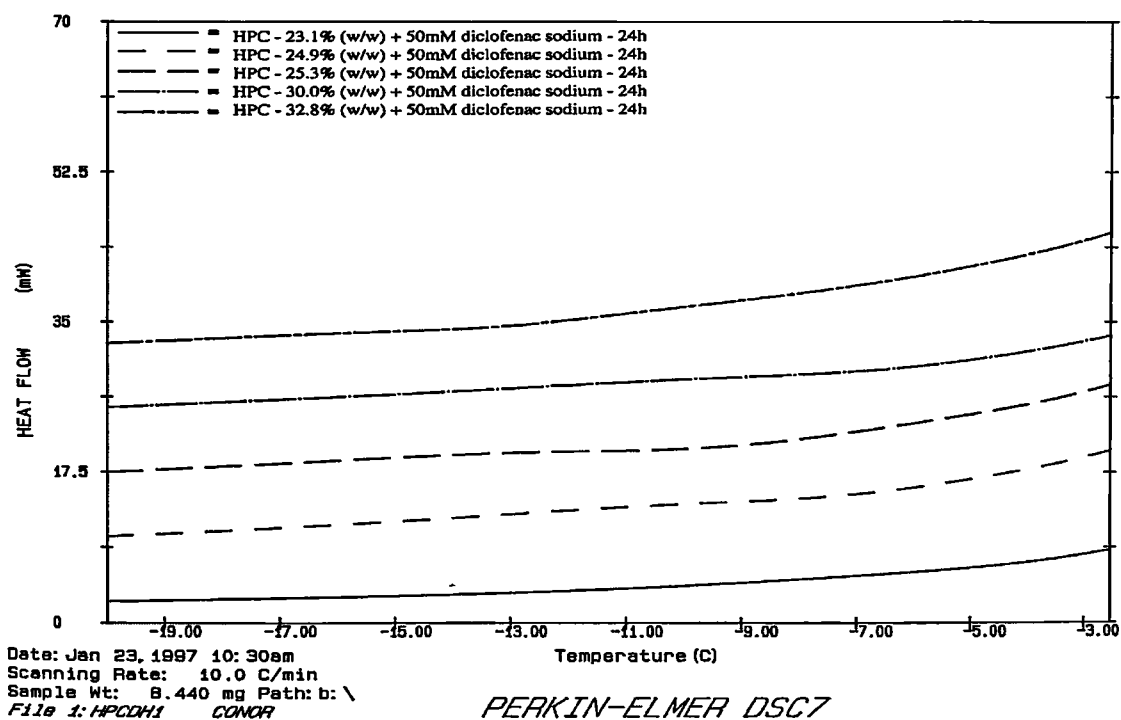
Figure 8.11 : DSC scans of 26.7 - 32.4% (w/w) HPMC K15M gels in the absence and presence of 50mM of diclofenac sodium cooled at $-10^{\circ}\text{Cmin}^{-1}$ and heated at $+10^{\circ}\text{Cmin}^{-1}$ after 24h storage

(a) from -32 to +20°C

(b) from -20 to -2.5°C



(a)



(b)

Figure 8.12 : DSC scans of 23.1 - 32.8% (w/w) HPC gels containing 50mM of diclofenac sodium cooled at $-10^{\circ}\text{Cmin}^{-1}$ and heated at $+10^{\circ}\text{Cmin}^{-1}$ after 24h storage
 (a) from -35 to $+20^{\circ}\text{C}$ (b) from -20 to -2.5°C

effect of diclofenac sodium. This may explain the appearance of pre-endothermic events in gels of all concentrations, molecular weights and substitution types when diclofenac sodium is added.

8.4.5 Effect of drug addition on the melting point of free water in HPMC K15M gels

Increasing HPMC K15M concentration from 5 to 25% (w/w) caused a depression of both the endothermic melting peak and the endothermic melting peak onset (section 5.4.1). With the addition of a drug, this depression of melting point may be expected regardless of polymer molecular weight or substitution type. For HPMC K15M gels, increasing polymer concentration from 5 to 25% (w/w) in the presence of propranolol hydrochloride (50mM) caused a depression of both the endothermic melting peak ($9.82 \pm 0.8^\circ\text{C}$ to $6.62 \pm 0.3^\circ\text{C}$) and the endothermic melting peak onset ($3.22 \pm 0.7^\circ\text{C}$ to $0.81 \pm 0.2^\circ\text{C}$). Similarly, increasing polymer concentration in HPMC K15M gels from 5 to 25% (w/w) in the presence of diclofenac sodium (50mM) caused a depression of both the endothermic melting peak ($10.41 \pm 1.5^\circ\text{C}$ to $8.33 \pm 0.3^\circ\text{C}$) and the endothermic melting peak onset ($2.90 \pm 0.5^\circ\text{C}$ to $1.26 \pm 0.2^\circ\text{C}$). In the absence of any drugs, increasing the concentration of HPMC K15M from 5 to 25% (w/w) caused a decrease of the endothermic melting peak ($8.9 \pm 0.35^\circ\text{C}$ to $6.17 \pm 0.53^\circ\text{C}$) and the endothermic melting peak onset (3.43 ± 0.16 to $1.82 \pm 0.48^\circ\text{C}$) after similar gel hydration periods.

8.4.6 Quantitative analysis of the effect of propranolol hydrochloride (50mM) and diclofenac sodium (50mM) on the bound water content of cellulose ether gels

The number of moles of bound water per PRU were calculated as previously described using the Ford and Mitchell (1995) method (section 5.4.3.1) and values chosen for the PRU were as listed in Table 5.9. In the majority of polymers studied here, propranolol

hydrochloride reduced the amount of water bound to the polymer (Table 8.3), i.e. less water required to fully hydrate the polymer, most likely due to its 'salting in' effect (section 8.4.3). No particular trend was apparent in the extent to which the amount of bound water was reduced by propranolol hydrochloride among the polymers studied.

Addition of propranolol hydrochloride to HPMC K100LV gels did not reduce the amount of bound water. The bound water content initially was very low in these gels. When diclofenac sodium was added to cellulose ether gels, with the exception of HPMC F4M and HPMC K100LV, the amount of water bound to the polymer was reduced in comparison with that bound in the absence of drug. More water was required to fully hydrate the polymer compared to when propranolol hydrochloride was added. Diclofenac sodium 'salts out' cellulose ether polymers making them less soluble. Therefore more water will be required to hydrate the polymer and thus the bound water content should increase. This effect was not seen in HPMC K100LV or HPMC F4M gels. For HPMC K100LV, addition of propranolol hydrochloride did not change the bound water content, while addition of diclofenac sodium caused an increase in the amount of water binding to the polymer. Addition of diclofenac sodium would certainly seem to make the polymer less soluble, causing an increase in water required to hydrate the polymer, as reflected in an increase in bound water. In the case of propranolol hydrochloride, the expected reduction in bound water content due to the 'salting in' effect of the drug did not occur. It may be that a certain minimum level of water is required to maintain the gel structure and remains tightly bound to the polymer. This amount of tightly bound water cannot be removed even with the addition of a drug like propranolol hydrochloride.

Differences in the bound water content of polymer gels of different molecular weights and substitution types were explained by the degree of substitution of hydrophilic and hydrophobic substituents on the polymer backbone in section 5.4.3. The bound water content of HPMC F4M in the absence or presence of drug did not follow the pattern shown by other polymer gels studied. HPMC F4M would be expected to have a fairly low bound water content on the basis that it has a high methoxyl substitution level

Table 8.3 : The effect of addition of 50mM of propranolol hydrochloride or diclofenac sodium on the water distribution within a range of cellulose ether gels after 24h equilibration

Polymer	Viscosity grade (cP)	Polymer (% w/w)	Water (% w/w)	Regression coefficient (R ²)	Moles bound water per PRU
HPMC K100LV	93	81.2	18.8	0.994	2.4
+ propranolol		80.3	18.3	0.976	2.4
+ diclofenac		70.0	28.5	0.986	4.3
HPMC K4M	4,196	59.6	40.4	0.996	7.1
+ propranolol		79.4	19.2	0.997	2.5
+ diclofenac		65.4	33.1	0.987	5.3
HPMC K15M	15,825	70.2	29.8	0.978	4.5
+ propranolol		76.6	21.9	0.975	3.0
+ diclofenac		71.8	26.8	0.992	3.9
HPMC K100M	119,768	64.1	35.9	0.970	6.0
+ propranolol		81.4	17.2	0.982	2.3
+ diclofenac		65.1	33.4	0.981	5.5
HPMC F4M	5,218	76.4	23.6	0.968	3.2
+ propranolol		76.3	22.2	0.986	3.0
+ diclofenac		83.3	15.3	0.992	1.9
HPMC E4M	3,970	63.1	36.9	0.974	6.2
+ propranolol		71.3	27.2	0.951	4.0
+ diclofenac		67.9	30.6	0.958	4.8
MC A4M	3,811	65.1	34.9	0.999	5.3
+ propranolol		77.4	21.2	0.995	2.7
+ diclofenac		71.8	26.8	0.998	3.7
HPC	5,950	61.6	38.4	0.983	5.5
+ propranolol		67.4	31.1	0.981	4.4
+ diclofenac		63.4	35.2	0.984	5.3

(28.9%) combined with a low hydroxypropoxyl substitution level (6.1%). This is found to be the case, however, while propranolol hydrochloride exhibits its 'salting in' effect, diclofenac sodium does not show its 'salting out' properties as in other polymers. A different mechanism may be operating in this case which requires further exploration.

8.4.7 Thermogravimetric analysis studies

8.4.7.1 Effect of propranolol hydrochloride and diclofenac sodium on thermal events in HPMC K15M gels

The effect of scanning rate on the nature of moisture loss from 15% (w/w) HPMC K15M gel samples was explored by thermogravimetric analysis (TGA) (section 4.4.1.2). More than one evaporation event became visible on the TGA derivative curve at scanning rates of $+10^{\circ}\text{Cmin}^{-1}$ and above. The appearance of such events were related to the presence of more than one type of water in HPMC polymer gels. This work was extended to identify whether the evaporation events were affected in the presence of drugs.

Tables 8.4 and 8.5 and Figure 8.13 show that few differences were apparent in the nature of moisture loss from $\sim 15\%$ (w/w) HPMC K15M gels in the absence or presence of propranolol hydrochloride. The differences in the derivative peak(s) shape(s) were not reproducible. Moisture was removed over a wider temperature range with increase in scanning rate and more than one evaporation event was visible at scanning temperatures of $\geq +10^{\circ}\text{Cmin}^{-1}$ as was seen in gels scanned in the absence of drug.

With addition of diclofenac sodium, separation of more than one evaporation event was poorly visible, even at the higher scanning rates studied (Figure 8.13).

When gels containing drugs were scanned in vented aluminium pans, water evaporated at higher temperatures in comparison to open pan TGA. A much more controlled release

Table 8.4 : Thermogravimetric analysis data showing the mean percentage weight loss and the temperature range over which moisture loss occurs in 14.2% (w/w) HPMC K15M gel samples containing 50mM of propranolol hydrochloride scanned at a variety of heating rates (n = 2)

HPMC K15M + 50mM propranolol HCl (% w/w)	Mean peak width (°C)	Mean % weight loss	Scanning rate (°Cmin ⁻¹)
14.2	36.40	-	+2
	46.39	78.96	
14.2	84.78	79.79	+5
	84.36	82.11	
14.2	119.17	80.79	+10
	96.13	81.84	
14.2	124.66	84.83	+15
	117.81	81.60	
14.2	119.18	82.15	+20
	116.31	81.57	

Table 8.5 : Thermogravimetric analysis data showing the mean percentage weight loss and the temperature range over which moisture loss occurs in 13.93% (w/w) HPMC K15M gel samples containing 50mM of diclofenac sodium scanned at a variety of heating rates (n = 2)

HPMC K15M + 50mM diclofenac sodium (% w/w)	Mean peak width (°C)	Mean % weight loss	Scanning rate (°Cmin ⁻¹)
13.93	52.73	84.07	+2
	51.36	83.91	
13.93	81.34	83.34	+5
	93.61	83.49	
13.93	99.92	83.77	+10
	97.57	83.77	
13.93	120.09	84.73	+15
	115.4	82.65	
13.93	119.64	84.15	+20
	125.45	84.72	

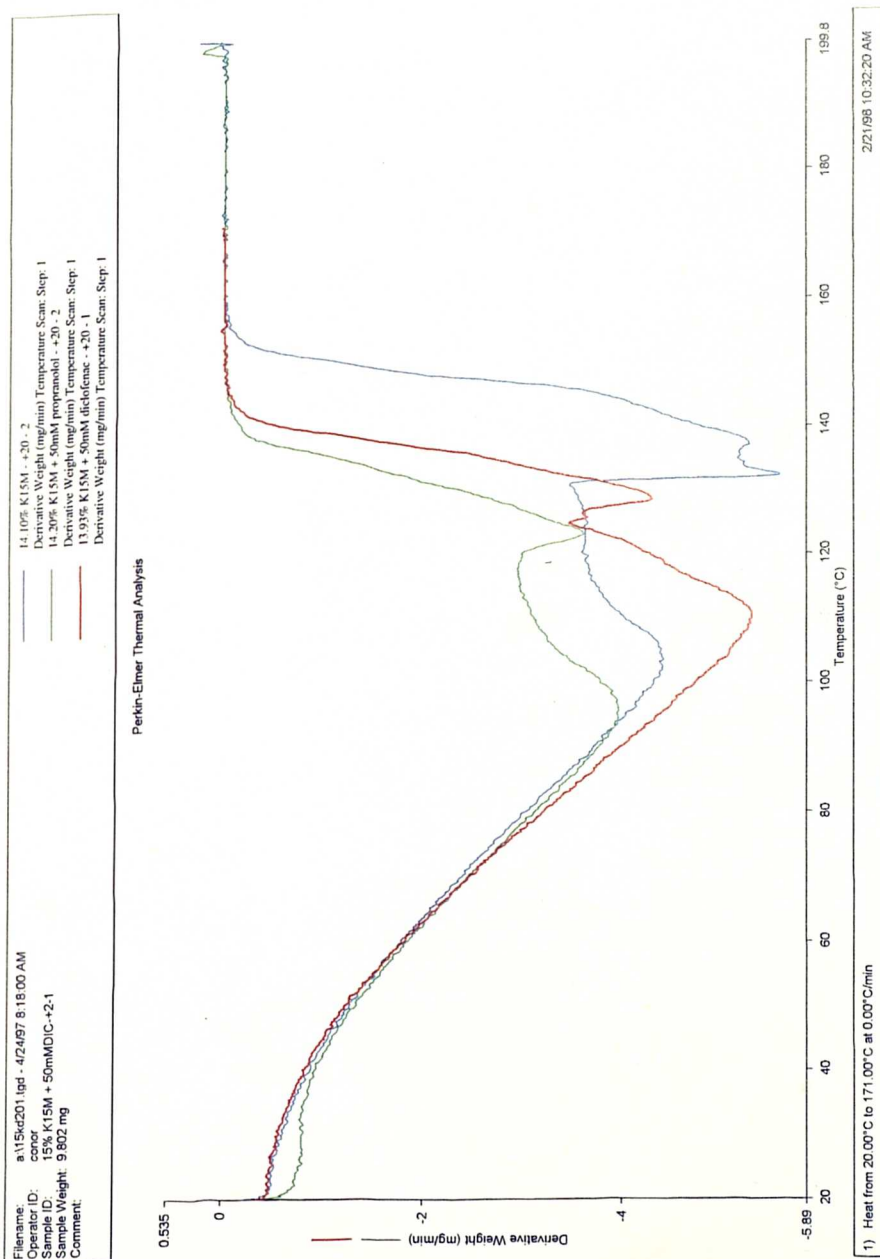


Figure 8.13 : TGA derivative curves of ~15% (w/w) HPMC K15M gels in the absence and presence of 50mM of propranolol hydrochloride or diclofenac sodium scanned at a heating rate of $+20^{\circ}\text{Cmin}^{-1}$ in open sample pans

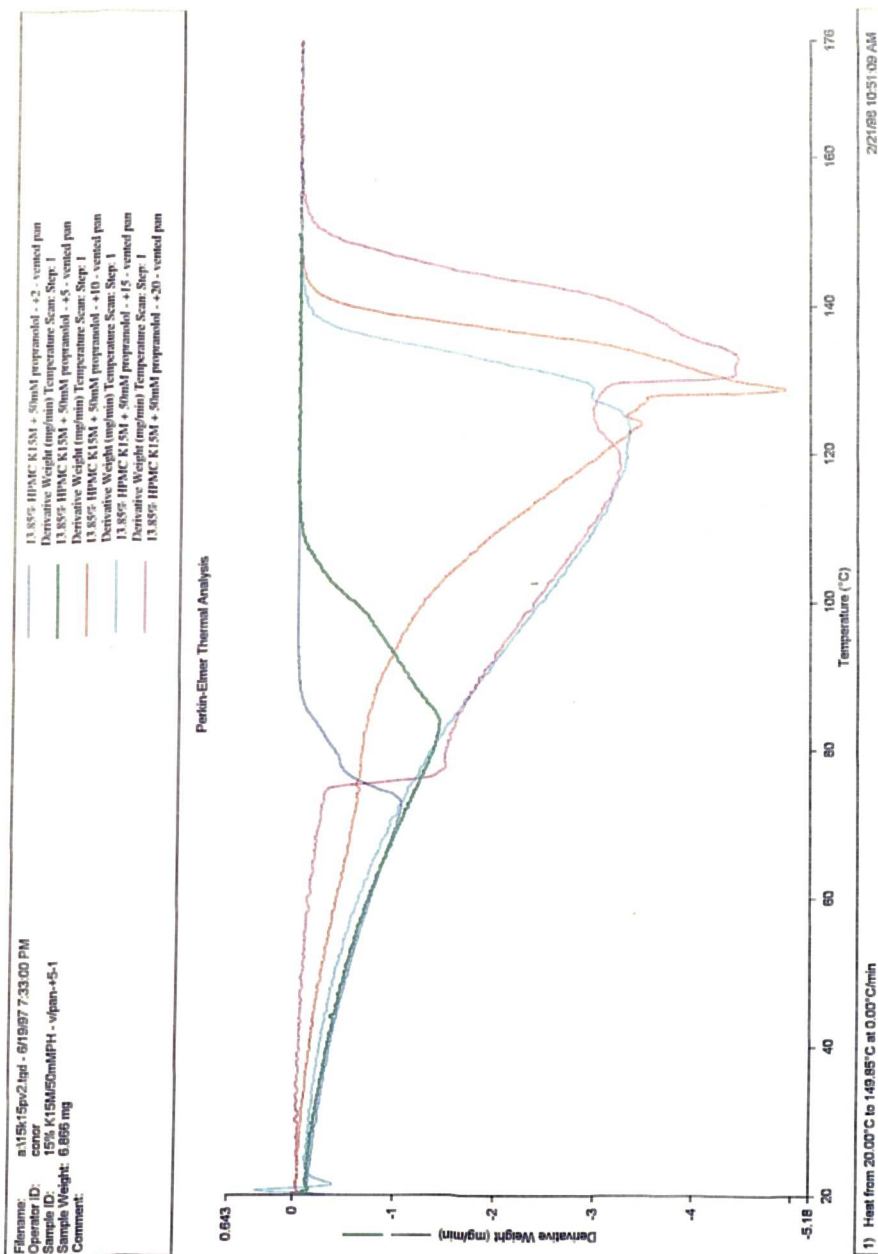


Figure 8.14 : TGA derivative curves of ~15% (w/w) HPMC K15M gels containing 50mM of propranolol hydrochloride scanned at heating rates of +2, +5, +10, +15 and +20°Cmin⁻¹ in vented sample pans

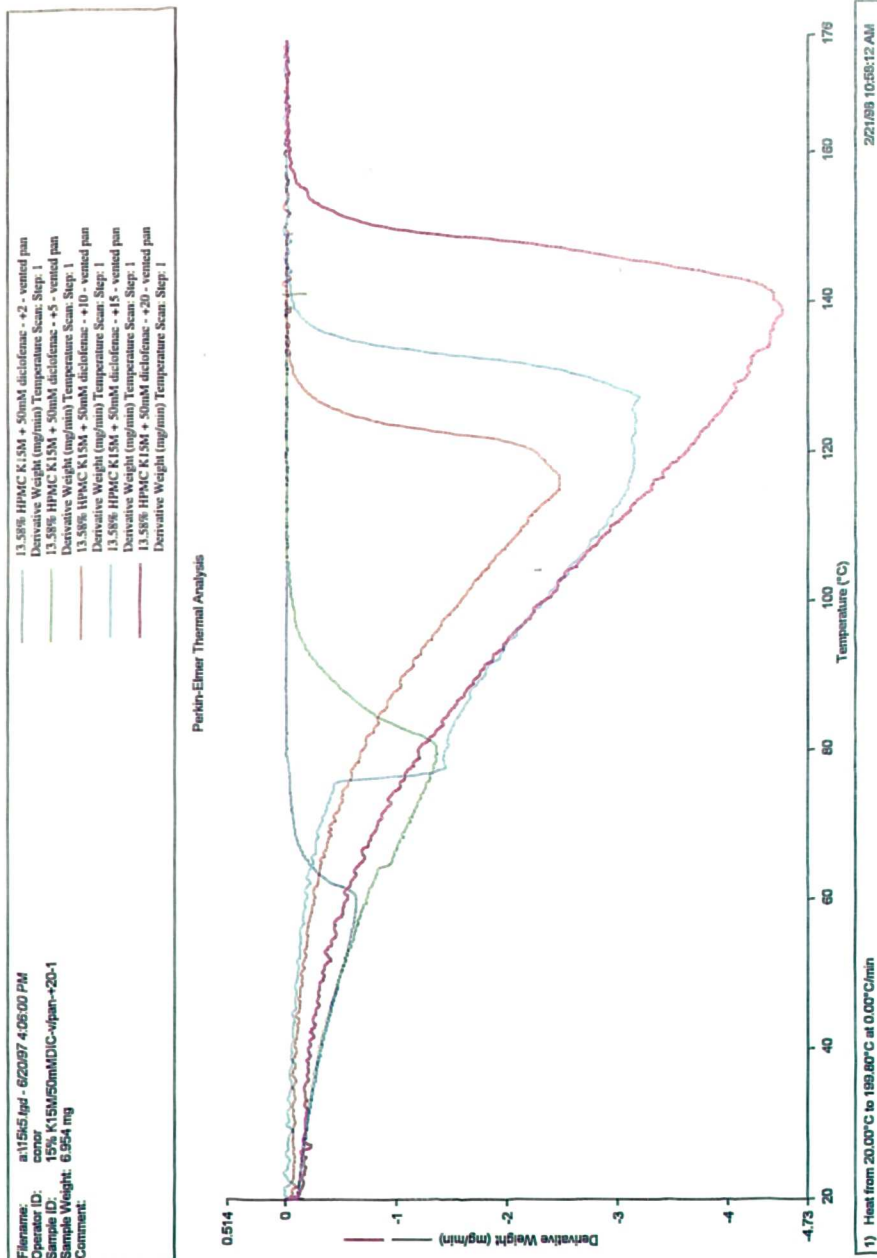


Figure 8.15 : TGA derivative curves of ~15% (w/w) HPMC K15M gels containing 50mM of diclofenac sodium scanned at heating rates of +2, +5, +10, +15 and +20°Cmin⁻¹ in vented sample pans

of water occurred. Figure 8.14 shows a clear separation of more than one evaporation event that occurred in HPMC K15M gels containing propranolol hydrochloride scanned in vented pans at high scanning rates. In comparison, Figure 8.15 shows a poorer separation of evaporation event(s) in HPMC K15M gels containing diclofenac sodium scanned under similar conditions.

8.4.7.2 Kinetic studies on the effect of drug addition on water loss from HPMC K15M gels

The data in section 8.4.2.1 (Table 8.4 and Table 8.5) were analysed using the Perkin-Elmer Decomposition Kinetics program (see section 4.4.1.3).

Statistical analysis of data in Tables 4.4, 8.6 and 8.7 indicate that no significant differences were observed in the values for E_a in HPMC K15M gels in the absence or presence of drugs. Table 8.6 and Table 8.7 also show that the highest E_a exists at the lowest conversion value, the point at which the reaction is in its early stages i.e the initial stages of moisture loss from the gel sample. This was also seen with HPMC K15M gels in the absence of drug (Table 4.4) and it was explained in section 4.4.1.3.

Gel samples containing diclofenac sodium showed very little spread in the E_a values obtained at any of the conversion values even at low conversion values. At low conversion values such gel systems are not at equilibrium, contain large quantities of free water and are at their most dynamic in nature, therefore the spread of E_a values were expected to be wider (as seen in the case of gels containing propranolol hydrochloride).

Table 8.6 : Activation energy (E_a) of gel samples of 14.2% (w/w) HPMC K15M containing 50mM of propranolol hydrochloride calculated at a number of different conversion values

HPMC K15M + 50mM propranolol HCl (% w/w)	conversion value (%)	E_a (KJ/mole)
14.20	2	123.1
		142.0
14.20	5	66.9
		86.4
14.20	10	49.1
		57.4
14.20	15	42.4
		48.0
14.20	20	38.7
		43.1

Table 8.7 : Activation energy (E_a) of gel samples of 14.2% (w/w) HPMC K15M containing 50mM of diclofenac sodium calculated at a number of different conversion values

HPMC K15M + 50mM diclofenac sodium (% w/w)	conversion value (%)	E_a (KJ/mole)
13.93	2	141.5
		140.6
13.93	5	70.8
		70.2
13.93	10	50.8
		50.1
13.93	15	43.9
		43.3
13.93	20	40.1
		39.7

8.5 Conclusions

The water distribution within cellulose ether polymer gels was affected by the presence of a drug. Pre-endothemic events indicative of loosely bound water were visible in HPMC K15M gels (15, 20 or 25% w/w) following the addition of 10, 20 or 30% (w/w) propranolol hydrochloride. These events were visible only in 20 and 25% (w/w) gels when 50mM of propranolol hydrochloride was incorporated. The events were exaggerated after 96h equilibration and the shape of the pre-endothemic events changed in the presence of 10 - 30% (w/w) propranolol hydrochloride. Generally, propranolol hydrochloride (50mM) had a negligible effect on the shape of pre-endothemic events in polymers of varying molecular weights or substitution types. In the case of HPMC F4M, which showed very little evidence of pre-endothemic events in the absence of drugs, some evidence of loosely bound water appeared in higher concentration gels, after addition of propranolol hydrochloride.

Diclofenac sodium had a marked effect on the appearance of pre-endothemic events in cellulose ether polymers. It appeared that after 24h equilibration, pre-endothemic events were visible in all HPMC K-series 5 to 25% (w/w) gels incorporating diclofenac sodium. Addition of diclofenac sodium resulted in the appearance of pre-endothemic events in HPMC E4M, HPMC F4M or MC A4M gels containing 5 - 25% (w/w) polymer. In HPC gels, however, no pre-endothemic events were visible after addition of 50mM of diclofenac sodium in gels of concentration 5 - 25% (w/w). However, pre-endothemic events appeared in HPC gels containing diclofenac sodium in the 25 - 35% (w/w) concentration range.

Quantitative studies have indicated that propranolol hydrochloride acts to 'salt in' the polymer, hence increasing its solubility. Less water is required to fully hydrate the polymer. This was shown in the reduced amount of water bound to the majority of polymers studied after propranolol hydrochloride addition when compared with the amount of water bound in the absence of drug. In contrast, when diclofenac sodium was

added to cellulose ethers gels, with the exception of HPMC F4M, more water was required to fully hydrate the polymer compared to when propranolol hydrochloride was added. Diclofenac sodium 'salts out' cellulose ether polymers making them less soluble. Therefore more water was required to hydrate the polymer and thus the bound water content was increased.

Thermogravimetric studies identified that HPMC K15M gels containing propranolol hydrochloride showed evidence of more than one evaporation event occurring at high scanning rates, similar to events seen in HPMC K15M gels in the absence of drugs. Separation of more than one evaporation event indicated the presence of more than one type of water in the gels. Thermogravimetric studies of HPMC K15M gels containing diclofenac sodium showed poor separation of evaporation events, even at the higher scanning rates studied. Kinetic analysis failed to distinguish any effects caused by addition of either propranolol hydrochloride or diclofenac sodium to the E_a of HPMC K15M gels.

CHAPTER 9

GENERAL DISCUSSION

Chapter 9 General Discussion

9.1 Introduction

The aims of this work were to characterise the fundamental interactions between water and cellulose ether polymers. A series of polymers were studied including a range of Methocels of similar substitution type and varying molecular weight; HPMC K100LV, HPMC K4M, HPMC K15M and HPMC K100M. Polymers were also studied which were of similar molecular weight but with varying substitution type; HPMC K4M, HPMC F4M, HPMC E4M, methylcellulose MC A4M and hydroxypropylcellulose (HPC). The behaviour of water within these gel systems was studied both in the presence and absence of drugs. A number of techniques were employed including the closely associated thermal techniques of differential scanning calorimetry (DSC) and thermogravimetric analysis (TGA). In addition, studies were carried out using dynamic vapour sorption (DVS) and low frequency dielectric spectroscopy (LFDS).

9.2 Characterisation of the interaction between water and HPMC K15M polymer gels

HPMC K15M was chosen as representative of other cellulose ethers commonly used as the rate controlling polymer in hydrophilic matrix systems. DSC studies showed the presence of one or more events appearing prior to the leading edge of the main endotherm for the melting of free water within HPMC K15M gels. These pre-endothermic events were thought to be related to the presence of different types of water within the gels, melting at different temperatures. Different types of water thought to be present in these systems include free (unbound) water, non-freezing water which is tightly bound to the polymer and freezing bound water (Nakamura et al, 1983b). The appearance of more than one endothermic peak around 0°C for the melting of frozen water has previously been reported in DSC traces. Murase (1993) has considered similar peaks in cross-linked dextrans as being related to the presence of water, different to bulk water. Hatakeyama and Hatakeyama (1998) have reported

that more than one endotherm, corresponding to the melting of different types of water, is present in various cellulose samples. They also reported that in some cases, a shoulder was found on the lower temperature side of an endothermic peak, similar to what was observed in HPMC K15M gels in the current study. Ratto et al (1995), have observed more than one endothermic peak for water in water/chitosan systems and have attributed this to cold crystallization. This occurs in systems where non-freezing and freezing bound water are present. Upon heating, some of the non-freezing water becomes mobile, comes into contact with solid freezing bound water and forms ice. A crystallization exotherm is subsequently visible. Liu and Lelièvre (1991, 1992) have identified more than one endothermic peak around 0°C in starch systems and have explained these as being due to either changes in machine resolution, the presence of a glass transition or due to division of moisture between water in the starch sample and water evaporating from the starch in the DSC pan and condensing on the pan lid. A number of authors have cast doubts on the existence of more than one type of water occurring within polymer systems (Levine and Slade, 1988; Roorda et al, 1988a, 1988b, 1994; Zografí, 1988; Bouwstra et al, 1995). They suggest that only a single class of water is present which is reduced in mobility due to the transition of the polymer from its rubbery to glassy state. Roos and Karel (1991) have attributed pre-endothermic events in DSC traces of ice melting in maltose and maltodextrins as being due to overlapping ice melting (first order) and glass transition (second order) phase transitions. Sodium chloride is present as an ionic contaminant in many cellulose ethers. The temperature of the sodium chloride : water eutectic is -21.2°C (Partington, 1954). It is possible that one or more of the transitions occurring below 0°C in cellulose ether gels may be due to this eutectic temperature.

TGA has previously been employed to differentiate between different types of water in various systems. Donescu et al (1993) have identified two types of water evaporating at different temperatures in polyvinylacetate (PVAc) emulsions. Three types of water have been observed evaporating from porcine stratum corneum (Liron et al, 1994). Hatakeyama and Hatakeyama (1998) have described water loss from hydrophilic polymers, using TGA, occurring in two or more stages. Further evidence

for the existence of more than one type of water within HPMC K15M gels has been provided by TGA. The first derivative of the TGA weight loss curve, showing the rate of water loss from gels, provides evidence of water evaporating in more than one event. It is hypothesised that free water evaporates at temperatures lower than water which is associated with the polymer which evaporates at higher temperatures.

Low Frequency Dielectric Spectroscopy (LFDS) has shown that the dielectric response of deionised water scanned from -30°C to $+20^{\circ}\text{C}$ at frequencies of 1 and 100 Hz is characterised by a sharp increase in both capacitance and dielectric loss at the melting point of ice (0°C). The presence of 25% (w/w) HPMC K15M gels resulted in a quite different dielectric response with the melting point of ice being depressed in both the capacitance and dielectric loss responses. In addition to the melting of free water, a number of other processes were visible as indicated by the shape of the dielectric response curves. These data are in agreement with the findings of DSC and TGA studies which showed the presence of more than one melting event in cellulose ether gels indicating the presence of more than one type of water melting at different temperatures. Dielectric analysis has previously been employed to characterise the behaviour of water within polymeric systems. Pathmanathan and Johari (1994) have found evidence of freezing and non-freezing water in a terpolymer hydrogel while Kyritsis et al (1995) have identified more than one type of water in poly (hydroxyethyl acrylate) hydrogels. Identification of different types of water in cellulose derivatives has not previously been carried out using dielectric analysis.

Both DSC and LFDS studies have shown that water associated with the polymer melts at lower temperatures than free or unbound water. This is explained by consideration of the cooling process which the gels are subjected to during both DSC and LFDS analysis. It is hypothesised that upon cooling, free water in the gel system forms larger crystals than those formed by water which is loosely bound to the polymer. Upon heating, the smaller crystals will melt first followed by the larger crystals formed by free water and thus different types of water melting at different temperatures are visible.

The pre-endothermic events in HPMC K15M gels were dependent on polymer concentration. In DSC studies, pre-endothermic events initially appeared at 16% (w/w) HPMC K15M gels and became more exaggerated as the concentration was further increased. Increase in HPMC K15M concentration resulted in a decrease in both DSC exothermic (cooling/ crystallization) and endothermic (heating/ melting) enthalpies (J/g) after gel storage for both 24 or 96h. Assuming that both these enthalpies relate, in the main, to the crystallization and melting of free water respectively, it is evident that there is a decrease in the amount of free water present with increase in HPMC concentration. It is thought that as polymer concentration increases, the amount of water required to hydrate the polymer increases and thus less free water is available. Increase in HPMC K15M concentration also resulted in a decrease of temperature of both the endothermic melting peak and the endothermic melting peak onset. This temperature decrease may be related to an increase in the quantity of loosely bound water, which melts at a lower temperature than free water. Hatakeyama and Hatakeyama (1998) have described how endothermic peak shape varies according to polymer water content in various cellulose samples.

Both TGA and dielectric studies reflected changes in water distribution occurring in HPMC K15M gels with increase in polymer concentration. The appearance of the TGA first derivative curve varied with HPMC K15M concentration (5 - 25% w/w) and this was thought to reflect the altered distribution of water within the gels. Higher temperatures were required to remove all of the water from gels with an increase in polymer concentration. It is thought that there is an increased amount of closely associated or loosely bound water with an increase in gel concentration. Dielectric response of HPMC K15M gels showed that with increase in polymer concentration from 5 to 25% (w/w), a transition beginning at -8.5°C became more pronounced. It is thought that such transitions may be similar to events seen on the lower temperature side of the main endotherm for the melting of free water only in higher concentration HPMC K15M gels using DSC.

The melting events visible in HPMC K15M gels were found to be dependent on polymer hydration time and on heating and cooling rates during DSC analysis. Pre-

endothermic events were visible in gels hydrated for 24 or 96h in DSC traces but were not visible in gels hydrated only for 2h. It is thought that 2h is insufficient time for gel equilibration to occur.

Pre-endothermic events were exaggerated at both low cooling and low heating rates during DSC analysis. Low cooling rates may allow water associated with the polymer to freeze slowly and combine more tightly with the polymer. This may lead to an increase in the amount of bound water which appears as a more pronounced peak to the left of the main endotherm for the melting of free water. When the heating rate is low, the resolution of the DSC increases and water melts as a number of separate events, possibly, indicating the presence of more than one type of closely associated water. Murase (1993) has previously identified how the shape of a small endotherm occurring to the left of the main peak for the melting of free water within cross-linked dextran gels, is dependent on the preceding cooling treatment. This has been suggested as evidence that such pre-endothermic events are not due to the glass transitions which should theoretically be independent of cooling and heating rates during DSC analysis. When a sample of HPMC K15M (20% w/w) gel was cooled to -50°C , then heated to the point at which secondary events first appeared ($\sim -9^{\circ}\text{C}$) and subsequently re-cooled and reheated to $+35^{\circ}\text{C}$, the secondary events remained visible. Further re-cooling to -50°C , heating to -9°C and holding for 10mins, and then re-cooling and reheating again indicated that the presence of the secondary events remained unaffected. These results indicated that such events are indeed quite 'real' and may be linked to the presence of different water types that exist in HPMC K15M gels.

Similarly, TGA heating rate influenced the evaporation of water from 25% (w/w) HPMC K15M gels. At heating rates of $+10^{\circ}\text{Cmin}^{-1}$ and above, more than one evaporation event was visible on the derivative TGA curve. It has been suggested that the appearance of such events at higher scanning rates only, may indicate that bubbling of the gel had occurred during heating at faster rates, providing a mechanism for release of loosely bound water from the gel. However, the fact that these events were reproducible may suggest that bubbling of the gel may not be

water may evaporate from gels at lower temperatures and is not visible as a separate evaporation event on the first derivative curve. Water evaporated at higher temperatures from HPMC K15M gels scanned in vented aluminium pans in comparison to open pans. Excellent separation of more than one evaporation event was visible on the dTGA curve at heating rates of $10^{\circ}\text{Cmin}^{-1}$ and above in gels scanned in vented pans. In vented aluminium pans, water vapour builds up inside the pan reaching equilibrium thus slowing down evaporation of water at lower temperatures from the gel.

The behaviour of HPMC K15M gel systems, as studied using DSC, was influenced both by gel preparation method and by batch to batch variation. Differences were identified qualitatively by the nature of the melting events visible on DSC traces and quantitatively by analysis of the number of moles of bound water (BW) per polymer repeating unit (PRU).

9.3 Characterisation of the interaction between water and a range of polymers of varying molecular weight and substitution type

DSC analysis was extended to the remaining HPMC K-series. Events occurring to the lower temperature side of the main endotherm for the melting of free water were again visible in these gels with their appearance being dependent on both polymer molecular weight and gel storage time. Decrease in the endothermic (melting) enthalpy and a decrease of melting point with increasing concentration of polymer occurred in all the polymers studied. DSC analysis of polymers with similar molecular weight but varying substitution type was completed. All polymers studied showed similar trends to those within the HPMC-K series with respect to decrease in the endothermic (melting) enthalpy and a decrease of melting point with increasing concentration of polymer. The presence of thermal events occurring to the left of the main endotherm for the melting of free water varied with polymer substitution type. No pre-endothermic events were visible in 5 - 30 % (w/w) HPC gels after either 24 or 96h storage. The dielectric response of the HPMC K-series varied with polymer molecular weight in terms of both the pattern of melting and the temperature at

molecular weight in terms of both the pattern of melting and the temperature at which melting begins. The dielectric response of polymers of similar molecular weight but different substitution types varied in a similar way. In all polymers studied the magnitude of the dielectric response varied from polymer to polymer and this was linked to the levels of ionic contaminants within the polymers.

Dynamic vapour sorption (DVS) studies provided information on the vapour sorption/ desorption properties of HPMC polymers. All polymers analysed, of varying molecular weights and substitution types, showed Type II isotherms. Type II isotherms are characteristic of either multilayer physical adsorption on non-porous solids with the formation of an adsorbed monolayer visible on the isotherm, or alternatively, typical of adsorption on microporous solids with condensation occurring in pores as well as monolayer adsorption on the surface (Shaw, 1992). Moisture sorption isotherms, constructed by plotting the mass of moisture taken up per unit mass of dry powder against the relative humidity, showed the existence of an hysteresis loop between the sorption and desorption cycles in all polymers studied. Polymers in the HPMC K-series have similar methoxyl and hydroxypropoxyl substitution levels and as a result one may expect them to be similar in terms of surface and particulate morphology. As a result, few differences in the moisture sorption and desorption properties of these polymers were expected. The moisture sorption isotherms showed that, as expected, polymer molecular weight had no effect on moisture sorption behaviour, however HPMC K100LV and HPMC K4M retained slightly more water during desorption than other members of the HPMC K-series. On the other hand, the DVS of cellulose ether polymers with different substitution types and levels showed that HPMC K4M sorbed more moisture at all RH values than the polymers of other substitution types studied. This was explained by the low percentage methoxyl substitution level (22.2%) of HPMC K4M in tandem with a high percentage hydroxypropoxyl level (8.4%). Three thermodynamic states of water have been previously identified in cellulose and starch based excipients (Zografis and Kontny, 1986) in similar water sorption studies.

It is hypothesised that the hysteresis area, the area between the moisture sorption/

desorption curves on the moisture sorption isotherm, is related to water being retained within the polymer. If this is indeed correct, this area may be related to the capability of a particular polymer to absorb water. HPMC K100LV and HPMC K4M have slightly larger hysteresis areas than HPMC K15M and HPMC K100M indicating that more water is transferred into these polymers and remains there. This follows the trend seen previously when HPMC K100LV and HPMC K4M retained slightly more moisture during desorption than HPMC K15M and HPMC K100M. The hysteresis area of HPMC K4M was larger than polymers of all other substitution levels studied. Previously, it has been shown that HPMC K4M tablets have a reduced water mobility within their gel layer (Rajabi-Siahboomi et al, 1996) and this has been proposed to explain slower drug release from HPMC K4M matrices. Here, it was also found that HPMC K4M retained more moisture within its structure than the other HPMCs studied.

The theory proposed by Young and Nelson (1967a, 1967b) assumes that three mechanisms exist by which water can associate with biological materials. These include adsorption of water onto the material surface to form initially a monomolecular layer followed by formation of multimolecular layers of water molecules. A certain amount of water is also transferred into the material and is known as absorbed moisture. The Young and Nelson theory (1967a, 1967b) was applied to the water vapour sorption data for all the HPMCs studied. The calculated data fitted closely with the experimental data indicating that the Young-Nelson theory may be accurately applied to characterise the interaction of water vapour with HPMC polymers. Polymer methoxyl/ hydroxypropoxyl substitution ratio was related to the water distribution as calculated using the Young-Nelson theory. The HPMC K-series have shown a good fit with the Young-Nelson model in agreement with previous work (Nokhodchi, 1996; Nokhodchi et al, 1997).

The amount of water tightly bound to the polymer was calculated using the method proposed by Ford and Mitchell (1995). The number of moles of BW per PRU was dependent on polymer molecular weight and substitution type as well as gel storage time. It was assumed that the amount of bound water present in the gels after 96h

gives a more accurate reflection of the water distribution within the gels due to an increased equilibration time. A number of conclusions were drawn regarding the amount of water bound to selected polymers based on the degree of substitution of hydrophilic and hydrophobic substituents on the polymer backbone. MC A4M gels contained the lowest amount of bound water of all the polymers studied after 96h storage. This may be linked to the structure of methylcellulose which has a high hydrophobic methoxyl content with no hydrophilic hydroxypropoxyl substitution. Such a structure will not favour large amounts of water binding to the polymer. In contrast, HPC contains no hydrophobic methoxyl substituents and only hydrophilic hydroxypropoxyl substituents and it was found that HPC gel systems contained large quantities of bound water. No loosely bound water is visible in 5 - 30 % (w/w) HPC gels and it is hypothesised that water attached to the polymer in this case is of the non-freezing bound type only. HPMC E4M and HPMC F4M gels have similar bound water contents after 96h. This may be a reflection of similar percentages of methoxyl substituents. The majority of polymers studied showed an increase in their bound water content from 24 to 96h storage. In contrast, HPMC K4M, HPMC E4M and MC A4M all showed a decrease in their bound water content during this equilibration period. For gels stored for 96h, an increase in the bound water content is visible with an increase in polymer molecular weight within the HPMC K-series. It is possible that as molecular weight increases, changes occur in the 3-D structure of the polymer due to folding of the polymer chains or changes in substitution along the cellulose backbone. The bound water content of the HPMC K-series of polymers has previously been characterised using the calculation methods proposed by Ford and Mitchell (1995) and Sung (1978) (Nokhodchi et al, 1997). The values reported varied between 6 and 7 (method of Sung) or 5 and 6 (method of Ford and Mitchell) for gels stored for 4 days. A value of 6.6 moles per PRU was also reported by Ford and Mitchell (1995) for HPMC K15M gels. However in this study it was found that differences between the BW values obtained using the method of Sung in the current work and those quoted by Nokhodchi et al (1997) were explained by considering the sample preparation method employed. Nokhodchi et al (1997) concluded that neither particle size nor viscosity grade of the HPMC K-series of polymers had any significant effect on the amount of BW per PRU.

The Brunauer, Emmett and Teller (BET) (1938) equation, for calculation of surface area, was applied to water vapour sorption isotherm data to compare with the results of BET analysis which was carried out on cellulose ether powders using nitrogen as the adsorbate gas. The values for specific surface area (SSA) obtained when water vapour was employed as the adsorbate gas, were much larger in comparison to the corresponding SSA achieved when nitrogen gas was employed. It is thought that nitrogen provides a truer estimate of the SSA because physical adsorption onto accessible internal and external surfaces are measured. When water vapour is employed, water is thought to interact with the anhydroglucose molecules within the cellulose polymer chain (Zografi et al, 1984) thus providing a much larger SSA.

9.4 Influence of drugs on the water distribution within cellulose ether polymer gels

The presence of a drug in a matrix tablet will affect the water distribution within cellulose ether polymer gels by affecting the way in which water is bound to, or taken up by, the cellulose ether. The effect of both propranolol hydrochloride (a water soluble drug) and diclofenac sodium (a poorly water soluble drug) on the distribution of water within HPMC K15M polymers was studied using DSC, dielectric spectroscopy and TGA.

The influence of drugs on cellulose ether polymers of varying molecular weight and substitution type was characterised using DSC analysis. The shape and appearance of pre-endothemic events in DSC scans of 5 - 25% (w/w) HPMC K15M gels were influenced by the concentration of added propranolol hydrochloride. Addition of 50mM (1.479% w/w) propranolol hydrochloride influenced the appearance of pre-endothemic events in 5 - 25% (w/w) HPMC K100M gels after 24h hydration but did not influence the appearance of these events in 5 - 25% (w/w) HPMC K100LV, HPMC K4M or HPMC K15M gels. Similar concentrations of propranolol hydrochloride influenced the appearance of pre-endothemic events in 5 - 25% (w/w) HPMC F4M gels, but did not influence their appearance in 5 - 25% (w/w) HPC, HPMC E4M or MC A4M gels. Diclofenac sodium (50mM) has a major influence on

the appearance of pre-endothemic events in cellulose ether polymer gels. Incorporation of diclofenac sodium results in the appearance of pre-endothemic events in all HPMC K-series and in HPMC E4M, HPMC F4M and in MC A4M gels at all concentrations studied (5 - 25% w/w). However, in 5 - 25% (w/w) HPC gels no pre-endothemic events were visible after diclofenac sodium addition. Pre-endothemic events were visible in 25 - 35% (w/w) HPC gels containing diclofenac sodium. The effect of drug addition on the bound water content of cellulose ether polymers after 24h storage was examined. In the majority of polymers studied, propranolol hydrochloride reduced the number of moles of bound water per PRU. This is in agreement with previous work in which the influence of propranolol hydrochloride on the interaction of water and polymer was examined by DSC Mitchell et al (1989) and in cloud-point studies (Mitchell et al, 1990a). This may be due to propranolol hydrochloride 'salting in' the polymer i.e. making it more soluble. By increasing the solubility of the polymer, less water is required to fully hydrate it (Mitchell et al, 1993c), and as a result less water is bound. In the majority of polymers studied, addition of diclofenac sodium reduced the amount of water binding to the polymer in comparison to that bound in the absence of drug. However, more water was required to fully hydrate the polymer in the presence of diclofenac sodium in comparison with the effects seen upon addition of propranolol hydrochloride. Diclofenac sodium 'salts out' cellulose ether polymers making them less soluble. This is in agreement with previous work which reported that diclofenac sodium decreased the hydration of HPMC polymers (Rajabi-Siahboomi et al, 1994) and modified the internal gel structure of HPMC matrices (Binns et al, 1990; Melia et al, 1990).

If different types of water are present in HPMC K15M gels which evaporate at different temperatures, then the presence of added drug, which interferes with the water distribution within the gel, should affect the appearance of these different water types in dTGA scans. The effect of drug addition on the interaction between water and HPMC K15M gels was analysed using TGA. The appearance of the evaporation events visible when propranolol hydrochloride (50mM) was added to HPMC K15M gels were similar to those seen in the absence of drug. In contrast, HPMC K15M gels

containing diclofenac sodium (50mM) showed poor separation of evaporation events at all scanning rates studied. Similar results occurred when gels containing drugs were scanned in vented sample pans. DSC studies have previously shown that diclofenac sodium caused an increase in polymer BW content in the majority of polymers studied. This increase in BW content may interfere with the melting events in these gel systems as detected by TGA. TGA kinetic studies were completed on the water evaporation process from HPMC K15M gels in the absence and presence of drugs. The activation energy (E_a) of dehydration of HPMC K15M gels scanned in both open and vented sample pans was influenced by the conversion (or % weight loss) chosen. The activation energy is described as the energy barrier or threshold that must be overcome to enable water to evaporate from the gels. The activation energy was also influenced by the build up of water vapour pressure in gels scanned in vented sample pans. Kinetic analysis failed to differentiate any effects resulting from addition of either propranolol hydrochloride or diclofenac sodium to HPMC K15M gels.

The melting of ice within HPMC K15M gels studied by dielectric spectroscopy was found to be affected by the addition of both propranolol hydrochloride and diclofenac sodium. The magnitude of the dielectric response over a temperature range of -30°C to $+20^{\circ}\text{C}$ at frequencies of 1 and 100Hz, was increased in gels containing propranolol hydrochloride in comparison with gels containing diclofenac sodium. It was hypothesised that different molar ratios of ionic species are released on drug dissociation with diclofenac sodium releasing less ionic species and showing a reduced dielectric response. In frequency sweeps at constant temperature, the nature of the dielectric response for HPMC K15M gels, which include either propranolol hydrochloride or diclofenac sodium is different when compared to the dielectric response of deionised water or HPMC K15M gels in the absence of drug. An increase in magnitude of both the capacitance and dielectric loss values occurs in the presence of added drug. This increase in magnitude is greater in HPMC K15M gels containing propranolol hydrochloride than those containing diclofenac sodium, which is consistent with the response previously seen in temperature scans at constant frequencies.

CHAPTER 10

CONCLUSIONS AND RECOMMENDATIONS FOR FUTURE WORK

Chapter 10 Conclusions and Recommendations for Future Work

10.1 Conclusions

The aims of this thesis were to characterise the interactions between water and cellulose ether polymers employed in hydrophilic matrices. Detailed analysis on the types of water existing within the gel layer are fundamental to the understanding of the mechanism of drug release and the factors that may affect it.

Distinctive thermal events appearing on the lower temperature side of the main endotherm for the melting of free water, were apparent in the DSC scans of HPMC K15M gels. These events were related to the presence of different types of water, melting at different temperatures, existing within the gels. Different types of water considered to be present within these systems include free water, freezing bound water and non-freezing bound water. Alternative explanations for the characteristic thermal events have been considered including the phenomenon of cold crystallization and overlapping ice melting and glass transition phase transitions.

Additional evidence for the existence of more than one type of water within HPMC K15M gels has been provided by both TGA and dielectric spectroscopy. Evidence of water evaporating in more than one event was visible from the first derivative of the TGA weight loss curve, which showed the rate of water loss from gels. Water which was associated with the polymer evaporated at higher temperatures than free water which evaporated at lower temperatures. LFDS has shown that deionised water scanned through 0°C at frequencies of 1 and 100 Hz exhibits a sharp increase in its dielectric response at the melting point of ice (0°C). In contrast, the melting point of ice was depressed in 25% (w/w) HPMC K15M gels in both the capacitance and dielectric loss responses. The shape of the dielectric response curves also indicated that in addition to the melting of free water, a number of other processes were occurring. These dielectric data are in agreement with the results of DSC and TGA studies which indicated that more than one type of water is present in HPMC K15M gels. The characteristic events occurring in HPMC K15M gels were found to be

dependent on polymer concentration (as seen in DSC, TGA and LFDS studies), polymer hydration time (DSC studies) and heating (DSC and TGA studies) and cooling (DSC studies) rates utilised during scanning.

Characteristic pre-endothermic events were present in the DSC scans of all polymer gels (5 – 25% w/w) studied which were dependent on polymer molecular weight and substitution type. Small pre-endothermic events were visible in HPC gels only at concentrations > 30 % (w/w). The amount of water bound per polymer repeating unit was dependent on hydration time and polymer molecular weight and substitution type and was related to the level of hydrophobic methoxyl and hydrophilic hydroxypropoxyl substitution. The dielectric response of polymer gels varied with both polymer molecular weight and substitution type in terms of both the pattern of melting and the temperature at which melting began.

Both propranolol hydrochloride (a water-soluble drug) and diclofenac sodium (a poorly water soluble drug) affected the distribution of water within cellulose ether polymer gels. Addition of propranolol hydrochloride influenced the appearance of pre-endothermic events in DSC scans of HPMC K100M and HPMC F4M gels only. Incorporation of diclofenac sodium resulted in appearance of pre-endothermic events in all polymers at all concentrations studied (5 – 25% w/w) except in 5 – 25% (w/w) HPC gels. In the majority of polymers studied, propranolol hydrochloride reduced the amount of water binding to the polymer. Diclofenac sodium reduced the amount of water binding to the polymer in comparison to that bound in the absence of drug. However, more water was required to fully hydrate the polymer in the presence of diclofenac sodium in comparison to the effects seen upon addition of propranolol hydrochloride. TGA studies identified differences in the separation of evaporation events in the absence and presence of drugs only when diclofenac sodium was added to HPMC K15M gels. Poor separation of evaporation events occurred after addition of diclofenac sodium to these gels at all scanning rates in both open and vented TGA pans. TGA kinetic analysis failed to differentiate any effects resulting from addition of either propranolol hydrochloride or diclofenac sodium to HPMC K15M gels. LFDS studies showed that drug addition affected the transitions occurring during the

melting of ice in HPMC K15M gels. The magnitude of the dielectric response was increased in gels containing propranolol hydrochloride in comparison to the response seen in gels containing diclofenac sodium.

The water vapour sorption/ desorption properties of cellulose ethers were investigated by dynamic vapour sorption. All polymers showed Type II isotherms irrespective of molecular weight and substitution type. Polymer molecular weight had little effect on their moisture sorption/ desorption behaviour. On the other hand, substitution level appeared to affect polymer water sorption/ desorption characteristics. HPMC K4M sorbed more water at all RH values compared to the other three substitution types. In addition, the hysteresis area of HPMC K4M was larger than HPMC E4M, HPMC F4M and MC A4M. Polymer methoxyl/ hydroxypropoxyl substitution ratio was related to water distribution as calculated using the Young-Nelson theory. The Young-Nelson theory fitted closely to the experimental water sorption/ desorption data indicating that this theory may be correctly applied to characterise the interaction of water vapour with HPMC polymers.

10.2 Recommendations for future work

(1) In this study, the interaction of water with individual polymers of varying molecular weight and substitution type were studied using DSC. Investigation of the interaction of water with polymer : polymer combinations (ionic and non-ionic polymers) using DSC may be useful to complete the study.

(2) In this thesis, DSC and TGA studies were carried out independently of each other. By using simultaneous DSC and TGA, bound (non-freezing) water may be directly determined by subtraction of bound (freezing) and free water (determined from DSC measurements) from total water (determined from TGA measurements).

(3) Further investigation is needed into the behaviour of HPMC F4M gels containing diclofenac sodium, as seen using DSC, in which the 'salting-out' effect of the drug on the polymer is not seen.

(4) The TGA work completed in this study provided information only on the evaporation of water from HPMC K15M gels. It may be interesting to investigate the evaporation of water from other cellulose ether polymers of varying molecular weights and substitution types, both in the absence and presence of drugs. Further investigations may be completed using vented sample pans in addition to open sample pans.

(5) Low Frequency Dielectric Spectroscopy studies in this thesis have highlighted the considerable potential of this technique to examine phase transitions occurring within cellulose ether gels. This work may be expanded to examine the effect of drugs, including non-ionizable drugs, on a range of other cellulose ether polymer gels.

(6) The effect of drug addition on the water vapour sorption/ desorption properties of cellulose ether polymers using DVS has yet to be studied and would expand the field in this particular area.

(7) There is considerable potential for examination of cellulose ether polymer systems using the relatively new technique of modulated DSC. This technique has the capacity to separate first and second order phase transitions. It has been suggested in some quarters that pre-endothemic events in various systems may be due to simultaneous melting (first order) and glass transitions (second order) occurring. If this is the case, modulated DSC may have the capacity to separate these events if indeed they are overlapping.

(8) The glass transition temperature of cellulose ether polymer films and the influence of moisture and drugs on this transition may be studied using modulated DSC.

REFERENCES

References

- Ahlneck, C. and Alderborn, G.,** Moisture adsorption and tableting. I. Effect on volume reduction properties and tablet strength for some crystalline materials, *Int. J. Pharm.*, 54, 131-141 (1989)
- Anderson, R. B.,** Modifications of the Brunauer, Emmett and Teller equation, *J. Amer. Chem. Soc.*, 68, 686-691 (1946)
- Aizawa, M. and Suzuki, S.,** Properties of water in macromolecular gels. III. Dilatometric studies of the properties of water in macromolecular gels, *Bull. Chem. Soc. Japan*, 44, 2967-2971 (1971)
- Aizawa, M., Mizuguchi, J., Suzuki, S., Hayashi, S., Suzuki, T., Mitomo, N. and Toyama, H.,** Properties of water in macromolecular gels. 4. Proton Magnetic Resonance studies of water in macromolecular gels, *Bull. Chem. Soc. Japan*, 45, 3031-3034 (1972)
- Alderman D. A.,** A review of cellulose ethers in hydrophilic matrices for oral controlled-release dosage forms, *Int. J. Pharm. Tech. & Prod. Mfr.*, 5 (3) 1-9 (1984)
- Angell, C. A., Oguni, M. and Sichina, W. J.,** Heat capacity of water at extremes of supercooling and superheating, *J. Phys. Chem.*, 86, 998-1002 (1982)
- Aoki, S., Ando, H., Ishii, M., Watanabe, S. and Ozawa, H.,** Water behavior during drug release from a matrix as observed using differential scanning calorimetry, *J. Control. Rel.*, 33, 365-374 (1995)
- Appelqvist, I. A. M., Cooke, D., Gidley, M. J. and Lane, S. J.,** Thermal properties of polysaccharides at low moisture: 1 - An endothermic melting process and water-carbohydrate interactions, *Carbohydrate Polym.*, 20, 291-299 (1993)

- Ashraf, M., Iuorno, V., Coffin-Beach, D., Anderson Evans, C. and Augsburger, L. L.,** A novel Nuclear Magnetic Resonance (NMR) imaging method for measuring the water front penetration rate in hydrophilic polymer matrix capsule plugs and its role in drug release, *Pharm. Res.*, 11 (5) 733-737 (1994)
- Astill, D. M., Hall, P. L. and McConnell, J. D. C.,** An automated vacuum microbalance for measurement of adsorption isotherms, *J. Phys. E: Sci. Instrum.*, 20, 19-21 (1987)
- Bamba, O., Puisieux, F., Marty, J.-P. and Carstensen, J. T.,** Release mechanisms in gel-forming sustained release preparations, *Int. J. Pharm.*, 2, 307-315 (1979)
- Banker, G., Peck, G., Jan, S., Pirakitikulr, P. and Taylor, D.,** Evaluation of hydroxypropyl cellulose and hydroxypropyl methyl cellulose as aqueous based film coatings, *Drug Dev. Ind. Pharm.*, 7 (6) 693-716 (1981)
- Bartell, L. S. and Huang, J.,** Supercooling of water below the anomalous range near 226K, *J. Phys. Chem.*, 98, 7455-7457 (1994)
- Barker, S. A., Craig, D. Q. M., Hill, R. M. and Taylor, K. M. G.,** Further studies on the low frequency dielectric spectroscopy of liposomes, *J. Pharm. Pharmacol.*, 41, 28P (1990)
- Bassez, M-P., Lee, J. and Robinson, G. W.,** Is liquid water really anomalous?, *J. Phys. Chem.*, 91, 5818-5825 (1987)
- Bergren, M. S.,** An automated controlled atmosphere microbalance for the measurement of moisture sorption, *Int. J. Pharm.*, 103, 103-114 (1994)

Bergren, M. S., Chao, R. S., Meulman, P. A., Sarver, R. W., Lyster, M. A., Havens, J. L. and Hawley, M., Solid phases of delavirdine mesylate, *J. Pharm. Sci.*, 85 (8) 834-841 (1996)

Berthold, J., Rinaudo, M. and Salmen, L., Association of water to polar groups; estimations by an adsorption model for ligno-cellulosic materials, *Colloids Surfaces A: Physicochem. Eng. Aspects*, 112, 117-129 (1996)

Binns, J. S., Davies, M. C. and Melia, C. D., A study of polymer hydration and drug distribution within hydrophilic polymer matrices by cryogenic SEM and EDX, *Proceed. Intern. Symp. Control. Rel. Bioact. Mater., Controll. Rel. Soc., Inc.*, 17, 339-340 (1990)

Binns, J. S., Craig, D. Q. M., Hill, R. M., Davies, M. C., Melia, C. D. and Newton, J. M., Dielectric characterisation of sodium alginate gels, *J. Mater. Chem.*, 2 (5) 545-549 (1992)

Biswas, A. B., Kumsah, C. A., Pass, G. and Phillips, G. O., The effect of carbohydrates on the heat of fusion of water, *J. Soln. Chem.*, 4 (7) 581-590 (1975)

Blair, T. C., Buckton, G., Beezer, A. E. and Bloomfield, S. F., The interaction of various types of microcrystalline cellulose and starch with water, *Int. J. Pharm.*, 63, 251-257 (1990)

Boчек, A. M. and Petropavlovsky, G. A., Structural-viscous characteristics of thermoreversible sol-gel transition of methylcellulose in systems with different critical dissolving temperatures, *Cell. Chem. Technol.*, 29, 567-574 (1995)

Boчек, A. M., Petropavlovskii, G. A. and Kallistov, O. V., Supramolecular structure of methyl cellulose in water and dimethylacetamide in the states of solution and transition to gel, *Russ. J. Appl. Chem.*, 69 (8) 1214-1218 (1996)

Bonferoni, M. C., Rossi, S., Ferrari, F., Bertoni, M. and Caramella, C., A study of three hydroxypropylmethylcellulose substitution types: effect of particle size and shape on hydrophilic matrix performances, *S. T. P. Pharma Sciences*, 6 (4) 277-284 (1996)

Bouwstra, J. A., Salomons-de Vries, M. A. and Van Miltenburg, J. C., The thermal behaviour of water in hydrogels, *Thermochim. Acta*, 248, 319-327 (1995)

British National Formulary (B. N. F.), Number 34 (September), BMA and RPSGB, 76-77, 421-422 (1997)

British Pharmacopoeia (B. P.), London, HMSO, 554-555 (1993)

Brunauer, S., Emmett, P. H. and Teller, E., Adsorption of gases in multimolecular layers, *J. Am. Chem. Soc.*, 60, 309-319 (1938)

Buckton, G. and Darcy, P., The use of gravimetric studies to assess the degree of crystallinity of predominantly crystalline powders, *Int. J. Pharm.*, 123, 265-271 (1995)

Buckton, G. and Darcy, P., Water mobility in amorphous lactose below and close to the glass transition temperature, *Int. J. Pharm.*, 136, 141-146 (1996)

Buri, P. and Doelker, E., Formulation of sustained release tablets II. Hydrophilic matrices, *Pharm. Acta. Kelv.*, 55 (7-8) 189-197 (1980)

Carstensen, J. T. (ed.), in: "Pharmaceutics of Solids and Solid Dosage Forms", Wiley, New York, 12-16 (1977)

Carstensen, J. T. and Li Wan Po, A., The state of water in drug decomposition in the moist solid state: Description and modelling, *Int. J. Pharm.*, 83, 87-94 (1992)

- Chatterjee, S. G., Ramarao, B. V. and Tien, C.,** Water-vapour sorption equilibria of a bleached-kraft paperboard - A study of the hysteresis region, *J. Pulp and Paper Sci.*, 23 (8), J366-J373 (1997)
- Christensen, G. L. and Dale, L. B.,** Sustained Release Tablet, *US Patent 3 065 143* (1962)
- Colombo, P., Gazzaniga, A., Conte, U., Sangali, M. E. and La Manna, A.,** Solvent front movement and release kinetics in compressed swellable matrices, *Proceed. Intern. Symp. Control. Rel. Bioact. Mater., Controll. Rel. Soc., Inc.*, 14, 83-84 (1987)
- Conte, U. and Maggi, L.,** Modulation of the dissolution profiles from Geomatrix multi-layer matrix tablets containing drugs of different solubility, *Biomaterials*, 17, 889-896 (1996)
- Conte, U., Maggi, L., Colombo, P. and La Manna, A.,** Multi-layered hydrophilic matrices as constant release devices (Geomatrix Systems), *J. Control. Rel.*, 26, 39-47 (1993)
- Craig, D. Q. M.,** Applications of low frequency dielectric spectroscopy to the pharmaceutical sciences, *Drug Dev. Ind. Pharm.*, 18 (11&12) 1207-1223 (1992)
- Craig, D. Q. M. (ed.):** "Dielectric Analysis of Pharmaceutical Systems", 1st ed. Taylor and Francis, London (1995)
- Craig, D. Q. M., Cook, G. D. and Parr, G. D.,** An investigation into B-cyclodextrin/acetoluide interactions using low frequency dielectric spectroscopy, *J. Mat. Sci.*, 27 (12) 3325-3329 (1992a)

Craig, D. Q. M., Tamburic, S., Buckton, G. and Newton, J. M., Analysis of bioadhesive Carbopol gels using dielectric spectroscopy and oscillatory rheometry, *Proceed. Intern. Symp. Control. Rel. Bioact. Mater., Controll. Rel. Soc., Inc.*, 19, 260-261 (1992b)

Craig, D. Q. M. and Newton, J. M., An investigation into the low-frequency dielectric response of polyethylene glycols, *J. Mat. Sci.*, 28, 405-410 (1993a)

Craig, D. Q. M., Hill, R. M. and Newton, J. M., Characterization of the structure of drug dispersions in polyethylene glycols using low frequency dielectric spectroscopy, *J. Mat. Sci.*, 28, 1978-1982 (1993b)

Craig, D. Q. M., Tamburic, S., Buckton, G. and Newton, J. M., An investigation into the structure and properties of Carbopol 934 gels using dielectric spectroscopy and oscillatory rheometry, *J. Control. Rel.*, 30, 213-223 (1994)

Dabbagh, M. A., Performance and characteristics of controlled release matrices composed of hydroxypropylmethylcellulose and other polymers. Ph. D. Thesis, Liverpool John Moores University (1996)

Dahlgren, L., Industrial utilisation, biotechnology, structure and properties, in: "Wood Cellulosics", **Kennedy, J., Fredrick, P. and Glyn, O. (eds.)**. Interscience, New York, 139-145 (1987)

Daly, P. B., Davis, S. S. and Kennerley, J. W., The effect of anionic surfactants on the release of chlorpheniramine from a polymer matrix tablet, *Int. J. Pharm.*, 18, 201-205 (1984)

Danjo, K., Nishio, F., Zhou, B. D. and Otsuka, A., Interactions between water and pharmaceutical polymers determined by water-vapor sorption measurement and differential scanning calorimetry, *Chem. Pharm. Bull.*, 43 (11) 1958-1960 (1995)

- Davè, V., Tamagno, M. and Foher, B.,** Hyaluronic acid - (hydroxypropyl) cellulose blends: a solution and solid state study, *Macromolecules*, 28, 3531-3539 (1995)
- Davies, R. E. M. and Rowson, J. M.,** Water-soluble cellulose derivatives. Factors affecting the viscosity of aqueous dispersions. Part 1, *J. Pharm. Pharmacol.*, 9, 672-680 (1957)
- Davies, R. E. M. and Rowson, J. M.,** Water-soluble cellulose derivatives. Factors affecting the viscosity of aqueous dispersions. Part 2, *J. Pharm. Pharmacol.*, 10, 30-39 (1958)
- Davies, R. E. M. and Rowson, J. M.,** Water-soluble cellulose derivatives. Uses as primary emulsifying agents. Part 1, *J. Pharm. Pharmacol.*, 12, 154-162 (1960)
- DeBoer, A. H. (ed.),** "The dynamical character of adsorption", 2nd ed., Clarendon Press, Oxford, 186-206 (1968)
- DeJong, G. I. W., Van den Berg, C., Kokelaar, A. J.,** Water vapour sorption behaviour of original and defatted wheat gluten, *Int. J. Food Sci. Tech.*, 31, 519-526 (1996)
- DeMali, K. A. and Williams, T. R.,** Determination of the content of water in bovine corneas by differential scanning calorimetry and thermogravimetric analysis, *Ophthalm. Res.*, 26, 105-109 (1994)
- Deodhar, S. and Luner, P.,** Measurement of bound (nonfreezing) water by differential scanning calorimetry, *ACS Symp. Ser.*, 127 (Water Polym.) 273 (1980)
- Doelker, H. E.,** in: "Hydrogels in Medicine and Pharmacy", **Peppas, N. A. (ed.)**, CRC Press, Florida, 164-166 (1987)

Donescu, D., Ciupitoiu, A., Gosa, K. and Languri, I., Water polymer interaction during emulsion polymerization of vinyl acetate, *Revue Roumaine de Chimie*, 38 (12) 1441-1448, (1993)

Dow Chemical Company, Handbook of Methocel cellulose ether products, Michigan (1983)

Duddu, S. P., Das, N. G., Kelly, T. P. and Sokoloski, T. D., Microcalorimetric investigation of phase transitions: 1. Is water desorption from theophylline. HOH a single-step process?, *Int. J. Pharm.*, 114, 247-256 (1995)

DVS Automated Water Sorption Analyser, Operations Manual, Surface Measurement Systems Ltd., Scientific and Medical Products Ltd., Shirley Institute, Manchester, U. K.

Entwistle, C. A. and Rowe, R. C., Plasticization of cellulose ethers used in the film coating of tablets, *J. Pharm. Pharmacol.*, 31, 269-272 (1979)

Fagan, P. G., Harrison, P. J. and Shankland, N., A Correlation between cloud point and disintegration of hydroxyalkylcellulose controlled release matrices, *J. Pharm. Pharmacol.*, 41 (suppl) 25P (1989)

Faroongsarng, D. and Peck, G. E., The swelling and water uptake of tablets III: moisture sorption behavior of tablet disintegrants, *Drug Dev. Ind. Pharm.*, 20 (5) 779-798 (1994a)

Faroongsarng, D. and Peck, G. E., Surface morphology study of solid powders evaluated by particle size distribution and nitrogen adsorption, *Drug Dev. Ind. Pharm.*, 20 (15) 2353-2367 (1994b)

Flynn, J. H. and Wall, L. A., A quick direct method for the determination of activation energy from thermogravimetric data, *Polymer Letters*, 4, 323-328 (1966)

Ford, J. L. and Mitchell, K., Thermal analysis of gels and matrix tablets containing cellulose ethers, *Thermochim. Acta*, 248, 329-345 (1995)

Ford, J. L., Rubinstein, M. H. and Hogan, J. E., Formulation of sustained release promethazine hydrochloride tablets using hydroxypropylmethylcellulose matrices, *Int. J. Pharm.*, 24, 327-338 (1985a)

Ford, J. L., Rubinstein, M. H. and Hogan, J. E., Propranolol hydrochloride and aminophylline release from matrix tablets containing hydroxypropylmethylcellulose, *Int. J. Pharm.*, 24, 339-350 (1985b)

Ford, J. L., Rubinstein, M. H. and Hogan, J. E., Dissolution of a poorly water soluble drug, Indomethacin, from hydroxypropylmethylcellulose controlled release tablets, *J. Pharm. Pharmacol.*, 37, 33P (1985c)

Ford, J. L., Rubinstein, M. H., McCaul, F., Hogan, J. E. and Edgar, P. J., Importance of drug-type, tablet shape and added diluents on drug release kinetics from hydroxypropylmethylcellulose matrix tablets, *Int. J. Pharm.*, 40, 223-234 (1987)

Galwey, A. K., Thermal reactions of selected solids including reactants that melt during chemical change, *J. Therm. Analys.*, 41, 267-286 (1994a)

Galwey, A. K., Magnitudes of Arrhenius parameters for decomposition reactions of solids, *Thermochim. Acta*, 242, 259-264 (1994b)

Galwey, A. K. and Brown, M. E., A theoretical justification for the application of the Arrhenius equation to kinetics of solid state reactions (mainly ionic crystals), *Proc. R. Soc. Lond.*, A 450, 501-512 (1995)

Gao, P. and Fagerness, P. E., Diffusion in HPMC Gels. 1. Determination of drug and water diffusivity by pulsed-field-gradient spin-echo NMR, *Pharm. Res.*, 12 (7) 955-964 (1995a)

Gao, P., Nixon, P. R. and Skoug, J. W., Diffusion in HPMC Gels. 2. Prediction of drug release rates from hydrophilic matrix extended-release dosage forms, *Pharm. Res.*, 12 (7) 965-971 (1995b)

Gao, P., Skoug, J. W., Nixon, P. R., Robert-Ju, T., Stemm, N. L. and Sung, K-C., Swelling of hydroxypropyl methylcellulose matrix tablets. 2. Mechanistic study of the influence of formulation variables on matrix performance and drug release, *J. Pharm. Sci.*, 85 (7) 732-740 (1996)

Gill, P. S., Sauerbrunn, S. R. and Reading, M., Modulated differential scanning calorimetry, *J. Therm. Analys.*, 40, 931-939 (1993)

Glicksman, M. (ed.), Cellulose Gums V. Methylcellulose and hydroxypropylmethylcellulose, in: "Gum Technology in the Food Industry", Academic Press, New York, 437-455 (1969)

Goring, D. A. I. and Timell, T. E., Molecular weight of native celluloses, *Tappi*, 45, 454 (1962)

Gregg, S. J. (ed.), in: "The Surface Chemistry of Solids," Reinhold, New York, N. Y., 24-26 (1951)

Greminger, G. K. J., Cellulose Derivatives, Ethers, in: "Encycl. Chem. Technol", **Eckroth, D.(ed.),** Wiley, New York, 143-163 (1979)

Greminger G. K. J. and Krumel K. L., Alkyl and hydroxyalkylcellulose, in: "Handbook of Water Soluble Gums and Resins", **Davidson R. L. (ed.)**, Academic Press, San Diego, 1-25 (1980)

Greminger G. K. J. and Savage A. B., Methylcellulose and its Derivatives, in: "Industrial Gums, Polysaccharides and their Derivatives", **Whistler R. L. (ed.)**, Academic Press, San Diego, 565-596 (1959)

Grover, J. A., Methylcellulose and its Derivatives, in: "Encycl. Polym. Sci. Technol.", **Whistler, R. L. and BeMiller, J. N. (eds.)**, Vol. 3. Interscience, New York, 475-504 (1993)

Haluska, R. J., Helms, D. S. and Porter, S. C., Application of a barrier film coating to achieve zero-order release from hydrophilic matrix tablets, *Proceed. Intern. Symp. Control. Rel. Bioact. Mater., Controll. Rel. Soc., Inc.*, 19, 12-13 (1992)

Hancock, B. C. and Zografi, G., The relationship between the glass transition temperature and the water content of amorphous pharmaceutical solids, *Pharm. Res.*, 11 (4) 471-477 (1994)

Haque, A. and Morris, E. R., Thermogelation of methylcellulose. Part 1: molecular structures and processes, *Carbohydr. Polym.*, 22, 161-173 (1993)

Haque, A., Richardson, R. K., Morris, E. R. and Caswell, D. C., Thermogelation of methylcellulose. Part 2: effect of hydroxypropyl substituents, *Carbohydr. Polym.*, 22, 175-186 (1993)

Haque, A., Morris, E. R. and Richardson, R. K., Polysaccharide substitutes for gluten in non-wheat bread, *Carbohydr. Polym.*, 25, 337-344 (1994)

- Harrison, G. (ed.):** "The Dynamic Properties of Supercooled Liquids", Academic Press, London (1976)
- Hatakeyama, T., Nakamura, K. and Hatakeyama, H.,** Determination of bound water contents adsorbed on polymers by differential scanning calorimetry, *Netsusokutei*, 6 (2) 50-52 (1979)
- Hatakeyama, T., Yamauchi, A. and Hatakeyama, H.,** Studies on bound water in poly(vinyl alcohol), *Eur. Polym. J.*, 20 (1) 61-64 (1984)
- Hatakeyama, T., Nakamura, K., Yoshida, H. and Hatakeyama, H.,** Phase transition on the water-sodium poly(styrenesulfonate) system, *Thermochim. Acta*, 88, 223-228 (1985)
- Hatakeyama, T., Yoshida, H. and Hatakeyama, H.,** A differential scanning calorimetry study of the phase transition of the water-sodium cellulose sulphate system, *Polymer*, 28, 1282-1286 (1987)
- Hatakeyama, T., Nakamura, K. and Hatakeyama, H.,** Determination of bound water content in polymers by DTA, DSC and TG, *Thermochim. Acta*, 123, 153-161 (1988)
- Hatakeyama, T., Nakamura, K., Yoshida, H. and Hatakeyama, H.,** Mesomorphic properties of highly concentrated aqueous solutions of polyelectrolytes from saccharides, *Food Hydrocolloids*, 3 (4) 301-311 (1989)
- Hatakeyama, T., Hatakeyama, H. and Nakamura, K.,** Non-freezing water content of mono- and divalent cation salts of polyelectrolyte-water systems studied by DSC, *Thermochim. Acta*, 253, 137-148 (1995)
- Hatakeyama, H. and Hatakeyama, T.,** Interaction between water and hydrophilic polymers, *Thermochim. Acta*, 308, 3-22 (1998)

Heymann, E., Studies on sol-gel transformations 1. The inverse sol-gel transformation of methyl cellulose in water, *Trans. Faraday*, 31, 849 (1935)

Heymann, E., Studies on sol-gel transformations. 2. Dilatometric investigations on iron hydroxide, gelatin, methylcellulose, silic acid and viscose, *Trans. Faraday*, 462-473 (1936)

Heymann, E., Bleakley, H. G. and Docking, R., Studies on the Lyotropic series .1. The adsorption of salts on methylcellulose, *J. Phys. Chem.*, 42, 353-368 (1938)

Higuchi, T., Mechanism of sustained-action medication. Theoretical analysis of rate of release of solid drugs dispersed in solid matrices, *J. Pharm. Sci.*, 52 (12) 1145-1149 (1963)

Higuchi, A. and Iijima, T., DSC investigation of the states of water in poly(vinyl alcohol) membranes, *Polymer*, 26, 1207-1211 (1985)

Hill, R. M. and Jonsher, A. K., The dielectric behaviour of condensed matter and its many-body interpretation, *Contemp. Phys.*, 24 (1) 75-110 (1983)

Hill, R. M. and Pickup, C., Barrier effects in dispersive media, *J. Mat. Sci.*, 20, 4431-4444 (1985)

Hodge, R. M., Edward, G. H. and Simon, G. P., Water absorption and states of water in semi-crystalline poly (vinyl alcohol) films, *Polymer*, 37 (8) 1371-1376 (1996)

Hogan, J. E., Hydroxypropylmethylcellulose sustained release technology, *Drug Dev. Ind. Pharm.*, 15 (6&7) 975-999 (1989)

- Hollenbeck, R. G., Peck, G. E. and Kildsig, D. O.**, Application of immersional calorimetry to investigation of solid-liquid interactions: microcrystalline cellulose-water system, *J. Pharm. Sci.*, 64 (11) 1599-1606 (1978)
- Huang, V. T., Haynes, L., Levine, H. and Slade, L.**, Glass transitions in starch, gluten and bread as measured, *J. Therm. Analys.*, 47, 1289-1298 (1996)
- Huber, H. E., Dale, L. B. and Christenson, G. L.**, Utilization of hydrophilic gums for the control of drug release from tablet formulations.1. Disintegration and dissolution behavior, *J. Pharm. Sci.*, 55 (9) 974-976 (1966)
- Ibbett, R. N., Philp, K. and Price, D. M.**, ¹³C N. M. R. studies of the thermal behaviour of aqueous solutions of cellulose ethers, *Polymer*, 33 (19) 4087-4094 (1992)
- Ingold, C. K. (ed.)**: "Structure and mechanism in organic chemistry", 2nd ed., 386-417, 559-563, Cornell University Press, London (1969) -
- Johnson, J. L., Holinej, J. and Williams, M. D.**, Influence of ionic strength on matrix integrity and drug release from hydroxypropyl cellulose compacts, *Int. J. Pharm.*, 90, 151-159 (1993)
- Joshi, H. N. and Topp, E. M.**, Hydration in hyaluronic acid and its esters using differential scanning calorimetry, *Int. J. Pharm.*, 80, 213-225 (1992)
- Joshi, H. N. and Wilson, T. D.**, Calorimetric studies on HPMC, *Proceed. Intern. Symp. Control. Rel. Bioact. Mater., Controll. Rel. Soc., Inc.*, 19, 262-263 (1992)
- Joshi, H. N. and Wilson, T. D.**, Calorimetric studies of dissolution of hydroxypropyl methylcellulose E5 (HPMC E5) in water, *J. Pharm. Sci.*, 82 (10) 1033-1038 (1993)

Ju, R. T. C., Nixon, P. R. and Patel, M. V., Drug release from hydrophilic matrices. 1. New scaling laws for predicting polymer and drug release based on the polymer disentanglement concentration and the diffusion layer, *J. Pharm. Sci.*, 84 (12) 1455-1463 (1995a)

Ju, R. T. C., Nixon, P. R., Patel, M. V. and Tong, D. M., Drug release from hydrophilic matrices. 2. A mathematical model based on the polymer disentanglement concentration and the diffusion layer, *J. Pharm. Sci.*, 84 (12) 1464-1477 (1995b)

Just, E. K. and Majewicz, T. G., Cellulose Ethers, in: "Encycl. Polym. Sci. Eng", **Kroschwitz, J. I. (ed.)**, Vol. 3. Wiley, New York, 226-269 (1985)

Kakar, S. and Bettelheim, F. A., The hydration of actin, *Investig. Ophthalmol. Vis. Sci.*, 32 (3) 562-566 (1991)

Kararli, T. T., Hurlbut, J. B. and Needham, T. E., Glass-Rubber transitions of cellulose polymers by dynamic mechanical analysis (DMA), *J. Pharm. Sci.*, 79 (9) 845-848 (1990)

Kato, T., Yokoyama, M. and Takahashi, A., Melting temperatures of thermally reversible gels. IV. Methyl cellulose-water gels, *Colloid & Polymer Sci.*, 256, 15-21 (1978)

Kato, T., Tokuya, T. and Takahashi, A., Measurements of molecular weight and molecular weight distributions for water-soluble cellulose derivatives used in the film coating of tablets, *Kobunshi Ronbunshu*, 39 (4) 293-298 (1982)

Katz, J. R. and Muschter, F. J. F., Die lyotrope reihe bei der quellung und ihre ausbreitung auf organische, auch nichtionisierende substanzen, *Biochem-Z*, 257, 385-396 (1933)

Khan, F. and Pilpel, N., The effect of particle size and moisture on the tensile strength of microcrystalline cellulose powder, *Powd. Tech.*, 48, 145-150 (1986)

Khan, F. and Pilpel, N., An investigation of moisture sorption in microcrystalline cellulose using sorption isotherms and dielectric response, *Powder Tech.*, 50, 237-241 (1987)

Khankari, R. K., Law, D. and Grant, D. J. W., Determination of water content in pharmaceutical hydrates by differential scanning calorimetry, *Int. J. Pharm.*, 82, 117-127 (1992)

Kim, E. H., Moon, B. Y., Jeon, S. and Jhon, M. S., The nature of water in copolymer hydrogels, *Bull. Kor. Chem. Soc.*, 4 (6) 251-256 (1983)

Kim, H. and Fassihi, R., Application of a binary polymer system in drug release rate modulation. 1. Characterization of release mechanism, *J. Pharm. Sci.*, 86 (3) 316-322 (1997)

Klug, E. D., Some properties of water-soluble hydroxyalkyl celluloses and their derivatives, *J. Polym. Sci.*, Part C, No.36, 491-508 (1971)

Kontny, M. J., Grandolfi, G. P. and Zografi, G., Water vapor sorption of water-soluble substances: Studies of crystalline solids below their critical relative humidities, *Pharm. Res.*, 4 (2) 104-112 (1987)

Kuhn, W., Moser, P. and Majer, H., Aggregation von Methylcellulose in Lösung, *Helv. Chim. Acta*, 44, 770-791 (1961)

Kumsah, C. A., Pass, G. and Phillips, G. O., The interaction between sodium carboxymethylcellulose and water, *J. Soln. Chem.*, 5 (11) 799-806 (1976)

Kyritsis, A., Pissis, P., Gómez Ribelles, J. L. and Monleón Pradas, M., Polymer-water interactions in poly(hydroxyethyl acrylate) hydrogels studied by dielectric, calorimetric and sorption isotherm measurements, *Polymer Gels and Networks*, 3, 445-469 (1995)

Lapidus, H. and Lordi, N. G., Some factors affecting the release of a water-soluble drug from a compressed hydrophilic matrix, *J. Pharm. Sci.*, 55 (8) 840-843 (1966)

Lapidus, H. and Lordi, N. G., Drug release from compressed hydrophilic matrices, *J. Pharm. Sci.*, 57, 1292-1301 (1968)

Lee, H. B., Jhon, M. S. and Andrade, J. D., Nature of water in synthetic hydrogels.1. Dilatometry, specific conductivity, and differential scanning calorimetry of polyhydroxyethyl methacrylate, *J. Coll. Interf. Sci.*, 51 (2) 225-231 (1975)

Lee, P. I., Kinetics of drug release from hydrogel matrices, *J. Control. Rel.*, 2, 277-288 (1985)

Lee, P. I. and Kim, C-J., Probing the mechanisms of drug release from hydrogels, *J. Control. Rel.*, 16, 229-236 (1991)

Lee, P. I. and Peppas, N. A., Prediction of polymer dissolution in swellable controlled release systems, *J. Control. Rel.*, 6, 207-215 (1987)

Levine, H. and Slade, L., Water as a plasticizer: physico-chemical aspects of low-moisture polymeric systems, in: "Water Science Reviews", **Franks, F. (ed.)**. Cambridge University Press, Cambridge, 79-185 (1988)

Levy, G. and Schwarz, T. W., The effect of certain additives on the gel point of methylcellulose, *J. Am. Pharm. Assoc.*, 47, 44-46 (1958)

Lillienfeld, L., *Chem. Abstracts* 73839, 3839-3840 (1913)

Ling, G. N., in: "Water Structure at the Water-Polymer Interface", **Jellinek, H. H. G.** (ed.), Plenum Press, London, 4-13 (1972)

Liron, Z., Wright, R. L. and McDougal, J. N., Water diffusivity in porcine stratum corneum measured by a thermal gravimetric analysis technique, *J. Pharm. Sci.*, 83 (4) 457-462 (1994)

Liu, C-H., Chen, S-C., Kao, Y-H., Kao, C-C., Soloski, T. D. and Sheu, M-T., Properties of hydroxypropylmethylcellulose granules produced by water spraying, *Int. J. Pharm.*, 100, 241-248 (1993)

Liu, C-H., Kao, Y-H., Chen, S-C., Sokoloski, T-D. and Sheu, M-T., In-vitro and in-vivo studies of the diclofenac sodium controlled-release matrix tablets, *J. Pharm. Pharmacol.*, 47, 360-364 (1995)

Liu, H. and Lelièvre, J., Effects of heating rate and sample size on differential scanning calorimetry traces of starch gelatinized at intermediate water levels, *Starch-Starke*, 43 (6) 225-227 (1991)

Liu, H. and Lelièvre, J., Transitions in frozen gelatinized-starch systems studied by differential scanning calorimetry, *Carbohydr. Polym.*, 19, 179-183 (1992)

Loewit, K., In vitro immobilization of human spermatozoa with hydroxypropylmethylcellulose, *Contraception*, 15 (2) 233-237 (1977)

Lorand, E. J., Cellulose Ethers. Variation of physical properties with composition, *Ind. Eng. Chem.*, 30, 527 (1938)

Malamataris, S. and Karidas, T., Effect of particle size and sorbed moisture on the tensile strength of some tableted hydroxypropylmethylcellulose (HPMC) polymers, *Int. J. Pharm.*, 104, 115-123 (1994)

Malamataris, S., Karidas, T. and Goidas, P., Effect of particle size and sorbed moisture on the compression behaviour of some hydroxypropylmethylcellulose (HPMC) polymers, *Int. J. Pharm.*, 103, 205-215 (1994)

Martin, A., Swarbrick, J. and Cammarata, A. (eds.): "Physical Pharmacy", 3rd ed. Lea and Febiger, Philadelphia, 74, 628-631 (1983)

Martindale: The Extra Pharmacopoeia, 31st ed., RPSGB, London, 36-37, 936-937 (1996)

Matsumoto, K., Nakai, Y., Yonemochi, E., Oguchi, T. and Yamamoto, K., Physicochemical characteristics of porous crystalline cellulose and formation of an amorphous state of ethenzamide by mixing, *Int. J. Pharm.*, 108, 167-172 (1994)

Mattha, A. G., Influence of some pharmaceutical adjuvants on the syneresis of *Plantago albicans* (Psyllium) seed gum gels, *Pharm. Acta. Helv.*, 52 (10) 233-235 (1977)

Matveeva, E. S., Diaz Calleja, R. and Parkhutik, V. P., Thermogravimetric and calorimetric studies of water absorbed in polyaniline, *Synthetic Metals*, 72, 105-110 (1995)

McBrierty, V. J., Wardell, G. E., Keely, G. E., O'Neill, E. P. and Prasad, M., The characterization of water in peat, *Soil Soc. Am. J.*, 60 (4) 991-1000 (1996)

Melia, C. D., Hydrophilic matrix sustained release systems based on polysaccharide carriers, *Crit. Rev. Drug Carrier Syst.*, 8 (4) 395-421 (1991)

- Melia, C. D., Binns, J. S. and Davies, M. C.,** Polymer hydration and drug distribution within the gel layer of hydrophilic matrix devices during drug release, *J. Pharm. Pharmacol.*, 42, 125 (1990)
- Mitchell, K.,** A study of factors controlling drug release from matrices containing cellulose ethers. Ph. D. Thesis, Liverpool John Moores University (1992)
- Mitchell, K., Ford, J. L., Armstrong, D. J., Elliott, P. N. C., Rostron, C. and Hogan, J. E.,** Differential thermal analysis of HPMC gels: Influence of water content and propranolol HCL, *J. Pharm. Pharmacol.*, 41, 59P (1989)
- Mitchell, K., Ford, J. L., Armstrong, D. J., Elliott, P. N. C., Rostron, C. and Hogan, J. E.,** The influence of additives on the cloud point, disintegration and dissolution of HPMC gels and matrix tablets, *Int. J. Pharm.*, 66, 233-242 (1990a)
- Mitchell, K., Sogo, T., Ford, J., Armstrong, D., Elliott, P., Rostron, C. and Hogan, J.,** Temperature effects on the dissolution of promethazine HCL from HPMC matrix tablets, *J. Pharm. Pharmacol.*, 42, 124P (1990b)
- Mitchell, K., Ford, J. L., Armstrong, D., Elliott, P., Rostron, C. and Hogan, J.,** The influence of substitution type on the performance of methylcellulose and hydroxypropylmethylcellulose in gels and matrices, *Int. J. Pharm.*, 100, 143-154 (1993a)
- Mitchell, K., Ford, J. L., Armstrong, D. J., Elliott, P. N. C., Rostron, C. and Hogan, J. E.,** The influence of concentration on the release of drugs from gels and matrices containing Methocel, *Int. J. Pharm.*, 100, 155-163 (1993b)
- Mitchell, K., Ford, J. L., Armstrong, D. J., Elliott, P. N. C., Hogan, J. E. and Rostron, C.,** The influence of drugs on the properties of gels and swelling characteristics of matrices containing methylcellulose or HPMC, *Int. J. Pharm.*, 100, 165-173 (1993c)

Mitchell, K., Ford, J. L., Armstrong, D. J., Elliott, P. N. C., Hogan, J. E. and Rostron, C., The influence of the particle size of hydroxypropylmethylcellulose K15M on its hydration and performance in matrix tablets, *Int. J. Pharm.*, 100, 175-179 (1993d)

Morrison, J. L. and Dzieciuch, M. A., *Can. J. Chem.*, 37, 1379 (1959)

Morss, N. M. and Ogg, J., Some special characteristics of cellulose ethers, *Soc. Chem. Ind. Mono.*, 24, 46-56 (1966)

Muffett, D. J. and Snyder, H. E., Measurement of unfrozen and free water in soy proteins by differential scanning calorimetry, *J. Agric. Food Chem.*, 28, 1303-1305 (1980)

Mullin, J. W., in: "Crystallization", 3rd Ed. Butterworths, Oxford (1993)

Munday, D. L., Bimodal in vitro release from polymeric matrix tablets containing centralised drug cores, *S. T. P. Pharma Sciences*, 6 (3) 182-187 (1996)

Murase, N., Origin of an endothermic trend observed prior to ice crystallization exotherm in the DSC rewarming trace for polymer gels, *Cryo-Letters*, 14, 365-374 (1993)

Nakamura, K., Hatakeyama, T. and Hatakeyama, H., Studies on bound water of cellulose by differential scanning calorimetry, *Text. Res. J.*, 1, 607-613 (1981)

Nakamura, K., Hatakeyama, T. and Hatakeyama, H., Effect of bound water on tensile properties of native cellulose, *Text. Res. J.*, 53, 682-689 (1983a)

Nakamura, K., Hatakeyama, T. and Hatakeyama, H., Relationship between hydrogen bonding and bound water in polyhydroxystyrene derivatives, *Polymer*, 24, 871-876 (1983b)

Nakano, M., Ohmori, N., Ogata, A., Sugimoto, K., Tobino, Y., Iwaoku, R. and Juni, K., Sustained release of theophylline from hydroxypropyl-cellulose tablets, *J. Pharm. Sci.*, 72, 378-380 (1983)

Neely, W. B., Solution properties of polysaccharides. IV. Molecular weight and aggregate formation in methylcellulose solutions, *J. Polym. Sci.*, 1, 311-320 (1963)

Nelson, R. A., The determination of moisture transitions in cellulosic materials using differential scanning calorimetry, *J. Appl. Polym. Sci.*, 21, 645-654 (1977)

Nicholson, M. D. and Merritt, F. M., Cellulose Ethers, in: "Cellulose Chemistry and its application", **NeVell, T. P. (ed.)**, Academic Press, San Diego, 363-383 (1985)

Noel, T. R., Parker, R. and Ring, S. G., A comparative study of the dielectric relaxation behaviour of glucose, maltose, and their mixtures with water in the liquid and glassy states, *Carbohydrate Research*, 282, 193-206 (1996)

Nokhodchi, A., Ford, J. L. and Rubinstein, M. H., Studies on the interaction between water and hydroxypropylmethylcellulose, *J. Pharm. Sci.*, 86 (5) 608-615 (1997)

Nokhodchi, A., The compaction properties of hydroxypropylmethylcellulose and ibuprofen. Ph. D. Thesis, Liverpool John Moores University (1996)

Ohno, H., Shibayama, M. and Tsuchida, E., DSC analyses of bound water in the microdomains of interpolymer complexes, *Die Makromolekulare Chemie*, 184, 1017-1024 (1983)

Okhamafe, A. O. and York, P., Interaction phenomena in some aqueous-based tablet coating polymer systems, *Pharm. Res.*, 2, 19-23 (1985)

- Oksanen, C. A. and Zografi, G.**, The relationship between the glass transition temperature and water vapor absorption by poly(vinylpyrrolidone), *Pharm. Res.*, 7 (6) 654-657 (1990)
- Oksanen, C. A. and Zografi, G.**, Molecular mobility in mixtures of absorbed water and solid poly(vinylpyrrolidone), *Pharm. Res.*, 10 (6) 791-799 (1993)
- Omelczuk, M. O. and McGinity, J. W.**, The influence of thermal treatment on the physical-mechanical and dissolution properties of tablets containing Poly (DL-Lactic Acid), *Pharm. Res.*, 10 (4) 542-548 (1993)
- Parker, R. and Ring, S. G.**, Diffusion in maltose-water mixtures at temperatures close to the glass transition, *Carbohydrate Research*, 273, 147-155 (1995)
- Partington, J.R. (ed.)**: "General and Inorganic Chemistry", 2nd ed. MacMillan and Co. Ltd., London, 64 (1954)
- Pathmanathan, K. and Johari, G. P.**, Relaxation and crystallization of water in a hydrogel, *J. Chem. Soc. Faraday Trans.*, 90 (8) 1143-1148 (1994)
- Peppas, N. A.**, Release of bioactive agents from swellable polymers: Theory and experiments, in: "Recent Advances in Drug Delivery Systems", **Anderson, J. M. and Kim, S. W. (eds.)**. Plenum Press, New York and London, 279-289 (1984)
- Peppas, N. A.**, Analysis of fickian and non-fickian drug release from polymers, *Pharm. Acta. Helv.*, 60 (4) 110-111 (1985)
- Peppas, N. A. and Sahlin, J. J.**, A simple equation for the description of solute release. 3. Coupling of diffusion and relaxation, *Int. J. Pharm.*, 57, 169-172 (1989)

Perez-Marcos, B., Ford, J. L., Armstrong, D. J., Elliott, P. N. C., Rostron, C. and Hogan, J. E., Release of propranolol hydrochloride from matrix tablets containing hydroxypropylmethylcellulose K4M and carbopol 974, *Int. J. Pharm.*, 111, 251-259 (1994)

Perkin-Elmer DSC7 Operator's Manual, Perkin-Elmer Corp., Norwalk, Connecticut (1986)

Perkin-Elmer TGA 7 Decomposition Kinetics Software Kit, Perkin-Elmer Corp., Norwalk, Connecticut (1989)

Perkin-Elmer TGA 7 Operators Manual, Perkin-Elmer Corp., Norwalk, Connecticut (1986)

Pham, A. T. and Lee, P. I., Probing the mechanisms of drug release from hydroxypropylmethylcellulose matrices, *Pharm. Res.*, 11 (10) 1379-1384 (1994)

Philippoff, W., *Cellulosechemie* 17, 57 (1936)

Pickett, G., Modification of the Brunauer-Emmett-Teller theory of multimolecular adsorption, *J. Amer. Chem. Soc.*, 67, 1958-1962 (1945)

Porter, S. C., Controlled-release film coatings based on ethylcellulose, *Drug Dev. Ind. Pharm.*, 15 (10) 1495-1521 (1989)

Porter, S. C. and Ridgway, K., An evaluation of the properties of enteric coating polymers: measurement of glass transition temperature, *J. Pharm. Pharmacol.*, 35, 341-344 (1983)

Proudfoot, S. G., Dosage regimens: their influence on the concentration-time profile of a drug in the body, in: "Pharmaceutics: The Science of Dosage Form design", **Aulton, M. (ed.)**, 1st ed. Churchill Livingstone, Edinburgh, 191-211 (1988)

Rajabi-Siahboomi, A. R., Bowtell, R. W., Mansfield, P., Henderson, A., Davies, M. C. and Melia, C. D., Structure and behaviour in hydrophilic matrix sustained release dosage forms: 2. NMR-imaging studies of dimensional changes in the gel layer and core of HPMC tablets undergoing hydration, *J. Control. Rel.*, 31 (2) 121-128 (1994)

Rajabi-Siahboomi, A. R., Bowtell, R. W., Mansfield, P., Davies, M. C. and Melia, C. D., Structure and behaviour in hydrophilic matrix sustained release dosage forms: 4. Studies of water mobility and diffusion coefficients in the gel layer of HPMC tablets using NMR Imaging., *Pharm. Res.*, 13 (3) 376-380 (1996)

Ranby, B. G., Accessibility of hydrogen bonds in cellulose, *J. Soc. Text. Cell. Ind. Japan*, 19, 695-704 (1963)

Ranga Rao, K. V. and Padmalatha Devi, K., Swelling controlled-release systems: recent developments and applications, *Int. J. Pharm.*, 48, 1-13 (1988)

Ranga Rao, K. V., Padmalatha Devi, K. and Buri, P., Influence of molecular size and water solubility of the solute on its release from swelling and erosion controlled polymeric matrices, *J. Control. Rel.*, 12, 133-141 (1990)

Rasmussen, M. D. and Akinc, M., Microcomputer-controlled gravimetric adsorption apparatus, *Rev. Sci. Instrum.*, 54 (11) 1558-1564 (1983)

Rasmussen, D. H., MacKenzie, A. P., Angell, C. A. and Tucker, J. C., Anomalous heat capacities of supercooled water and heavy water, *Science*, 181, 342-344 (1973)

Ratto, J., Hatakeyama, T. and Blumstein, R. B., Differential scanning calorimetry investigation of phase transitions in water/ chitosan systems, *Polymer*, 36 (15) 2915-2919 (1995)

Rees, D. A., Structure, conformation and mechanism in the formation of polysaccharide gels and networks, in: "Advances in Carbohydrate Chemistry and Biochemistry", **Wolfrom, M. L. and Tipson, R. S. (eds.)**. Academic Press, San Diego, 267 (1969)

Rees, D. A., Polysaccharide Gels: A molecular view, *Chem. and Ind.*, 19th August, 630-637 (1972)

Ritger, P. L. and Peppas, N. A., A simple equation for description of solute release 1. Fickian and non-fickian release from non-swellable devices in the form of slabs, spheres, cylinders or discs, *J. Control. Rel.*, 5, 23-36 (1987a)

Ritger, P. L. and Peppas, N. A., A simple equation for description of solute release II. Fickian and anomalous release from swellable devices, *J. Control. Rel.*, 5, 37-42, (1987b)

Roorda, W., Do hydrogels contain different classes of water?, *J. Biomat. Sci. Polym. Ed.*, 5 (5) 383-395 (1994)

Roorda, W. E., Bouwstra, J. A. and deVries, M. A., Thermal analysis of water in p(HEMA) hydrogels, *Biomaterials*, 9, 494-499 (1988a)

Roorda, W. E., Bouwstra, J. A., deVries, M. A. and Junginger, H. E., Thermal behaviour of poly hydroxy ethyl methacrylate (pHEMA) hydrogels, *Pharm. Res.*, 5 (11) 722-725 (1988b)

Roos, Y. and Karel, M., Water and molecular weight effects on glass transitions in amorphous carbohydrates and carbohydrate solutions, *J. Food Sci.*, 56 (6) 1676-1681 (1991)

Roots, J., Moseley, M. E. and Nystrom, B., NMR Study of the sol-gel transition of aqueous methyl cellulose, *Chemica Scripta*, 16 (5) 201-202 (1980)

Rowe, R. C., The effect of molecular weight on the properties of films prepared from hydroxypropyl methylcellulose, *Pharm. Acta. Helv.*, 51 (11) 330-334 (1976)

Rowe, R. C., The molecular weight and molecular weight distribution of hydroxypropylmethylcellulose used in the film coating of tablets, *J. Pharm. Pharmacol.*, 32 116-119 (1980)

Rowe, R. C., Molecular weight studies on hydroxypropyl methylcellulose phthalate (HP 55), *Acta Pharmaceutica Technologica*, 28 (2) 127-130 (1982a)

Rowe, R. C., The molecular weight of methylcellulose used in pharmaceutical formulation, *Int. J. Pharm.*, 11, 175-179 (1982b)

Rowe, R. C., Kotaras, A. D. and White, E. F. T., An evaluation of the plasticizing efficiency of the dialkyl phthalates in ethylcellulose films using the torsional braid pendulum, *Int. J. Pharm.*, 22, 57-62 (1984)

Rowland, S. P. and Wade, C. P., Microstructural order in cotton fibers by relative availability of O(3)H: Never-Dried Fibers, *J. Polym. Sci., Polymer Chem. Ed.*, 18, 2577-2583 (1980)

Rowland, S. P., Roberts, E. J. and Wade, C. P., Selective accessibilities of hydroxyl groups in the microstructure of cotton cellulose, *Text. Res. J.*, 39, 530 (1969)

- Rowland, S. P., Roberts, E. J. and Bose, J. L.,** Availability and state of order of hydroxyl groups on the surfaces of microstructural units of crystalline cotton cellulose, *J. Polym. Sci.*, A-19, 1431-1440 (1971)
- Rubel, G. O.,** A non-intrusive method for the measurement of water vapour sorption by bacterial spores, *J. Appl. Micro.*, 83, 243-247 (1997)
- Sadeghnejad, G. R., York, P. and Stanley-Wood, N. G.,** Water vapour interaction with pharmaceutical cellulose powders, *Drug Dev. Ind. Pharm.*, 12 (11-13) 2171-2192 (1986)
- Sadek, H. M. and Olsen, J. L.,** Determination of water-adsorption isotherms of hydrophilic polymers, *Pharm. Tech.*, Feb., 40-48 (1981)
- Sakellariou, P., Rowe, R. C. and White, E. F. T.,** The thermomechanical properties and glass transition temperatures of some cellulose derivatives used in film coating, *Int. J. Pharm.*, 27, 267-277 (1985)
- Salomon, J. L., Doelker, E. and Buri, P.,** Sustained release of a water-soluble drug from hydrophilic compressed dosage forms, *Pharm. Ind.*, 41 (8) 799-802 (1979)
- Sarkar, N.,** Thermal gelation properties of methyl and hydroxypropylmethylcellulose, *J. Appl. Polym. Sci.*, 24, 1073-1087 (1979)
- Sarkar, N.,** Kinetics of thermal gelation of methylcellulose and hydroxypropylmethylcellulose in aqueous solutions, *Carbohydr. Polym.*, 26, 195-203 (1995)
- Sarkar, N. and Walker, L. C.,** Hydration-dehydration properties of methylcellulose and hydroxypropylmethylcellulose, *Carbohydr. Polym.*, 27, 177-185 (1995)

Savage, A. B., Derivatives of cellulose ethers, in: "High Polymers, Structures and Properties of cellulose fibres", **Ott, E., Spurlin, H. M. and Graffin, M. W. (eds.)**. Interscience, New York, 785-810 (1954)

Savage, A. B., Temperature-viscosity relationships for water soluble cellulose ethers, *Ind. Eng. Chem.*, 49, 99-103 (1957)

Savage, A. B., Cellulose Ethers, *Encycl. Polym. Sci. Technol.*, 3, 459-510 (1965)

Savage, A. B., Young, A. E. and Maasberg, A. T., Structures and properties of cellulose ethers, in: "High Polymers, Structures and Properties of cellulose fibres", **Ott, E., Spurlin, H. M. and Graffin, M. W. (eds.)**. Interscience, New York, 882-958 (1954)

Schenz, T. W., Glass transitions and product stability - an overview, *Food Hydrocolloids*, 9 (4) 307-315 (1995)

Shaw, D. J. (ed.), "Introduction to Colloid and Surface Chemistry," 4th ed., Chapter 5: The solid-gas interface, Butterworth-Heinemann, Oxford, 115-136 (1989)

Sheu, M-T., Chou, H-L., Kao, C-C., Liu, C-H. and Sokoloski, T. D., Dissolution of diclofenac sodium from matrix tablets, *Int. J. Pharm.*, 85, 57-63 (1992)

Skoug, J. W., Mikelsons, M. V., Vigneron, C. N. and Stemm, N. L., Qualitative evaluation of the mechanism of release of matrix sustained release dosage forms by measurement of polymer release, *J. Control. Rel.*, 27, 227-245 (1993)

Slade, L. and Levine, H., Non-equilibrium melting of native granular starch: I Temperature location of the glass transition associated with gelatinization of A-type cereal starches, *Carbohydr. Polym.*, 8, 183-208 (1988)

Slade, L. and Levine, H., Beyond water activity: Recent advances based on an alternative approach to the assessment of food quality and safety, *Crit. Rev. Food Sci. Nutr.*, 30 (2-3) 115-360 (1991)

Slade, L. and Levine, H., Water relationships in starch transitions, *Carbohydr. Polym.*, 21, 105-131 (1993)

Sönnerskog, S., The positions occupied by the substituents in water soluble cellulose ethers, *Svensk Papperstidning*, 51, 50-51 (1948)

Sonaglio, D., Bataille, B., Terol, A., Jacob, M., Pauvert, B. and Cassanas, G., Physical characterization of two types of microcrystalline cellulose and feasibility of microspheres by extrusion/ spheronization, *Drug Dev. Ind. Pharm.*, 21 (5) 537-547 (1995)

Spurlin, H. M., Arrangement of substituents in cellulose derivatives, *J. Am. Chem. Soc.*, 61, 2222-2227 (1939)

Sung, K. C., Nixon, P. R., Skoug, J. W., Robert Ju, T., Gao, P., Topp, E. M. and Patel, M. V., Effect of formulation variables on drug and polymer release from HPMC-based matrix tablets, *Int. J. Pharm.*, 142, 53-60 (1996)

Sung, Y. K., Interaction of water with hydrophilic methacrylate polymers. Ph. D. Thesis, University of Utah (1978)

Sung, Y. K., Pulse NMR and thermal analysis of water-swelling polymers for biomedical and pharmaceutical applications, *Polymer (Korea)*, 10 (6) 576-583 (1986)

Sung, Y. K., Gregonis, D. E., John, M. S. and Andrade, J. D., Thermal and pulse NMR analysis of water in poly(2-hydroxyethyl methacrylate), *J. Appl. Polym. Sci.*, 26, 3719-3728 (1981)

- Svetlik, J. and Pouchly, J.**, Sorption of water in hydrophilic polymers - I, *Eur. Polym. J.*, 12, 123-127 (1976)
- Tahara, K., Yamamoto, K. and Nishihata, T.**, Overall mechanism behind matrix sustained release (SR) tablets prepared with hydroxypropyl methylcellulose 2910, *J. Control. Rel.*, 35, 59-66 (1995)
- Tahara, K., Yamamoto, K. and Nishihata, T.**, Application of model-independent and model analysis for the investigation of effect of drug solubility on its release rate from hydroxypropyl methylcellulose sustained release tablets, *Int. J. Pharm.*, 133, 17-27 (1996)
- Talukdar, M. M. and Kinget, R.**, Comparative study on xanthan gum and hydroxypropylmethylcellulose as matrices for controlled-release drug delivery. II. Drug diffusion in hydrated matrices, *Int. J. Pharm.*, 151, 99-107 (1997)
- Tamburic, S. and Craig, D. Q. M.**, An investigation into the rheological, dielectric and mucoadhesive properties of poly(acrylic acid) gel systems, *J. Control. Rel.*, 37, 59-68 (1995)
- Tamburic, S. and Craig, D. Q. M.**, The effects of ageing on the rheological, dielectric and mucoadhesive properties of poly(acrylic acid) gel systems, *Pharm. Res.*, 13 (2) 279-283 (1996)
- Tanaka, H., Koga, N. and Galwey, A. K.**, Thermal dehydration of crystalline hydrates, *J. Chem. Ed.*, 72 (3) 251-256 (1995)
- Taniguchi, Y. and Horigome, S.**, The states of water in cellulose acetate membranes, *J. Appl. Polym. Sci.*, 19, 2743-2748 (1975)

Tomioka, M. and Matsumura, G., Effects of concentration and degree of polymerization on the rheological properties of methylcellulose aqueous solution, *Chem. Pharm. Bull.*, 35 (6) 2510-2518 (1987)

Touitou, E. and Donbrow, M., Influence of additives on (hydroxyethyl)methylcellulose properties:relation between gelation temp. change, compressed matrix integrity and drug release profile, *Int. J. Pharm.*, 11, 131-148 (1982)

Touzinsky, G. F., The substituent group distribution in a Michael reaction, Carboxymethyl cellulose, *J. Org. Chem.*, 30, 426-428 (1965)

Udupa, N., Tatwawadi, S. V. and Gode, K. D., Studies on physicochemical properties of viscosity building agents used in contact lens solutions, *Ind. J. Hosp. Pharm.*, 13, 184-189 (1976)

Vacher, J., Formation d'une texture fibreuse dans les barres de cuivre écrouies, *Chim. Ind. (Paris)*, 43, 214 (1940)

Van Krevelen, D. W. (ed.), B. Molecular Weight and Distribution of Molecular Weights, in: "Properties of Polymers-Correlation with Chemical Structure", Elsevier, North Holland, 17-19 (1972)

Vázquez, M. J., Iglesias, R., Gómez-Amoza, J. L., Martínez-Pachece, R., Souto, C. and Concheiro, A., Influence of technological variables on the drug-release properties of atenolol-hydroxypropyl methylcellulose hydrophilic matrix tablets, *Proceed. Intern. Symp. Control. Rel. Bioact. Mater., Controll. Rel. Soc., Inc.*, 18, 447-448, (1991)

Vázquez, M. J., Gómez-Amoza, J. L., Martínez-Pacheco, R., Souto, C. and Concheiro, A., Relationships between drug dissolution profile and gelling agent viscosity in tablets prepared with hydroxypropylmethylcellulose (HPMC) and sodium carboxymethylcellulose (NaCMC) matrices, *Drug Dev. Ind. Pharm.*, 21 (16) 1859-1874 (1995)

Vedamuthu, M., Singh, S. and Wilse Robinson, G., Properties of liquid water: Origin of the density anomalies, *J. Phys. Chem.*, 98, 2222-2230 (1994)

Vigouret, M., Rinaudo, M. and Desbrières, J., Thermogelation of methylcellulose in aqueous solutions, *J. Chim. Phys.*, 93, 858-869 (1996)

Vyas, S. P., Jain, N. K. and Khanna, S., Formulation and performance evaluation of controlled release diclofenac tablets, *J. Control. Rel.*, 10, 219-223 (1989)

Wadsö, L., Describing non-fickian water-vapour sorption in wood, *J. Mat. Sci.*, 29 (9) 2367-2372 (1994)

Wadsö, I and Wadsö, L., A new method for determination of vapour sorption isotherms using a twin double microcalorimeter, *Thermochim. Acta*, 271, 179-187 (1996)

Wan, L. S. C., Heng, P. W. S. and Wong, L. F., The effect of hydroxypropylmethylcellulose on water penetration into a matrix system, *Int. J. Pharm.*, 73, 111-116 (1991)

Wendlandt, W. W. : "Thermal Analysis", 3rd ed. (Chemical Analysis Series, 19, Monographs on Analytical Chemistry and Applications), **Elving, P. J. and Windfordover, J. D. (ed.).** J. Wiley and Sons, London (1986)

Yasuda, H., Olf, H. G., Crist, B., Lamaze, C. E. and Peterlin, A., Movement of water in homogeneous water-swollen polymers, in: "Water Structure at the Water-Polymer Interface", **Jellinek, H. H. G. (ed.)**. Plenum Press, London, 39-55 (1972)

York, P., Analysis of moisture sorption hysteresis in hard gelatin capsules, maize starch, and maize starch : drug powder mixtures, *J. Pharm. Pharmacol.*, 33, 269-273 (1981)

Young, J. H. and Nelson, G. L., Theory of hysteresis between sorption and desorption isotherms in biological materials, *Trans. Am. Soc. Agric. Eng.*, 10, 260 - 263 (1967a)

Young, J. H. and Nelson, G. L., Research of hysteresis between sorption and desorption isotherms of wheat, *Trans. Am. Soc. Agric. Eng.*, 10, 756 - 761 (1967b)

Zhang, W.-Z., Satoh, M. and Komiyama, J., A differential scanning calorimetry study of the states of water in swollen poly(vinyl alcohol) membranes containing non-volatile additives, *J. Memb. Sci.*, 42, 303-314 (1989)

Zhu, H., Padden, B. E., Munson, E. J. and Grant, D. J. W., Physicochemical characterization of nedocromil bivalent metal salt hydrates. 2. Nedocromil zinc, *J. Pharm. Sci.*, 86 (4) 418-429 (1997)

Zografi, G., States of water associated with solids, *Drug Dev. Ind. Pharm.*, 14 (14) 1905-1926 (1988)

Zografi, G. and Kontny, M. J., The interactions of water with cellulose- and starch-derived pharmaceutical excipients, *Pharm. Res.*, 3 (4) 187-194 (1986)

Zografi, G., Kontny, M. J., Yang, A. Y. S. and Brenner, G. S., Surface area and water vapor sorption of microcrystalline cellulose, *Int. J. Pharm.*, 18, 99-116 (1984)

PUBLICATIONS

Research Publications

McCrystal, C.B., Ford, J.L. and Rajabi-Siahboomi, A-R.,

A study on the interaction of water and cellulose ethers using DSC.

UK National Thermal Analysis and Calorimetry Symposium (TAC 96), Leeds, U.K.
(1996)

McCrystal, C.B., Ford, J.L. and Rajabi-Siahboomi, A-R.,

Characterisation of the fundamental interactions between water and cellulose ether polymers.

Post-graduate research seminar (oral presentation), Liverpool John Moores University, School of Pharmacy & Chemistry (1996)

McCrystal, C.B., Ford, J.L. and Rajabi-Siahboomi, A-R., Molecular interactions between water and HPMC polymers.

3rd European Congress of Pharmaceutical Sciences, Edinburgh, U.K., P3.037
(1996)

Rajabi-Siahboomi, A-R., Leung, W.S.W., Al-Suwailem, A. and McCrystal, C.B., Effect of Bile Salts on drug release from HPMC matrices.

3rd European Congress of Pharmaceutical Sciences, Edinburgh, U.K., P2.105
(1996)

McCrystal, C.B., Ford, J.L. and Rajabi-Siahboomi, A-R., A study on the interaction of water and cellulose ethers using differential scanning calorimetry,

Thermochimica Acta 294, 91-98 (1997)

McCrystal, C.B., Ford, J.L. and Rajabi-Siahboomi, A-R.,

A study on the molecular interactions between water and cellulose ether polymers using DSC.

3rd UKCRS Symposium on Controlled Drug Delivery (UKCRS), Manchester, U.K.
(1997)

McCrystal, C.B., Ford, J.L. and Rajabi-Siahboomi, A-R.,
Influence of drugs on water distribution within cellulose ether polymers.
2nd UK National Thermal Analysis and Calorimetry Symposium (TAC 97), Oxford, U.K. (1997)

McCrystal, C.B., Ford, J.L., Vyas, K, Dennis, A.B. and Rajabi-Siahboomi, A-R.,
Influence of molecular weight and substitution type on dynamic vapour sorption of cellulose ether polymers.
J. Pharm. Pharmacol. Suppl. 49 (4) 38 (1997)
134th British Pharmaceutical Conference (BPC 97), Scarborough (1997)

McCrystal, C.B., Ford, J.L. and Rajabi-Siahboomi, A-R.,
Investigation of the molecular interactions between water and cellulose ether polymers using thermal analysis.
Pharm. Res. Suppl. 14 (11) S627 (1997)
AAPS Annual Meeting and Exposition (oral presentation), Boston, Massachusetts, (1997)

McCrystal, C.B., Ford, J.L., He, R., Craig, D.Q.M., Rajabi-Siahboomi, A-R.,
Characterisation of the interactions between water and cellulose ether polymers using dielectric spectroscopy.
The 17th Pharmaceutical Technology Conference and Exhibition (oral presentation), Trinity College, Dublin, 60 (1998)

McCrystal, C.B., Ford, J.L., He, R., Craig, D.Q.M., Rajabi-Siahboomi, A-R.,
Dielectric response of gels containing cellulose ether polymers.
135th British Pharmaceutical Conference (BPC 98), Eastbourne, U.K. (1998)
(accepted)